ЖУРНАЛ
ЭКСПЕРИМЕНТАЛЬНОЙ И ТЕОРЕТИЧЕСКОЙ
ФИЗИКИ
АКАДЕМИЯ НАУК СССР

SOVIET PHYSICS

JETP

VOLUME 3 NUMBER 5

A Translation

of the

Journal of Experimental and Theoretical Physics

of the

Academy of Sciences of the USSR

DECEMBER, 1956

Published by the

AMERICAN INSTITUTE OF PHYSICS
INCORPORATED

SOVIET PHYSICS
JETP

A translation of the Journal of Experimental and Theoretical Physics of the USSR.

SOVIET PHYSICS is a monthly journal published by the American Institute of Physics for the purpose of making available in English reports of current Soviet research in physics as contained in the Journal of Experimental and Theoretical Physics of the Academy of Sciences of the USSR. The page size of SOVIET PHYSICS will be 7⅛" x 10½", the same as other Institute journals.

Transliteration of the names of Russian authors follows the system employed by the Library of Congress.

This translating and publishing project was undertaken by the Institute in the conviction that dissemination of the results of researches everywhere in the world is invaluable to the advancement of science. The National Science Foundation of the United States encouraged the project initially and is supporting it in large part by a grant.

The American Institute of Physics and its translators propose to translate faithfully all the material in the Journal of EXPERIMENTAL AND THEORETICAL PHYSICS OF THE USSR appearing after January 1, 1955. The views expressed in the translated material, therefore, are intended to be those expressed by the original authors, and not those of the translators nor of the American Institute of Physics.

Two volumes are published annually, each of six issues. Each volume contains the translation of one volume of the Journal of EXPERIMENTAL AND THEORETICAL PHYSICS OF THE USSR. New volumes begin in February and August.

Subscription Prices:

Per year (12 issues)	
United States and Canada	$60.00
Elsewhere	64.00
Back Numbers	
Single copies	$ 6.00

Subscriptions should be addressed to the American Institute of Physics, 57 East 55 Street, New York 22, New York.

SOVIET PHYSICS

JETP

SOVIET PHYSICS JETP VOLUME 3, NUMBER 5 DECEMBER, 1956

Shape of the Spectral Line of a Generator with Fluctuating Frequency

A. N. MALAKHOV
Riazan' Radio Engineering Institute
(Submitted to JETP editor March 12, 1955)
J. Exptl. Theoret. Phys. (U.S.S.R.) 30, 884-888 (May, 1956)

The present paper is a continuation and further development of Bershtein's work[1-3] on the natural line width, and Gorelik's work[4,5] on the "technical" width of a vacuum tube generator.

IN any actual vacuum tube generator there are always fluctuations of the frequency (or phase) which produce a smearing of the spectral line. If we consider fluctuations arising from shot or thermal noise (i.e., from "natural" causes), then we speak of the natural line width. If on the other hand we consider "technical" causes of fluctuation, such as "microscopic" effects, then we speak of the technical line width. It is of interest to consider the general question of the relation of the shape of the spectral line of a generator to various characteristics of the frequency fluctuations, which depend on the method of generation of the fluctuations. The present paper treats this problem.

1. THE GENERAL EXPRESSION FOR THE SPECTRAL DENSITY OF THE OSCILLATION

We consider an oscillation whose frequency fluctuates:

$$z_t = A\cos(\omega_0 t + \varphi_t), \tag{1}$$

$$\varphi_t = \int_{t_0}^{t} \Delta\omega_\xi \, d\xi. \tag{2}$$

A is the amplitude, ω_0 is the average value of the frequency, φ_t is the phase of the oscillation and $\Delta\omega_t$ is the frequency fluctuation, whose average value is zero.

The spectral density $S_z(\omega)$ is equal to

$$S_z(\omega) = \frac{2}{\pi}\int_0^\infty \Phi_z(\tau)\cos\omega\tau\, d\tau, \tag{3}$$

where

$$\Phi_z(\tau) = \lim_{T\to\infty}\frac{1}{T}\int_0^T z_t z_{t+\tau}\, dt \tag{4}$$

is the correlation function for the quantity z_t. Substituting (1) in (4), we obtain, after some simple transformations:

$$\Phi_z(\tau) = \lim_{T\to\infty}\frac{A^2}{2T}\int_0^T \cos(\omega_0\tau + \Delta\varphi)\, dt,$$

where

$$\Delta\varphi = \varphi_{t+\tau} - \varphi_t = \int_t^{t+\tau}\Delta\omega_\xi\, d\xi. \tag{5}$$

We shall assume that the frequency fluctuations represent a stationary random process and are a superposition of a large number of random, statistically independent, disturbances. In this case, $\Delta\varphi$ also describes a stationary process and, in addition, has a normal distribution around zero value. Consequently, on the basis of the quasi-ergodic theorem[6], the time average of a function of $\Delta\varphi$ can be identified with the statistical average over the corresponding ensemble (which we shall denote by a bar over the symbol which is averaged). Thus,

$$\Phi_z(\tau) = {}^1/_2 A^2 \overline{\cos(\omega_0\tau + \Delta\varphi)} = {}^1/_2 A^2 \cos\omega_0\tau\ \overline{\cos\Delta\varphi}, \quad (6)$$

since

$$\overline{\sin\Delta\varphi} = 0.$$

To find the average value of the cosine we use the well-known formula

$$\int_{-\infty}^{+\infty} e^{-\alpha x^2}\cos qx\,dx = \sqrt{\frac{\pi}{\alpha}}\,e^{-q^2/4\alpha}$$

and obtain

$$\overline{\cos\Delta\varphi} = \exp(-{}^1/_2\,\overline{\Delta\varphi^2}). \quad (7)$$

Combining (7) and (6), we find

$$\Phi_z(\tau) = {}^1/_2 A^2\cos\omega_0\tau\exp(-{}^1/_2\,\overline{\Delta\varphi^2}). \quad (8)$$

To get $\overline{\Delta\varphi^2}$ we square both sides of (5) and average them:

$$\overline{\Delta\varphi^2} = \int_t^{t+\tau}\int_t^{t+\tau}\overline{\Delta\omega_\xi\,\Delta\omega_\eta}\,d\xi\,d\eta = \int_t^{t+\tau}\int_t^{t+\tau}\Phi(\xi-\eta)\,d\xi\,d\eta,$$

where $\Phi(\tau)$ is the correlation function of the frequency fluctuations, which we shall assume to be given. If we change variables in the double integral and use the fact that the correlation function is even, we get

$$\overline{\Delta\varphi^2} = 2\int_0^\tau(\tau-\xi)\,\Phi(\xi)\,d\xi. \quad (9)$$

We write the correlation function in the form

$$\Phi(\tau) = \overline{\Delta\omega^2}\,R(\tau), \quad (10)$$

where $R(\tau)$ is the correlation coefficient of the frequency fluctuation $\Delta\omega_t$ and $\overline{\Delta\omega^2}$ is the mean square deviation of the frequency.

Combining (10), (9) and (7), we get the final expression for the correlation function:

$$\Phi_z(\tau) = {}^1/_2\,A^2\cos\omega_0\,\tau\,\exp\Big[-\overline{\Delta\omega^2}\int_0^\tau(\tau-\xi)\,R(\xi)\,d\xi\Big]. \quad (11)$$

We shall discuss some of the features of this result. Formula (9) shows that $\overline{\Delta\varphi^2}$ does not depend on the time coordinate t, but depends only on the time interval τ, i.e., the distribution of $\Delta\varphi$ actually does not depend on the time, but is stationary. However, this is not the case for the phase φ_t itself or the quantity φ_t^2, which do depend on the time. This means that the distribution of the phase, though normal, is not stationary.

The problem of finding the spectrum of the oscillations in the presence of frequency fluctuations has also been considered by Middleton[7]. For example, he treated the case where the spectral density of the frequency fluctuations has a Gaussian shape. However, in our opinion, Middleton made the mistake in his calculations of setting $\overline{\varphi_t^2} \equiv \overline{\varphi_{t+\tau}^2}$. Actually, one can show that even for small τ,

$$\overline{\varphi^2{}_{t+\tau}} - \overline{\varphi^2}_t = 2\tau\int_0^\infty\Phi(\xi)\,d\xi \not\equiv 0.$$

By finding the parameters of the normal probability distribution for the quantity φ_t, one can show that the phase fluctuations follow a diffusion law, which clearly should be the case, since the phase shifts due to frequency fluctuations pile up [because of the time integral in Eq. (2)]. This diffusion law for the phase fluctuations was considered in more detail earlier by Bershtein in the papers mentioned, in which he investigated the phase fluctuations of a tube generator arising from shot and thermal noise*.

Substituting the value (11) for the correlation function in Eq. (3), we find the spectral density

$$S_z(\omega) = S(\omega) + S(-\omega),$$

where

$$S(\omega) = \frac{A^2}{2\pi}\int_0^\infty\cos(\omega_0-\omega)\,\tau\times\exp\Big[-\overline{\Delta\omega^2}\int_0^\tau(\tau-\xi)\,R(\xi)\,d\xi\Big]\,d\tau. \quad (12)$$

The spectral density in the neighborhood of the average frequency ω_0 is determined mainly by the first term $S(\omega)$, since it had a singularity just at the point $\omega = \omega_0$. The second integral $S(-\omega)$ produces no essential change in the spectral density $S_z(\omega)$ at $\omega = \omega_0$.

Thus Eq. (12) gives the "shape" of the spectral line.

2. GENERAL INVESTIGATION OF THE SHAPE OF THE SPECTRAL LINE

Let the frequency fluctuation $\Delta\omega_t$ be characterized by its correlation time τ_0, defined so that for $\tau > \tau_0$ the quantities $\Delta\omega_t$ and $\Delta\omega_{t+\tau}$ may be treated as practically independent.

Let us first consider the limiting case when the frequency fluctuations are slow or large, i.e., the case when $\overline{\Delta\omega^2}\,\tau_0^2 \gg 1$. To find the spectral density for this case, we consider the expression

$$\int_0^\tau(\tau-\xi)\,R(\xi)\,d\xi.$$

If τ is taken outside the integral, then after changing variables, we get

$$\int_0^{\tau} (\tau - \xi)\, R(\xi)\, d\xi = \tau^2 \int_0^1 (1 - \xi)\, R(\tau\xi)\, d\xi.$$

In this case the spectral density (12) is given by

$$S(\omega) = \frac{A^2}{2\pi} \int_0^{\infty} \cos(\omega_0 - \omega)\tau \times \exp\left[-\overline{\Delta\omega^2}\,\tau^2 \int_0^1 (1 - \xi)\, R(\tau\xi)\, d\xi\right] d\tau. \quad (13)$$

It can be shown that for $\overline{\Delta\omega^2}\,\tau_0^2 \gg 1$, the quantity $R(\tau\xi)$ in Eq. (13) can be set equal to unity without significant error. As a result, we get

$$S(\omega) = \frac{A^2}{2\pi} \int_0^{\infty} \cos(\omega_0 - \omega)\tau \exp\left[-\frac{1}{2}\overline{\Delta\omega^2}\,\tau^2\right] d\tau.$$

Calculating this integral, we get finally,

$$S(\omega) = \frac{A^2}{2}(2\pi\,\overline{\Delta\omega^2})^{1/2} \exp\left\{-\frac{(\omega_0 - \omega)^2}{2\,\overline{\Delta\omega^2}}\right\}. \quad (14)$$

Thus if there are slow or large fluctuations of the frequency, so that $\overline{\Delta\omega^2}\,\tau_0^2 \gg 1$, the line is broadened and coincides in shape with a Doppler broadened line, with "line width" equal to $2(2\overline{\Delta\omega^2})^{1/2}$.

We now consider a second limiting case, opposite to the first. Suppose that there are rapid or small fluctuations of the oscillation frequency, so that $\overline{\Delta\omega^2}\,\tau_0^2 \ll 1$. To find $S(\omega)$, we introduce the auxiliary quantity $k = k(\tau_0)$, such that

$$k(\tau_0) \int_{-\infty}^{+\infty} R(\tau)\, d\tau = 1 \quad (15)$$

for all values of τ_0. Since for $\tau_0 \to 0$ the quantity $R(\tau)$ differs from zero only for small values of τ [we recall that $R(0) = 1$], it is obvious that

$$\lim_{\tau_0 \to 0} k(\tau_0)\, R(\tau) = \delta(\tau),$$

where $\delta(\tau)$ is the delta function.

We write (13) in the form

$$S(\omega) = \frac{A^2}{2\pi} \int_0^{\infty} \cos(\omega_0 - \omega)\tau \times \exp\left[-\frac{\overline{\Delta\omega^2}}{k}\,\tau^2 \int_0^1 (1 - \xi)\, kR(\tau\xi)\, d\xi\right] d\tau.$$

One can show that for $\overline{\Delta\omega^2}\tau_0^2 \ll 1$, the quantity $kR(\tau\xi)$ in this expression can be set equal to $\delta(\tau\xi)$ without serious error, so that

$$S(\omega) = \frac{A^2}{2\pi} \int_0^{\infty} \cos(\omega_0 - \omega)\tau \exp\left[-\frac{\overline{\Delta\omega^2}}{2k}\tau\right] d\tau.$$

Computing this integral, we get finally

$$S(\omega) = \frac{A^2}{2\pi} \frac{\overline{\Delta\omega^2}/2k}{(\overline{\Delta\omega^2}/2k)^2 + (\omega_0 - \omega)^2}. \quad (16)$$

This spectral density coincides in shape with that obtained by Bershtein for the natural broadening of the line.

Thus if there are rapid or small frequency fluctuations, so that $\overline{\Delta\omega^2}\,\tau_0^2 \ll 1$, the line emitted by the oscillator suffers a broadening, and has a line shape identical with that for natural broadening with a "line width" equal to $\overline{\Delta\omega^2}/k$.

We note that from Eqs. (14) and (16) it follows that the Doppler and natural broadening may, in general, represent different special cases of the same process of "smearing" of the line emitted by an oscillator.

3. EXAMPLE

We consider the special case where the fluctuation of the generator frequency has a correlation coefficient equal to

$$R(\tau) = e^{-\alpha|\tau|}, \quad \tau_0 = 1/\alpha.$$

The first limiting case, where $\overline{\Delta\omega^2} \gg \alpha^2$, leads without change to Eq. (14). To consider the second limiting case, where $\overline{\Delta\omega^2} \ll \alpha^2$, we determined the auxiliary quantity $k(\tau_0)$. From the definition (15) we find that $k(\tau_0) = \alpha/2$. Thus, for the second limiting case,

$$S(\omega) = \frac{A^2}{2\pi} \frac{\overline{\Delta\omega^2}/\alpha}{(\overline{\Delta\omega^2}/\alpha)^2 + (\omega_0 - \omega)^2}. \quad (17)$$

Now suppose that there is some arbitrary ratio between $\overline{\Delta\omega^2}$ and α^2. Returning to Eq. (12) and computing the integral in the argument of the exponential, we get:

$$S(\omega) = \frac{A^2}{2\pi} e^C \int_0^{\infty} \cos(\omega_0 - \omega)\tau \exp\left[-B\tau - Ce^{-\alpha\tau}\right] d\tau,$$

where $C = \overline{\Delta\omega^2}/\alpha^2$, $B = \alpha C$. Computing this integral by expanding in series, we get the general expression for the spectral density for our example in the form

* The validity of the diffusion law for the phase fluctuations of a tube generator for arbitrary τ is also shown by the work of Rytov[8,9]

$$S(\omega) = \frac{A^2}{2\pi} e^{\Delta\overline{\omega^2}/\alpha^2} \tag{18}$$

$$\times \sum_{m=0}^{\infty} \frac{(-1)^m}{m!} \left(\frac{\overline{\Delta\omega^2}}{\alpha^2}\right)^m \frac{(\overline{\Delta\omega^2}/\alpha) + \alpha m}{[(\overline{\Delta\omega^2}/\alpha) + \alpha m]^2 + (\omega_0 - \omega)^2}.$$

If $\overline{\Delta\omega^2} \ll \alpha^2$, then only the first terms in the series (18) are important:

$$S(\omega) = \frac{A^2}{2\pi}\left[\frac{\overline{\Delta\omega^2}/\alpha}{(\overline{\Delta\omega^2}/\alpha)^2 + (\omega_0 - \omega)^2} - \frac{\overline{\Delta\omega^2}/\alpha}{\alpha^2 + (\omega_0 - \omega)^2} + \ldots\right]$$

where, as expected, the first term of the series coincides with Eq. (17).

[1] I. L. Bershtein, Dokl. Akad. Nauk SSSR 20, 11 (1938).

[2] I. L. Bershtein, J. Tech. Phys. (U.S.S.R.) 11, 305 (1941).

[3] I. L. Bershtein, Izv. Akad. Nauk SSSR, Ser. Fiz. 14, 145 (1950).

[4] G. S. Gorelik, J. Exptl. Theoret. Phys. (U.S.S.R.) 20, 351 (1950).

[5] G. S. Gorelik, Izv. Akad. Nauk SSSR, Ser. Fiz. 14, 187 (1950).

[6] M. A. Leontovich, *Statistical Physics* (Moscow, Leningrad), 1944.

[7] D. Middleton, Phil. Mag. 42, 689 (1951).

[8] S. M. Rytov, J. Exptl. Theoret. Phys. (U.S.S.R.) 29, 304, 315 (1955); Soviet Phys. JETP 2, 217, 225 (1956).

[9] S. M. Rytov, Radiotekhnika i elektronika 1, 114 (1956).

Translated by M. Hamermesh
182

SOVIET PHYSICS JETP VOLUME 3, NUMBER 5 DECEMBER, 1956

Vibration Spectrum of Disordered Crystal Lattices

I. M. LIFSHITZ AND G. I. STEPANOVA

Physico-Technical Institute, Ukrainian Academy of Sciences

(Submitted to JETP editor, April 6, 1955)
J. Exptl. Theoret. Phys. (U.S.S.R.) 30, 938-946 (May, 1956)

The vibration spectrum of a disordered crystal is studied. Calculations are made for an isotopic mixture, although the method could be applied under more general conditions. The mass of each atom is taken to be a random variable, and the deviation of the mass from its average value is not assumed to be small. The spectral density and the vibrational part of the free energy of the mixed crystal are determined.

THE determination of the vibration spectrum of a disordered system, for example a mixed solid, is a highly interesting problem. A similar problem was considered by one of the authors[1] in connection with the optical properties of mixed solids; at that time we investigated thoroughly only those aspects of the problem which are directly relevant to infra-red spectroscopy, (in particular the question of the existence of impurity frequencies). Dyson[2] considered the same problem for the special case of a disordered linear chain with nearest-neighbor interactions. But Dyson's method is by its very nature not capable of extension to three-dimensional systems.

In the present paper we describe a method which is free from these limitations. The method is an extension of earlier work by one of us.[3-6] We apply the method here to the case in which the atoms in the system differ only in mass (a mixture of isotopes). For the sake of clarity and simplicity of exposition, we consider only an idealized lattice in which all vibrations take place in one direction. This shortens the analysis considerably, without changing the essential nature of the problem.

There exists a deep-lying similarity in the effects of the destruction of translational invariance upon the energy spectra of phonons and of electrons. Hence the results of this investigation should be qualitatively valid also for electronic spectra.

1. THE METHOD OF TRACES

The equation for the vibrations of a lattice composed of a mixture of isotopes of a single element has the form

$$\sum_{\mathbf{r}'} \frac{A_{\mathbf{r}-\mathbf{r}'}}{m_{\mathbf{r}}} \chi(\mathbf{r}') - \omega^2 \chi(\mathbf{r}) = 0. \tag{1}$$

Here $\chi(r)$ is the displacement of an atom from its equilibrium position, and $A_{r-r'}$ is an interaction coefficient; $r=n_1 a_1 + n_2 a_2 + n_3 a_3$, where the n_i are integers and the a_i are the periods of the lattice. In what follows we take the periods to be the unit of length. The masses m_r are random variables taking two values (for a binary mixture) with probabilities equal to the corresponding isotopic abundances. The quantity to be determined is the expectation value of the spectral density, or of the number of energy levels in a given interval. For a sufficiently large crystal, the actual value of the spectral density will coincide with its expectation value.

Considering the difference between m_r and a constant mass m as a perturbation, we may write equation (1) in the form

$$(\hat{L} + \hat{\varepsilon}\hat{L})\chi - \omega^2\chi = 0, \tag{2}$$

with

$$L_{r,r'} \equiv L_{r-r'} = A_{r-r'}/m; \tag{3}$$

$$\hat{\varepsilon}_{r,r'} = \varepsilon'_r \delta_{rr'}, \qquad \varepsilon'_r = (m - m_r)/m_r. \tag{4}$$

To make the operators Hermitian, we write Equation (2) in the symmetrized form

$$(\hat{L} + \hat{\Lambda})\chi' = \omega^2\chi', \tag{5}$$

$$\hat{\Lambda} = \hat{L}^{1/2}\hat{\varepsilon}\hat{L}^{1/2}, \qquad \chi' = \hat{L}^{1/2}\chi.$$

In future we drop the primes and write χ for χ'. The eigenfunctions of the unperturbed operator $\hat{L}$ are the plane waves $\chi^0_k = e^{2\pi i k r}$. The corresponding eigenvalues are the squares of the unperturbed frequencies

$$\omega^2(\mathbf{k}) = \sum_{\mathbf{r}} L_{\mathbf{r}} e^{-2\pi i\, \mathbf{k}\mathbf{r}}.$$

In the representation defined by the states χ^0_k, the perturbation $\hat{\Lambda}$ has matrix elements given by

$$\Lambda_{k,k'} = (\hat{L}^{1/2}\hat{\varepsilon}\hat{L}^{1/2}\chi^0_k, \chi^0_{k'}) = (\hat{\varepsilon}\hat{L}^{1/2}\chi^0_k, \hat{L}^{1/2}\chi^0_{k'}) \tag{6}$$

$$= \omega(\mathbf{k})\,\omega(\mathbf{k}') \sum_{\mathbf{r}} \varepsilon'_{\mathbf{r}} e^{2\pi i(\mathbf{k}-\mathbf{k}')\mathbf{r}}.$$

We shall calculate the difference in vibrational free energy between the unperturbed and perturbed crystals, namely

$$F - F_0 = \mathrm{Sp}\,\{\varphi(\hat{L} + \hat{\Lambda}) - \varphi(\hat{L})\}, \tag{7}$$

$$\varphi(z) = \Theta \ln(1 - e^{-\hbar\sqrt{z}/\Theta}) + {}^1\!/_2\,\hbar\sqrt{z}. \tag{8}$$

Here Θ is the temperature and h is Planck's constant. In principle we could equally well carry through the calculation with some other function ϕ, but this choice has the advantage of yielding directly the free energy which is a physically interesting quantity.

The quantity (7) is related to the difference between the spectral densities by the equation

$$F - F_0 = N\int \varphi(z)\,[\nu(z) - \nu_0(z)]\,dz \tag{9}$$

$$= -N\int dz\varphi'(z)\int_0^z [\nu(\mu) - \nu_0(\mu)]\,d\mu.$$

Here and henceforth, the letter z denotes the square of a frequency, $z = \omega^2$. N is the number of atoms if the lattice and $N\nu(z)$ is the spectral density. For the unperturbed lattice,

$$\nu_0(z) = \int d\Omega/|\nabla\omega^2|, \tag{10}$$

the integration being over the surface $\omega^2(k) = z$ in k-space; $d\Omega$ is an element of area on the surface, and $\nabla\omega^2$ means the gradient of ω^2 in k-space.

2. EXPANSION IN POWERS OF CONCENTRATION

We set the "unperturbed mass" m equal to the mass m_1 of one isotope, and consider as a perturbation the replacement of m_1 by the mass m_2 of the other isotope at certain lattice-points. Asymptotically for large N, the expansion of the vibrational free energy in powers of the concentration c of the second isotope has the form

$$F - F_0 = Ncf_1 + N\frac{c^2}{2}f_2 + \ldots, \tag{11}$$

$$Nf_1 = (\partial F/\partial c)|_{c=0} = N(\bar{F}_1 - F_0), \tag{12}$$

$$Nf_2 = (\partial^2 F/\partial c^2)|_{c=0} = N^2(\bar{F}_2 - 2\bar{F}_1 + F_0). \tag{13}$$

Here F_n is the free energy of a lattice containing precisely n impurity atoms, averaged over the possible positions of these atoms. Let $\psi_n(r_1, \ldots, r_n$ (be the addition to the unperturbed free energy, in the case when the impurity atoms are at the positions $r_1, \ldots, r_n$. Clearly $\psi_1(r) = \psi_1$ is independent of r, and $\psi_2(r_1, r_2) \equiv \psi_2(r_1 - r_2)$, while $\psi_2(r) \to 2\psi_1$ as $r \to \infty$. Further, let $W_{r_1 - r_2, \ldots, r_{n-1} - r_n}$

be the correlation function defining the probability $P_{r_1 \ldots r_n}$ for finding n impurity atoms at the positions $r_1, \ldots, r_n$,

$$P_{\mathbf{r}} = c, \quad P_{\mathbf{r}_1, \mathbf{r}_2} = c^2 W_{\mathbf{r}_1 - \mathbf{r}_2} \cdots$$

In the absence of long-range order, $W_r \to 1$ as $r \to \infty$. If there is no correlation between the positions of impurity atoms, then $W_r = 1$ for all r. In any case,

$$f_1 = \psi_1, \quad f_2 = \sum_{\mathbf{r} \neq 0} W_{\mathbf{r}} [\psi_2(\mathbf{r}) - 2\psi_1], \tag{14}$$

and therefore

$$F - F_0 = N \left\{ c\psi_1 + \frac{c^2}{2} \sum_{\mathbf{r} \neq 0} W_{\mathbf{r}} [\psi_2(\mathbf{r}) - 2\psi_1] + \ldots \right\}. \tag{15}$$

If there is no correlation ($W_r = 1$), then

$$F - F_0 = N \left\{ c\psi_1 + \frac{c^2}{2} \sum_{\mathbf{r} \neq 0} [\psi_2(\mathbf{r}) - 2\psi_1] + \ldots \right\}. \tag{16}$$

Thus, to determine the free energy of the mixture correctly to terms of the order c^n, it is sufficient to calculate the addition to the free energy produced by inserting not more than n impurity atoms into the lattice. When n atoms are inserted, the contribution to the free energy is

$$\psi_n(\mathbf{r}_1, \ldots, \mathbf{r}_n) = \mathrm{Sp}\, \{\varphi(\hat{L} + \hat{\Lambda}_n(\mathbf{r}_1, \ldots, \mathbf{r}_n)) - \varphi(\hat{L})\}, \tag{17}$$

with

$$(\hat{\Lambda}_n)_{\mathbf{k},\mathbf{k}'} = \varepsilon' \omega(\mathbf{k})\, \omega(\mathbf{k}') \sum_{p=1}^{n} e^{2\pi i (\mathbf{k} - \mathbf{k}') \mathbf{r}_p}, \tag{18}$$

$$\varepsilon' = (m_1 - m_2)/m_2. \tag{19}$$

In our problem, the perturbation operator is finite-dimensional, the number of dimensions being equal to the number of impurity atoms. The analysis of such perturbation operators in the physics of crystal lattices has been carried out earlier.[3-6] The problem of calculating the trace of a difference of two operators of the form (7) has been solved[6,7] quite generally. Using the results of the earlier papers, we have

$$\psi_n(\mathbf{r}_1, \ldots, \mathbf{r}_n) = \int \xi_n(z, \mathbf{r}_1, \ldots, \mathbf{r}_n)\, \varphi'(z)\, dz; \tag{20}$$

$$\xi_n(z, \mathbf{r}_1, \ldots, \mathbf{r}_n) = \frac{1}{\pi} \arg D \tag{21}$$

$$\times \left(\delta_{pk} + \varepsilon z \int_0^{z_g^0} \frac{J_{\mathbf{r}_p - \mathbf{r}_k}(\mu)}{\mu - z - i0} d\mu \right) \quad (p, k = 1, \ldots, n);$$

$$\varepsilon = (m_1 - m_2)/m_1, \tag{22}$$

$$J_{\mathbf{r}}(\mu) = \int_{\omega^2(\mathbf{k}) = \mu} \frac{d\Omega}{|\nabla \omega^2|} e^{2\pi i \mathbf{k} \mathbf{r}}. \tag{23}$$

Here $D(\alpha_{ik})$ means the determinant whose elements are α_{ik}. For $z > z_g^0$, the determinant D is real, and ξ_n takes the value zero or one according as D is positive or negative. The contribution to ψ_n supplied by the function ξ_n in this range is

$$\sum_j (\varphi(z_j) - \varphi(z_g^0)), \tag{24}$$

where the z_i are the roots of the equation

$$D \left(\delta_{ik} + \varepsilon z \int_0^{z_g^0} \frac{J_{\mathbf{r}_i - \mathbf{r}_k}(\mu)}{\mu - z} d\mu \right) = 0. \tag{25}$$

In the region of the continuous spectrum ($0 < z < z_g^0$) we have

$$\int \frac{J_{\mathbf{r}_i - \mathbf{r}_k}(\mu)}{\mu - z - i0} d\mu = \int' \frac{J_{\mathbf{r}_i - \mathbf{r}_k}(\mu)}{\mu - z} d\mu + i\pi J_{\mathbf{r}_i - \mathbf{r}_k}(z),$$

where $\int'$ means a principal value integral, and so the argument of the determinant may take any value from $-\pi$ to π. In the special case of one impurity atom, with z in the continuous spectrum range,

$$\xi_1(z) = \frac{1}{\pi} \mathrm{arctg} \left\{ \pi \varepsilon z \nu_0(z) \left[1 + \varepsilon z \int' \frac{\nu_0(\mu)}{\mu - z} d\mu \right]^{-1} \right\}. \tag{26}$$

To make the meaning of the above equations clear, we now carry through the calculations of Ref. 6 for the simplest case, in which there is only one impurity atom. Without loss of generality we suppose this atom to be placed at the coordinate origin. Then the perturbation operator becomes

$$(\hat{\Lambda}_1)_{k,k'} = \varepsilon' \omega(k)\,\omega(k').$$

We introduce a sequence of operators L_α, having the same eigenfunctions $\chi_k^0 = e^{2\pi i k r}$ as L, but with eigenvalues $\mu_n = \alpha [\omega^2(k)/\alpha]$, where $[q]$ denotes the integer part of a real number q. Each eigenvalue $\mu_n = \alpha n$ of $\hat{L}_\alpha$ is infinitely degenerate, the crystal being supposed infinite. It was proved previously [3] that, for an operator with a degenerate spectrum, the addition of a one-dimensional operator $\hat{\Lambda}_1$ produces a decrease by one unit in the multiplicity of each eigenvalue, the multiple eigenvalues maintaining their positions unchanged. One eigenvalue is split off from each multiplet and takes a displaced position between μ_n and μ_{n+1}. Thus the new eigenvalues of $(L_\alpha + \hat{\Lambda}_1)$ may be written in the form

$$z_n = \mu_n + \alpha \xi_1(\mu_n). \tag{27}$$

with an error small compared with α. The equation for the eigenfunctions corresponding to the new eigenvalues is

$$f(r) = -(\hat{L}_\alpha - z)^{-1}\hat{\Lambda}_1 f(r) \tag{28}$$

$$= \sum_n \frac{1}{z-\mu_n} \int\limits_{\alpha n < \omega^2(k) < \alpha(n+1)} (\hat{\Lambda}_1 f, \chi_k)\,\chi_k\, dk$$

$$= \varepsilon' f(0) \sum_n \frac{\alpha \mu_n}{z-\mu_n} \int\limits_{\omega^2(k)=\mu_n} \frac{d\Omega}{|\nabla \omega^2|} e^{2\pi i k r}.$$

Putting $r = 0$ on both sides of this equation and dividing by $f(0)$, we obtain

$$1 = \varepsilon' \sum_n \frac{\alpha \mu_n \nu_0(\mu_n)}{z-\mu_n}. \tag{29}$$

We now write $z_n = \mu_n + \alpha\xi_1(\mu_n)$, and go to the limit $\alpha \to 0$. After a few transforamtions,[6] we obtain

$$1 = \pi\varepsilon' z \nu_0(z) \operatorname{ctg} \pi\xi_1(z) + \varepsilon' \int' \frac{\mu \nu_0(\mu)}{z-\mu} d\mu, \tag{30}$$

Remembering that $\int dk = 1$ and $\varepsilon = \varepsilon'/(1+\varepsilon')$, we find that (30) reduces to the desired result (26). These displaced eigenvalues tend to a continuous spectrum as $\alpha \to 0$. If there exist other eigenvalues in the range $z < z_g^0$ of the discrete spectrum, they are solutions of the limiting equation

$$1 = \varepsilon' \int_0^{z_g^0} \frac{\mu \nu_0(\mu)}{z-\mu} d\mu. \tag{31}$$

In our case, such discrete eigenvalues can exist only if ϵ' is positive and sufficiently large, i.e., if the impurity atom is much lighter than the others. In what follows, except in Sec. 4, we assume that such discrete eigenvalues are absent.

From the foregoing expressions for the eigenvalues of the perturbed operator, we deduce the value of the difference of traces.

$$\gamma_1 = \operatorname{Sp}\{\varphi(\hat{L} + \hat{\Lambda}_1) - \varphi(\hat{L})\} \tag{32}$$

$$= \lim_{\alpha \to 0} \operatorname{Sp}\{\varphi(\hat{L}_\alpha + \hat{\Lambda}_1) - \varphi(\hat{L}_\alpha)\}$$

$$= \lim_{\alpha \to 0} \sum_n [\varphi(\mu_n + \alpha\xi_1(\mu_n)) - \varphi(\mu_n)]$$

$$= \int \xi_1(\mu)\,\varphi'(\mu)\, d\mu,$$

in agreement with Eq. (20).

Turning now to the evaluation of the free energy (15) and using Eq. (20), we find

$$F - F_0 = N \int dz \varphi'(z) \left\{ c\xi_1(z) + \frac{c^2}{2} \right. \tag{33}$$

$$\left. \times \sum_{r \neq 0} W_r [\xi_2(z, r) - 2\xi_1(z)] + \ldots \right\}.$$

The sum over r in Eq. (33) is convergent. In fact, the quantity $(\xi_2(r) - 2\xi_1)$ is according to Eq. (21)

$$\xi_2(r) - 2\xi_1 \tag{34}$$

$$= \frac{1}{\pi} \arg\left(1 - \frac{\varepsilon^2 z^2 \int \frac{J_r'(\mu)}{\mu - z - i0}\, d\mu \int \frac{J_{-r}(\mu')}{\mu' - z - i0}\, d\mu'}{\left(1 + \varepsilon z \int \frac{\nu_0(\mu'')}{\mu'' - z - i0}\, d\mu''\right)^2}\right),$$

and decreases rapidly for large r by virtue of the decrease of the integrands $J_r(\mu)$ which contain exponential factors. If there is no correlation, the sum in Eq. (33) becomes

$$\sum_r (\xi_2(z, r) - 2\xi_1(z)) = \frac{1}{\pi} \arg \prod_r \tag{35}$$

$$\times \left(1 - \frac{\varepsilon^2 z^2 \int \frac{J_r(\mu)}{\mu - z - i0}\, d\mu \int \frac{J_{-r}(\mu')}{\mu' - z - i0}\, d\mu'}{\left(1 + \varepsilon z \int \frac{\nu_0(\mu'')}{\mu'' - z - i0}\, d\mu''\right)^2}\right).$$

We used the fact that the argument of a product is equal to the sum of the arguments of the factors.

Within the interval of unperturbed frequencies ($0 < z < z_g^0$), the vibrational spectrum density $\nu(z)$ of the mixed crystal is obtained by a comparison of Eq. (9) with (33),

$$\nu(z) - \nu_0(z) = -\frac{d}{dz}\left\{c\xi_1(z) + \frac{c^2}{2} \times \sum_{\mathbf{r}\neq 0} W_{\mathbf{r}}[\xi_2(z,\mathbf{r}) - 2\xi_1(z)] + \ldots\right\}. \quad (36)$$

Near the end-frequency z_g^0 this formula is incorrect. Indeed, the endpoints of the continuous spectrum of the perturbed and unperturbed crystals will not be identical. In Sec. 4 we determine the perturbation of the end-points, and the spectral density throughout the whole range of perturbed frequencies.

3. EXPANSION IN POWERS OF ϵ

When the mass-differences are small ($\epsilon \ll 1$), the foregoing results simplify greatly. Retaining terms up to the order ϵ^2, we find

$$\xi_1(z) = \varepsilon z \nu_0(z)\left[1 - \varepsilon z \int' \frac{\nu_0(\mu)}{\mu - z}\, d\mu\right], \quad (37)$$

$$\xi_2(z,\mathbf{r}) - 2\xi_1(z) = -2\varepsilon^2 z^2 \operatorname{Re} J_{-\mathbf{r}}(z) \int' \frac{J_{\mathbf{r}}(\mu)}{\mu - z}\, d\mu. \quad (38)$$

Substituting Eqs. (37) and (38) into the expressions (33) for the free energy and (36) for the vibration spectrum density, we obtain to the same accuracy, assuming no correlations exist,

$$F - F_0 = N\left\{\varepsilon c \int z\varphi'(z)\nu_0(z)\,dz + \varepsilon^2\left[c^2 \int z\varphi'(z)\nu_0(z)\,dz + \frac{c^2}{2}\int z^2\varphi''(z)\nu_0(z)\,dz + \frac{c(1-c)}{2} \times \int \frac{z^2\varphi'(z) - \mu^2\varphi'(\mu)}{z-\mu}\nu_0(z)\nu_0(\mu)\,dz\,d\mu\right] + \ldots\right\}; \quad (39)$$

$$\nu(z) - \nu_0(z) = -\frac{d}{dz}\left\{\varepsilon c z \nu_0(z) - \varepsilon^2\left[c(1-c)z^2\nu_0(z)\int' \frac{\nu_0(\mu)}{\mu - z}\, d\mu + \frac{c^2}{2} z^2 \nu_0'(z)\right] + \ldots\right\}. \quad (40)$$

In the derivation we have used the identity

$$\int_{\omega(\mathbf{k})=z} \frac{d\Omega}{|\nabla\omega^2|} \int d\mathbf{k}'\, f(\mathbf{k},\mathbf{k}') = \int d\mathbf{k}\, d\mathbf{k}'\, \delta(\omega^2(\mathbf{k}) - z)\, f(\mathbf{k},\mathbf{k}').$$

Equations (39) and (40), considered as expansions in powers of ϵ, are valid for any value of the concentration c. This is because the higher terms in the expansion in powers of c all carry higher powers of ϵ.

Equation (39) could have been derived directly from Equations (2) – (6) by making an expansion in powers of ϵ. If we apply the analogs of Equations (17), (20) and (21)) to the entire perturbation operator $\hat{\Lambda}$ (Equation 6) and expand $\xi(z)$ in powers of ϵ, we find*

$$F - F_0 = \sum_{\mathbf{r}} \bar{\varepsilon}_{\mathbf{r}} \int z\varphi'(z)\nu_0(z)\,dz + \sum_{\mathbf{r},\mathbf{r}'} \overline{\varepsilon_{\mathbf{r}}\varepsilon_{\mathbf{r}'}} \int' \frac{z^2\varphi'(z)}{z-\mu} J_{\mathbf{r}-\mathbf{r}'}(z) J_{\mathbf{r}'-\mathbf{r}}(\mu)\,dz\,d\mu. \quad (41)$$

Here $\varepsilon_{\mathbf{r}} = (m - m_{\mathbf{r}})/m_{\mathbf{r}}$ is treated as a random variable, and the bar means a statistical average. The $\epsilon_{\mathbf{r}}$ appear in Equation (41) in place of the $\epsilon'_{\mathbf{r}}$ which appear in Eq (6), because we changed from integrals of the form $\int' \frac{\mu J_{\mathbf{r}}(\mu)}{\mu - z}\, d\mu$ to integrals of the form $\int' \frac{J_{\mathbf{r}}(\mu)}{\mu - z}\, d\mu$. The same thing happened in passing from Eq. (30) to (26). If the original unperturbed mass was m_1, then

$$\bar{\varepsilon}_{\mathbf{r}} = c(m_1 - m_2)/m_1 = c\varepsilon,$$

$$\overline{\varepsilon_{\mathbf{r}}^2} = c\varepsilon^2,\ \overline{\varepsilon_{\mathbf{r}'}\varepsilon_{\mathbf{r}'+\mathbf{r}}} = c^2 W_{\mathbf{r}}\varepsilon^2,$$

and Eqs. (39) and (40) follow.

If ϵ is small, it is convenient to choose for the unperturbed mass the mean mass $m = m_1(1-\epsilon)$. In this case Equation (41) should be used with

$$\bar{\varepsilon}_{\mathbf{r}} = 0,\ \overline{\varepsilon_{\mathbf{r}}^2} = c(1-c)\varepsilon^2,\ \overline{\varepsilon_{\mathbf{r}'}\varepsilon_{\mathbf{r}'+\mathbf{r}}} = 0$$

if there are no correlations. The correction to the free energy is then quadratic in ϵ. The unperturbed spectrum density in this case will be $\nu^0(z) = \nu_0[z/(1-\varepsilon c)]$.

*To justify the use of these equations, we should imagine that we have an infinite crystal composed of identical atoms of mass m, with a finite perturbed region containing N lattice -sites at which the perturbation operator $\hat{\Lambda}$ is different from zero. Afterwards the value of N can be made as large as we please.

Finally, we shall state without proof the formula for the correction to the free energy for $\epsilon \ll 1$, in a real crystal where the vibrations have several modes of polarization. The unperturbed mass is again the mean mass $\bar{m}$.

$$F - F_0 = \sum_{\mathbf{r},\mathbf{r}'} \overline{\varepsilon_{\mathbf{r}}\varepsilon_{\mathbf{r}'}} \int' \frac{z^2\varphi'(z)}{z-\mu} \times \sum_{\beta,\beta'} J^{\beta\beta'}_{\mathbf{r}-\mathbf{r}'}(z)\, J^{\beta\beta'}_{\mathbf{r}'-\mathbf{r}}(\mu)\, dz\, d\mu, \tag{42}$$

$$J^{\beta'\beta}_{\mathbf{r}}(z) = \sum_j \int_{\omega_j^2(\mathbf{k})=z} \frac{d\Omega}{|\nabla\omega_j^2|} u^j_\beta(\mathbf{k})\, u^{j*}_{\beta'}(\mathbf{k}')\, e^{2\pi i \mathbf{k}\mathbf{r}}. \tag{43}$$

Here the index j denotes a particular mode of polarization of the unperturbed crystal vibration, and u^j (u^j_1, u^j_2, u^j_3) is the corresponding normalized polarization vector. The eigenfunctions of the unperturbed system are now of the form $\mathbf{u}^j(\mathbf{k})\, e^{2\pi i \mathbf{k}\mathbf{r}})$. . It is more convenient to write Equation (42) as an integral over k-space, the integration volume being one cell of the reciprocal lattice.

$$F - F_0 = \frac{1}{2} \sum_{\mathbf{r},\mathbf{r}'} \overline{\varepsilon_{\mathbf{r}}\varepsilon_{\mathbf{r}'}} \times \int d\mathbf{k}\, d\mathbf{k}'\, e^{2\pi i(\mathbf{k}-\mathbf{k}')(\mathbf{r}-\mathbf{r}')} \Phi(\mathbf{k},\mathbf{k}'), \tag{44}$$

$$\Phi(\mathbf{k},\mathbf{k}') = \sum_{jj'} |\mathbf{u}^j(\mathbf{k}), \mathbf{u}^{j'}(\mathbf{k}')|^2 \times \frac{\omega_j^4(\mathbf{k})\varphi'(\omega_j^2(\mathbf{k})) - \omega_{j'}^4(\mathbf{k}')\varphi'(\omega_{j'}^2(\mathbf{k}'))}{\omega_j^2(\mathbf{k}) - \omega_{j'}^2(\mathbf{k}')}. \tag{45}$$

If there is no correlation, then

$$F - F_0 = \frac{1}{2} Nc(1-c)\varepsilon^2 \int d\mathbf{k}\, d\mathbf{k}'\, \Phi(\mathbf{k},\mathbf{k}'). \tag{46}$$

4. STRUCTURE OF THE SPECTRUM

Equations (36) and (40), obtained formally from the difference of traces, are incorrect near the end-points z^0_g of the unperturbed spectrum. This is connected with the fact that the range of eigenvalues of the perturbed operator $\hat{L} + \hat{\Lambda}$ does not coincide with the range $(0, z^0_g)$ of the continuous spectrum of the unperturbed operator $\hat{L}$ (i.e., the range of frequencies of the monoisotopic crystal). The difficulty arises mathematically from the singularities of the derivatives $\nu_0^{(n)}(z)$ at the point z^0_g. In the neighborhood of z^0_g, the spectrum usually has the shape $\nu_0(z) \sim (z^0_g - z)^{1/2}$, and the expansion (40) containing the $\nu_0^{(n)}(z)$ is meaningless. It is not difficult to express $\nu(z)$ in a form free from divergences, and to determine the displacement of the end-point. For this purpose we consider first the case $\epsilon \ll 1$. Then Eq. (39) may be written in the form

$$F = N \int \nu_0(z) \Big\{ \varphi(z) + \Big[\varepsilon c z + \varepsilon^2 c^2 z + \varepsilon^2 c(1-c) z^2 \int' \frac{\nu_0(\mu)}{z-\mu} d\mu \Big] \varphi'(z) + \frac{\varepsilon^2 z^2 c^2}{2} \varphi''(z) + \ldots \Big\} dz. \tag{47}$$

The point z^0_g is not a singularity of the function $\phi(z)$, and the coefficients of $\phi'(z), \phi''(z), \ldots$ in the curly bracket are finite at z^0_g. Therefore we may regard the whole expression in the curly bracket as an expansion in powers of ϵ of the quantity

$$\varphi(z + \varepsilon c z + \varepsilon^2 \eta(z) + \ldots), \tag{48}$$

$$\eta(z) = c^2 z + c(1-c) z^2 \int' \frac{\nu_0(\mu)}{z-\mu} d\mu. \tag{49}$$

Then a simple change of variable in the integral gives

$$F = \int_0^{z^0_g} \nu_0(t)\, \varphi(t + \varepsilon c t + \varepsilon^2 \eta(t))\, dt = \int_0^{z_g} \nu_0(t(z)) \frac{dt}{dz} \varphi(z)\, dz, \tag{50}$$

$$z = t + \varepsilon c t + \varepsilon^2 \eta(t), \tag{51}$$

$$z_g = z^0_g + \varepsilon c z^0_g + \varepsilon^2 \eta(z^0_g).$$

Hence

$$\nu(z) = \nu_0(t(z))\, (dt/dz). \tag{52}$$

A similar method applies to the case when we make an expansion in powers of the concentration of one isotope. The result, correct to terms of order c, is then

$$\nu(z) = \nu_0\left(z - c\frac{\xi_1(z)}{\nu_0(z)}\right)\left[1 + c\left(\frac{\xi_1(z)}{\nu_0(z)}\right)'\right]^{-1}, \quad (53)$$

$$z_g = z_g^0 + c\xi_1(z_g^0)/\nu_0(z_g^0). \quad (54)$$

Up to now we assumed that there were no discrete eigenvalues of the perturbed operator. If such eigenvalues exist, then terms of the form (24) must be added to the expression (33) for the free energy. Let $z_j^{(n)}$ be the j'th discrete eigenvalue for a crystal with n impurity atoms. The value of $z_j^{(n)}$ is determined by Equation (25). Then the relevant difference between free energies becomes

$$F - F_0 = N\left\{\int\varphi'(z)\left[c\xi_1(z) + \frac{c^2}{2}\right.\right. \quad (55)$$

$$\times\sum_{\mathbf{r}\neq 0} W_{\mathbf{r}}(\xi_2(z,\mathbf{r}) - 2\xi_1(z)) + \ldots\Big]dz$$

$$+ c\left[\varphi(z_1^{(1)}) - \varphi(z_g^0)\right] + \frac{c^2}{2}$$

$$\left.\times\sum_{\mathbf{r}\neq 0} W_{\mathbf{r}}\left[\varphi(z_1^{(2)}(\mathbf{r})) + \varphi(z_2^{(2)}(r)) - 2\varphi(z_1^{(1)})\right] + \ldots\right\}.$$

Since $z_{1,2}^{(2)} \to z_1^{(1)}$ as $r \to \infty$, the terms in square brackets decrease rapidly, and the sum over r converges.

From equation (21), or from a consideration of the physical meaning of the eigenvalues, the value $z_1^{(1)}$ is the limit of a sequence of values $z^{(2)}$ which appear in the terms of order c^2. Each value $z^{(2)}$ is in turn the limit of a sequence of values $z^{(3)}$, belonging to the crystal with three impurity atoms and appearing in terms of order c^3. And so on.

The correction to the free energy arising from the discrete eigenvalues van be expanded in powers of the concentration c, and this expansion formally corresponds to a spectrum with the peculiar structure which we have described. However, an expression for the expectation value of the spectral density cannot be immediately obtained. A formal expansion of the density function gives a meaningless and divergent sum of δ– functions. We are always interested physically, not in the spectral density itself, but only in expectation values of the form (7) constructed from the spectral density. For example, the vibrational energy of the crystal is given by Eq. 7 with

$$\varphi(z) = \hbar\sqrt{z}\left[(e^{\hbar\sqrt{z}/\theta} - 1)^{-1} + \frac{1}{2}\right],$$

Thus the expansion in powers of the concentration provides in principle the solution of our problem.

---

[1] I. M. Lifshitz, J. Exptl. Theoret. Phys. (U.S.S.R.) 12, 117 (1942).

[2] F. J. Dyson, Phys. Rev. 92, 1331 (1953).

[3] I. M. Lifshitz, J. Exptl. Theoret. Phys. (U.S.S.R.) 17, 1017 (1947).

[4] I. M. Lifshitz, J. Exptl Theoret. Phys. (U.S.S.R.) 17, 1076 (1947).

[5] I. M. Lifshitz, J. Exptl. Theoret. Phys. (U.S.S.R.) 18, 233 (1948).

[6] I. M. Lifshitz, Usp. Mat. Nauk 7, 171 (1952).

[7] M. G. Krein, Mat. Sbornik 33 (75), 597 (1953).

Translated by F. J. Dyson
187

Electron Spectra of Pu^{239}, Pu^{240} and Pu^{241}

K. N. SHLIAGIN

(Submitted to JETP editor, December 26, 1955)
J. Exptl. Theoret. Phys. (U.S.S.R.) 30, 817-823 (May, 1956)

Two plutonium samples, containing different amounts of Pu^{239}, Pu^{240}, and Pu^{241}, have been analyzed on a 180° magnetic β-spectrometer. Using thin celluloid films and radioactive sources, spectra were taken in an energy range beginning at ≈ 1 kev.

From the conversion lines it was possible to determine the following energies for γ-transitions in U^{235} and U^{236}: for U^{235} – 3 (?), 12.5, 38.3, 50.8, 117 (?) kev and for U^{236} – 44.6 kev.

The Pu^{241} β-spectrum has the allowed shape with end point $E_0 = 20.8$ kev.

INTRODUCTION

IMPORTANT data about the energy levels of radioactive nuclei can be obtained both from their electron spectra and their α and γ spectra. Thus, by observing the spectra of conversion electrons from α-active isotopes of plutonium, one can obtain information about γ-transitions in the uranium isotopes. However, up to the present time, no investigations of the electron spectra from Pu^{239}, Pu^{240}, or Pu^{241} have been published.

We summarize briefly the published work on the decay of Pu^{239}, Pu^{240}, and Pu^{241}. The fact that Pu^{239} is α-active was first apparent in the years 1944–1946. The results of Ghiorso, Sullivan et al,[1] and Rosenblum, Valadares and Goldschmidt [2] indicate that the α-spectrum is complicated. According to their results, U^{235}, the daughter nucleus of Pu^{239}, should emit γ-rays of energies about 0.05, 0.2 (weak), 0.3 (weak) and 0.42 (weak) mev. According to Skaggs et al[3], the half life of Pu^{239} is about 24,400 years.

The only information available about Pu^{240} was that it was α-active, with a half life of about 6000 years.[4]

Seaborg, James and Morgan[5] showed tha Pu^{241} is mostly β-active (the α-activity amounting to only 0.002% of the total) with a half life of about 10 years. The electron energy is 10 to 20 kev.

It was with the above scarcity of information about the radiations from these isotopes in mind, that the present work was undertaken.* The results of several other investigations, carried out concurrently with the one described here, and also in the last year, agree with ours.

Albouy and Teillac[6], and Dunlavey and Seaborg[7] used electron sensitive emulsions to detect the conversion electrons, and found transitions in U^{235} (obtained by the α-decay of Pu^{239}) at energies about 35, 50, 115 and 200 kev. Using a proportional counter, West and Dawson[8] found α-rays of energies 38.5, 51.8, 101 (?) and 115 (very weak) kev for U^{235} and another at 45.1 kev belonging, apparently, to U^{236} (from the α-decay of Pu^{240}). The α-spectra of Pu^{239} and Pu^{240} have been examined with a magnetic α-spectrometer by Asaro and Perlman[9] and also by Gol'din, Tretiakov and Novikov.[10]. Their results confirm the fact that these spectra are very complicated, and point to the possibility that U^{235} might have γ-rays at about 13, 38, and 51 kev, while U^{236} might have a γ-ray at about 45 kev.

The only work besides ours, on the electron spectra of Pu^{239}, Pu^{240}, and Pu^{241} was carried out by Freedman, Wagner and Engelkemeir,[11] on a magnetic lens β-spectrometer. These authors also investigated the γ-rays, using a proportional counter and a scintillation spectrometer. γ-transitions were found at 39, 53, 100 and 120 kev for U^{235}, 46.9 kev for U^{236}, and 100 and 145 kev for U^{237} (from the decay of Pu^{241}). The β-spectrum of Pu^{241} taken by these authors is strongly distorted. According to their data, the upper limit of the β-spectrum is at 20.5 kev. The electron spectrum is not shown in their paper.

There are great experimental difficulties in the study of the soft β-radiations from the decay of plutonium, which might explain why so little work has been done on them.

1. EXPERIMENTAL TECHNIQUE

a) β-SPECTROMETER

The electron spectra reported in this paper were taken on a conventional, magnetic β-spectrometer with 180° focussing. The middle electron orbit had a radius of curvature of 15 cm. The spectrometer resolution, as measured by the relative half width of the Hg^{198} conversion line (E_γ=411.2 kev Au^{198}), was about 2% in one experiment and about 1% in the other. The same conversion line was used to calibrate the spectrometer. The relative solid angle was about 0.06% of 4π. A mercury diffusion pump, with a liquid air trap, gave a vacuum of about

*The work was done in 1951.

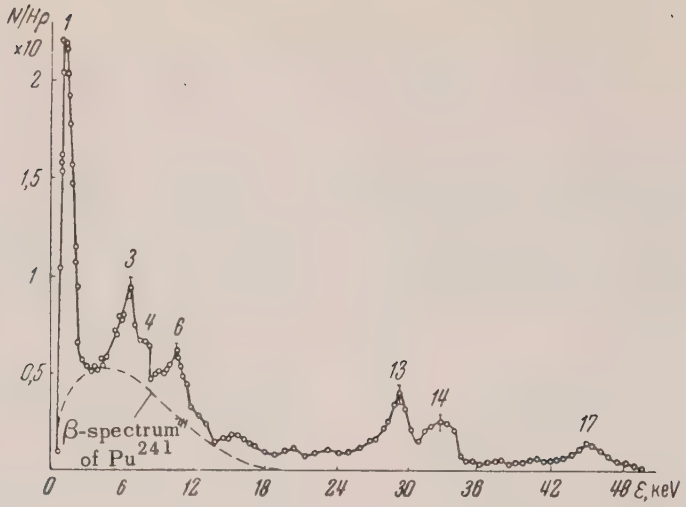

FIG. 1. Electron spectrum of sample No. 1 (source on film)

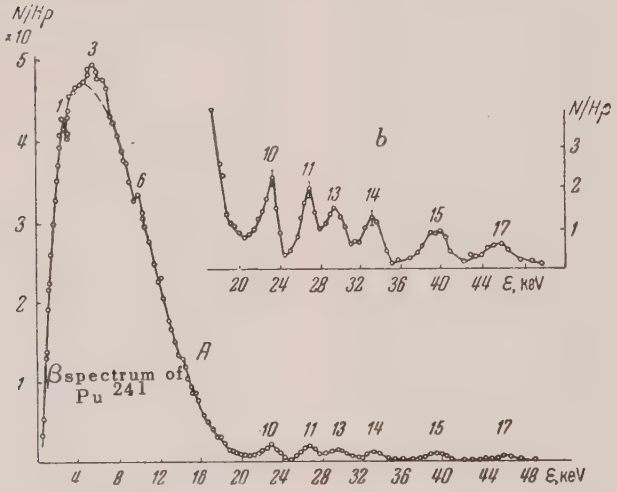

FIG. 2. Electron spectrum of sample No. 2 (source on film)

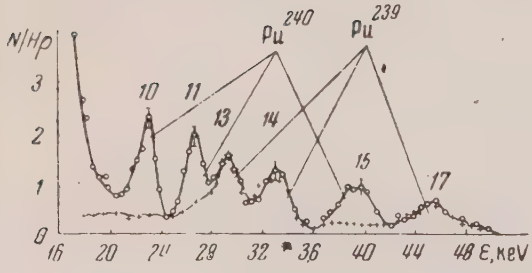

FIG. 3. Superposition of spectra from samples No. 1 and 2

10^{-5} mm Hg in the spectrometer. A constant current electromagnet, made of "Armco" soft iron, generated the magnetic field. The electromagnet current was supplied by high capacity storage batteries ($\sim$3000 amp-hr). The field was measured to 1% by a search coil and ballistic galvanometer.

A Geiger-Muller counter, with a slit to admit electrons, was used as a detector. The celluloid window was $5\,\mu\ g/cm^2$ thick, and was supported by a wolfram wire net (wire thickness 0.04 mm, separation 0.3 mm) giving about 80% transmission. The counter was filled with a gaseous mixture of argon (90%) and ethyl alcohol (10%) at a pressure of 20 to 40 mm. Hg. The counter pulses were recorded by a conventional electronic circuit.

b) PREPARATION OF SOURCES

Plutonium is usually prepared by irradiating uranium with slow neutrons. Pu^{239} is formed by the reaction

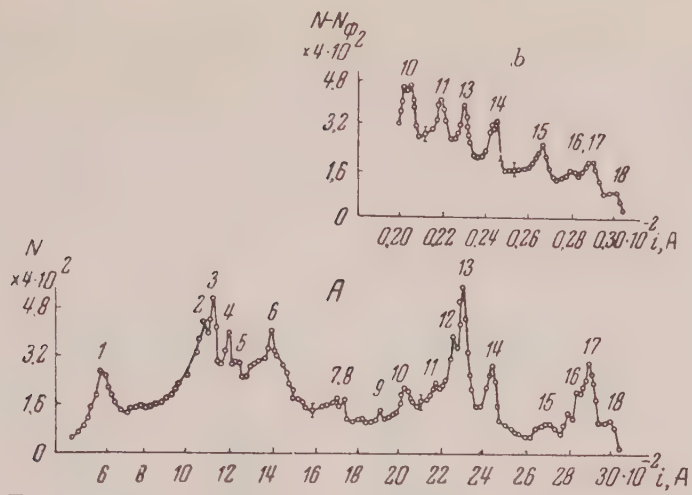

FIG. 4. Electron spectra: A – sample No. 1, B – sample No. 2; sources on aluminum foil. Spectrometer resolution ~ 1%.

$$U^{238}(n, \gamma)\, U^{239} \xrightarrow[23.5\ \text{min}]{\beta} Np^{239}$$

$$\xrightarrow[2.3\ \text{days}]{\beta} Pu^{239}\ (T \sim 24\,400\ \text{yr}).$$

Further neutron irradiation of Pu^{239} leads to the formation of Pu^{240} and Pu^{241}:

$$Pu^{239}(n, \gamma)\, Pu^{240}\ (T \sim 6000\ \text{yr});$$

$$Pu^{240}(n, \gamma)\, Pu^{241}\ (T \sim 13\ \text{yr}).$$

Two plutonium samples, No. 1 and No. 2, were used in the present experiment. They differed in the relative amounts of Pu^{239}, Pu^{240}, and Pu^{241} contained, sample No. 2 being richer in the Pu^{240} and Pu^{241} isotopes than sample No. 1. The plutonium samples were carefully purefied chemically to rid them of products from the fission of uranium and plutonium. The radioactive source (in the form of a strip 1 to 2×30 mm^2) was precipitated out from an aqueous solution of plutonium nitrate on a celluloid film 10 $\mu g/$ cm^2 thick. To avoid charging, a layer of aluminum (about 1$\mu g/$cm^2 thick) was evaporated in vacuum on the radioactive source. The surface density of the sources was measured by their α-activity and was ~ 3 to 10 $\mu g/$cm^2. Each run was long because the sources were weak.

2. RESULTS

Figures 1 and 2 show the electron spectra from samples No. 1 (surface density ~6$g/$ cm^2) and No. 2 (surface density ~ 3$g/$ cm^2) taken on the spectrometer with 2% resolution. Part of the spectrum from No. 2, starting from 18 kev, is shown in Fig. 2 on an enlarged scale (curve B). In the energy interval from 1 to 50 kev, the figures show a β-spectrum and several conversion lines.*

In order to interpret lines 10, 11, 13, 14, 15, 17, the electron spectra were superposed in the energy region from 18 to 50 kev (Fig. 3).

From a knowledge of the concentrations of the various plutonium isotopes in the samples used, together with the intensities and positions of the lines in the β-spectra, it was possible to establish the following:

a) lines No. 1, 3, 4, 6, 13, 14, 17 are conversion lines from U^{235}.

b) lines 10, 11, 15 are conversion lines of U^{236}.

c) the β-spectrum shown in Figs. 1 and 2 is that of Pu^{241}.

It was difficult to determine the γ-transition energies accurately from the conversion lines in Figs. 1 and 2, because these lines were poorly resolved. Because of this, we took the spectra of the same samples (Nos. 1 and 2) again, this time with better resolution (~ 1%). Figure 4 shows these spectra (curve A for sample No. 1, curve B for sample No. 2), using sources with surface densities ~ 10 $g/$ cm.^{2} An aluminum foil was used as source backing.

In addition to the earlier, intense lines, several new, weak lines appear in the spectra of Fig. 4. The results of measurements on the conversion lines of the Pu^{239} and Pu^{240} isotopes are shown in the table. In the spectra of all the figures,

*The electron spectrum of Pu^{240} does not appear in Fig. 1 because little of this isotope was present.

TABLE

Interpretation of lines in the electron spectra of plutonium samples Nos. 1 and 2.

Line number from Fig. 4		Electron kinetic energy (in kev)	Conversion Shell	Transition energy in kev		Plutonium isotope	Notes
Line	Curve						
1	*A* Not Shown	~2 ~95(?)	*K* *L*	117 117	117(?)	Pu^{239}	Very weak radiation
1	*A*	~2	*N,O*	~3(?)		Pu^{239}	
2	*A*	6.7	M_I	12.3			
3	*A*	7,2	M_{II}	12.4			
4	*A*	8.3	M_{III}	12.6	12.5	Pu^{239}	
5	*A*	8.8	$M_{IV,V}$	12.4			
6	*A*	11.1	N_I	12.5			
7	*A*	16.7	L_I	38.5			
8	*A*	17.4	L_{II}	33.3	38.3	Pu^{239}	Very weak radiation
9	*A*	20.9	L_{III}	38.1			
10	*A*	23	L_I	44.8			
10	*B*	23.8	L_{II}	44.7			
11	*B*	27.3	L_{III}	44.5		Pu^{240}	
11	*A*	27.1	L_{III}	44.3	44.6		
15	*B*	40.4	$M_{I\div V}$	~45			
15	*A*	40.4	$M_{I\div V}$	~45			
16	*B*	44.2	*N,O*	~45			
12	*A*	28.8	L_I	50.6			
13	*A*	29,8	L_{II}	50.7			
13	*B*	29.9	L_{III}	50.8			
14	*A*	33.6	L_{III}	50.8			
14	*B*	33.9	L_{III}	51	50.8	Pu^{239}	
17	*B*	46.5	$M_{I\div V}$	~51			
17	*A*	49.5	$M_{I\div V}$	~51			
18	*A*	50.7	*O*	~51			
18	*A*	50.9	*O*	~51			

1–4, identical conversion lines are labeled by the same indices,

In the energy region 0.05 to 2 mev, none of the electron lines from Pu^{239}, Pu^{240} or Pu^{241}, nor any of the β-spectra, were more than a factor 2 above the background.

The most intense line, 1 (see Fig. 1 at electron energy about 2 kev), is difficult to interpret because it is somewhat different from the nearest conversion lines. If we take line 1 to be a K-conversion line, then the corresponding γ-ray energy, as calculated from the energy of the conversion electrons, is about 117 kev. The presence of a weak L-conversion line (electron energy ~ 95 kev, intensity

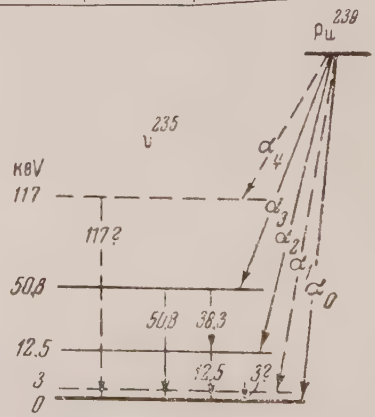

FIG. 5. Decay scheme of Pu^{239}

$\sim$ 1.5 times the background) lends some support to this view. Approximate calculations indicate that the intensity of the K-conversion line should be considerably less than the observed intensity of line 1. Hence, we cannot take line 1 as due only to K-conversion electrons. Similarly, we are not justified in considering line 1 to be due only to Auger-electrons. Similar Auger-lines should appear at energies > 3 kev, but are not observed on the experimental spectra.

Hence, it is difficult to explain the large intensity* of line 1, except as due to K-conversion and Auger-electrons combined.

We cannot exclude the possibility that line 1 is due to conversion electrons from the *N* and *O* shells. In this case, the γ-ray energy would have to be about 3 kev. If such a ray is actually present in the γ-decay of Pu^{239}, we would have to assume that one of the excited levels in U^{235} lies $\sim$ 3 kev above the ground state. Another effect that might contribute significantly is the ionization of plutonium when it decays by α-emission. These conjectures need confirmation.

The data in the table show that the observed conversion lines are associated with the following γ-transitions in U^{235} (from the α-decay of Pu^{239}): 3 (?), 12.5, 38.3, 50.8, 117 (?) kev and in U^{236} (from the α-decay of Pu^{240}) – 44.6 kev. The 12.5 kev γ-ray in U^{235}, which certainly exists, is reported here for the first time. The 3 and 117 kev transitions need to be checked. Figure 5 shows the proposed α-decay scheme of Pu^{239}. A Kurie plot of the Pu^{241} β-spectrum shows that this spectrum has the allowed shape.** The experimental points in this graph lie close to a straight line in the energy interval 3 to 19 kev. The upper limit of the β-spectrum is at 20.8 $\pm$ 0.2 kev.

In conclusion it is my pleasant duty to express my gratitutde to G. N. Iakovlev and G. A. Chistiakova for preparing the chemically pure plutonium samples.

*The observed line intensity is considerably lessened by electron absorption in the source itself and in the window of the Geiger-Muller counter.

**A more detailed discussion of the Pu^{241} β-decay will be given in another paper.[12]

Note added in proof: The level sequence 0, 50.8 and 117 kev can be described by the well known theoretical formula of Bohr and Mottelson[13] for the rotational energy levels of nuclei. Assuming that the ground state of U^{235} is the first rotational level, with spin 7/2 $\pm$,[14] then the spins of the first and second levels will be 9/2 $\pm$ and 11/2 $\pm$. In our case, the ratio $E_2 : E_1$ for these levels is 117: 50.8 = 2.3, which agrees with the value 2.22 given by the Bohr–Mottelson formula. Better agreement is obtained by taking the spin of the first rotational level to be 5/2 $\pm$.

[1] A. Ghiorso (1944), W. H. Sullivan, T. P. Kohman, and J. A. Swartout (1945). Reported by Seaborg and Perlman, Rev. Mod. Phys. 20, 585 (1948).

[2] Rosenblum, Valdares and Goldschmidt, Compt. rend. 230, 638 (1950).

[3] Skaggs, Laughlin, Hanson and Orlin, Phys. Rev. 73, 420 (1948).

[4] James, Florin, Hopkins and Ghiorso (1948). Results given in Rev. Mod. Phys. 20, 585 (1948).

[5] Seaborg, James and Morgan. Cited in Seaborg and Perlman, Rev. Mod. Phys. 20, 585 (1948).

[6] G. Albouy and Teillac, Compt. Rend. 232, 326 (1951).

[7] D. C. Dunlavey and G. T. Seaborg, Phys. Rev. 87, 165 (1952).

[8] D. West and J. K. Dawson, Proc. Phys. Soc. A64, 586 (1951). D. West, J. K. Dawson, and C. J. Mandleberg, Phil. Mag. 43, 875 (1952).

[9] F. Asaro and I. Perlman, Phys. Rev. 88, 828 (1952).

[10] L. L. Gol'din, E. F. Tret'iakov and G. I. Novikova, Paper given to the conference on peaceful uses of atomic energy, sponsored by the Academy of Sciences of the USSR and published by the Academy in 1955.

[11] Freedman, Wagner, and Engelkemeir, Phys. Rev. 88, 1155 (1952).

[12] K. N. Shliagin, Izv. Akad. Nauk SSSR, Ser. Fiz. To be published.

[13] A. Bohr and B. R. Mottelson, Phys. Rev. 90, 717 (1953); 89, 316 (1953).

[14] K. L. V. Sluis and J. R. McNally, Jr., J. Opt. Soc. Am. 45, 65 (1955).

Translated by A. Krotkov
173

Dielectric Constant and Loss Angle of Several Solid Dielectrics at a Wavelength of 3 cm, and Their Temperature and Frequency Dependence

G. I. SKANAVI AND G. A. LIPAEVA
P. N. Lebedev Physical Institute, Academy of Sciences, USSR

(Submitted to JETP editor August 13, 1955)
J. Exptl. Theoret. Phys. (U.S.S.R.) 30, 824-832 (May, 1956)

The results of measurements of ϵ and $\tan\delta$ at a wavelength of 3 cm are given for magnesium, zinc, calcium, strontium and bismuth titanates, barium tetratitanate and steatite. A cylindrical resonator was used. The frequency dependences of ϵ and $\tan\delta$ were determined for these materials over a wide range of frequencies, and the temperatures were determined at frequencies of 10^3, 10^6 and 10^{10} cps. The results are discussed from the point of view of present ideas concerning the dielectric constant.

1. STATEMENT OF THE PROBLEM

IT is known[1,2] that the dielectric constant of polycrystalline dielectrics of the ceramic type may have different values, lying in a wide range (from 6 to several thousand), depending on their composition and structure. High values of ϵ for nonpiezoelectric titanates of the perovskite and rutile structure depend on a favorable internal field[3]. On introducing weakly bound ions into such dielectrics, in a manner dependent on the structural defects, for example, a thermal ionic relaxation polarization is produced which strongly increases the dielectric constant (up to 1000)[3] and leads to a rather strong frequency and temperature dependence of ϵ and $\tan\delta$.

The indicated dependence agrees satisfactorily with the results of relaxation theory, provided the internal field is taken into account correctly[4]. In the further development of the theory of polarization of solid dielectrics, the investigation of their dielectric properties in ultrahigh frequency region and in the long wavelength part of the infrared region of the spectrum will be of very great significance. Actually, in dielectrics with purely elastic polarization the dielectric constant should not depend on the frequency until the frequency of the ions in the crystal lattice ($10^{12} - 10^{13}$ sec^{-1}). In dielectrics with relaxation polarization a decrease in ϵ with frequency should take place at lower frequencies and can arise at room temperature in the centimeter wavelength region. Suggestions as to the existence of a suitable dispersion for piezoelectrics, for example, are to be found in the literature[5].

In the infrared region of the spectrum all crystals, as is well known, display anomalous dispersion and absorption. The lower the frequency corresponding to maximum absorption, the greater must be the elastic ionic polarizability. Generally speaking, a high value of the dielectric constant can depend not only on a suitable internal field and, in the case of dielectrics with relaxation polarization, increased thermal ionic (or dipole) polarizability, but also on a high value of elastic polarizability.

Dielectric losses in solid dielectrics have been investigated by many authors. In the most recent works[6,7], it has been shown that more or less clearly manisfested dielectric losses are superimposed on the loss of conductivity even in simple ionic crystals. In these dielectrics, in which relaxation polarization leads to a high value of the dielectric constant, dielectric losses are ordinarily comparatively large, and the loss angle has temperature and frequency maxima in the region of electrotechnical and radio frequencies. Dielectrics with elastic polarization ordinarily have small losses. In a rather wide frequency interval the loss angle of these dielectrics does not depend on the frequency and begins to increase with temperature only in the region of comparatively high temperatures. The mechanism of these small dielectric losses is still insufficiently clear. On going to ultrahigh frequencies, the loss angle of solid dielectrics with elastic polarization may increase if the region of resonance absorption corresponds to the long wavelength part of the infrared region of the spectrum.

The investigation of dielectrics in the centimeter wavelength region also has a practical value in connection with their use in high frequency techniques.

As a rule, the works mentioned involve great procedural difficulties, the surmounting of which is possible only by use of good ultrahigh frequency and special optical apparatus, and development and utilization of new methods are needed.

In the present work, ultrahigh procedures published in the literature[5] are used with certain small

but essential improvements, allowing the measurement of the dielectric constant of solid dielectrics over a rather wide range of values (from 1.5 to 200) at a wavelength of 3.1 cm.

For the measurements at audio and radio frequencies an audio bridge of type 716-V and Q meters of types KV-1 and UK-1 were used.

2. METHODS OF MEASUREMENT AT 3.1 CM WAVELENGTH

The basic part of the ultrahigh frequency apparatus is the circular cylindrical resonator, operating in the H_{01} mode. This mode is excited through two openings in the end wall of the cavity joined to a thin wall of a rectangular waveguide in which the wave is propagated[8]. By a careful choice of the dimensions, form and position of the output loop in the coupler, we were able, first, to obtain a signal in the basic mode H_{01} exceeding by 200-400 times the signals in other modes which were unavoidably present in the resonator, and, second, to obtain a loaded resonator Q approaching that of the resonator itself, that is, to make the energy losses in the coupler negligibly small in comparison with the energy losses in the walls of the cavity. The resonator was constructed of brass and was silvered. Its diameter was 45 mm. The Q of the empty resonator for the H_{01} mode is 20,000. The samples being measured are prepared in the form of disks of diameter 1 mm less than that of the cylinder, but the optical thickness depends on the magnitudes of ϵ and $\tan\delta$. The thickness error in the preparation of the disks is not more than 0.01 mm. The disks are set tightly against the electrically unconnected movable plunger serving as the second end wall of the cavity. For good contact of the samples with the plunger, the resonator is positioned vertically. The samples are placed in the resonator through a cut in the side wall located below the working positions of the plunger. The plunger is moved with the aid of a micrometric screw with steps of 1 mm and a distance of travel of 100 mm. The position of the plunger is read on a scale, shown in Fig. 1, with an accuracy of 0.01 mm; this accuracy is assured by the quality of the micrometric screw.

The changes in the resonance length and Q of the cavity which occur when a dielectric is placed in it allow the calculation of ϵ and $\tan\delta$ for the sample under investigation. The scheme of the calculation is given in detail in reference 5 and briefly in reference 8. In the calculation it is assumed that the propagation constant of the electromagnetic wave in the dielectric under investigation $\gamma = \alpha + j\beta \approx j\beta$, that is, that $\alpha \ll \beta$. A block

FIG. 1. The cavity resonator.

diagram of the apparatus is shown in Fig. 2; it contains five assemblies: 1, a generator of type 43-I; 2, the measuring resonator; 3, a wavemeter; 4, an amplifier-mixer; 5, a cathode ray oscillograph of type EO-7. In addition, in order to isolate the resonator from the wavemeter, there is introduced into the rectangular waveguide 6 an attenuator 7. The modulation is fed into the reflex klystron oscillator through a condenser and potentiometer from the horizontal sweep of the oscillograph.

The precision wavemeter is in the form of a cylindrical cavity resonator, excited, like the measuring resonator, through two openings in an end wall and operating in the H_{01} mode. The signal for the measurements is taken through an output coupler in the side wall, exciting the H_{01} mode in a rectangular waveguide. The signal taken out through the coupler into the rectangular waveguide is detected and fed to the input of the amplifier-mixer. The peak value of the intensity of the signals from the resonator and wavemeter applied to the input of the amplifier is about 0.2 mv. The amplifier-mixer contains three amplifiers in cascade: two single 6Zh6 amplifiers, into one of which is fed the signal from the resonator and into the other of which is fed the signal from the wavemeter, and a single 6N9 mixer. The amplification factor is about 2000. The pass band includes all of 50-20,000 cps and assures the preservation of the form of the signals from the resonator and the wavemeter. The horizontal sweep of the oscillograph (with a frequency of 50 cps) appears as a frequency

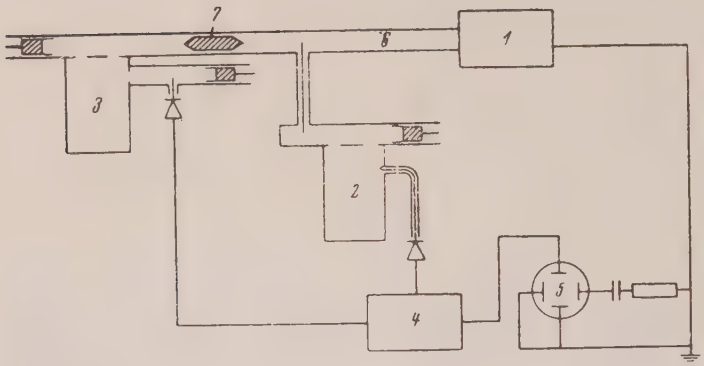

FIG. 2. Block diagram of the apparatus: *1*, generator; *2*, resonator; *3*, wavemeter; *4*, amplifier; *5*, oscillograph; *6*, waveguide; *7*, attenuator.

in the resultant display; hence with a quadratic detector the width of the resonance curve obtained on the oscillograph screen gives the width of the resonance curve of the resonator, which may be measured with the aid of the wavemeter. The wavemeter allows increasing the accuracy of the determination of the resonance-length setting of the resonator when a sample is put into it even with poor generator stability, since the wavemeter fixes the working frequency with great accuracy.

In taking the temperature characteristics of the samples, experimentally determined corrections are applied to the Q of the resonator and to the other measurements which are changed by heating. The resonator is heated by means of a heating spiral surrounding its side walls. The temperature of the sample is determined by a thermocouple placed in a hole in the plunger next to the lower surface of the sample. An estimate of the relative error in the determination of ϵ and tan δ at room temperature gives ±1 to 1.5% and ±15%, respectively, for all the values of ϵ and tan δ mentioned below. The average relative errors in ϵ and tan δ found from the experimental spread in the values of ϵ and tan δ for various samples did not, as a rule, exceed these values. At elevated temperatures the error in the determination of tan δ was increased threefold.

3. RESULTS OF THE MEASUREMENTS

The values of the dielectric constant and loss angle at a wavelength of 3.1 cm are given for a number of substances in Tables 1-8. From these tables it is clear that for a correct choice of sample thickness, results are obtained which are reproducible and lie close together for different samples.

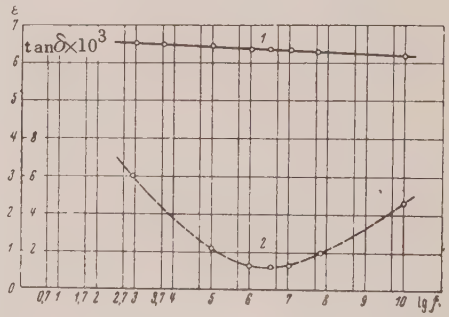

FIG. 3. Frequency dependence of ϵ and tan δ for steatite. Curve 1 gives ϵ and curve 2 gives tan δ.

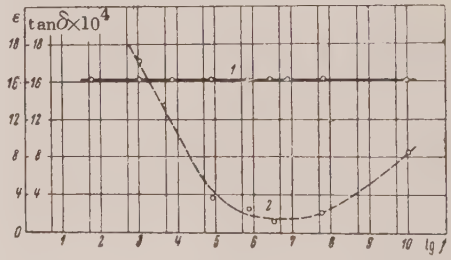

FIG. 4. Frequency dependence of ϵ and tanδ for magnesium titanate to which a small amount of calcium titanate and flux has been added. Curve 1 gives ϵ and curve 2 gives tanδ.

Curves showing the dependence of ϵ and tanδ on frequency over a wide range of frequencies are given in Figs. 3-9. Practically complete absence of any frequency dependence of the dielectric constant is found for magnesium titanate, barium titanate, zinc titanate and fused strontium titanate (Figs. 4, 5, 6, 9). This fact fully confirms our

idea that only elastic polarization occurs in these materials (the question as to whether strontium titanate belongs to the piezoelectrics seems open to discussion).

In the case of the frequency dependence of steatite and calcium titanate, it is clear from Figs. 3 and 8 that with increasing frequency a rather weak, almost linear decrease in the dielectric constant takes place. This could not occur for purely elastic polarization. It is possible that in these materials weakly expressed relaxation processes occur. The dielectric constant of bismuth titanate decreases rather strongly with frequency in the region of low frequencies (Fig. 7). This can be explained only by the presence of relaxation processes with long relaxation times.

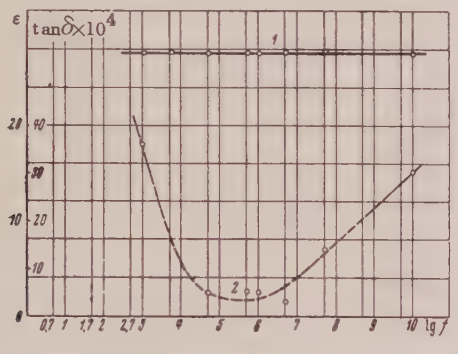

FIG. 5. Frequency dependence of ϵ and $\tan\delta$ for fused barium titanate. Curve 1 gives ϵ and curve 2 gives $\tan\delta$.

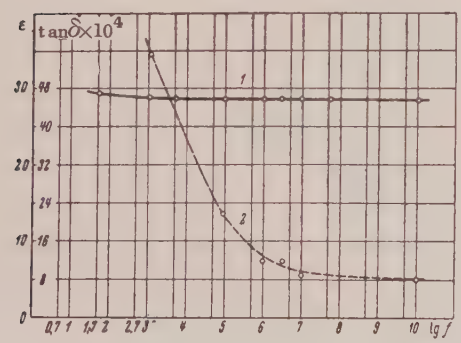

FIG. 6. Frequency dependence of ϵ and $\tan\delta$ for zinc titanate. Curve 1 gives ϵ and curve 2 gives $\tan\delta$.

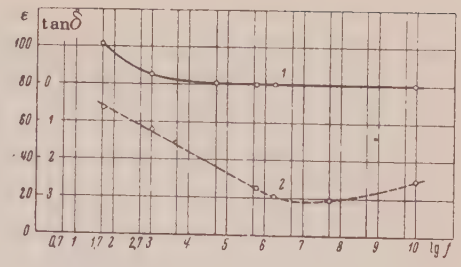

FIG. 7. Frequency dependence of ϵ and $\tan\delta$ for bismuth titanate. Curve 1 gives ϵ and curve 2 gives $\tan\delta$.

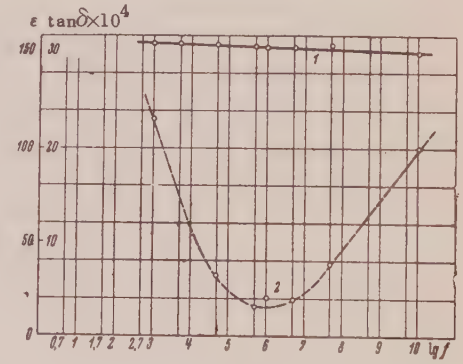

FIG. 8. Frequency dependence of ϵ and $\tan\delta$ for calcium titanate. Curve 1 gives ϵ and curve 2 gives $\tan\delta$.

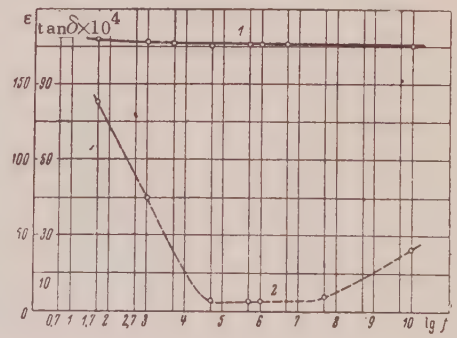

FIG. 9. Frequency dependence of ϵ and $\tan\delta$ for fused strontium titanate. Curve 1 gives ϵ and curve 2 gives $\tan\delta$.

The dielectric loss angle of all the dielectrics investigated, with the exception of zinc titanate, shows an unsymmetrical but definite minimum in the frequency region 10^5-10^8 cps. The increase in the loss angle at low frequencies is ordinarily connected with conductivity losses, for which the loss

TABLE 1

Material	Sample no.	Sample thickness in mm	ε	$\tan\delta$	Average ε	Average $\tan\delta$
Steatite	1	2.19	6.51	0.0023	6.50	0.0026
	2	2.11	6.51	0.0027		
	3	2.41	6.49	0.0025		
	4	2.40	6.51	0.0026		
	5	2.30	6.46	0.0028		
	6	2.50	6.51	0.0024		
	7	2.60	6.48	0.0032		

TABLE 2

Material	Sample no.	Sample thickness in mm	ε	$\tan\delta$	Average ε	Average $\tan\delta$
Magnesium titanate	1	1.79	16.1	0.00077	16.0	0.00086
	2	1.79	16.2	0.00094		
	3	1.78	16.0	0.00099		
	4	2.37	15.9	0.00082		
	5	1.80	15.8	0.00086		
	6	2.23	16.1	0.00079		
	7	2.23	16.0	0.00069		
	8	2.23	15.9	0.00077		

TABLE 3

Material	Sample no.	Sample thickness in mm	ε	$\tan\delta$	Average ε	Average $\tan\delta$
Barium tetra-titanate	1	1.88	28.1	0.0031	27.6	0.0030
	2	2.00	27.9	0.0028		
	3	2.00	27.7	0.0030		
	4	3.76	27.8	0.0028		
	5	1.73	27.7	0.0027		
	6	1.75	27.4	0.0031		
	7	1.29	27.5	0.0033		
	8	1.29	27.4	0.0032		
	9	1.29	28.0	0.0033		
	10	1.75	27.3	0.0030		
	11	1.75	27.9	0.0028		
	12	1.75	27.2	0.0030		

TABLE 4

Material	Sample no.	Sample thickness in mm	ε	$\tan\delta$	Average ε	Average $\tan\delta$
Zinc titanate	1	4.70	27.8	0.00090	27.9	0.00079
	2	4.70	27.9	0.00064		
	3	4.70	27.9	0.00078		
	4	1.70	28.0	0.00074		
	5	1.80	27.7	0.00090		

TABLE 5

Material	Sample no.	Sample thickness in mm	ε	tan δ	Average ϵ	Average tan δ
Calcium titanate	1	3.30	152	0.0020	152	0.0020
	2	3.30	152	0.0020		
	3	1.80	151	0.0022		
	4	4.30	152	0.0015		
	5	4.30	151	0.0022		
	6	1.81	151	0.0019		

TABLE 6

Material	Sample No.	Sample thickness in mm	ε	tan δ	Average ϵ	Average tan δ
Bismuth titanate	1	2.82	81.0	0.0031	80.8	0.0033
	2	2.82	81.0	0.0028		
	3	2.82	80.0	0.0026		
	4	3.95	81.5	0.0034		
	5	2.82	83.0	0.0043		
	6	3.81	80.3	0.0037		
	7	3.80	80.7	0.0033		
	8	3.80	79.8	0.0032		

TABLE 7

Material	Sample No.	Sample thickness in mm	ε	tan δ	Average ϵ	Average tan δ
Strontium titanate	1	3.90	175	0.0023	176	0,0025
	2	4.99	177	0,0021		
	3	1.60	176	0,0031		
	4	4.99	176	0.0025		
	5	4.99	172	0,0031		
	6	2.75	178	0.0024		
	7	4.26	175	0.0019		
	8	4.26	175	0.0026		
	9	1.95	175	—		

TABLE 8

Material	Sample No.	Sample thickness in mm	ε	tan δ	Average ϵ	average tan δ
Porcelain	1	2.50	5.47	0.0084	5.39	0.0113
	2	2.60	5.34	0.0101		
	3	2.41	5.35	0.0104		
	4	2.39	5.42	0.0142		
	5	2.40	5.39	0.0135		

angle is inversely proportional to frequency. However, it is possible to consider that in the cases where the dielectric constant decreases with frequency in the region of large values of $\tan\delta$, relaxation polarization occurs. This polarization, which is especially strongly manifested in bismuth titanate takes place, perhaps, in calcium titanate and steatite.

The loss angle of zinc titanate (see Fig. 6) decreases strongly with increasing frequency, and in the region of high frequencies (above 10^7 cps) it has a small frequency-independent value. This may be of significance for the practical use of zinc titanate in high frequency equipment.

The increase of loss angle with frequency in the region of high frequencies for all the remaining materials can be connected equally well with high frequency relaxation and with resonance absorption in the region of long infrared wavelengths. The unambiguous decision of this question requires further investigation in the shorter radio wavelength region and in the infrared region of the spectrum.

The temperature dependence of ϵ and $\tan\delta$ at frequencies of 10^3, 10^6, and 10^{10} cps is shown in Figs. 10-13 for the dielectrics investigated. As is clear from Figs. 10 and 11, the temperature dependence of the dielectric constant of fused strontium titanate and calcium titanate at a frequency of 10^{10} cps is completely analogous to the temperature dependence of ϵ at frequencies of 10^3 and 10^6 cps. For strontium titanate all three curves practically merge into one (Fig. 11). For calcium titanate, in

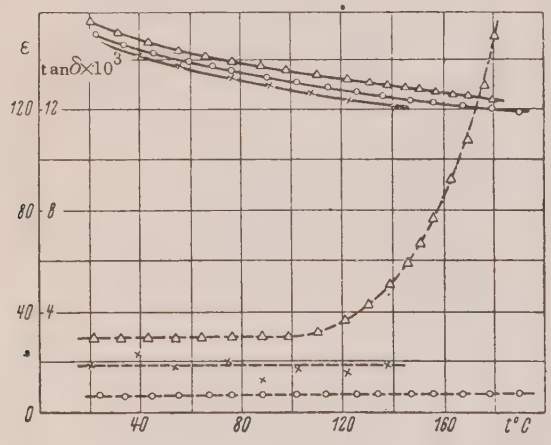

FIG. 10. Temperature dependence of ϵ and $\tan\delta$ for calcium titanate. The continuous curve gives ϵ and the dashed curve gives $\tan\delta$. Points Δ are for $f = 10^3$ cps, O for $f = 10^6$ cps, $\times$ for $f = 10^{10}$ cps.

connection with the occurrence of some decrease in ϵ with frequency (see Fig. 8), the curves $\epsilon = f(t^\circ)$ (t is in °C) do not coincide for different frequencies. However, they have the same slope. From this there follows the practically important consequence that the temperature coefficient of capacity for ceramic condensers based on strontium and calcium titanates, cannot depend strongly on frequency right up to frequencies of $\sim 10^{10}$ cps. As is well known, the temperature coefficient of the dielectric constant of magnesium titanate and barium tetratitanate is comparatively small $(1/\epsilon)(d\epsilon/dT) \approx (10\text{-}40) \times 10^{-6}$ degree^{-1}; hence it does not seem possible to show the change in ϵ with temperature for these materials by means of the measuring apparatus used in the present work. The practical constancy of the dielectric constants of magnesium titanate and barium tetratitanate with change in temperature (Fig. 12) only emphasizes the possibility of temperature measurements by means of a resonator with a heating coil, for changes in ϵ which are not very small.

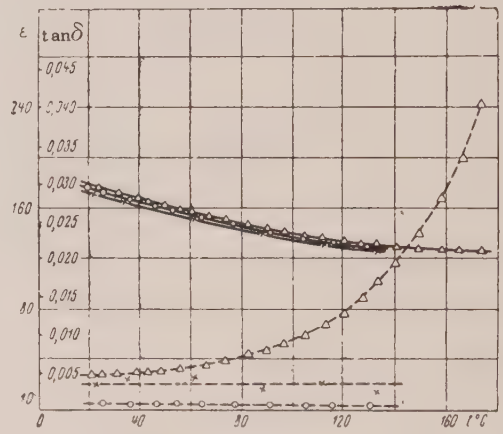

FIG. 11. Temperature dependence of ϵ and $\tan\delta$ for strontium titanate. The continuous curve gives ϵ and the dashed curve gives $\tan\delta$. Points Δ are for $f = 10^3$ cps, O for $f = 10^6$ cps, $\times$ for $f = 10^{10}$ cps.

The increase in ϵ with temperature for bismuth titanate (Fig. 13), occurring especially at a frequency of 10^3 cps, emphasizes the presence of relaxation polarization with a comparatively large relaxation time. The essential thing is that even at high frequencies the ϵ of bismuth titanate grows with temperature. It should be noted that the bismuth titanate investigated in the present work has a complex structure, differing strongly from the structure of rutile and perovskite, and hence it is very difficult to determine to what extent its structure favors the polarization. It may clearly be asserted that in bismuth titanate there are weakly bound ions or groups of ions giving rise to relaxation (thermal ionic) polarization.

The dielectric loss angle of calcium titanate

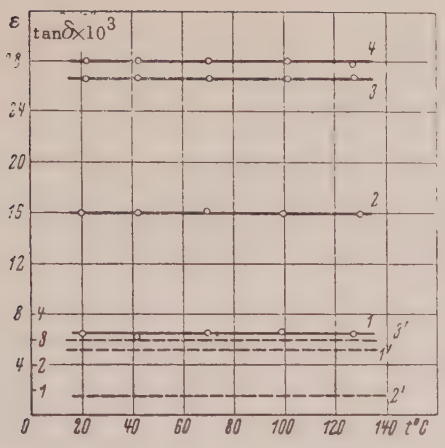

FIG. 12. Temperature dependence: The continuous curves give ϵ and the dashed curves $\tan\delta$; *1* and *1′* — steatite, *2* and *2″* — magnesium titanate, *3* and *3′* — barium tetratitanate, *4* — zinc titanate. The points of curves *1′*, *2′* and *3′* give a scatter of (20 — 50)%.

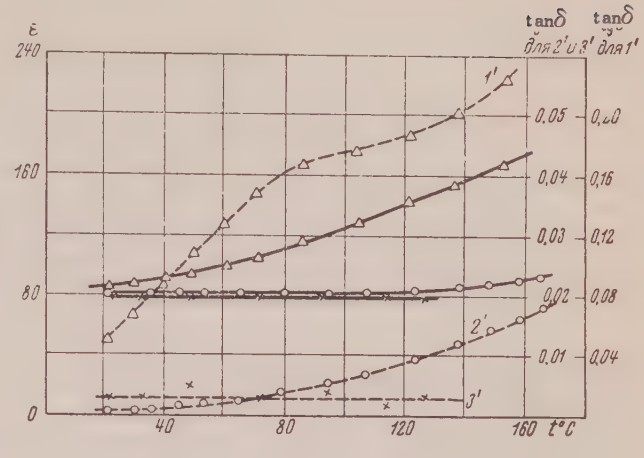

FIG. 13. Temperature dependence of ϵ and $\tan\delta$ for bismuth titanate. The continuous curve gives ϵ, the dashed curve gives $\tan\delta$. Points Δ are for $f = 10^3$ cps, O for $f = 10^6$ cps, × for $f = 10^{10}$ cps.

and fused strontium titanate in the temperature region from room temperature to 160° increases strongly with temperature only at low frequencies ($f = 10^3$ cps, Figs. 10 and 11). At frequencies of 10^6 and 10^{10} cps the $\tan\delta$ of these dielectrics is constant in this temperature interval. The loss angle of magnesium titanate and barium tetratitanate at a frequency of 10^{10} cps does not change in the temperature interval 20-120°.

It is evident from Fig. 13 that the loss angle of bismuth titanate is independent of temperature in the interval 20-160° only for a frequency of 10^{10} cps. At lower frequencies (10^6, 10^3 cps) the loss angle of bismuth titanate increases more strongly with temperature the lower the frequency. This fact is connected with the presence of relaxation polarization. The investigation of solid dielectrics in the long wavelength part of the infrared region of the spectrum will permit our conclusions concerning the nature of dielectric polarization and loss to be developed and made more precise.

[1] G. I. Skanavi, *The Physics of Dielectrics, Weak Field Region*, GTTI, Moscow-Leningrad, 1949.

[2] G. I. Skanavi, *Dielectric Constant and Losses in Glasses in Polycrystalline Materials of the Ceramic Type*, Gosenergoizdat, 1952.

[3] G. I. Skanavi and A. I. Demeshina, J. Exptl. Theoret. Phys. (U.S.S.R.) **19**, 3 (1949).

[4] G. I. Skanavi and A. N. Gubkin, J. Exptl. Theoret. Phys. (U.S.S.R.) **28**, 85 (1955); Soviet Phys. JETP 1, 71 (1955).

[5] Horner, Taylor, Dunsmuir, Lamb and Jackson, J. Inst. Elec. Engrs. (London) **93**, 53 (1946).

[6] R. G. Breckenridge, J. Chem. Phys. **16**, 959 (1948).

[7] R. G. Breckenridge, J. Chem. Phys. **18**, 913 (1950).

[8] *Measurements at Ultrahigh Frequencies*, translated from the English under the editorship of V. B. Steinschläger, Soviet Radio Press Moscow, 1952.

Translated by M. G. Gibbons
174

Dark Conductivity of Silver Bromide Crystals

V. V. Gladkovskii and P. V. Meikliar
Vologod State Pedagogical Institute
(Submitted to JETP editor September 8, 1955)
J. Exptl. Theoret. Phys. (U.S.S.R.) 30, 833-839 (May, 1956)

The conductivity of large silver halide crystals in weak fields is shown to be electronic. In stronger fields the ions start moving through the defects and over the surface, and this is accompanied by a growth of dendrites. When the crystals are exposed to light, their conductivity first rises and then falls. The result of the exposure depends on the medium in which the crystal is located.

IT is customary to assume that the dark conductivity of most ionic crystals, including that of silver halide crystals, is ionic. This conclusion is based principally on experiments by Tubandt,[1] who showed that at higher temperatures specimens made of compressed powders of many salts obeyed the Faraday electrolysis law.

Tubandt's determination of the transport numbers has shown that the conductivity of all three silver halides is caused by the positive silver ions. Application of the Frenkel defect theory to these crystals has led to the conclusion that in addition to the interstitial silver ions the vacant sites of these ions also affect the conductivity. The Frenkel defect formation hypothesis was confirmed by many experiments,[2] and at the present time there is no doubt that no defects are formed in silver halides by the Schottky mechanism, with the exception of the single case when the crystal temperature is close to the melting point. Experiments[3] with the diffusion of radioactive bromine and silver in crystals have shown that the diffusion coefficient of the silver ions is considerably higher than that of the bromine ions, while bromine atoms diffuse with relative ease. Incidentally, pressed powders were used in the experiments on the diffusion of radioactive isotopes, as in the Tubandt experiment.

It was further shown[4] that the conductivity of pressed powders at temperatures below 80-100°C is proportional to the surface area of the crystals. This last dependence indicates that at room temperatures the conductivity of pressed powders, with which many investigators perform their experiments, is determined by the motion of the ions over the surface. Room-temperature investigation of the conductivity of silver halide monocrystals is reported only in Ref. 5, and its results make it clear that at room temperature the dark conductivity of large silver halide monocrystals is electronic. At room temperature the surface conductivity of the silver halide crystals is thus determined by the silver ions, while only electrons move deep within the crystal.

It is known from the Kirillov and Levi[6] experiments that the dark conductivity changes after the crystal has been exposed to light, and it was shown in that investigation that the observed change in conductivity is reversible. The electrons that were fixed at local levels during the crystal exposure become thermally free after the conclusion of the exposure. Barshchevskii[7] observed an increase in photoconductivity during the exposure of the crystal.

Investigation of silver halide crystal conductivity is made difficult by the formation of so-called dendrites, i.e., silver filaments that grow from the cathode to the anode and short circuit the crystal. At the same time, investigation of the dendrite formation process is of importance in the explanation of the conductivity mechanism. The structure of dendrites was studied in reference 8.

This article reports the results of an investigation of the dark conductivity and of the electrolysis of silver halide crystals, and also the effect of exposure on these processes.

EXPERIMENTAL PROCEDURE

Specimens were prepared by pouring fused salt between two glass plates followed by prolonged annealing, as described by Meikliar.[9] Added pads of suitable thickness were placed between the plates to obtain thick crystals. During the experiment the crystals were uncovered by stripping one or both glass plates. To check whether the Faraday electrolysis law is obeyed, a setup similar to that described in Ref. 5 was assembled. A silver bromide crystal, several tenths of a millimeter thick, was placed over a silver plate, serving as the anode. A glass tube, into which a solution of potassium nitrate was poured, was pressed against the upper surface of the crystal through a rubber washer. A platinum plate serving as a cathode was placed in the solution. The circuit was energized and the amount of electricity passing through the crystal was measured with a coulomb meter, consisting of a platinum crucible containing a solution of silver nitrate and a silver

plate immersed in this solution. The crucible acted as the cathode, and the silver plate as the anode. The electrolysis current was several microamperes; each experiment lasted as much as several days. Whenever a silver filament grew in the crystal during the time of the experiment the current increased sharply and the experiment was discarded as a failure. The weights gained by the coulomb-meter crucible and lost by the anodes of the coulomb meter and the crystal were measured by a precision balance accurate to 5×10^{-5} grams. It was impossible to determine the weight gained by the cathode immersed in the potassium nitrate solution, for the silver was deposited on this cathode as thin filaments which broke easily.

We also made observations on the growth of the dendrites. For this purpose graphite electrodes were coated over the crystal which was placed on the flat surface of a small electric furnace. A potential difference on the order of several tens of volts was applied to the electrodes to raise the crystal temperature, and the growth of dendrites was examined with the aid of a microscope, occasional microphotographs being taken. The same setup was used to heat the exposed crystal. In the latter case graphite, or metal (platinum, copper, cadmium or silver) electrodes were used. The metal electrodes were deposited on the crystal either by evaporation or by cathode spattering.

The effect of crystal exposure on the value of its dark conductivity was then investigated. The exposure was made in air, in vacuum, or in various gas atmospheres. For this purpose the crystal was placed in an evacuated container, the upper portion of which had a flange with a quartz plate inserted. As required, the exposure was made either without evacuation, or after evacuation followed by additional admission of some gas. The source of light was a PRK-4 mercury tube with a set of light filters to separate the spectral lines. The thermal conductivity was measured without removing the crystal from the container. For this purpose, leads passing through the lower portion of the glass container were pressed against the graphite electrodes of the crystal. These conductors were used to connect the crystal alternately to a mirror galvanometer and to the power source.

In some cases the photoconductivity was measured simultaneously with the dark conductivity. In such a case the source of light was also a mercury tube with light filters. Sometimes the crystals were exposed while immersed in a solution of caustic potassium of varying concentration. When convenient, the absorption spectrum of the crystals was measured simultaneously, using a dual monochromator made by the experimental machine shop of the Leningrad State University Physics Institute.

RESULTS OF MEASUREMENTS

The table gives the results of measurements made to verify the applicability of the Faraday law. It can be seen here that at a relatively low potential difference (less than 4 volts) the weight lost by the crystal anode is noticeably less than that lost by the coulomb-meter anode and that gained by the coulomb-meter crucible, while at high potential differences the corresponding quantities are of the same order of magnitude. This means that if the fields inside the crystal are weak its conductivity is purely or predominantly electronic, becoming ionic in strong fields. The ionic conductivity produced by the increase in the field is accompanied by a growth of silver filaments at places where the crystal is inhomogeneous. The more perfect the crystal, i.e., the smaller the number of defects in which ions can move and form metallic filaments, the higher the potential difference at which the conductivity becomes ionic.

Figures 1 and 2 show microphotographs of a silver filament growing on the surface of the crystal from the cathode. Examination under the microscope shows how the filament grows. Measurements have shown that at a temperature of 100°C and an electric field intensity of 50v/cm the filament grows at an approximate rate of $10^{-3} - 10^{-2}$ mm/sec. Reversing the electric field causes the length of the filaments at the electrode (which now becomes an anode) to diminish until it vanishes completely. At the same time filaments begin to grow from the second electrode (now the cathode). Treating such a crystal with its silver filaments in a hydrogen sulfide atmosphere forms silver sulfide on the surface of the crystal with the exception of the places that are directly adjacent to the filaments. This can be seen from Fig. 3. The growth of silver filaments during electrolysis of silver halide crystals was reported in Ref. 8. However, this work was previously unknown to us and our observations were made independently. Heating an exposed crystal in an electric field causes resorption of the photolytic silver near the anode. Figure 4 is a photograph of a crystal uniformly exposed over the entire surface and shows such brightening at the anode. Figure 5 shows a crystal first dusted with silver. When an alternating electric field is applied, the brightening forms at both electrodes, although at a slower rate. We observed this brightening only with graphite and platinum electrodes. When the crystal was

TABLE

Results of Electrolysis Experiments

Weight, milligrams	First Experiment with Crystal			Second Experiment with the Same Crystal		
	Before Experiment	After Experiment	Difference	Before Experiment	After Experiment	Difference
Crystal No. 1	potential — 2 volts			potential — 30 volts		
Coulomb-meter crucible	6465.40	6467.60	+2.20	6465.40	6466.50	+1.10
Coulomb-meter anode	2115.80	2113.55	—2.25	2113.55	2112.50	—1.05
Crystal anode	3571.70	3571.70	0.00	3570.00	3568.90	—1.10
Crystal No. 2	potential — 2 volts			potential — 20 volts		
Coulomb-meter crucible	6346.80	6349.50	+2.70	6346.40	6347.60	+1.20
Coulomb-meter anode	2227.95	2225.10	—2.85	2222.90	2221.80	—1.10
Crystal anode	3423.70	3423.60	—0.10	3422.85	3421.80	—1.05

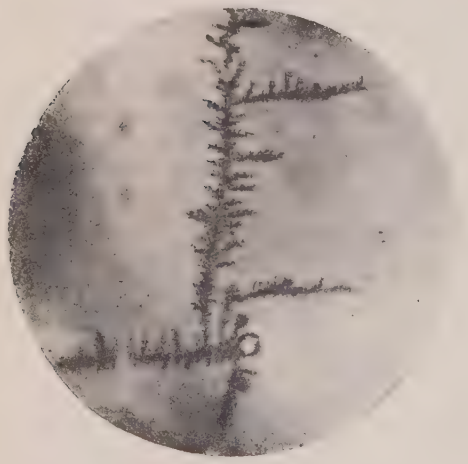

FIG. 1. Microphotograph of silver filament growing from the cathode in the electrolysis of silver bromide. Magnification 40 x, field intensity 60 v/cm, temperature 100-150.°

FIG. 2. Microphotograph of portion of the silver filament shown in Fig. 1; magnification 160 x.

coated with silver or copper electrodes, no bright areas were observed near the anode and the flow of current caused a gradual breakdown of the anode itself.

Figure 6 shows the increments of the optical density of the exposed crystal before and after this brightening.

We learned recently that thermal resorption of the photolytic silver near the anode is reported also in Ref. 10. However, in that investigation the experiments were with silver bromide crystals to which silver sulfide was added, and we consider this phenomenon to occur only with such mixed crystals. Our experiments, performed independently, were carried out with silver bromide crystals without any admixtures.

We next investigated the effect of the exposure on the value of the dark conductivity. We observed there that the separation of the photolytic silver depends to a large extent on the nature of the medium in which the crystal is placed during

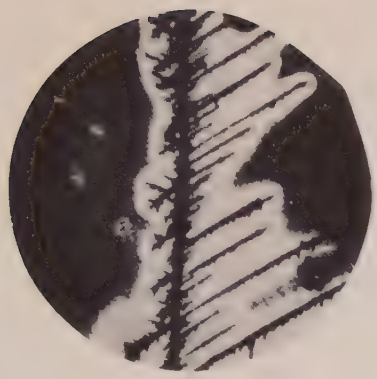

FIG. 3. Microphotograph of a portion of a crystal with a silver filament, treated in hydrogen sulfide; magnification 400 x.

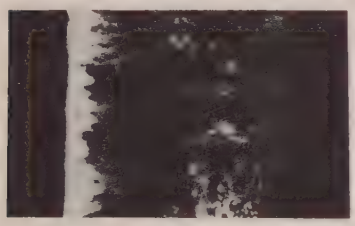

anode *cathode*

FIG. 4. Regression of photolitic silver in the electric field at the anode. Potential difference 70 v, interelectrode distance 25 mm, experiment temperature 210.°

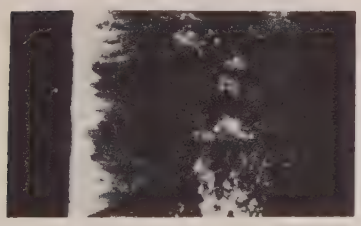

anode *cathode*

FIG. 5. Regression of silver dusted on the surface of the crystal at the anode, under the same conditions as in Fig. 4.

the exposure. Experiments show that the photolytic silver is separated most intensely when the crystal is exposed in a hydrogen sulfide stmosphere or in a vacuum. Exposure in a hydrogen or an oxygen atmosphere produces approximately the same results as in air. This is illustrated by Fig. 7, which shows the increments of the optical density of the various portions of the same crystal exposed in different gaseous media.

The photochemical sensitivity of the crystals increases noticeably also when the crystals are immersed in a solution of potassium hydroxide; as the concentration of the potassium hydroxide increases, the photochemical sensitivity first rises, and then stays constant as the concentration reaches approximately 5%. This is illustrated by Fig. 8, showing the increments of the optical density of crystals exposed in air and in 5% potassium hydroxide.

The effect of crystal exposure on the value of its dark conductivity is quite complicated in character. With respect to this, crystals can be divided into two types: 1) those with high dark resistivity and low photoconductivity and 2) those with low dark resistivity and high photoconductivity.

Exposed crystals of the first type exhibit a gradual and irreversible decrease in the dark conductivity and their photoconductivity at first increases somewhat and then also decreases. This is seen from the curves of Fig. 9. When crystals of the second type are exposed, an increase is observed in the dark conductivity and in the photoconductivity followed, starting with a certain exposure time, by a decrease in both (Fig. 10). If the crystal exposure is stopped at a time when its conductivity is on the rise, both the dark conductivity and the photoconductivity return after a certain time to their initial values, i.e., to the values before the start of the exposure; this is in agreement with the data obtained by Kirillov and Levi.[6] But if the exposure is interrupted while the conductivity decreases, the latter does not return to its initial value; the changes occurring in the crystal in this case appear to be irreversible.

In certain cases the variation of crystal photoconductivity with exposure time is even more complicated and passes through several minima and maxima. However, spectral measurements of the crystal light absorption have shown in all cases that the photoconductivity vs. exposure time curve has a minimum corresponding to light absorption in the spectral interval 400-460 millimicrons, and, conversely, the maximum of this curve corresponds to a lower absorption of light in the above region of the spectrum. Further experiments have shown that the first group of crystals, characterized by low photoconductivity, has a noticeably higher photochemical sensitivity than the second group of crystals with the higher photoconductivity. This is illustrated by Fig. 11, which shows incremental optical density curves of crystals of the first (curve a) and second type (curve b) exposed under

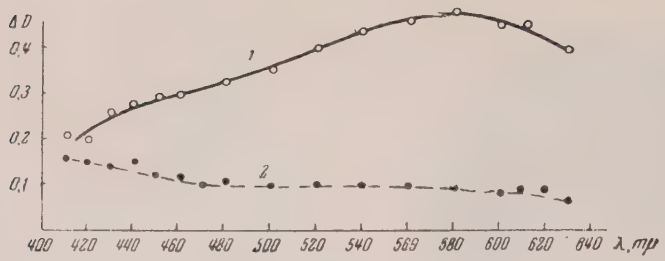

FIG. 6. Curves showing increments of crystal optical density: *1* — after exposure, *2* — after exposure and anode brightening.

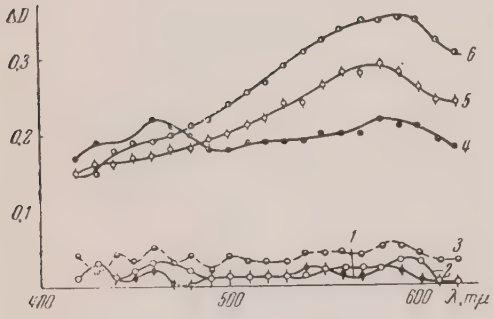

FIG. 7. Curves showing increment of optical density after exposing the crystal for 30 minutes with a mercury-arc lamp in: *1* — oxygen, *2* — hydrogen, *3* — air, *4* — vacuum. Also curves obtained by exposing the crystal: *5* — ten minutes in hydrogen sulfide, *6* — three minutes in potassium hydroxide.

identical conditions. Measurements of the absorption spectra of these crystals have shown that in the 400-460 millimicron spectral region the crystals of the first group have a noticeably higher absorption than those of the second type. This is illustrated in Fig. 12, where curves refer to crystals of the first and second type respectively. Both curves were obtained by comparison with a crystal having an average photoconductivity.

DISCUSSION OF RESULTS

It follws from the data given that the dark conductivity of large silver halide crystals is electronic. The conductivity becomes ionic when the electric field in the crystal is increased, because of the motion of the ions over the defects of the crystal, in which the field reduces the activation energy for the motion of the ions. Such a hypothesis is corroborated by the fact that silver dendrites grow out of the defects as the electric field is increased. The silver ions move over the surface of the crystal. When an electric field is superposed these ions move to the cathode where they absorb electrons and turn into atoms. This is how silver filaments grow at the cathode. Subsequent silver ions reach the sharp point of the filament, where they are discharged and the filament continues to grow. When the field direction is reversed the filament decomposes. Apparently, the silver ions become thermally separated from the positively charged filament (anode). During the growth of the filament, the crystal surface in the direct vicinity of the filaments becomes poor in silver ions, and therefore no silver sulfide is formed in the vicinity of the filaments when such a crystal is developed in hydrogen vapor. The thermal decomposition of particles of metallic silver near the anodes can be explained by the fact that the decomposition starts with the separation of electrons, which migrate to the anode, followed by thermal decomposition of the positively-charged silver particles, as can be seen from the absorption curves on Fig. 6. The silver ions formed move away to the cathode. If the anode is made of graphite or platinum, no new ions arrive to replace the silver ions that move to the cathode. But if the anode is made of another metal, the ions of this metal come to replace the silver ion, and the anode itself becomes decomposed rather than the metal particles. Such a hypothesis concerning the mechanism of the thermal decomposition of silver particles is in agreement with the data by Kazantsev and Meikliar[11] on the regression of the centers of the latent photographic image. The relationship between the dark conductivity and the photoconductivity of the crystal, described above, can be explained in the following manner. Since a relatively large light absorption is observed in the case of crystals of the first type, which have a low photoconductivity in the 400-460 millimicron spectral region (Fig. 12), i.e., in the region where light is absorbed by the F-centers[12], we must assume that the concentration of such centers is relatively high in these crystals. The light absorption in such crystals has an exciton character,[13] and no thermal electrons are liberated

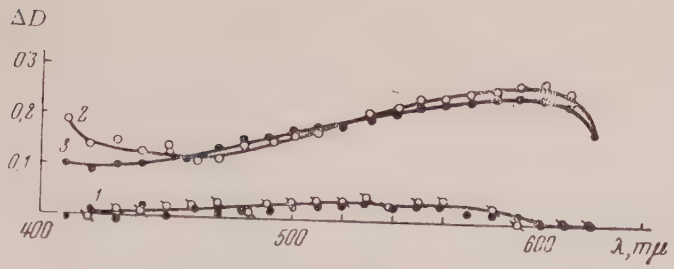

FIG. 8. Increment of optical density of crystal after exposure of 10 minutes in air (1), 10 minutes in 5% potassium hydroxide solution (2) and 5 minutes in potassium hydroxide solution (3).

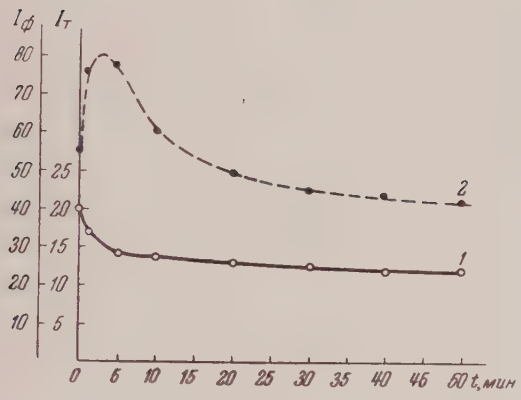

FIG. 9. Dark conductivity (1) and photoconductivity (2) vs. exposure time for a crystal with high dark resistivity ($R = 2.5 \times 10^9$ ohm) and low photoconductivity ($I_{ph}/I_d = 3$).

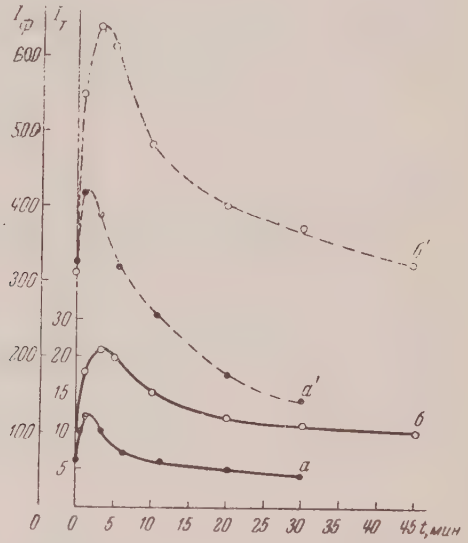

FIG. 10. Dependence of exposure time on dark conductivity (a,b) and on photoconductivity (a′,b′) for two crystals with low dark resistivity ($R = 4 \times 10^8$ and 2×10^8 ohms) and high photoconductivity ($I_{ph}/I_d = 52$ and 35).

from the F-centers. This is why the dark conductivity of such crystals is low and is determined only by the silver ions moving along the surface. When such crystals are exposed the electrons liberated by the light are captured by the silver ions and the conductivity of the crystals decreases monotonically.

The crystals of the second type, which have a high photoconductivity, are characterized by low absorption of light in the 400-460 millimicron region (Fig. 12), and consequently, by a low F-center concentration. Here the electrons can be thermally liberated from the F-centers at the start of the exposure and the increase in the number of F-centers during exposure first causes an increase in the dark conductivity. As the exposure time is increased the concentration of the F-centers becomes greater, the absorption of light assumes an exciton character, and this leads to a reduction in the dark conductivity and in the photoconductivity. This agrees with the data on the determination of the photochemical sensitivity of crystals. Crystals of the first type contain more F-centers than those of the second type, and accordingly their photochemical sensitivity is noticeably higher (see Fig. 11).

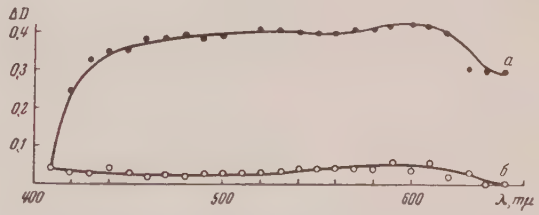

FIG. 11. Curves showing increments of optical density of crystals exposed under identical conditions: *a* — first type, *b* — second type.

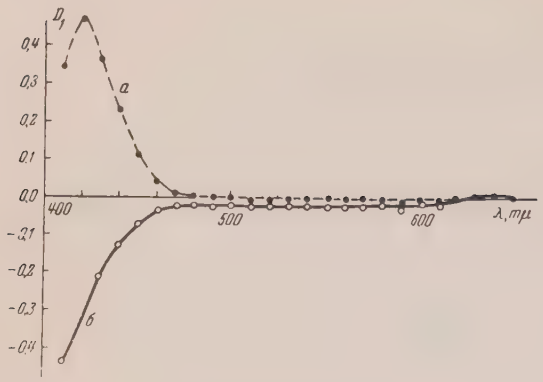

FIG. 12. Comparison of optical density of crystals of the first (a) and second (b) types with that of a crystal having an average photoconductivity ($D_1 = \ln I_0 / I_1$).

[1] C. Tubandt, Handb. d. Experimentalphysik, 12, Part 1, Ch. 3.

[2] Cf. for example, H. Keith and J. Mitchell, *Physical Foundations of Photographic Sensitivity* (Russian Translation), IIL, Moscow 1953, p. 41.

[3] A. H. Murin and Iu. Taush, Dokl. Akad. Nauk SSSR 80, 579, 1951; A. N. Murin, G. N. Kazakova and B. G. Lur'e, Dokl. Akad. Nauk SSSR, 99, 529 (1954).

[4] I. Shapiro and E. I. Kol'tgof, *Physical Foundations of Photographic Sensitivity*, IIL, Moscow 1953, p. 17). (Tr. Note – apparently book title is wrong – cf. Ref. 2).

[5] Pfeiffer, Hauffe and Jehnke, *Physical Chemistry of Photographic Processes* (Russian Translation) IIL, Moscow 1954, p. 73.

[6] E. Kirillov and Z. A. Levi, J. Exptl. Theoret. Phys. (U.S.S.R.) 17, 336, (1947).

[7] B. A. Barshchevskii, J. Exptl. Theoret. Phys. (U.S.S.R.) 16, 815, (1946).

[8] J. Mitchell, *Physical Chemistry of Photographic Processes*, (Russian Translation) IIL, M 1954, p. 92.

[9] P. V. Meikliar, J. Exptl. Theoret. Phys. (U.S.S.R.) 21, 42, (1951).

[10] S. Suzuki, Sc. ind. phot., 25, 70 (1954).

[11] B. I. Kazantsev and P. V. Meikliar, J. Exptl. Theoret. Phys. (U.S.S.R.) 28, 70, (1955); Soviet. Phys. JETP 1, 45 (1955).

[12] E. K. Putseiko and P. V. Meikliar, J. Exptl. Theoret. Phys. (U.S.S.R.) 21, 341 (1951).

[13] M. S. Egorova and P. V. Meikliar, J. Exptl. Theoret. Phys. (U.S.S.R.) 30, 60 (1956); Soviet Phys. JETP 3, 4 (1956).

Translated by J. G. Adashko
175

Ionization Spectrum of the Cosmic Ray Soft Component at Sea Level

A. G. Meshkovskii and L. I. Sokolov

(Submitted to JETP editor October 8, 1955)
J. Exptl. Theoret. Phys. (U.S.S.R.) 30, 840-849 (May, 1956)

A new method for the investigation of ionization spectra of cosmic ray particles is worked out. Ionization spectra are taken for particles with penetration in the intervals 2-3, 3-5, 5-9, and 9-15 cm of lead. Conclusions are reached about the distribution of the proton component at sea level among these penetration intervals.

1. INTRODUCTION

BY investigating the ionization spectra of cosmic ray particles of known penetration, it is possible to determine the composition of cosmic rays.[1] The basic difficulty of this method is the poor separation of various mass particles. The insufficient resolution is determined by the nature of the ionization energy loss fluctuations, which for most cosmic ray particles, obey the Landau distribution.[2] The distinguishing characteristic of this distribution is the high probability of fluctuations in the direction of large energy loss. However, it is particularly in the region of large ionization that the ionization spectra of hyperons, protons, or K-mesons of the soft cosmic ray component are located. Since the percentage of these particles in the composition of cosmic rays at sea level or at mountain altitudes is relatively small, it turns out that the ionization spectra of these particles can not be successfully separated from those parts of the ionization spectra of cosmic ray μ-mesons and electrons which are caused by fluctuations in the direction of large energy loss. In the method proposed below, this difficulty is overcome to a large extent.

2. THE BASIC IDEA

Let each particle of the analyzable particle flux pass successively through n layers of matter, in each of which it loses some energy by ionization. The basic idea of our method is to measure the smallest value of the totality of ionization losses $\Delta_1, \Delta_2, \ldots \Delta_n$. A suitable arrangement of equipment automatically selects this value for measurement, and rejects all others. We assume here that the material of all layers is the same, and that all layers have the same thickness.*

*The selection of the smallest value of ionization as an experimental method using two gas proportional counters was proposed by L. D. Landau and first carried out by Nikitin.[1]

Let us examine, in such a measuring set up, the probability of finding a particle in the interval of ionization loss Δ, $\Delta + d\Delta$. If the ionization loss in each of the n identical layers obeys a Landau distribution, the desired probability is

$$n\frac{1}{\xi}\varphi\left(\frac{\Delta-\Delta_0}{\xi}\right)\left[\psi\left(\frac{\Delta-\Delta_0}{\xi}\right)\right]^{n-1}d\Delta = \frac{1}{\xi}\Phi_n\left(\frac{\Delta-\Delta_0}{\xi}\right)d\Delta, \quad (1)$$

where we introduce the general function

$$\Phi_n(\lambda) = n\varphi(\lambda)[\psi(\lambda)]^{n-1}, \quad (2)$$

in which φ and ψ are Landau's general functions[2] (see Ref. 2 for remaining definitions). Thus, instead of an ionization spectrum which can be described by Landau's distribution function

$$f(x, \Delta) = \frac{1}{\xi}\varphi\left(\frac{\Delta-\Delta_0}{\xi}\right), \quad (3)$$

the above method of measurement will yield a spectrum which obeys the distribution

$$f_n(x, \Delta) = \frac{1}{\xi}\Phi_n\left(\frac{\Delta-\Delta_0}{\xi}\right). \quad (4)$$

Let us now evaluate the probability of ionization loss larger than a particular value, i.e., we calculate the integral

$$S(\Delta_a) = \int_{\Delta_a}^{\infty} f_n(x, \Delta)\,d\Delta. \quad (5)$$

Since we are interested in large values of Δ_a, we shall use the asymptotic expressions for the general functions φ and ψ, as developed in Landau's paper. We then easily obtain, for large values of Δ_a,

$$S(\Delta_a) = 1/\omega_a^n, \quad (6)$$

where ω_a is connected to Δ_a by the equation

$$(\Delta_a - \Delta_0)/\xi = \omega_a + \ln \omega_a - 0.37. \qquad (7)$$

It follows from Eq. 6 that the number of particles with ionization higher than the given value Δ_a is ω_a^{n-1} times smaller with the present method of measurement (i.e., selection of the smallest value) than with the ordinary method where the particle passes through only a single layer of matter (a single proportional counter). For the majority of cosmic ray particles and the counters used in the work described here, $\omega_a \approx 15$ if $\Delta_a = 2\Delta_0$. This means that if ionization spectra are taken with three counters ($n = 3$) the number of μ-mesons or electrons with more than twice the expected value of ionization is some 200 times smaller than for ionization spectra taken with a single counter. Consequently, with a large enough number of counters, it is possible to measure the ionization spectra of hyperons or protons of the soft cosmic ray component under conditions almost completely free of background caused by parts of meson and electron ionization spectra.

3. DESCRIPTION OF THE EQUIPMENT

We have chosen to use scintillation counters as a method of measuring ionization loss. The possibility of using scintillation counters for this purpose, and their superiority to gas proportional counters has been proved earlier by Meshkovskii and Shebanov[3] and other workers.[4,5]

The physical arrangements are shown in Fig. 1. Here 1 – 5 are five layers of scintillator material. The scintillators, especially prepared for this experiment, were polystyrene plastic activated with 1, 1, 4, 4 – tetraphenylbutadine – 1, 3 in a concentration of 1.8 %. The polymerization of the doubly distilled styrene was carried out at 200° C in the course of 12 – 15 hours. The tetraphenylbutadine was prepared by the method of Valeur.[6] Scintillater size was $1 \times 3.5 \times 7.5$ cm. After machining, the scintillater plates were carefully polished, mounted in reflecting housings and glued to the photocathodes of type FEU – 19 photomultipliers for better optical contact.

For this experiment, exceptional photomultipliers were selected in order to give the least instrumental line broadening. A scintillation γ spectrometer based on the Compton effect was set up, and photomultipliers selected for least line width from a Co^{60} source.

The numbers 6 – 10 on Fig. 1 are lead filters. The thickness of filter 6 was chosen such that the penetration of particles passing through it was greater than 2 cm of lead. The roman numerals denote arrays of Geiger-Muller counters. For the measurement of ionization spectra of particles with 2 – 3 cm penetration, a gating pulse due to the coincidence of I + II + III – IV – IVa – V was used; for particles with penetration 3 – 5 cm — the coincidence I + II + III + IV – IVa – V – Va – VI ; for penetration 5 – 9 cm. — I + II + III +V – VI – VIa – VII; for penetration 9 – 15 cm.— I + II + III + VI – VII; for penetration greater than 9 cm. — I + II + III + VI.

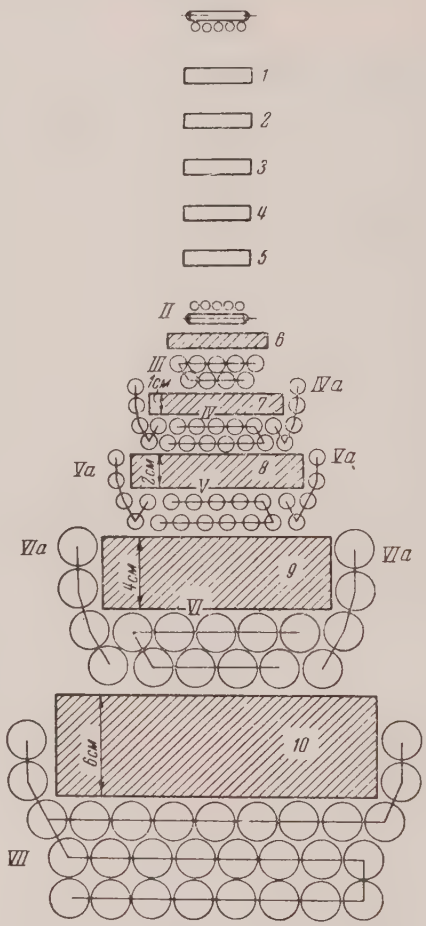

FIG. 1. Diagram of the apparatus

In the selected solid angle, path length of particles through the scintillaters varied by ± 5%. Material over the apparatus was kept to a minimum (0.5 cm plywood and roofing iron). The apparatus was placed in a thermostatically controlled enclosure where the temperature was held constant to ± 0.2°. The temperature controlled enclosure was found necessary in order to keep the photomultiplier gains constant. Voltages on the photomultipliers was held constant to ± 0.1 %.

Photomultiplier gains were checked once in 24 hours by the following method. Simultaneously

with the measurements described above, integral ionization spectra of the cosmic ray hard component were taken for all five scintillation counters. Using the integral spectra taken in the course of twenty four hours, the maxima of the differential spectra were found by a method described in reference 3. In the event of a shift in the position of the maximum for any of the counters, the high voltage on the photomultiplier was adjusted. Over long periods of operation the equipment showed no sharp fluctuations of photomultiplier gain as long as the temperature and voltage were held constant within the stated limits.

A block diagram of the electronics is shown in Fig. 2. Pulses from scintillation counters 1–5 were put through linear amplifiers with negative

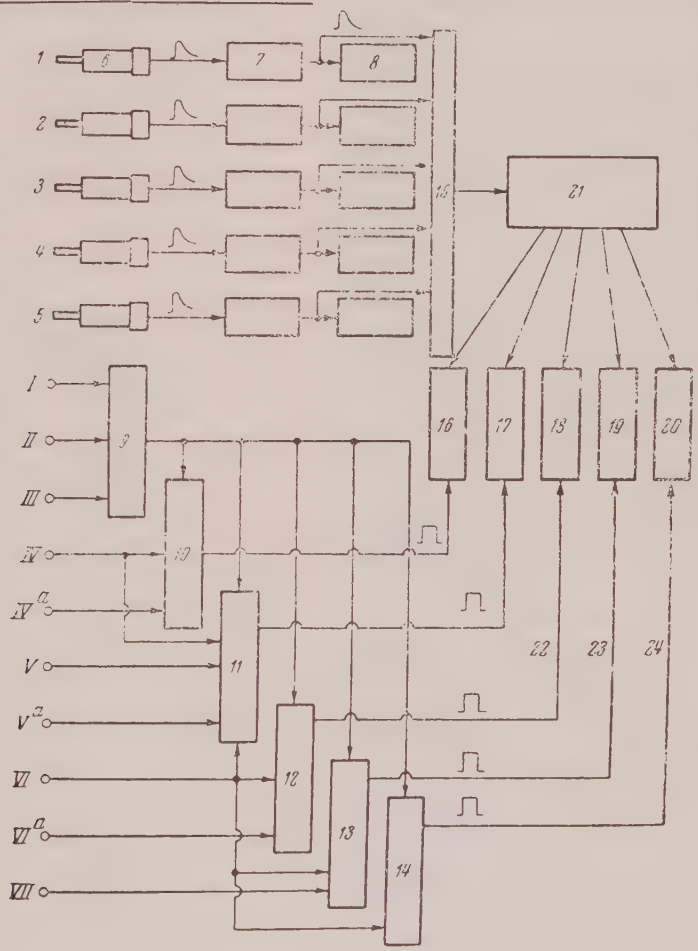

FIG. 2. Block diagram of the electronics: *1–5* — scintillationcounters, *6* – FEU – 19 photomultiplier, *7* – amplifier, *8* – integral analyser, *9–14* – coincidence circuits, *10–13* anticoincidence circuits, *15* – circuit to select the smallest pulse, *16–20* – groups of 25 registers, *21* – 25 channel pulse height analyser, *22–24* – gating pulses, *I – VII* –arrays of Geiger-Muller counters.

feedback. Subsequently, pulses were fed into integral registers, as well as a circuit which selected the smallest pulse. The latter consisted of a coincidence circuit using crystal diodes. The linearity of this minimum pulse selection circuit was checked with generator in the amplitude interval 2 – 40 V.

The selected smallest pulse was measured by a 25 channel differential pulse height analyser, which made use of two type LP – 1 electronic switches.* Each channel of the pulse height

*The differential analyzer was built by E. V. Kuznetsov, to be published.

analyser was connected to five mechanical registers. Gating pulses, corresponding to particular intervals of particle penetration were also fed to the registers. The output of the pulse height analyser was registered only if the gating pulse was present. Thus a single 25 channel analyser fed 125 mechanical registers, and made it possible to take 5 simultaneous ionization spectra corresponding to various intervals of particle penetration.

In the interpretation of heavy particle ionization spectra it was important to know that events recorded in the region of high ionization were not the result of the passage of several particles. To eliminate multiple events from the results, we constructed a special system.

Sets I and II of 5 mm diameter Geiger-Muller tubes each consisted of two layers, the tube axes of one layer being perpendicular to those of the other. Thus sets I and II defined a coordinate system. A circuit with a neon lamp (type MTX – 90) was connected to each counter tube in sets I and II in such a way as to light when a charged particle passed through the counter tube. A similar circuit was connected to each of the sets of counters III, IV, IVa, V, VI, VIa, and VII. Neon lamps were also connected to each channel of the pulse height analyser. All lamps were displayed on a single panel.

During passage of a particle through the system (coincidence I + II + III), the corresponding neon lamps lit, and the panel was photographed by a motion picture camera. In this way it was possible to differentiate between the passage of a single particle and the passage of several and at the same time measure the amount of ionization caused by either type of event. A system to register the multiple events could work simultaneously with the equipment used to make the basic measurements.

4. EXPERIMENTAL RESULTS

Measurements were carried out during 1300 hours of equipment operation. During 900 of these hours, i.e., about 70% of the total time, multiple events were registered in addition to the basic measurements. During the 900 hours, in the soft component there was only one case of simultaneous passage of two particles through the equipment (and 5000 single events). The one multiple event was found in the penetration interval 2 – 3 cm lead and showed twice minimum ionization. The measurement of multiple passage events shows that this type of background was essentially absent in our ionization spectra of the soft component of cosmic rays.

The ionization spectra are shown in Figs. 3–6.

FIG. 3. Ionization spectrum for particles with penetration of 2–3 cm Pb.

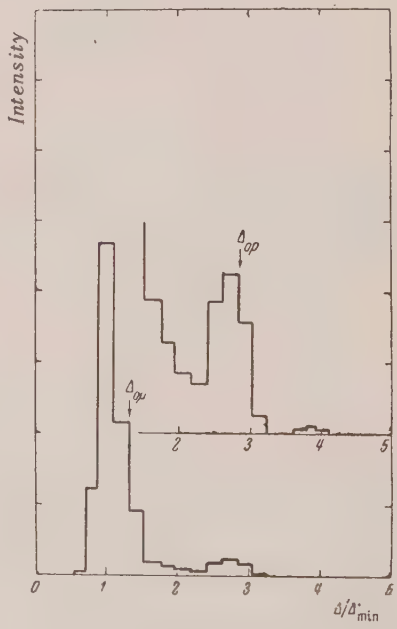

FIG. 4. Ionization spectrum for particles with penetration of 3–5 cm Pb

The abscissa is ionization in units of minimum ionization, the ordinate is the relative intensity in a particular differential interval of ionization. In the

upper portions of Figs. 3–6 the right portion of each spectrum is shown in a larger scale. We note that two groups are clearly seen on each drawing. As will be shown in Sec. 5, the right group is the ionization spectrum of the proton component of cosmic rays. The left group corresponds to mesons and electrons of the soft component.

FIG. 5. Ionization spectrum for particles with penetration of 5–9 cm Pb.

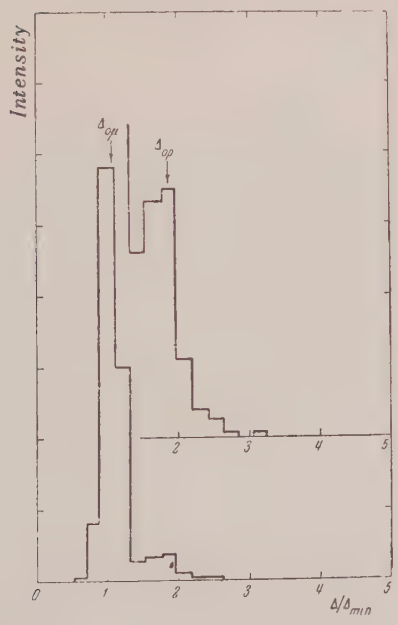

FIG. 6. Ionization spectrum for particles with penetration of 9–15 cm Pb.

As has been described above, in our method of measuring ionization an electronic circuit automatically selects the smallest pulse from an array of five scintillation counters for measurement. This method of measurement can lead to serious errors if there are background pulses in a single counter which are small compared to the pulse magnitude at the maximum of the ionization spectrum, which, according to Landau's theory, decreases very rapidly in the direction of small energy losses. It is clear that the appearance of such small pulses which have nothing to do with the ionization spectrum can strongly distort the results of our method of measurement. To investigate this possibility we performed a separate experiment in which the ionization spectrum of the hard component was measured with a single scintillation counter, and the position of the maximum was found in the vicinity of the proton maximum(see Fig. 3). The results, taken with good statistical accuracy, showed the absence of pulses to the left of the ionization curve of a single scintillator.

Another control experiment evaluated the background due to possible inefficiencies of the anti-coincidence schemes. Results showed that the anti-coincidence arrays of our apparatus were at least 99.9% efficient, i.e., the number of particles which are falsely registered as having been absorbed in a particular filter do not exceed 0.1 % of the number of particles passing through the filter. In the proton spectrum region this anti-coincidence inefficiency can give no visible background since a majority of the particles passing through a given filter of our apparatus are mesons whose background in the region of high ionization is already eliminated by the selection of the smallest pulse. An insignificant background (order 2–3%) due to this inefficiency applies to the left portion of the spectra (Figs. 3–6).

5. DISCUSSION OF THE RESULTS

For interpretation of the results the abscissa of figures 3–6 were given in units of minimum ionization $\Delta_{0\,min}$. Simultaneously with measurements of the soft component spectra, measurements were made of the hard component (particles with penetration greater than 9 cm of lead), and the position of the ionization maximum Δ_0 calculated by averaging the values of Δ_0 for mesons from a momentum spectrum of mesons at sea level.

The magnitude of the most probable value of ionization Δ_0 was calculated from the equation:

$$\Delta_0 = \xi [\ln \xi + 2 \ln (p/\mu) + \ln (2m/I^2) - \beta^2 + 0.37 - \delta] \quad (8)$$

where δ is a correction for density (Eq. 8 without the quantity δ has been given by Landau in Ref. 2).

We computed the density correction from data of Sternheimer. [7] As in that reference, the ionization potential I for styrene was taken as 60 ev.

For the calculation of Δ_0 we used the known meson spectrum as given by Rossi, [8] taking into account more recent work. [9-20] The results of these workers, together with Rossi's spectrum are plotted in Fig. 7. The results of references 14 and 15 are not shown because they differed too much from all others; results of Glaser et al [11] are not shown because their spectrum is very similar to Rossi's. We see that notwithstanding the large number of papers which came out after Rossi's review, no important modifications need be made. We feel, however, that some changes should be made in the regions of high and low momenta . For momenta $p > 10000$ mev/ c we used the exponential law $S(p) \sim p^{-2,44}$, as found by Owen and Wilson [ref 20]. For momenta below 1000 mev/ c we adopted the spectrum given by a dotted line on Fig. 7. For the region below 500 mev/c the curve is determined by taking $S(R) = \text{const}$, if S is measured in gm^{-1} sec^{-1} $sterad^{-1}$ and R in gm/cm^2 of air. The existence of a plateau in this momentum region is shown in several papers. [12, 18, 19]

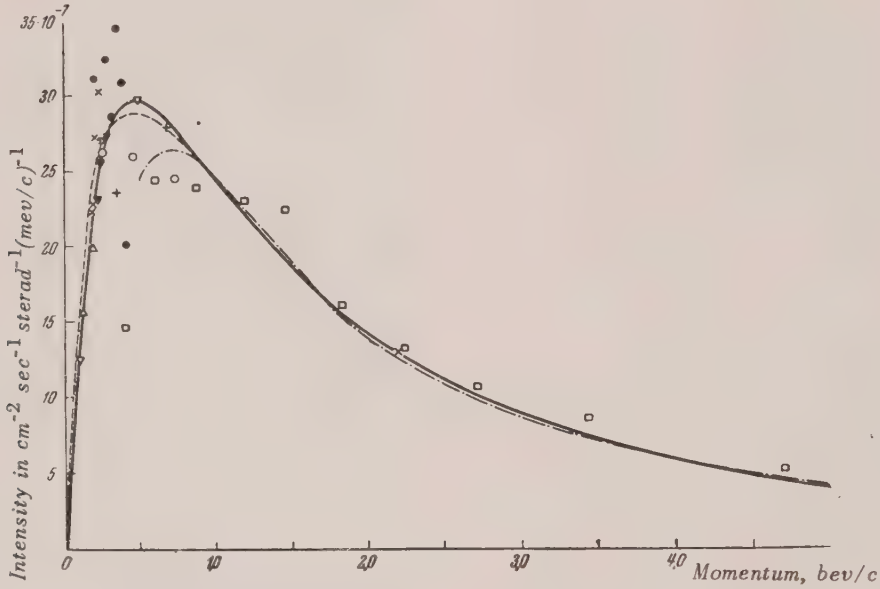

FIG. 7. Meson spectrum at sea level. ---Rossi[8], ——Owen and Wilson[20], Δ — Ref. 9, ▼ — Ref. 10, O — Ref. 12, ▽ — Ref. 13, + — Ref. 16, □ — Ref. 17, × — Ref. 18, ● — Ref. 19.

The result of averaging the values of Δ_0 on the meson spectrum, for the hard component, was $\bar{\Delta}_0 = 1.01\ \Delta_{0\,min}$. Thus the position of the maximum in the hard component spectra was calibrated in units of minimum ionization. The closeness of the magnitude of Δ_0 to that of minimum ionization is explained by our use of scintillation counters made of polystyrene, for which, as for some other organic scintillators, [3-5] theory predicts almost no increase of ionization with increase of particle energy due to the density effect, as expressed in Eq. 8.

In the calculation of Δ_0 for μ-mesons of the soft component we must take into account that in the described method of measuring ionization loss, i.e., by selection of the least loss, the maximum of the ionization spectrum are shifted to smaller values of ionization compared to the maxima obtained with a single counter. This circumstance follows from the fact that with selection of the least pulse the spectrum does not obey differential distribution of a single counter, but is the result of multiplying the differential curve by the $(n-1)$ power of the integral curve, as has been mentioned in Sec. 2. It follows that the new position of the maximum depends on the shape of the distribution for a single counter. If the single

counter obeys the Landau distribution, it is easy to derive an expression for the position of the ionization curve maximum Δ_{0n} which would be obtained in a system of n counters:

$$\Delta_{0n} = \Delta_0 (1 + \lambda_n \xi / \Delta_0), \qquad (9)$$

where λ_n is the number for which the general function $\varphi_n(\lambda)$, introduced in Sec. 2, has a maximum. For example, in our case of five counters $\lambda_5 \approx -1.0$.

It follows from equation 9 that the shift of the maximum, i.e., the ratio Δ_{0n} / Δ_0, varies slowly with the speed of the particle since the magnitude

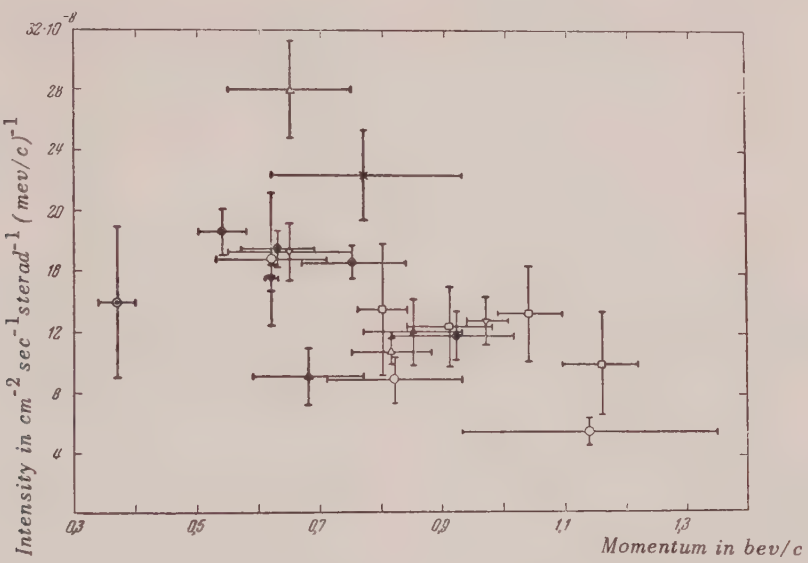

FIG. 8. Proton spectrum of cosmic rays at sea level: ⊙—Ref. 22, O— Ref. 24, Δ — Ref. 18, ▽— Ref. 25, ▼ — Ref. 26, ▲— Ref. 27, □— Ref. 28, •—data of this paper.

of ξ / Δ_0 depends only little on speed, as seen in Eq. 8. Numerical calculation shows that, within the limits of Landau's theory, the maximum spread of values of Δ_{0n} / Δ_0 for $n = 5$ is not greater than 0.5%. Thus the apparatus described above can be considered to a sufficient degree of accuracy as a linear device with respect to the various groups of particles whose ionization losses obey the Landau distribution.

Proceeding from this it is possible to calculate the value of Δ_0 for μ-mesons in the penetration intervals we investigated without the use of Eq. 8. These values are shown in Figs. 3–6 and are labeled with the letter $\Delta_{0\mu}$. The absence of a well defined μ-meson maximum in Figs. 3–6 is not surprising, since according to the literature[19] there are few μ-mesons in the soft component of cosmic rays. The left ends of the spectra in these figures are chiefly caused by electrons. In particular these particles are in the penetration interval 2–3 cm of lead, in which the number of μ-mesons is about 15% of the number of electrons.

It can be seen in Fig. 3 that the maximum of the electrons spectrum coincides with the value of minimum ionization, as would be expected from calculation with Eq. 8.

In calculating the magnitude of Δ_0 for protons in the measured penetration intervals we can not use Eq. 8, which comes from Landau's theory, since for protons of this penetration and for such counters as we used the basic condition for applicability of the theory is not fulfilled:

$$G = (\xi / E_{max}) \ll 1 \qquad (10)$$

(E_{max} is the maximum transferable energy). Therefore we made use of Symon's results, as described in Rossi's book[21], where calculations are made for more general cases, up to $G = 10$.

Using Symon's results we also calculated the shift of the maximum Δ_{0n} / Δ_0 for particles with various large values of G. It turned out that the value of Δ_{0n} / Δ_0 for such particles is quite close to that of Δ_{0n} / Δ_0 for particles obeying a

Landau distribution. Variations in this quantity of more than 0.5% begin only for $G \gtrsim 1.5$. Since the protons in the measured penetration interval have $G < 1.4$, we may conclude that our equipment is linear for the position of the proton spectra maxima.

Penetration interval in cm of lead	Observed number of protons		The number of protons in percent	
	Data of preliminary measurements	Data from which the spectra of Figs. 3–6 were obtained	of all particles in the penetration interval	of all particles with penetration greater than 9 cm lead.
2 — 3	47	95	4.34 ± 0.45	0.193 ± 0.017
3 — 5	70	109	7.33 ± 0.68	0.247 ± 0.019
5 — 9	75	166	8.62 ± 0.70	0.350 ± 0.023
9 — 15	—	130	7.90 ± 1.26	0.295 ± 0.041

Results of the calculation of Δ_0 according to Symon are indicated in Figs. 3–6 by the letter Δ_{0p}. We see that the positions of the right spectrum maxima are quite close to the calculated value Δ_{0p}, although still different. In particular the experimentally observed position of the maxima is smaller than the theoretical value by 4–5%. We have not been able to formulate a sufficiently convincing hypothesis to explain this discrepancy.

From the above discussion it follows that the right portion of the curves in Figs. 3–6 are the ionization spectra of the proton component of cosmic radiation. It is then possible to draw conclusions about the number of protons in cosmic rays at sea level in the measured penetration intervals. The results are given in a table, and presented as a momentum spectrum of protons (Figure 8) where the results of previous work are also given[18, 22-28]. In drawing our points on Fig. 8 and in calculating the statistical errors we took into account the data of preliminary experiments which are not included in the spectra of Figs. 3–6, although indicated in the table. With regard to the number of protons the results of the preliminary experiments are as accurate as the results which were used to construct the spectra of Figs. 3–6. The absolute intensity of the vertical proton flux was evaluated relative to the mesons of more than 9 cm lead penetration, whose flux was taken as 0.81×10^{-2} cm^{-2} sec^{-1} sterad^{-1}, in accordance with the spectrum of figure 7 and the exponential law $p^{-2.44}$ for $p > 10000$ mev/c.

In conclusion we express deep appreciation to V. P. Rumiantsev for aid in the work, and to Iu. F. Orlov for fruitful discussions of the results.

[1] S. Ia. Nikitin, J. Exptl. Theoret. Phys. (U.S.S.R.) 18, 577, (1948).

[2] L. Landau, J. Phys. USSR 8, 201 (1944).

[3] A. G. Meshkovskii, V. A. Shebanov, Dokl. Akad. Nauk SSSR 82, 233 (1952).

[4] T. Bowen, F. X. Roser, Phys. Rev. 85, 992, (1952).

[5] T. Bowen, Phys. Rev. 96, 754, (1954).

[6] A. Valeur, Bull. Soc. Chim. 29, 683, (1903).

[7] R. M. Sternheimer, Phys. Rev. 88, 851 (1952).

[8] B. Rossi, Rev. Mod. Phys. 20, 537, (1948).

[9] W. L. Kraushaar, Phys. Rev. 76, 1045 (1949).

[10] E. W. Kellermann and K. Westerman, Proc. Phys. Soc. (London) A62, 365 (1949).

[11] Glaser, Hamermesh and Safonov, Phys. Rev. 80, 625 (1950).

[12] M. Conversi, Phys. Rev. 79, 749 (1950).

[13] M. Sands, Phys. Rev. 77, 180 (1950).

[14] L. Germain, Phys. Rev. 80, 616 (1950).

[15] Caro, Parry and Rathgeber, Aust. J. Sci. Res., A4, 16 (1951).

[16] J. L. Zar, Phys. Rev. 83, 761 (1951).

[17] W. L. Wittemore and R. P. Shutt, Phys. Rev. 86, 940 (1952).

[18] C. M. York, Phys. Rev. 85, 998 (1952).

[19] P. G. Lichtenstein, Phys. Rev. 93, 858 (1954).

[20] B. G. Owen and J. G. Wilson, Proc. Phys. Soc. (London) A68, 409 (1955).

[21] Rossi, *High-energy Particles*, Prentice-Hall, New York, 1952 pp 29–37.

[22] G. D. Rochester and M. Bound, Nature 146, 745 (1940).

[23] Merkle, Goldwasser and Brode, Phys. Rev. 79, 926 (1950).

[24] M. G. Mylroi and J. G. Wilson, Proc. Phys. Soc. (London) A64, 404 (1951).

[25] A. I. Alikhanov and G. P. Eliseev, J. Exptl. Theoret. Phys. (U.S.S.R.) 21, 1009 (1951).

[26] A. I. Alikhanov and G. P. Eliseev, J. Exptl. Theoret. Phys. (U.S.S.R.) 25, 368 (1953).

[27] A. Z. Rosen, Phys. Rev. 93, 211, (1954).

[28] J. Ballam and P. G. Lichtenstein, Phys. Rev. 93, 851 (1954).

Translated by G. L. Gerstein
176

SOVIET PHYSICS JETP VOLUME 3, NUMBER 5 DECEMBER, 1956

Generalized Method for Calculating Damping in Relativistic Quantum Field Theory

V. I. GRIGORIEV
Moscow State University

(Submitted to JETP editor, March 1, 1955)
J. Exptl. Theoret. Phys. (U.S.S.R.) 30, 873-880 (May, 1956)

An infinite system of coupled equations is constructed, of which each describes a process involving the emission and absorption of a certain number of particles. This system is shown to be equivalent to the Tomonaga-Schwinger equation. The solution, which is derived by a process of successive substitutions, leads to results for the *S*-matrix which generalize the results of the theory of radiation damping.

IT has often been pointed out that the solution of the problems of the quantum theory of fields by means of perturbation theory leads to difficulties in a number of cases. In order to eliminate these difficulties, and to study the limits of applicability of the results obtained by means of perturbation theory, one has to develop a more consistent method of solving the equations of field theory. The present paper represents an attempt to develop a method of solution which guarantees that the normalization remains correct, and from which one obtains as an approximation the results of damping theory, and, as a zero-order approximation, perturbation theory.

We start from the usual equation for the scattering matrix:

$$i\hbar c \delta U[\sigma] / \delta \sigma(x) = \mathcal{H}(x) U[\sigma], \qquad (1)$$

where $\mathcal{H}(x)$ as usual, is the operator of the interaction Hamiltonian, which, if we limit the discussion to the case of the electron-positron and the electromagnetic fields (we consider these fields for definiteness, although the result can be generalized directly) takes the form

$$\mathcal{H}(x) = -j_\mu A_\mu \qquad (2)$$

$$= -\frac{e}{2}[\bar{\psi}(x)\gamma_\mu\psi(x) - \psi(x)\bar{\psi}(x)\gamma_\mu] A_\mu(x).$$

The operators $\bar{\psi}$, ψ, A_μ satisfy the equations of free fields and therefore, if we write

$$\bar{\psi}(x) = \bar{u}(x) + v(x); \quad \psi(x) = u(x) + \bar{v}(x); \qquad (3)$$

$$A_\mu(x) = A_\mu^{(+)}(x) + A_\mu^{(-)}(x),$$

we may interpret $A_\mu^{(+)}$, $\bar{u}$ and v as free-particle creation operators (creating photons, electrons and positrons, respectively) and $A_\mu^{(-)}$, u and $\bar{v}$ as absorption operators for the same free particles.

This basic equation is quite general, i.e., it describes any arbitrary process involving the creation and annihilation of particles in arbitrary states due to their mutual interaction. Moreover, as has already been pointed out, [1] Eq. (1) does not describe each of these processes separately, but contains them all simultaneously. In the process of solving the equation by perturbation theory, this connection between different processes is lost sight of in practice, and each is considered in isolation. We shall try to put forward a method of solution which is free from this disadavantage, and which uses this connection between different processes as a starting-point.

The physical picture behind this change is the following: As a result of the interactions between the particles the probability of the initial state decreases in the course of time, while simultaneously the probabilities of the mutually com-

peting transitions into new states are building up; the transitions themselves look like the absorption of free particles with certain energies and momenta, and the creation of particles with others.

Our task is to construct a solution which corresponds to this physical picture. One of the simplest ways to this end is to put

$$U = \sum_{\xi=0}^{\infty} U^{(\xi)}, \tag{4}$$

where (ξ) stands as a symbol for the set of suffixes $(i, j; n, m; \rho, \sigma)$. The operator $U^{(\xi)}$ which we have introduced represents the transition matrix for a transition in which i photons, n electrons and p positrons present in the initial state are absorbed, and j photons, m electrons, and σ positrons emitted (the emitted particles belong to the final state). In this way we clearly take into account the fact that the general scattering matrix consists of a sum of the operators of all particular types of transition.

However, the mere "splitting" of the transition matrix U into a sum of partial transition matrices $U^{(\xi)}$ is not enough. One has to find a set of equations which connect all the $U^{(\xi)}$ and solve these with some or other degree of accuracy. We have previously given such equations [1] for a simplified problem. The method used here of "splitting" the equations can be extended to the general case. The essence of the method is to replace the basic equation (10), which, with the use of (4), may be written in the form

$$i\hbar c \frac{\delta \sum_{\xi} U^{(\xi)}}{\delta\sigma(x)} = -\frac{e}{2}[(\bar{u}(x) + v(x))\gamma_\mu (u(x) + \bar{v}(x)) - (u(x) + \bar{v}(x))(\bar{u}(x) + v(x))\gamma_\mu](A_\mu^{(+)}(x) + A_\mu^{(-)}(x))\sum_{\xi} U^{(\xi)}[\sigma], \tag{5}$$

by a system of equations which (a) when added together replace (5), (b) when taken separately, would each describe a process with the emission and absorption of a given number of particles, as distinct from (5) which contains the whole set of possible processes. The fact that an equation describes a process with a fixed number of emitted and absorbed particles means that each term in the equation must describe the emission and absorption of the same number of particles.

In "splitting" Eq. (5) one must note that $U^{(\xi)}$ contains i photon absorption operators $A^{(-)}$, and j photon creation operators $A^{(+)}$. Similarly, it contains n operators u, m operators $\bar{u}$, ρ operators v and σ operators $\bar{v}$. The system of equations obtained after this "splitting" may be written schematically in the form

$$i\hbar c \delta U^{(\xi)} / \delta\sigma = \sum H^{(\xi)}_{(\xi')} U^{(\xi')}, \tag{6}$$

where $H^{(\xi)}_{(\xi')}$ is an interaction operator which represents one of the sixteen terms in $\mathfrak{H}(x)$, and where the labels in ξ' may differ from the corresponding labels in ξ on the left-hand side at most be one each (some of the numbers n, n' m, m'; ρ, ρ'; σ, σ' may also be the same). One may show without difficulty that the system of equations (6) is consistent, but we shall not give the proof here.

We shall not write out the right-hand side of Eq (6) explicitly, because of its unwieldy form (it contains 128 terms) but we shall only discuss the method of construction of these terms, and consider a number of typical examples.

The values which the labels ξ' may take in a term on the right-hand side of (6) depend on which of the operators $A^{(+)}$, $A^{(-)}$, $\bar{u}$, u, $\bar{v}$, v occur in that term. For terms containing $A^{(-)}$, $i' = i-1$; $j' = j$, or $i' = i$, $j' = j+1$. In the terms with $A^{(+)}$, $i' = i$, $j' = j-1$, or $i' = i+1$; $j' = j$. In quite a similar way one can express the labels n', m' and $\rho'\sigma'$ in terms of n, m, ρ and σ according to which operators of the electron-positron field occur in the term under discussion. The only difference is that each term contains two electron-positron field operators, which may be grouped in pairs: u and $\bar{u}$, v and $\bar{v}$, u and v, and $\bar{u}$ and $\bar{v}$, whereas the electromagnetic field operator occurs only once. This difference reflects the inportant fact that photons are absorbed and emitted singly, whereas the creation and annihilation of the particles of the electron-positron field can occur only in pairs (electron and positron). This causes no essential complication in the determination of the labels n', m', ρ' and σ', but in writing them down one has to remember the effect of the various spinor operators.

Consider a few terms as examples:

1) $\bar{u}\gamma_\mu A_\mu^{(-)} u U^{(i-1,\ j;\ n-1,\ m-1;\ \rho,\ \sigma)}$.

This term describes the absorption of a photon, and the absorption of an electron in one state, and its emission in another; the total number of spinor particles therefore remains the same, and the process looks like the transition of an electron from one state to another with the absorption of a photon.

2) $\bar{u}\gamma_\mu A_\mu^{(+)} u U^{(i,\ j-1;\ n,\ m;\ \rho,\ \sigma)}$.

This term corresponds to the emission of a photon in the transition of an electron from one state to another. However, in distinction from the case considered above, the last transition is connected withthe absorption (and emission) of an electron which was previously emitted (absorbed), and not withthe absorption or emission of "new" electrons.

3) $\bar{u}\gamma_\mu A_\mu^{(-)}\bar{v}U^{(i,\,j+1;\,n,\,m-1;\,\rho,\,\sigma-1)}$.

This term corresponds to the absorption of a previously emitted photon and the simultaneous creation of an electron-positron pair.

4) $v\gamma_\mu A_\mu^{(+)}uU^{(i+1,\,j;\,n,\,m+1;\,\rho,\,\sigma+1)}$.

This term corresponds to the emission of a photon which was previously absorbed, and the absorption of a previously emitted electron-positron pair.

5) $v\gamma_\mu A_\mu^{(+)}\bar{v}U^{(i,\,j-1;\,n,\,m;\,\rho-1,\,\sigma-1)}$.

This term corresponds tothetransition of a positron from one state to another with the emission of a photon.

These examples will suffice to showthat all kinds of possible processes find their expression in the equations (6).

The unwieldy form ofthe equations (6) is no unsurmountable obstacle for their analysis. In a number of cases a kind of "operator dimension rule" proves convenient: all terms in the equation must contain $A^{(+)}$, $A^{(-)}$, u, $\bar{u}$, v, $\bar{v}$ to similar degrees; it should, however, be remembered that certain bilinear combinations of creation and annihilation operators of certain fields have "zero" dimension (if the operators relate to the same particles) in other words they are c-numbers.

It is easy to see that the sum of all the equations (6) gives the original Eq (5) , as it should do. Indeed, the sum of the left-hand sides of (6) gives

$$i\hbar c\sum_\xi \frac{\delta U^{(\xi)}}{\delta\sigma} = i\hbar c\,\frac{\delta}{\delta\sigma}\left[\sum_\xi U^{(\xi)}\right] = i\hbar c\,\frac{\delta U}{\delta\sigma}\,. \tag{7}$$

The sum of the right-hand sides is

$$\sum_\xi\sum_{\xi'} H^{(\xi)}_{(\xi')}U^{(\xi')} = \sum_{\xi'}\mathcal{H}U^{(\xi')} = \mathcal{H}U. \tag{8}$$

It is easy to see that the sum of (6) contains all the terms which occur on the right-hand side of (5) and that each term occurs only once.

One can also show that the original equation (10) and the requirements (a) and (b) determine the system (6) uniquely. Indeed, if we add to the various equations (6) further terms whose sum vanishes, then requirement (a) would remain satisfied, but (b) would be violated. And, similarly, any addition to (6) which would satisfy (b), would violate (a). Hence the transition from (1) to (6) subject to the conditions (a) and (b) is unambiguous.

We now turn to the problem of solving (6), i.e.,, of finding $U^{(\xi)}$. Consider first time-dependent problems (stationary states will be discussed later) i.e. we require a solution which satisfies the initial condition

$$U^{(0)}[\sigma_0] = 1,\quad U^{(\xi)}[\sigma_0] = 0, \tag{9}$$

if (ξ) (i.e. at least one of the labels i, j; n, m; ρ, σ) differs from zero.

We look for the solution by the method of substitution, which consists in inserting, on the right-hand side of (6) for the operator $U^{(\xi')}$ its value

$$U^{(\xi')} = -\frac{i}{\hbar c}\left(\frac{\delta}{\delta\sigma}\right)^{-1}\sum_{\xi''} H^{(\xi')}_{(\xi'')}U^{\xi''}. \tag{10}$$

The operator $(\delta/\delta\sigma)^{-1}$ which is the inverse of a functional derivative, may in all the cases which we shall meet here, be interpreted as an integral over the four-dimensional region bounded by the hypersurfaces σ_0 and σ.

As a result of substituting (10) on the right-hand side of (6) there occurs a $U^{(\xi'')}$ with new labels (ξ''). This we can in turn express in terms of $U^{(\xi)}$, etc. As a result of such successive substitutions one obtains an equation of the type

$$\frac{\delta U^{(\xi)}}{\delta\sigma} = \sum_{q,\,\xi',\,\xi'',\,\ldots}\left(\frac{-i}{\hbar c}\right)^{i+j+2q} \left[H^{(\xi)}_{(\xi')}\left(\frac{\delta}{\delta\sigma}\right)^{-1}\cdots\left(\frac{\delta}{\delta\sigma}\right)^{-1}H^{(\xi_{i+j+2q-1})}_{(\xi_{i+j+2q})}\right]U^{(0)} + \sum_{l,\,\xi',\,\xi'',\,\ldots}\left(\frac{-i}{\hbar c}\right)^{2l} \left[H^{(\xi)}_{(\xi')}\left(\frac{\delta}{\delta\sigma}\right)^{1}\cdots\left(\frac{\delta}{\delta\sigma}\right)^{-1}H^{(\xi_{2l-1})}_{(\xi_{2l})}\right]U^{(\xi)} + Q. \tag{11}$$

Here we have divided the terms on the right-hand side into three groups. The first consists of the terms which contain $U^{(0)}$. Each of these contains i, n, ρ annihilation and j, m, σ creation operators for photons, electrons and positrons, respectively. In addition, these terms may contain q operators $A^{(+)}$ and q operators $A^{(-)}$, which form a combination $(A^{(+)}A^{(-)})$ of "operator dimension zero".*

*And a corresponding number of combinations of "operator dimension zero" of electron-photon field operators (uu), (vv) since to every electromagnetic field operator belong two operators of the electron-positron field.

The second group of terms in (11) contains $U^{(\xi)}$, where (ξ) is that label which occurs on the left-hand side of the equation. The structure of the terms of this second group differs from that of the first group in that the numbers of photon emission and absorption operators contained in them are equal (and equal to l).

Finally, a third group of terms, which we have denoted by Q, contain those operators $U^{(\xi')}$ whose labels (ξ') are neither zero, nor equal to that which stands on the left-hand side of (11). By carrying the process of substitution far enough, we may make the order of the terms Q as high as we like, so that, at any rate in electrodynamics where the coupling constant is small, Q may be neglected.

In solving concrete problems, we shall restrict the discussion to terms of a certain order, and neglect Q. To neglect Q is similar to the device of cutting off the chain of linked equations in the Tamm Dancoff method.[2] Omitting Q, we are left with the following equation to be solved:

$$\delta U^{(\xi)}[\sigma]/\delta\sigma(x) = K_0^{(\xi)} U^{(0)}[\sigma] + K_l^{(\xi)} U^{(\xi)}[\sigma], \tag{12}$$

where

$$K_0^{(\xi)} = \sum_{q=0}^{\infty} \left(\frac{-i}{\hbar c}\right)^{i+j+2q} B^{(i+q,\, j+q)} \left\{ H_{(\xi')}^{(\xi)} \left(\frac{\delta}{\delta\sigma}\right)^{-1} \cdots \left(\frac{\delta}{\delta\sigma}\right)^{-1} H_{(\xi_{i+j+2q})}^{(\xi_{i+j+2q-1})} \right\}; \tag{13}$$

$$K_l^{(\xi)} = \sum_{l=1}^{\infty} \left(\frac{-i}{\hbar c}\right)^{2l} B^{(l,\, l)} \left\{ H_{(\xi')}^{(\xi)} \left(\frac{\delta}{\delta\sigma}\right)^{-1} \cdots \left(\frac{\delta}{\delta\sigma}\right)^{-1} H_{(\xi_{2l})}^{(\xi_{2l-1})} \right\}.$$

In line with what was said above, the operators $B^{(i+q,\, j+q)}\{\ldots\}$ denote the sum of all possible permutations of $A^{(+)}$ and $A^{(-)}$ in operators of the type

$$H_{(\xi')}^{(\xi)} \left(\frac{\delta}{\delta\sigma}\right)^{-1} \cdots \left(\frac{\delta}{\delta\sigma}\right)^{-1} H_{(\xi_i)}^{(\xi_{i-1})},$$

containing $i + q$ operators $A^{(-)}$ and $j + q$ operators $A^{(+)}$, in such a way that q pairs of such operators refer to the same photon states (and form bilinear combinations which are c-numbers).

Equation (12) by itself is not sufficient. For a complete formulation of the problem, we must also write down an equation for $U^{(0)}[\sigma]$. This equation could be derived by the method of successive substitutions from the system (6); however, we shall not derive it in that manner, but obtain it directly from (12) by putting there $(\xi) = (0)$:

$$\frac{\delta U^{(0)}[\sigma]}{\delta\sigma(x)} = \sum_{l=1}^{\infty} \left(\frac{-i}{\hbar c}\right)^{2l} B^{(l,\, l)} \left\{ H_{(\xi')}^{(\xi)} \left(\frac{\delta}{\delta\sigma}\right)^{-1} \cdots \left(\frac{\delta}{\delta\sigma}\right)^{-1} H_{(\xi_{2l})}^{(\xi_{2l-1})} \right\} U^{(0)}[\sigma] = K^{(0)} U^{(0)}[\sigma]. \tag{14}$$

The final form of the equations to be investigated is

$$U^{(\xi)}[\sigma] = \int_{\sigma_0}^{\sigma} K_0^{(\xi)} U^{(0)}[\sigma]\, d\omega + \int_{\sigma_0}^{\sigma} K_l^{(\xi)} U^{(\xi)}[\sigma]\, d\omega; \tag{15a}$$

$$U^{(0)}[\sigma] = 1 + \int_{\sigma_0}^{\sigma} K^0 U^{(0)}[\sigma]\, d\omega. \tag{15b}$$

In forming the Eqs. (15) we have made use of the initial condition (9).

Our next task consists in considering the Eq. (15).

It goes without saying that the method of successive substitutions, with the omission of the Q terms, which we used in obtaining (15) is not the only way of solving the fundamental set (6). Even considering only approximate solutions one could have given other ways of approach, which might be more convenient, for example, in the case of strong coupling. However, we shall confine our attention to the discussion of the Eqs. (15) in view of their relative simplicity. Indeed, as has already been stated, our initial set (6) is most unwieldy. Although we have obtained our Eqs. (15) from (6), they can in practice also be written down directly without reference to (6). For this purpose we must only observe the rule of "operator dimensions", according to which all the terms in each equation must describe the emission and absorption of the same number of particles (not only of photons, but of each other kind). One must then also allow for the fact that bilinear expressions of absorption and

emission operators relating to the same particle have "operator dimension" zero.

From this "operator dimension" rule it is at once evident, in particular, that $U^{(\xi)}$ may differ from the corresponding quantity obtained from perturbation theory, $U^{(\xi)}_{\text{pert}} = U^{(\xi)}_0$ only by a c-number factor (i.e., a factor of "operator dimension" zero). Using this fact, and noting also that

$$U_0^{(\xi)} = \int_{\sigma_0}^{\sigma} K_0^{(\xi)}\, d\omega, \tag{16}$$

we shall look for a solution of (15) in the form

$$U^{(\xi)}[\sigma] = \int_{\sigma_0}^{\sigma} K_0^{(\xi)}\, U^{(0)}\, \varepsilon^{(\xi)}\, d\omega, \tag{17}$$

where $\epsilon^{(\xi)}$ is a certain unknown c-number quantity which remains to be determined, and $U^{(0)}[\sigma]$ is found from Eq. (15b). It is easy to see that the insertion in (12) of the value of $U^{(0)}[\sigma]$ obtained from (15b) by iteration is equivalent to an increase of q in the expression for $K_0^{(\xi)}$.

We may therefore write down the following equation for the determination of the quantity $\epsilon^{(\xi)}$:

$$K_0^{(\xi)}\, \varepsilon^{(\xi)} = K_0^{(\xi)} + K_l^{(\xi)} \int_{\sigma_0}^{\sigma} K_0^{(\xi)}\, \varepsilon^{(\xi)}\, d\omega. \tag{18}$$

We shall be interested only in the asymptotic solution for $\sigma \to \infty$, $\sigma_0 \to -\infty$, and this makes it possible to write the equation for $\epsilon^{(\xi)}$ in the form

$$\varepsilon^{(\xi)} = 1 + \overline{K}_0^{(\xi)} K_l^{(\xi)} \int_{-\infty}^{\infty} K_0^{(\xi)}\, \varepsilon^{(\xi)}\, d\omega \,/\, \overline{K}_0^{(\xi)} K_0^{(\xi)}, \tag{19}$$

where $\overline{K}_0(\lambda)$ is the conjugate of $K_0^{(\xi)}$.

We have written (19) in a form which makes it obvious that $\xi^{(\xi)}$ is a c-number. Indeed all coefficients in (19) are operators in diagonal form, and this proves our statement that $\xi^{(\xi)}$ is a c-number.

We see from the relation (17) that the result of perturbation theory corresponds to the zero-order approximation $\xi^{(\xi)} = 1$ in the solution of (19).

If we represent $\xi^{(\xi)}$ in the form

$$\varepsilon^{(\xi)} = \frac{1}{(1 - R^{(\xi)})}, \quad R^{(\xi)} = \frac{K_0^{(\xi)} K_l^{(\xi)} \int_{-\infty}^{\infty} K_0^{(\xi)}\, d\omega}{\overline{K}_0^{(\xi)} K_0^{(\xi)}}, \tag{20}$$

we find the following expression for the S matrix:

$$S^{(\xi)} = \int_{-\infty}^{\infty} K_0^{(\xi)} \frac{d\omega}{1 - R^{(\xi)}}. \tag{21}$$

If we restrict the discussion to one-electron problems, and neglect in the expression for $K^{(\xi)}$ all terms with $q > 0$, then the value (21) for $S^{(\xi)}$ reduces to that obtained earlier from the generalized damping theory. Thus our solution reduces, in appropriate limits, to damping theory and to perturbation theory.

We do not need to investigate specially whether the normalization is correct, since this is already proved within the framework of damping theory. Thus the solution which we have constructed satisfies the requirements set out in the beginning of this paper. *

We see from (20) that the perturbation theory gives a satisfactory approximation when $R^{(\xi)} \to 0$, which is usually the case at low energies. But if $R^{(\xi)}$ is appreciable, then the result may differ appreciably from that of perturbation theory. It has been shown in a number of examples that $\xi^{(\xi)}$ may play the part of a cut-off factor, which will reduce the general magnitude of the cross sections at high energies. However, the appearance of the general solution does not in general exclude other possibilities. The detailed discussion has to be carried out separately for each case.

We still have to refer to the elimination of divergences. Since the whole theory has been formulated in a manifestly covariant way, we may use the same methods for eliminating the divergences as in the usual theory. The results obtained after removing the infinities, may, however, differ from the results of perturbation theory. We shall not examine the questions of self-energy and charge, since they do not lie within the scope of this paper.

The method explained above is applicable not only to the case of the electron-positron and the electromagnetic fields, but also to any arbitrary combination of fields. As we increase the number of interactions which are considered, we must add to (ξ) more labels; the total number of pairs of labels in (ξ) equals the number of types of elementary particles.

However, our method is general not only in its applicability to any types of field. This method may be used also to study various kinds of generalized theory (those containing derivatives of higher order, nonlinear interactions, some kind of nonlocal generalizations, etc.). We note incidentally that in theories with nonlinear interactions ($H \sim \varphi^n$)[3] the damping must play a much more significant part than

* Actually our solution corresponds to a partial summation of a series of successive approximations.

with the usual linear interactions.

The method may also be generalized to stationary problems for which one cannot determine initial conditions. In that case the problem reduces to a set of homogeneous integral equations which may be obtained from (12) by omitting the terms in U^0. In solving stationary problems one may use the method of residues. Problems involving several particles lead to equations of the Bethe-Salpeter type.

In the region of low energies the method proposed above leads, as a rule, to the same results as perturbation theory (in corresponding approximations). At high energies, however, the corrections may be appreciable, in particular as regards the relative importance of various processes.

It is a valuable duty to thank I. M. Lomsadze for valuable discussions.

[1]V. I. Grigoriev, J. Exptl. Theoret. Phys. (U.S.S.R.) 25, 40 (1953).

[2]I. Tamm, J. Phys. USSR 9, 449 (1945).

[3]D. Ivanenko and V. Lebedev, Dokl. Akad. Nauk SSSR 80, 357 (1951).

Translated by R. E. Peierls
180

SOVIET PHYSICS, JETP VOLUME 3, NUMBER 5 DECEMBER, 1956

Theory of Wave Motion of an Electron Plasma

A. I. Akhiezer and R. V. Polovin
Physico-Technical Institute, Acacemy of Sciences, Ukrainian SSR
Kharkov State University

(Submitted to JETP editor March 19, 1955)
J. Exptl. Theoret. Phys. (U.S.S.R.) 30, 915-928 (May, 1956)

A general investigation of the nonlinear wave motions of an electron plasma has been carried out for arbitrary electron velocities. Temperature effects are not taken into account, and the state of the plasma is characterized not by a distribution function, but by the particle density. A correspondence is established between the wave motion of the plasma and the motion of a nonrelativistic particle in a certain potential field. The variation of the frequency of longitudinal vibrations on the velocity amplitude has been determined. Nonlinear transverse vibrations of the plasma, and vibrations close to these, are also considered, and their frequencies determined. A number of relations are established for the complicated longitudinal transverse plasma oscillations.

---

1. FUNDAMENTAL EQUATIONS

IN the study of the oscillatory behavior of an electron plasma, i.e., of an electron gas neutralized by ions, or a neutralized electron beam, it is usually assumed that the electron velocities and the density fluctuations are small, so that one may use a linearized system of equations. This scheme makes it possible to determine the frequencies of oscillation and to discuss, by means of gas-kinetic considerations, the part played by temperature effects[1,2], which turn out in general to be unimportant.

Nonlinear plasma oscillations were considered in a previous paper[3], in which temperature effects were neglected, and the electron velocity was assumed to be finite, but essentially nonrelativistic. Under these assumptions it is found that the oscillation frequency is independent of the velocity amplitude, and obeys the classical formula of Langmuir.

The purpose of the present paper is to investigate the oscillatory motion of the plasma quite generally, for arbitrary velocities. But, as in Ref. 3, we shall neglect temperature effects, i.e, we shall assume the plasma temperature to be zero. This approximation is very natural when we are investigating nonlinear oscillations even in a "high-temperature" plasma, and even more so in the study of plasma oscillations in electron beams, where the temperature is practically zero. Under these conditions it is not necessary to introduce a distribution function to specify the state of the plasma, but one

may use the electron density, which depends on the coordinates and time. Some of the conclusions derived below apply also to the case of a plasma in an external magnetic field.

Assuming the plasma infinitely extended, we shall start from the following fundamental equations for the quantities E, H, the density n and the electron velocity v:

$$\operatorname{curl} \mathbf{E} = -\frac{1}{c}\frac{\partial \mathbf{H}}{\partial t}; \tag{1}$$

$$\operatorname{curl} \mathbf{H} = \frac{1}{c}\frac{\partial \mathbf{E}}{\partial t} + \frac{4\pi}{c} ne\,\mathbf{v}; \qquad \operatorname{div} \mathbf{H} = 0;$$

$$\operatorname{div} \mathbf{E} = 4\pi e\,(n - n_0);$$

$$\frac{\partial \mathbf{p}}{\partial t} + (\mathbf{v}\nabla)\,\mathbf{p} = e\,\mathbf{E} + \frac{e}{c}[\mathbf{v}\times\mathbf{H}]$$

Here n_0 is the equilibrium density of electrons, equal also to the density of the ions, which are assumed infinitely heavy and immobile; p is the electron momentum, equal to $m\mathbf{v}[1-(v^2/c^2)]^{-1/2}$.

Our problem consists of the general investigation of the wave motions of the plasma, i.e., of such electron motions for which all the variables entering into Eq. (1) are functions not of r and t separately, but only of the combination $\mathbf{i}\cdot\mathbf{r} - Vt$, where i is a constant unit vector, and V a constant. The meaning of this type of solution is that it represents plane waves travelling in the direction i with speed V.

If we denote derivatives with respect to this argument by a prime, we can rewrite Eqs. (1) in the form

$$[\mathbf{i}\times\mathbf{E}'] = \beta\,\mathbf{H}', \tag{2}$$

$$[\mathbf{i}\times\mathbf{H}'] = -\beta\mathbf{E}' + \frac{4\pi}{c} en\,\mathbf{v}, \tag{3}$$

$$\mathbf{i}\cdot\mathbf{H}' = 0, \tag{4}$$

$$\mathbf{i}\cdot\mathbf{E}' = 4\pi e\,(n - n_0), \tag{5}$$

$$(\mathbf{i}\cdot\mathbf{v} - V)\,\mathbf{p}' = e\,\mathbf{E} + \frac{e}{c}[\mathbf{v}\times\mathbf{H}], \tag{6}$$

where $\beta = V/c$. By integrating (2) we obtain

$$\mathbf{H} = \beta^{-1}[\mathbf{i}\times\mathbf{E}] + \mathbf{H}_0, \tag{7}$$

where $\mathbf{H}_0$ is the intensity of the external magnetic field acting on the plasma. If there is no such field, and the plasma performs self-oscillations, then $\mathbf{H} = \beta^{-1}\,\mathbf{i}\times\mathbf{E}$. In that case

$$\mathbf{i}\cdot\mathbf{H} = 0, \qquad \mathbf{E}\cdot\mathbf{H} = 0. \tag{8}$$

In other words, the magnetic field is in that case transverse and perpendicular to the electric field.

From (3) and (5) we see that

$$n = n_0 V/(V - \mathbf{i}\cdot\mathbf{v}). \tag{9}$$

Since $n > 0$ it follows that $\mathbf{i}\cdot\mathbf{v} < V$, i.e., the component of the electron velocity in the direction of propagation of the wave must always be less than the phase velocity.

We multiply (6) on the left vectorially by i and use (7). This gives

$$\mathbf{H} = -\frac{c}{e}[\mathbf{i}\times\mathbf{p}'] + \frac{V\mathbf{H}_0 - \mathbf{v}\,(\mathbf{i}\mathbf{H}_0)}{V - \mathbf{i}\cdot\mathbf{v}}. \tag{10}$$

Next we multiply (3) on the left vectorially by i and find

$$\mathbf{H}' = (4\pi/c)\,en\,(\beta^2 - 1)^{-1}[\mathbf{i}\times\mathbf{v}] \tag{11}$$

From (10) and (11) it follows that

$$[\mathbf{i}\times\mathbf{p}]'' + \frac{4\pi e^2 n}{(\beta^2-1)c^2}[\mathbf{i}\times\mathbf{v}] = \frac{e}{c}\left(\frac{V\mathbf{H}_0 - \mathbf{v}\,(\mathbf{i}\mathbf{H}_0)}{V - \mathbf{i}\cdot\mathbf{v}}\right)'. \tag{12}$$

Taking the scalar product of (6) with i and using (5) we find

$$\left((\mathbf{i}\cdot\mathbf{v} - V)\,\mathbf{i}\cdot\mathbf{p}' + [\mathbf{i}\times\mathbf{v}]\,[\mathbf{i}\times\mathbf{p}]' - e\beta\frac{\mathbf{i}\,[\mathbf{v}\mathbf{H}_0]}{V - \mathbf{i}\cdot\mathbf{v}}\right)' \tag{13}$$

$$\operatorname{div} \mathbf{E} = 4\pi e\,(n -$$

The Eqs. (12) and (13) determine the transverse and longitudinal velocity components in the general case when $\mathbf{H}_0$ does not vanish.

Taking the vector i in the z direction, and introducing the dimensionless momentum $\rho = \mathbf{P}/mc$ and the dimensionless velocity $\mathbf{u} = \mathbf{v}/c$, we bring (12) and (13) to the form

$$\frac{d^2\rho_x}{d\tau^2} + \omega_0^2\frac{\beta^2}{\beta^2-1}\frac{\beta}{\beta - u_z}u_x + \beta\frac{d}{d\tau}\frac{\beta\Omega_y - u_y\Omega_z}{\beta - u_z} = 0;$$

$$\frac{d^2\rho_y}{d\tau^2} + \omega_0^2\frac{\beta^2}{\beta^2-1}\frac{\beta}{\beta - u_z}u_y - \beta\frac{d}{d\tau}\frac{\beta\Omega_x - u_x\Omega_z}{\beta - u_z} = 0;$$

$$\frac{d}{d\tau}\left\{(u_z - \beta)\frac{d\rho_z}{d\tau} + u_x\frac{d\rho_x}{d\tau}\right.$$

$$\left. + u_y\frac{d\rho_x}{d\tau} + \frac{\beta^2}{\beta - u_z}(u_x\Omega_y - u_y\Omega_x)\right\} = \omega_0^2\frac{\beta^2 u}{\beta - u_z}, \tag{14}$$

where $\tau = t - (\mathbf{i}\cdot\mathbf{r}/V)$, $\omega_0^2 = 4\pi e^2 n_0/m$, $\Omega = e\mathbf{H}_0/mc$:

In the absence of the external field $\mathbf{H}_0$ the equations of motion (14) take the form

$$\frac{d^2\rho_x}{d\tau^2} + \omega_0^2 \frac{\beta^2}{\beta^2-1}\frac{\beta}{\beta-u_z}u_x = 0;$$

$$\frac{d^2\rho_y}{d\tau^2} + \omega_0^2 \frac{\beta^2}{\beta^2-1}\frac{\beta}{\beta-u_z}u_y = 0; \qquad (15)$$

$$\frac{d}{d\tau}\left\{(u_z-\beta)\frac{d\rho_z}{d\tau} + u_x\frac{d\rho_x}{d\tau} + u_y\frac{d\rho_y}{d\tau}\right\} = \omega_0^2\frac{\beta^2 u_z}{\beta-u_z}.$$

or

$$\frac{d^2\rho_x}{d\tau^2} + \omega_0^2\frac{\beta^2}{\beta^2-1}\frac{\beta\rho_x}{\beta\sqrt{1+\rho^2}-\rho_z} = 0;$$

$$\frac{d^2\rho_y}{d\tau^2} + \omega_0^2\frac{\beta^2}{\beta^2-1}\frac{\beta\rho_y}{\beta\sqrt{1+\rho^2}-\rho_z} = 0; \qquad (15')$$

$$\frac{d^2}{d\tau^2}(\beta\rho_z - \sqrt{1+\rho^2}) + \omega_0^2\frac{\beta^2\rho_z}{\beta\sqrt{1+\rho^2}-\rho_z} = 0.$$

The first two equations (15) for the transverse components evidently admit finite solutions only if $\beta > 1$, i.e., $V > c$. As regards the third equation (15) for the longitudinal velocity component u_z, it has finite solutions for arbitrary β, if $u_x = u_y = 0$. Such purely longitudinal motions for $\beta < 1$ are, however, unstable because of the coupling between longitudinal and transverse motion.

If we introduce, in place of the momentum components, the new variables

$$\xi = \sqrt{\beta^2-1}\,\rho_x,$$

$$\eta = \sqrt{\beta^2-1}\,\rho_y, \qquad \zeta = \beta\rho_z - \sqrt{1+\rho^2},$$

we obtain (15′) in the form

$$\frac{d^2\xi}{d\tau^2} + \omega_0^2\frac{\beta^2}{\beta^2-1}\frac{\beta\xi}{\sqrt{\beta^2-1+\xi^2+\eta^2+\zeta^2}} = 0; \qquad (16)$$

$$\frac{d^2\eta}{d\tau^2} + \omega_0^2\frac{\beta^2}{\beta^2-1}\frac{\beta\eta}{\sqrt{\beta^2-1+\xi^2+\eta^2+\zeta^2}} = 0;$$

$$\frac{d^2\zeta}{d\tau^2} + \omega_0^2\frac{\beta^2}{\beta^2-1}\frac{\beta\zeta}{\sqrt{\beta^2-1+\xi^2+\eta^2+\zeta^2}} + \omega_0^2\frac{\beta^2}{\beta^2-1} = 0.$$

These equations can be derived from the Lagrangian

$$L = \frac{1}{2}\left[\left(\frac{d\xi}{d\tau}\right)^2 + \left(\frac{d\eta}{d\tau}\right)^2 + \left(\frac{d\zeta}{d\tau}\right)^2\right] \qquad (17)$$

$$- \omega_0^2\frac{\beta^2}{\beta^2-1}[\beta\sqrt{\beta^2-1+\xi^2+\eta^2+\zeta^2}+\zeta].$$

Hence, the general problem of the wave motion of the plasma in the absence of an external magnetic field is equivalent to that of the nonrelativistic motion of a particle of unit mass in a field with potential energy

$$U = \omega_0^2\frac{\beta^2}{\beta^2-1} \qquad (17')$$

$$(\beta\sqrt{\beta^2-1+\xi^2+\eta^2+\zeta^2}+\zeta).$$

From the form of the Lagrangian follows immediately the laws of conservation of energy and momentum:

$$\frac{1}{2}\left[\left(\frac{d\xi}{d\tau}\right)^2 + \left(\frac{d\eta}{d\tau}\right)^2 + \left(\frac{d\zeta}{d\tau}\right)^2\right]$$

$$+ \omega_0^2\frac{\beta^2}{\beta^2-1}[\beta\sqrt{\beta^2-1+\xi^2+\eta^2+\zeta^2}+\zeta] = \mathcal{E};$$

$$\xi d\eta/d\tau - \eta d\xi/d\tau = M.$$

If we go back from the variables ξ, η, ζ to the fields $\mathbf{E}$ and $\mathbf{H}$, and the velocity $\mathbf{v}$, these laws take the following form:

$$\frac{\beta}{8\pi}(\mathbf{E}^2+\mathbf{H}^2) + \beta n_0\frac{mc^2}{\sqrt{1-v^2/c^2}} \qquad (18)$$

$$- \frac{1}{4\pi}\mathbf{i}\cdot[\mathbf{E}\times\mathbf{H}] = \text{const};$$

$$\mathbf{p}\times\mathbf{H} = \text{const}.$$

We note that these relations are simple consequences of our fundamental equations. Indeed, taking the scalar product of (3) with $\mathbf{H}'$, one sees easily that $\mathbf{v}\cdot\mathbf{H}' = 0$, i.e., $\mathbf{p}\cdot\mathbf{H}' = 0$. From the scalar product of $\mathbf{H}$ with (6) we see also that $\mathbf{p}'\cdot\mathbf{H} = 0$. Adding these two results gives us the second part of (18). The first part can be derived in a similar manner.

2. PLASMA OSCILLATIONS OF SMALL AMPLITUDE

Turning now to a detailed investigation of the general equations of motion of the plasma, we

shall first consider the well-known case of oscillations of small amplitude. We introduce in place of $\mathbf{u}$ a new variable $\mathbf{w} = \mathbf{v}/V$, and assume that $w \ll 1$. Then (15) takes the form

$$\frac{d^2w_x}{d\tau^2} + \omega_\perp^2 \frac{w_x}{1 - w_z} = 0; \qquad (19)$$

$$\frac{d^2w_y}{d\tau^2} + \omega_\perp^2 \frac{w_y}{1 - w_z} = 0;$$

$$\frac{d}{d\tau}\left[(w_z - 1)\frac{dw_z}{d\tau} + w_x \frac{dw_x}{d\tau} + w_y \frac{dw_y}{d\tau}\right] = \omega_0^2 \frac{w_z}{1 - w_z},$$

where $\omega_\perp^2 = \omega_0^2 \beta^2/(\beta^2 - 1)$.

The Eqs. (19) can be solved by successive approximations. If we neglect w_z compared to unity, and also the terms quadratic in $\mathbf{w}$, we find in first approximation uncoupled longitudinal and transverse waves, with the frequencies ω_0 and $\omega_\perp$:

$$w_x^{(0)} = W_x \cos \omega_\perp \tau; \qquad (20)$$

$$w_y^{(0)} = W_y \sin \omega_\perp \tau; \quad w_z^{(0)} = W_z \cos(\omega_0 \tau + \alpha).$$

Note that the transverse frequency $\omega_\perp$ corresponds to a dielectric constant of the plasma:

$$\varepsilon = 1 - (\omega_0/\omega_\perp)^2.$$

Indeed, if we define the phase velocity as $c/\sqrt{\epsilon}$, and insert the above value of ϵ, we obtain V.

In the next approximation the longitudinal and transverse oscillations are already coupled. To find the velocity components in this approximation, let $\mathbf{w} = \mathbf{w}^{(0)} + \mathbf{w}^{(1)}$ in (19), where $\mathbf{w}^{(0)}$ is given by (20). Retaining terms of order $w^{(0)2}$ and neglecting $w^{(0)}w^{(1)}$ and $w^{(1)2}$, we obtain

$$w_x = w_x^{(0)} + w_x^{(1)} = W_x \cos \omega_\perp \tau - \frac{1}{2} W_x W_z \omega_\perp^2 \frac{\cos[(\omega_0 + \omega_\perp)\tau + \alpha]}{\omega_\perp^2 - (\omega_0 + \omega_\perp)^2} - \frac{1}{2} W_x W_z \omega_\perp^2 \frac{\cos[(\omega_0 - \omega_\perp)\tau + \alpha]}{\omega_\perp^2 - (\omega_0 - \omega_\perp)^2};$$

$$w_y = w_y^{(0)} + w_y^{(1)} = W_y \sin \omega_\perp \tau - \frac{1}{2} W_y W_z \omega_\perp^2 \frac{\sin[(\omega_0 + \omega_\perp)\tau + \alpha]}{\omega_\perp^2 - (\omega_0 + \omega_\perp)^2} - \frac{1}{2} W_y W_z \omega_\perp^2 \frac{\sin[(\omega_0 - \omega_\perp)\tau - \alpha]}{\omega_\perp^2 - (\omega_0 - \omega_\perp)^2}; \qquad (20')$$

$$w_z = w_z^{(0)} + w_z^{(1)} = W_z \cos(\omega_0 \tau + \alpha) - \frac{1}{2} W_z^2 + \frac{\beta^2}{3\beta^3 + 1}(W_x^2 - W_y^2) \cos 2\omega_\perp \tau + \frac{1}{2} W_z^2 \cos 2(\omega_0 \tau + \alpha).$$

We now have obtained anharmonic oscillations, in which the transverse anharmonicity contains the combination frequencies $\omega_\perp + \omega_0$ and $\omega_\perp - \omega_0$, whereas the longitudianl anharmonicity contains the double frequencies $2\omega_0$ and $2\omega_\perp$. Note that the average of w_z does not vanish; however, the average of the current density $n\mathbf{w}$ vanishes.

If the field $\mathbf{H}_0$ does not vanish, oscillations of small amplitude obey [according to (14)] the equations

$$d^2u_x/d\tau^2 + \Omega_y du_z/d\tau - \Omega_z du_y/d\tau + \beta^2(\beta^2 - 1)^{-1}\omega_0^2 u_x = 0;$$

$$d^2u_y/d\tau^2 + \Omega_z du_x/d\tau - \Omega_x du_z/d\tau + \beta^2(\beta^2 - 1)^{-1}\omega_0^2 u_y = 0;$$

$$d^2u_z/d\tau^2 + \Omega_x du_y/d\tau - \Omega_y du_x/d\tau + \omega_0^2 u_z = 0.$$

Setting $u_x = U_x e^{i\omega t}$, etc., we find the well-known expression for the refractive index

$$\frac{1}{\beta_{1,2}^2} = 1 - \omega_0^2\left[\omega^2 + \frac{\Omega^2\omega^2\sin^2\vartheta}{2(\omega_0^2-\omega^2)} \pm \left(\frac{\Omega^4\omega^4\sin^4\vartheta}{4(\omega_0^2-\omega^2)^2} + \Omega^2\omega^2\cos^2\vartheta\right)^{1/2}\right]^{-1}, \tag{21}$$

where ϑ is the angle between the field and the direction of propagation.

Since β^2 must be real, we can determine from this the range of frequencies which may be propagated in the plasma. We see from (21) that in the presence of an external magnetic field the quantity β may be greater, as well as less than, unity.

3. LONGITUDINAL OSCILLATIONS

Next we consider longitudinal plasma oscillations, without assuming the amplitude to be small. Assuming in (16) that $u_x = u_y = 0$, we find

$$(d/d\tau)\{(u-\beta)\,d\rho/d\tau\} = \omega_0^2\beta^2 u/(\beta-u),$$

where $u = u_z$ and $\rho = \rho_z$ are the dimensionless velocity and momentum of the electron. By expressing the momentum in terms of the velocity we can bring this equation into the form

$$\frac{d^2}{d\tau^2}\frac{1-\beta u}{\sqrt{1-u^2}} = \omega_0^2\frac{\beta^2 u}{\beta-u}.$$

If we now multiply by $(d/d\tau)[(1-\beta u)/(\sqrt{1-u^2})]$ and integrate, we find

$$\frac{1}{2}\left(\frac{d}{d\tau}\frac{1-\beta u}{\sqrt{1-u^2}}\right)^2 = \beta^2\omega_0^2\left(C - (1-u^2)^{-1/2}\right),$$

where C is a constant of integration. Putting $C = (1-u_m^2)^{-1/2}$, we see that u must lie in the interval $-u_m \le u \le u_m$. By a further integration we find

$$\int_0^u [(1-u_m^2)^{-1/2} - (1-u^2)^{-1/2}]^{-1/2}\frac{(\beta-u)\,du}{(1-u^2)^{3/2}} = \sqrt{2}\,\beta\omega_0\tau. \tag{22}$$

This formula solves our problem in principle, since it expresses u as a function of $\tau = t - (z/V)$.

By introducing in place of u a new independent variable λ,

$$u = \tanh\lambda,\quad u_m = \tanh\lambda_0,$$

one can put (22) in the form

$$\int_0^{\lambda}\beta\,\frac{\cosh\lambda - \sinh\lambda}{\cosh\lambda_0 - \cosh\lambda}\,d\lambda = \sqrt{2}\,\beta\omega_0\tau. \tag{22'}$$

Evidently u is a periodic function of τ. Its period, which we shall denote by T is determined by the equation

$$2\int_{-u_m}^{+u_m}[(1-u_m^2)^{-1/2} - (1-u^2)^{-1/2}]^{-1/2}\frac{(\beta-u)\,du}{(1-u^2)^{1/2}} = \sqrt{2}\,\beta\omega_0 T.$$

Or, in terms of the frequency $\omega = 2\pi/T$:

$$\omega = \omega_0\frac{\pi}{\sqrt{2}\,I(u_m)},\quad I(u_m) = \int_0^{u_m}\left[\left(\frac{1-u^2}{1-u_m^2}\right)^{1/2} - 1\right]^{-1/2}\frac{du}{(1-u^2)^{3/4}}. \tag{23}$$

We thus see that the period of longitudinal oscillations depends on the velocity amplitude u_m.

Simple expressions can be obtained in the two limiting cases of small and large velocity amplitude. In the first case, $u_m \ll 1$, the frequency is

$$\omega = \omega_0\left(1 - \frac{3}{16}u_m^2\right),\quad u_m \ll 1. \tag{24}$$

In the second case, $1 - u_m \ll 1$, the frequency becomes

$$\omega = 2^{-3/2}\pi\omega_0(1-u_m^2)^{1/4},\quad 1-u_m \ll 1. \tag{25}$$

As $u_m \to 0$, the frequency tends to zero. This is connected with the fact that for $u_m \to 1$ the electron mass tends to infinity.

In the general case of intermediate values of u_m the integral in (22) and the period can be expressed in terms of elliptic functions. Indeed, with the substitution

$$u = \frac{2k\,\mathrm{sn}(x;k)}{1+k^2\,\mathrm{sn}^2(x;k)},$$

$$k = \left[\frac{1-\sqrt{1-u_m^2}}{1+\sqrt{1-u_m^2}}\right]^{1/2},\quad k' = \sqrt{1-k^2},$$

we find

$$\frac{k}{\beta k'}\,\frac{\mathrm{cn}\,(x;\,k)}{\mathrm{dn}\,(x;\,k)} \tag{26}$$

$$-k'x+\frac{1}{k'K}\left[2E_x+\frac{\vartheta_3'\,(x/2K;\,q)}{\vartheta_3\,(x/2K;\,q)}\right]=\omega_0\tau,$$

where

$$\frac{\vartheta_3'\,(z;\,q)}{\vartheta_3\,(z;\,q)}=4\pi\sum_{n=1}^{\infty}\frac{(-1)^n q^n\sin 2\pi nz}{1-q^{2n}};\quad q=e^{-\pi k'/K};$$

$$K=\int_0^1\frac{dx}{\sqrt{(1+x^2)\,(1-k^2x^2)}};$$

$$K'=\int_0^1\frac{dx}{\sqrt{(1-x^2)\,(1-k'^2x^2)}};$$

$$E=\int_0^1\sqrt{\frac{1-k^2x^2}{1-x^2}}\,dx.$$

Setting in (26) $u=u_m$, $\tau=1/4\,T$, and noting that $x=K$ when $u=u_m$, we find the following expression for the oscillation frequency

$$\omega=\omega\,(\pi/2)\,k'/(2E-k'^2K). \tag{27}$$

From u we can easily obtain the particle density, and the electric field, which is in the direction of propagation. From (6) and (9), we find

$$n\,(\tau)=\frac{n_0\beta}{\beta-u};\quad eE\,(\tau) \tag{28}$$

$$=\pm\sqrt{2}\,m\omega_0 c\left[\frac{1}{\sqrt{1-u_m^2}}-\frac{1}{\sqrt{1-u^2}}\right]^{1/4}.$$

The maximum value of the field is, for small amplitude, proportional to u_m; for $1-u_m\ll 1$, it is given by

$$eE_m=\sqrt{2}\,m\omega_0 c\,(1-u_m^2)^{1/4}, \tag{28'}$$

If $1-u_m\ll 1$,

$$u=\begin{cases} u_m & \text{for}\quad 0<\theta<2\sqrt{2}\,(1-1/2\beta);\\ -u_m & \text{for}\quad -2\sqrt{2}\,(1+1/2\beta)<\theta<0,\end{cases}$$

where $\theta=\omega_0\,\tau(1-u_m^2)^{1/4}$. Using these expressions we may consider almost longitudinal oscillations in the case $1-u_m\ll 1$. They are described according to (14) by the equation

$$d^2\rho_x/d\theta^2+f\,(\theta)\,\rho_x=0$$

with a given function $f(\theta)$. This function $f(\theta)$ may be approximately expressed in the form

$$f\,(\theta)=f_0\,(\theta)+h\Big\{\sum_n\delta\,(\theta-4\sqrt{2}\,n)$$

$$+\sum_n\delta\left(\theta-2\sqrt{2}\left(1-\frac{1}{2\beta}\right)-4\sqrt{2}\,n\right)\Big\}.$$

Here $f_0\,(\theta)$ is a periodic function, defined by the relations

$$f_0\,(\theta)=\frac{\beta^2}{\beta^2-1}\,\frac{\beta}{\beta-1}$$

$$\text{for}\quad 0<\theta<2\sqrt{2}\left(1-\frac{1}{2\beta}\right);$$

and

$$f_0\,(\theta)=\frac{\beta^2}{\beta^2-1}\,\frac{\beta}{\beta+1}$$

$$\text{for}\quad -2\sqrt{2}\left(1+\frac{1}{2\beta}\right)<\theta<0;$$

$$h=\frac{\sqrt{2}\,\beta^2}{\beta^2-1}\left(2\ln\frac{2\sqrt{2}}{(1-u_m^2)^{1/4}}-\frac{2\beta^2-1}{\beta^2-1)}\right).$$

The solution of this equation is of the form $\rho_x=e^{ik\theta}\,\varphi(\theta)$ where $\varphi(\theta)$ is a periodic function and k is defined by

$$\cos 4\sqrt{2}\,k$$

$$=\cos k_1a_1\cos k_2a_2-\frac{k_1^2+k_2^2-h^2}{2k_1k_2}\sin k_1a\sin k_2a$$

$$-\frac{h}{k_1}\sin k_1a_1\cos k_2a_2-\frac{h}{k_2}\sin k_2a_2\cos k_1a_1;$$

$$a_1=\sqrt{2}\,\frac{2\beta-1}{\beta};\quad a_2=\sqrt{2}\,\frac{2\beta+1}{\beta};$$

$$k_1^2=\frac{\beta^2}{\beta^2-1}\,\frac{\beta}{\beta-1};\quad k_2^2=\frac{\beta^2}{\beta^2-1}\,\frac{\beta}{\beta+1}.$$

4. TRANSVERSE OSCILLATIONS

For purely transverse oscillations $u_z=0$, and the third Eq. (15′) gives $p^2=\text{const}$. This follows also with H_0 present, provided H_0 is parallel to

the direction of propagation.

Putting $\rho_z = 0$ in the first two Eqs. (15′) we obtain

$$\rho_x = \rho \cos \omega\tau; \quad \rho_y = \rho \sin \omega\tau,$$

where

$$\omega = \omega_0 \beta (\beta^2 - 1)^{-1/2} (1 + \rho^2)^{-1/4}. \tag{29}$$

Therefore, the wave velocity β may be expressed in the form $\beta = \epsilon^{-1/2}$, where

$$\epsilon = 1 - \frac{\omega_0'^2}{\omega^2};$$

$$\omega_0' = \sqrt{\frac{4\pi e^2 n_0}{m'}}; \quad m' = \frac{m}{\sqrt{1 - v^2/c^2}}$$

(v is the electron velocity).

Thus in the case of purely transverse waves the electrons move around in circular orbits with angular velocity ω, and there can exist only waves with circular polarization*. This is connected with the fact that for large amplitude one cannot superimpose two oscillations of opposite circular polarization because of the nonlinearity of the equations. For small amplitude, when the oscillations are linear, such a superposition is possible, and this leads to the appearance of linearly polarized oscillations, as has been shown.

From (10) (with $H_0 = 0$) and (29) it is easily shown that the magnetic field H is parallel to the electron momentum, and is given by the relations

$$eH_x = -(mc\omega/\beta)\rho_x = -(mc\omega\rho/\beta)\cos\omega\tau;$$

$$eH_y = -(mc\omega/\beta)\rho_y = -(mc\omega\rho/\beta)\sin\omega\tau.$$

The electric field is, according to (7),

$$eE_x = mc\omega\rho \sin\omega\tau; \quad eE_y = -mc\omega\rho\cos\omega\tau.$$

If the external magnetic field is not zero, and is parallel to the direction of propagation, the equations of motion for transverse oscillations take the form $\frac{d^2\rho_x}{d\tau^2} - \Omega\frac{du_y}{d\tau} + \frac{\beta^2}{\beta^2-1}\omega_0^2 u_x = 0;$

$$\frac{d^2\rho_y}{d\tau^2} + \Omega\frac{du_x}{d\tau} + \frac{\beta^2}{\beta^2-1}\omega_0^2 u_y = 0,$$

where, as before, $u_x^2 + u_y^2 = \text{const}$. Remembering that $\rho = u(1-u^2)^{-1/2}$ and putting $u_x = U\cos\omega\tau$, $u_y = U\sin\omega\tau$, we find the following expression for the frequency ω:

$$\omega = \left[\frac{\Omega'^2}{4} + \frac{\beta^2}{\beta^2-1}\omega_0'^2\right]^{1/2}, \tag{30}$$

and, therefore,

$$\beta^{-2} = 1 - \omega_0'^2/(\omega^2 \pm \omega\Omega),$$

where

$$\omega_0'^2 = \omega_0^2\sqrt{1-u^2}, \quad \Omega' = \Omega\sqrt{1-u^2}.$$

Note that the present expression for β^{-2} is formally identical with (21) for $\vartheta = 0$. However, the difference consists in the fact that (21) refers to linear oscillations, and one may therefore superimpose two waves for which the sign of the root in (21) is different, whereas the nonlinear oscillations to which (30) relates, may not be so superimposed. In this case we may therefore either have the solution with the positive or that with the negative sign in the expression for the frequency.

We now turn to the case of almost transverse oscillations, for which the electron trajectories are almost circles. For this purpose we replace ρ_x and ρ_y in the fundamental Eq. (18) by the new variables $\rho_\perp$ and φ, related to ρ_x and ρ_y by the relation $\rho_x + i\rho_y = \rho_\perp e^{i\varphi}$. The first two Eqs. (15′) can then be written in the form

$$\frac{d^2\rho_\perp}{d\tau_2} - \rho_\perp\left(\frac{d\varphi}{d\tau}\right)^2 + \frac{\beta^2}{\beta^2-1}\omega_0^2\frac{\beta\rho_\perp}{\beta\sqrt{1+\rho_\perp^2+\rho_z^2}-\rho_z} = 0;$$

$$2\rho_\perp\frac{d\rho_\perp}{d\tau}\frac{d\varphi}{d\tau} + \rho_\perp^2\frac{d^2\varphi}{d\tau^2} = 0.$$

Integration of the second of these gives

$$\rho_\perp^2\, d\varphi/d\tau = M,$$

where M is a constant. Therefore, the first equation becomes

$$\frac{d^2\rho_\perp}{d\tau^2} - \frac{M^2}{\rho_\perp^3} + \omega_0^2\frac{\beta^2}{\beta^2-1}\frac{\beta\rho_\perp}{\beta\sqrt{1+\rho_\perp^2+\rho_z^2}-\rho_z} = 0. \tag{31}$$

* This argument loses its usefulness in practice when $\beta \gg 1$ since, because of the small longitudinal velocity component, almost transverse oscillations then become possible which are linearly polarized (see Sec. 5 below).

If we put here $\rho_z = 0$, we obtain transverse oscillations with constant $\rho_\perp$. If we call this constant value ρ_0, we find from (31)

$$\omega_\perp^2 = \omega_0^2\beta^2/(\beta^2 - 1). \tag{32}$$

Consider now small oscillations of the quantity $\rho_\perp$ about the value ρ_0. Letting $\rho_\perp = \rho_0 + \delta$ and assuming δ and ρ_z small compared to ρ_0, we obtain from (31) with the help of (32):

$$\frac{d^2\delta}{d\tau^2} + \frac{\omega_\perp^2(4+3\rho_\perp^2)}{(1+\rho_0^2)^{3/2}}\delta + \frac{\omega_\perp^2\rho_0\rho_z}{\beta(1+\rho_0^2)} = 0.$$

By a similar expansion in the third Eq. (15′) we obtain a second equation for δ and ρ_0:

$$\beta\frac{d^2\rho_z}{d\tau^2} - \frac{\rho_0}{\sqrt{1+\rho_0^2}}\frac{d^2\delta}{d\tau^2} + \omega_0^2\frac{\beta\rho_z}{\sqrt{1+\rho_0^2}} = 0.$$

Putting $\delta = De^{i\omega t}$, $\rho_z = Re^{i\omega t}$, we find the following equations for the frequencies of coupled transverse-longitudinal oscillations:

$$\omega^4 - \frac{\omega_0^2(4\beta^2\rho_0^2 + 5\beta^2 - 1)}{(\beta^2-1)(1+\rho_0^2)^{3/2}}\omega^2 - \frac{\omega_0^4\beta^2(4+3\rho_0^2)}{(\beta^2-1)(1+\rho_0^2)^2} = 0,$$

and hence

$$\omega_{1,2} = \frac{\omega_\perp}{\sqrt{1+\rho_0^2}}\left\{\frac{4\beta^2\rho_0^2 + 5\beta^2 - 1}{2\beta\sqrt{1+\rho_0^2}} \pm \left[\left(\frac{4\beta^2\rho_0^2 + 5\beta^2 - 1}{2\beta^2\sqrt{1+\rho_0^2}}\right)^2 - \frac{(\beta^2-1)(4+3\rho_0^2)}{\beta^2}\right]^{1/2}\right\}^{1/2} \tag{33}$$

Some limiting cases are of interest.

If $\rho \ll 1$,

$$\omega_1 = 2\omega_\perp, \qquad \omega_2 = \omega_0, \tag{34}$$

in agreement with the result found previously for the frequencies of longitudinal and transverse oscillations in the linear approximation. (We have found here twice the value of $\omega_\perp$, since we are here concerned with oscillations of the resultant, which evidently have a period equal to one-half that of the oscillations of ρ_x and ρ_y.)

If $\rho_0 \gg 1$,

$$\omega_{1,2} = \omega_\perp\rho_0^{-1/2}\left[2 \pm \beta^{-1}(3+\beta^2)^{1/2}\right]^{1/2}. \tag{35}$$

In the case $\beta - 1 \ll 1$, the frequencies of coupled oscillations are, for arbitrary ρ_0, given by

$$\omega_1 = 0, \quad \omega_2 = 2\omega_\perp(1+\rho_0^2)^{-1/2}. \tag{36}$$

If $\beta \gg 1$, then for any ρ_0

$$\omega_1 = \omega_0\frac{(4+3\rho_0^2)^{1/2}}{(1+\rho_0^2)^{3/4}}; \quad \omega_2 = \frac{\omega_0}{(1+\rho_0^2)^{1/4}}. \tag{37}$$

5. COUPLED LONGITUDINAL-TRANSVERSE OSCILLATIONS

In the preceding sections we considered longitudinal, transverse and almost transverse plasma oscillations. The investigation of the general case which might be called the case of longitudinal-transverse oscillations, amounts to the integration of Eq. (16) and represents a very complicated problem, which is soluble only in some limiting cases, viz., for very large β and for β close to unity*.

Consider first the case $\beta \gg 1$. We shall assume that β^2 and $\xi^2 + \eta^2 + \zeta^2$ are quantities of the same order. (If $\xi^2 + \eta^2 + \zeta^2 \ll \beta^2$, then we get back to the case of small oscillations, which has already been discussed, since in that case ξ, η, ζ are proportional to ρ_x, ρ_y, ρ_z**.) With these assumptions we may neglect the term ζ in the potential energy U defined by (17′), which determines the motion of the plasma. The problem therefore reduces to the integration of the equations of motion for a particle in a central field whose Lagrangian is, according to (17),

$$L = \frac{1}{2}\left[\left(\frac{d\xi}{d\tau}\right)^2 + \left(\frac{d\eta}{d\tau}\right)^2 + \left(\frac{d\zeta}{d\tau}\right)^2\right] - \omega_0^2\beta\sqrt{\beta^2 + \xi^2 + \eta^2 + \zeta^2}.$$

We replace $\xi, \eta, \zeta, \tau, L$ by the new variables $X, Y, Z, \theta, \mathcal{L}$, defined by $X = \xi/\beta$, $Y = \eta/\beta$, $Z = \zeta/\beta$, $\theta = \omega_0\tau$, $\mathcal{L} = \omega_0^2\beta^2 L$ and find

$$\mathcal{L} = \frac{1}{2}\left\{\left(\frac{dX}{d\theta}\right)^2 + \left(\frac{dY}{d\theta}\right)^2 + \left(\frac{dZ}{d\theta}\right)^2\right\} - \sqrt{1+R^2},$$

* The possibility of a solution for these cases was pointed out to us by L. D. Landau.

** From $\rho_z = [\beta\zeta + (\beta^2 - 1 + \xi^2 + \eta^2 + \zeta^2)^{1/2}](\beta^2-1)^{-1}$ follows, if $\beta^2 \gg \xi^2 + \eta^2 + \zeta^2$ and $\beta^2 \gg 1$, that $\rho_z = \zeta + 1/\beta$. In addition, $\rho_x = \xi/\beta$ and $\rho_y = \eta/\beta$.

where $R^2 = X^2 + Y^2 + Z^2$. Since the motion in this problem takes place in a plane, it is convenient to rotate the coordinate axes so as to make the X-Y plane perpendicular to the direction of the angular momentum. The Lagrangian then takes the form:

$$\mathcal{L} = \frac{1}{2}\{(dR/d\theta)^2 + R^2(d\varphi/d\theta)^2\} - \sqrt{1+R^2},$$

where φ is the polar angle. We write down the energy and angular momentum equations

$$\frac{1}{2}\left(\frac{dR}{d\theta}\right)^2 + \frac{M^2}{2R^2} + \sqrt{1+R^2} = \mathcal{E}; \qquad R^2\frac{d\varphi}{d\theta} = M,$$

and hence find finally the solution

$$\omega_0\tau = \int\left[2\mathcal{E} - \frac{M^2}{R^2} - 2\sqrt{1+R^2}\right]^{-1/2} dR. \quad (38)$$

The quantity R which occurs here is connected with the dimensionless momentum ρ by

$$R^2 = \rho^2 - (2\rho_z/\beta)\sqrt{1+\rho^2} + \beta^{-2}.$$

For large ρ, R practically coincides with ρ. We see from (38) that the quantity R oscillates between two limits R_0 and R_1, which are related to $\mathcal{E}$ and M by

$$M^2 = \frac{2R_0^2R_1^2}{\sqrt{1+R_1^2}+\sqrt{1+R_0^2}};$$

$$\mathcal{E} = \frac{R_0^2+R_1^2+1+\sqrt{(1+R_0^2)(1+R_1^2)}}{\sqrt{1+R_0^2}+\sqrt{1+R_1^2}}.$$

The frequency of oscillation is

$$\omega = \frac{\pi\omega_0}{\sqrt{2}\,I(R_0, R_1)}, \qquad I(R_0, R_1) \quad (39)$$

$$= \int_{R_0}^{R_1}\left[\mathcal{E} - \frac{M^2}{2R^2} - \sqrt{1+R^2}\right]^{-1/2} dR.$$

For $R_0 = 0$, this integral becomes identical with the integral $I(u_m)$ which gave the frequency of longitudinal vibrations, if we put $R_1 = u_m(1-u_m^2)^{-1/2}$. However, the case considered here does not, for $R_0 = 0$, reduce to the case of purely longitudinal oscillations which we had considered before, since we may here be dealing with oscillations which are almost linearly polarized in an arbitrary direction. In particular, we may have oscillations which are approximately transverse and linearly polarized, and for which ρ_x is non-zero, $\rho_y = 0$, and ρ_z is non-zero, but much less than ρ_x, of the order $\rho_z \sim \rho_x/\beta$. The existence of such oscillations does not conflict with the statement made earlier that purely transverse oscillations have circular rather than linear polarization. Indeed, it is clear from the third part of (15) that for $\beta \gg 1$, $\rho_x \sim 1$ and $\rho_z \sim 1/\beta$ the quantity ρ_y may vanish, i.e., the oscillation may be approximately transverse and linearly polarized.

If $R_0 = R_1$ (R = const) the vector $\mathbf{R}$ describes a circle with angular velocity

$$\omega = \omega_0(1+R^2)^{-1/4}.$$

This formula agrees with (29) for the frequency of transverse oscillations for $\beta \gg 1$. The present type of oscillation is then for $R_0 = R$, very similar to oscillations with circular polarization, for which, however, the plane of oscillation is not necessarily at right angles to the direction of propagation.

We now turn to the case when β is close to unity, $\beta - 1 \ll 1$. The basic Eqs. (15′) may then be written in the form

$$\frac{d^2\rho_x}{d\theta^2} + \frac{\rho_x}{\sqrt{1+\rho^2}-\rho_z} = 0; \quad (40)$$

$$\frac{d^2\rho_y}{d\theta^2} + \frac{\rho_y}{\sqrt{1+\rho^2}-\rho_z} = 0;$$

$$\frac{d^2}{d\theta^2}\left(\rho_z - \sqrt{1+\rho^2}\right) + \frac{(\beta^2-1)\rho_z}{\sqrt{1+\rho^2}-\rho_z} = 0,$$

where $\theta = \omega_0\tau(\beta^2-1)^{-1/2}$. Neglecting the last term in the third equation, we find

$$\sqrt{1+\rho^2} - \rho_z = C^2, \quad (40')$$

where C is a constant. The first two Eqs. (40) then take the form

$$\frac{d^2\rho_x}{d\theta^2} + \frac{\rho_x}{C^2} = 0; \qquad \frac{d^2\rho_y}{d\theta^2} + \frac{\rho_y}{C^2} = 0,$$

and hence

$$\rho_x = R_x\cos(\theta/C); \quad (41)$$

$$\rho_y = R_y\sin(\theta/C).$$

Inserting these expressions in (40′) we find

$$\rho_z = \frac{1}{4C^2}\left\{R_x^2 + R_y^2 - 2(C^4 - 1) - (R_x^2 - R_y^2)\cos\frac{2\theta}{C}\right\}. \quad (41')$$

The constants C, R_x and R_y are connected by a relation which follows from the fact that nv_z vanishes on the average. [This condition follows from the fact that $\mathbf{E}'$ and $\mathbf{H}'$ vanish on the average, see (3).] Noting that $u_z = (1+\rho^2)^{-1/2}$ and using (9) and (40′), we find for $\beta - 1 \ll 1$:

$$nu_z \approx \frac{n_0 u_z}{1-u_z} = \frac{n_0\rho_z}{\sqrt{1+\rho^2}-\rho_z} = \frac{n_0}{C^2}\rho_z.$$

Since the average of nu_z vanishes, it follows therefore that also the average of ρ_z must vanish. We can therefore put in (41′)

$$R_x^2 + R_y^2 = 2(C^4 - 1),$$

$$C^2 = \sqrt{1 + {}^1/_2(R_x^2 + R_y^2)}.$$

Finally, ρ_x, ρ_y, ρ_z take the form

$$\rho_x = R_x\cos\omega\tau; \qquad \rho_y = R_y\sin\omega\tau; \quad (42)$$

$$\rho_z = \frac{R_x^2 - R_y^2}{4\sqrt{1+{}^1/_2(R_x^2+R_y^2)}}\cos 2\omega\tau,$$

where

$$\omega = \omega_0(\beta^2-1)^{-1/4}\left[1 + {}^1/_2(R_x^2+R_y^2)\right]^{-1/4}. \quad (42')$$

These results agree with the Eqs. (29) and (36) which describe oscillations which are approximately perpendicular with circular polarization. Indeed, when $R_x \approx R_y$, the frequency of oscillation of the quantity R_z takes the value given by (36).

We may further consider the case of high energies, when the inequality $\xi^2 + \eta^2 + \zeta^2 \gg \beta^2 - 1$ is satisfied, β being arbitrary ($\beta > 1$). The Lagrangian of the plasma motion can then be written in the form

$$L = \frac{1}{2}\left[\left(\frac{d\xi}{d\tau}\right)^2 + \left(\frac{d\eta}{d\tau}\right)^2 + \left(\frac{d\zeta}{d\tau}\right)^2\right] - \omega_0^2\frac{\beta^2}{\beta^2-1}\left[\beta\sqrt{\xi^2+\eta^2+\zeta^2} + \zeta\right].$$

Under the substitution

$$\xi = \mu\xi', \quad \eta = \mu\eta', \quad \zeta = \mu\zeta', \quad \tau = \sqrt{\mu}\tau',$$

where μ is an arbitrary constant, the Lagrangian is multiplied by μ. This shows that, if the motion $\xi = \xi(\tau)$; $\eta = \eta(\tau)$; $\zeta = \zeta(\tau)$ is possible, then also the similar motion $\xi' = \xi(\tau')$; $\eta' = \eta(\tau')$; $\zeta' = \zeta(\tau')$ is possible. In particular, we can deduce from this a definite dependence of the oscillation frequency on the quantity p_0 which characterizes the electron momentum. The result is that the frequency must be inversely proportional to $\sqrt{p_0}$:

$$\omega = \text{const}\, p_0^{-1/2}. \quad (43)$$

This formula is in agreement with the results obtained previously for the frequency in the region of high energies [Eqs. (25), (29), (35) and (42′)].

In conclusion, the authors would like to express their gratitude to L. D. Landau for valuable advice and for his interest in the work, and to N. I. Akhiezer and I. B. Fainberg for valuable discussions.

---

[1] A. Vlasov, J. Exptl. Theoret. Phys. (U.S.S.R.) 8, 291 (1938).

[2] L. Landau, J. Exptl. Theoret. Phys. (U.S.S.R.) 16, 193 (1951).

[3] A. Akhiezer and G. Liuburskii, Dokl. Akad. Nauk SSSR 80, 193 (1951).

Translated by R. E. Peierls
185

Experiments in Enrichment of Helium with Isotope He^3

V. P. Peshkov

Institute for Physical Problems, Academy of Sciences, USSR

(Submitted to JETP editor October 24, 1955)
J. Exptl. Theoret. Phys. (U.S.S.R.) 30, 850-854 (May, 1956)

Equipment is described for the enrichment of helium with isotope He^3 based on the use of thermomechanical effect and rectification. An evaluation is made of the possible degree of enrichment and extraction of He^3 by means of thermal diffusion.

As is well known natural helium consists basically of the isotope of mass 4 and contains very small amounts of the mass 3 isotope. The usual fraction of He^3 is only 10^{-8} --10^{-7} of He^4. Therefore, in order to obtain even a small amount of helium with a significant concentration of He^3 from natural helium it is necessary to enrich it by a factor of several hundred thousand. Pollard and Davidson[1] first proposed to use the thermomechanical effect for this purpose. The most effective method was developed by Esel'son and Lazarev[2]. In the method of Ref. 2 the apparatus worked cyclically and the enrichment per one cycle was about 200. The purpose of the present work, which has been conducted with considerable interruptions since 1949, was to develop equipment of sufficient yield for the extraction of He^3 from its mixture with He^4 and its further purification from He^4.

1. EQUIPMENT FOR EXTRACTION OF He^3

Several types of apparatus for the extraction of He^3 from natural helium have been devloped and tested. The first is shown in Fig. 1. The temperature in the Dewar flask *1* containing liquid helium (from which H^3 was extracted) was maintained at 2.3° K. A temperature of 1.8° K was established in the internal Dewar flask *2*. Helium entered from the external flask through the regulating valve *3* and a copper tube 0.4 diameter × 1.0 mm into the collector *4*. The level in the collector was maintained near the center of the top ball. The temperature in the collector was measured with the thermometer *8* and was somewhat lower than the λ point (2.19° K). Since the temperature in flask *1* was higher than in the collector *4*, the thermal flow was upward due to conduction of heat along the copper tupe and to the heat carried by the helium from the bottom of the collector. The thermal flow carried with it He^3 and the liquid helium depleted of He^3 was pressed into flask *2* through the copper tube *5* (0.4 × 1.0 mm). The speed of the pressure transfer was regulated by valve *6*. In this as in other apparatus the transitions from glass to metal were accomplished by welds between the copper and glass. The evaporated He^3 enriched helium in the collector *4* was passed into the rectification column *7*, the upper portion of which was cooled by contact with the helium contained in flask *2*. The column consisted

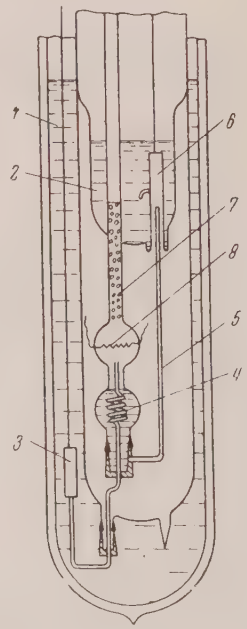

FIG. 1. Apparatus for the extraction of He^3 by thermal flow and rectification.

of a glass tube 3 mm in diameter and 100 mm long. The tube was filled with rings of 0.15 mm constantan wire cut from a spiral 1 mm diam. The more readily boiling He^3 was collected in the region of lower temperatures at the top of the column and the more readily condensable He^4 flowed back into the collector.

Enrichment up to 0.2% of He^3 was obtained with this equipment which corresponds to an increase in concentration by a factor of 10^5. It was further established that the concentration of He^3 in the output was of the order of 10^{-8}. The equipment was cyclic in operation and permitted the processing, with a single loading, of 0.75 liter of liquid helium in four hours.

Since the equipment described above was of insufficient output and did not permit the uninterrupted processing of helium, another apparatus was constructed and set up which could be operated continuously with the helium added at atmospheric pressure without interrupting the operation of the equipment. In this apparatus, as in the method of Esel'son and Lazarev[2], the enrichment of He^4 was obtained by making use of the diverted He^4 in the form of a superfluid flow through a filter due to the action of thermal diffusion and besides this, by the simultaneous diversion of the He^4 enriched gas by rectification in the tube. The apparatus is shown in Fig. 2. The helium in the external flask *1* was at atmospheric pressure being replensihed as it was used up from the liquefying machine without interrupting the operation of the equipment. In the internal flask *2* the temperature was held between the limits 1.9° and 2° K by pumping and the use of heater *3*. Helium from the outer flask *1* entered collector *4* through the regulating valve *5* and the 6 mm in diameter 1.4 × 20 mm copper tubing. The tube in the inner flask was bent in the form of a spiral of an overall length of 35 cm in order to effect cooling of the helium carried by this tube. In addition, this tube was soldered to a similar tube *7* for a length of 2 cms. Due to the heat received by tube *7* at the soldered surface and the heat emitted by the heater *8*, the helium flowed in the manner of a superfluid from collector *4* through filter *9* into the inner flask. The filter consisted of a brass cartridge 7 mm in diameter, 35 mm long, densely packed with rouge. The He^3 remaining in the collector passed into the gaseous state and was enriched by rectification in tube *10* and removed from the apparatus through the same tube. According to computation the small difference in temperature formed between the collector and flask *2* was quite sufficient for the normal operation of the

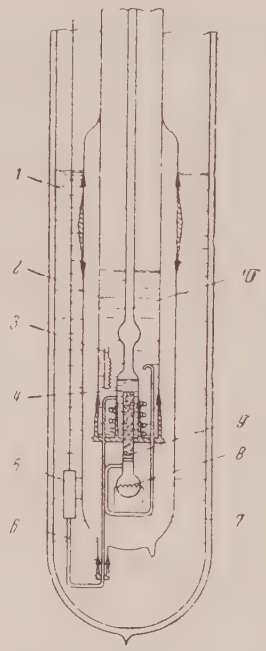

FIG. 2. Apparatus for extraction of He^3 by the thermomechanical effect and rectification.

tubular column. The evaluation of the operation of tubular columns is presented in Ref. 3. The rate of helium processing was limited by the pumping of the helium vapor from the inner flask *2*. All the processed helium was to be pumped out by pumps at pressures from 20 to 30 mm of mercury. The equipment was capable of processing helium at the rate of 3 m^3/hr (at normal temperature and pressure) with the capactity of the vacuum pumps about 100 m^3/hr, power of the heater 82 watts and of the evaporator 31 watts. The gas collected in the first experiments was enriched to 0.02% of He^3. To determine the extraction coefficient the once-processed helium was worked over for the second time. The result showed that, within the limits of measurements errors (which amounted to 5-10%), the extraction was complete. On the basis of balance relationships the concentration of the output gas should be taken as 10^{-8} and enrichment coefficient as 2×20^4. Since the concentration of the processed helium could not be measured with sufficient accuracy it can only be stated that the common division coefficient was greater than 2×10^5. The described apparatus could be operated continuously as long as desired. The duration of its operation was determined by the operation of the liquefying equipment.

1. EVALUATION OF THE EFFECTIVENESS OF SEPARATION METHODS

Theoretically, the coefficient of separation of He^3 by the superfluid filtration can be evaluated from the following considerations. If we assume that superflow and diffusion take place through the same effective cross section of the filter and that the velocity of the superflow is limited by the critical velocity $v_s = 20$ cm/sec, then the value of the superflow through a unit of cross section is

$$\omega_1 = \rho_s v_s,$$

and the flow of He^3 determined by diffusion will be

$$\omega_2 = D\rho m_3 X_0 / m_4 l,$$

where D nenoted the diffusion coefficient of He^3, l the length of the filter, ρ_s, the density of the superflowing helium, X_0, the molar concentration before the filter, m_3 and m_4, atomic masses of He_3 and He_4, respectively.

The molar concentration of the passing helium will be determined by:

$$X = \omega_2 m_4 / m_3 \omega_1 = D\rho X_0 / l\rho_s v_s,$$

i.e., the limit of the attainable separation coefficient is equal to

$$A = X_0 / X = l\rho_s v_s / D\rho.$$

The diffusion coefficient of He^3 in liquid helium II was determined experimentally by Beenakker et al.[4]. Their results show that the coefficient decreases rapidly from 10^2 cm^2/sec at 1.3° K to 10^{-3} cm/sec at 1.6° K and 4×10^{-5} cm^2/sec at 2.1° K. Thus, for the filter length $l = 5$ cm, we will obtain for the separation coefficient at 1.3° K $A = 10^4$, at 1.6° K $A = 8 \times 10^4$, at 2° K $A = 6 \times 10^5$ and at 2.1° K $A = 5 \times 10^5$, i.e., the separation coefficient reaches a maximum at about 2° K. In practice, the obtainable coefficient is less due to interruptions in the process when the diffusion continues and there is no superflow.

It should be noted that enrichment by thermal diffusion cannot take place at any desired high concentration. As the measurements in Refs. 5 and 6 have shown, the λ-transition is displaced with increase of concentrations into the region of lower temperatures. Thus in a 50% solution of He^3 and He^4 the superflow is already lost at 1° K. Besides, the following relation for thermal diffusion given in the work of Pomeranchuk[7] holds for not too high concentrations of He^3:

$$-SdT + \frac{dp}{\rho} - \frac{k}{m_4} d(XT) = 0,$$

where S denotes the entropy 1 gm He^4, ρ density, p pressure, m_4 the atomic mass of He^4, k Boltzman's constant and x the molar concentration of He^3. The entropy of He II in the temperature region above 1° K can be expressed by the formula $S = 0.405\,(T/2.19)^{5.5}$ cal/gm, deg, i.e., $SdT = (1/6.5)d(ST)$. Since the density of He^4 changes very little, the entire expression can be written in the form

$$d\left\{\left(\frac{kX}{m_4} + \frac{S}{6.5}\right)T - \frac{p}{\rho}\right\} = 0$$

or, along the thermal diffusion path,

$$\left(\frac{kX}{m_4} + \frac{S}{6.5}\right)T - \frac{p}{\rho} = \text{const}.$$

Since with the extraction of He^3 by thermal diffusion the concentration on one side is practically equal to zero, we obtain

$$\left(\frac{kX}{m_4} + \frac{S}{6.5}\right)T - \frac{p}{\rho} = \frac{S_0 T_0}{6.5} - \frac{p_0}{\rho}$$

or

$$X = \frac{m_4}{kT}\left(\frac{S_0 T_0 - ST}{6.5} - \frac{p_0 - p}{\rho}\right).$$

The line of λ-transitions and also the values of X computed for different values of T by the given formula are shown graphically in Fig. 3. As seen from Fig. 3 the process of thermal diffusion cannot proceed to any desired high concentrations. Therefore, the enrichment of mixtures with concentrations of He^3 higher than 10% and the purification of He^4 are more appropriately carried out by rectification. Evaluation of the operation of the rectification column was presented in Ref. 3. It was possible on the basis of these evaluations to reduce considerably the volume of experimental work in the development of the concentration equipment.

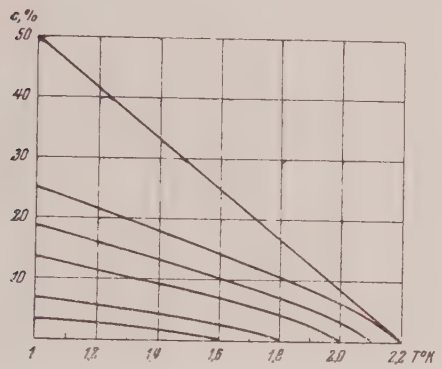

FIG. 3. The line of λ-transitions (upper) and lines $(k\epsilon/m+S_0/6.5)T-p/\rho = \text{const}$ for various values of T_0.

3. CONCENTRATION EQUIPMENT

A series of apparatus has been developed for the concentration of He^3 from mixtures of 0.1% and higher. The most effective was the apparatus shown in Fig. 4. It operates on the same principle as the one previously described. However, since it is impossible to obtain high concentration of He^3 by the thermomechanical effect, the rectification column was noticeably increased and it was in this column that the basic enrichment took place. In addition, the resulting mixture was condensed directly in the apparatus and after reprocessing collected in a special collector. The apparatus was placed in a Dewar flask *1* containing liquid helium, the resulting mixture was passed through a German silver coiled tube 1.5 × 2 mm of a total length of 800 cms. The helium condensed in the coiled tube was collected in the evaporator *3*. From the evaporator He^4 entered the glass collector *4* by superfluid flow through the filter *5* with the aid of the warmer *6*. In order to prevent diffusion of He^3 through the filter during the absence of superfluid motion, the exit opening of the filter was closed by valve *7*. The filter consisted of copper tube 2 × 4 mm, 45 mm long, densely packed with rouge. The processed helium was pumped out from the collector *4* through tube *8*.

The helium remaining in the evaporator entered the rectification column *9*, where the more readily boiling He^3 was collecting in the cold upper portion. The temperature in the upper portion of the column was maintained at the expense of the evaporation of helium from the collector *10*. Liquid helium was supplied from flask *1* through tube *11* and valve *12* by the pressure difference. Helium was added as required to make up for loss due to boiling.

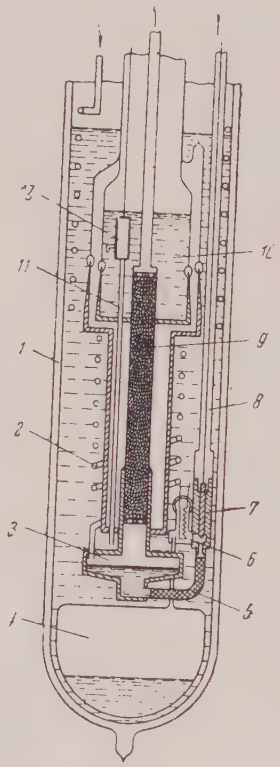

FIG. 4. Apparatus for the concentration of He^3.

The rectification column consisted of a stainless steel tube, inside diameter 9.6 mm, 0.2 mm wall thickness, 200 mm long. The entire column was filled with rings 1.5 mm diameter of 0.2 mm constantan wire.

Inasmuch as the rectification process is considerably slower than the enrichment by superflow, it was appropriate to carry out the concentration process in two cycles. The first cycle (excitation cycle) was carried out with full loading of the filter at a temperature of 1.95° K and heater power of 0.01 watt. The rate of processing of the initial gas mixture was thereby equal to 100 *l*/hr (at 0° C and 760 mm of mercury). At this processing rate, especially since the initial concentration was about 1 to 2% of He^3, the rectification column could not operate effectively and only slightly improved the singular enrichment as a result of the difference in concentrations between the liquid and gaseous state. At the top of the column the temperature was maintained at 1.5° K with the removal of the gas taking place at a pressure inside the column of 20 mm of mercury. The concentration of the removed gas was of the order of 30 to 50%. To begin the superfluid flow through the filter it was necessary to fill the collector 4 with gaseous He^4 up to equilibrium pressure, because otherwise the helium would pass through the filter by diffusion, i.e., would bring with it noticeable quantities of He^3 which decreases the degree of extraction. By following this procedure the obtained degree of extraction was 99.98% and the general division coefficient was 10^4, which is only several times smaller than the attainable limit.

When small quantities of the initial mixture were processed valve 7 was closed immediately after the cessation of the superfluid flow, all the removed gas was again condensed and the second cycle (enrichment) was carried out.

In the second cycle the temperature of the bottom of the column was set at the beginning of the process at 2.0° K, and at the top to 1.46° K. It was not possible to attain a lower temperature at the top of the column with the available pump which had a capacity of 50 m^3/hr. The pressure inside the column was thereby of the order of 45 mm of mercury. After equilibrium was reached, removal of the product began at a rate of 0.6 *l*/hr (at 0° and 760 mm of mercury). As the He^3 was being extracted, it was necessary to raise the temperature of the bath in order to maintain a pressure of 45 mm of mercury at the top of the column. The extraction process ended when the temperature of the bath reached 2.5° K. The concentration of He^3 in the removed product was 99.95 to 99.97%. After removal of the 99.95% gas and with 2.5 *l* still remaining in the apparatus, the concentration of the remaining mixture proved to be 16%.

With 2 liters of liquid helium poured initially into the outer flask, the apparatus could operate for about 4 to 5 hours.

I consider it my pleasant duty to express my sincere thanks to Mr. A. I. Filimonov, who had constructed most of the equipment and with whom I conducted most of the experiments; also, to V.M. Kuznetsov and A. I. Uriutov who helped with the experiments; to Professor N. E. Alekseevskii/ in whose laboratory the mass spectroscopic analyses were carried out; and to T. K. Shusalova who performed the analyses with the mass spectroscope.

---

[1] E. Pollard and W. Davidson, *Applied Nuclear Physics* (New York, London), 1945.

[2] V. N. Esel'son and B. G. Lazarev, J. Exptl. Theoret. Phys. (U.S.S.R.) 20, 742 (1950).

[3] V. P. Peshkov, J. Tech. Phys. (U.S.S.R.) **26**, 178 (1956).

[4] J. J. M. Beenakker et al., Physica **18**, 433 (1952).

[5] V. N. Esel'son et al., J. Exptl. Theoret. Phys. (U.S.S.R.) 20, 748 (1950).

[6] J. G. Daunt and C. V. Heer, Phys. Rev. 79, 46 (1950)

[7] I. Pomeranchuk, J. Exptl. Theoret. Phys. (U.S.S.R.) 19, 42 (1949).

Translated by J. L. Herson
177

The Effect of Noncentral Forces on Bremsstrahlung in Neutron-Proton Collisions

B. L. TIMAN
Dnepropetrovsk Mining Institute
(Submitted to JETP editor March 10, 1955)
J. Exptl. Theoret. Phys. (U.S.S.R.) 30, 881-883 (May, 1956)

The differential cross section for bremsstrahlung in the collision of high energy nucleons is calculated, including the effect of noncentral forces.

BREMSSTRAHLUNG during collision of high energy nucleons has been studied in a series of theoretical papers [1-5]. In addition, there are many experimental papers which deal with this problem [6]. It is of interest to consider the effect of noncentral forces on the bremsstrahlung during such collisions.

In calculating the differential cross section for bremsstrahlung during neutron-proton collisions, including noncentral forces, we shall, as in the earlier work, use the Born approximation and solve the problem for the nonrelativistic case. We choose the operator describing the nuclear interaction of the particles to be

$$V(r, \vec{\sigma}_p, \vec{\sigma}_n) \tag{1}$$
$$= (\alpha + \beta\vec{\sigma}_p\cdot\vec{\sigma}_n + \gamma S_{pn}) P_M g_i e^{-\lambda r}/r;$$

here P_M is the Majorana operator, $\lambda^{-1} = 1.18 \times 10^{-13}$ cm, g_1 and g_3 are the depths of the potential well for single and triplet states, respectively [7]

$$g_1 = 0{,}280\,\hbar c,\quad g_3 = 0{,}404\,\hbar c, \tag{2}$$
$$\alpha = 1 - {}^1/_2 g,\quad \beta = g/2,\quad g = 0{,}07,\quad \gamma = 0{,}775,$$

$$S_{pn} = 6(\mathbf{S}\cdot\mathbf{r})^2/r^2 - 2\mathbf{S}^2. \tag{3}$$

In order to shorten the calculations we consider only exchange forces, as shown in earlier work [1]; the intensity of the radiation in neutron-proton collisions under the action of exchange forces is greater than the intensity of the radiation under the action of ordinary forces.

The operator describing the interaction of the proton with the radiation field is

$$H = -(e/Mc)\,\mathbf{p}\cdot\mathbf{A}, \tag{4}$$

where

$$\mathbf{A} = (2\pi)^{1/2}\hbar c \sum_{\varkappa} \frac{\vec{\varepsilon}_{\varkappa}}{\omega_{\varkappa}^{1/2}} \exp\{i\vec{\varkappa}\cdot\mathbf{r}\}\,(a_{\varkappa} + a_{-\varkappa}); \tag{5}$$

$a_{\varkappa}$ and $a_{-\varkappa}$ correspond to emission and absorption of a photon, respectively, $\omega_{\varkappa} = \hbar\nu_{\varkappa}$ is the photon energy. Thus we shall consider only electric radiation.

We shall calculate the matrix element H' which determines the probability of radiation of a photon:

$$H' = \frac{H_{AI}V_{IF}}{E_A - E_I} + \frac{V_{AII}H_{IIF}}{E_A - E_{II}}. \tag{6}$$

The wave functions for the neutron-proton system in Born approximation are:

$$\psi_A = \exp\left\{\frac{i}{\hbar}\mathbf{p}_0\cdot\mathbf{r}\right\}\chi^{S^0}_{m_{S^0}};\quad \psi_I = \exp\left\{\frac{i}{\hbar}\mathbf{p}_I\cdot\mathbf{r}\right\}\chi^{S'}_{m_{S'}};$$

$$\psi_F = \exp\left\{\frac{i}{\hbar}\mathbf{p}\cdot\mathbf{r}\right\}\chi^{S}_{m_S};$$

$$\psi_{II} = \exp\left\{\frac{i}{\hbar}\left(\mathbf{p}_{II}\cdot\mathbf{r}\right)\right\}\chi^{S''}_{m_{S''}}.$$

The index A refers to the initial state, I indicates the intermediate state in which the photon has been emitted but the nuclear interaction has not yet occurred, II indicates the intermediate state in which the nuclear interaction has already occurred but the photon has not yet been emitted, while F refers to the final state of the system.

$\chi^{S^0}_{m_{S^0}}$, $\chi^{S'}_{m_{S'}}$, $\chi^{S''}_{m_{S''}}$, $\chi^{S}_{m_S}$ are spin functions characterizing, respectively, the initial, intermediate and final states of the spin and its projection on the axis of quantization. The superscript indicates the value of the total spin in the corresponding state, while the subscript is the value of the spin projection on the axis of quantization. $\mathbf{p}_0$, $\mathbf{p}_I$, $\mathbf{p}_{II}$ and $\mathbf{p}$ are the relative momenta of neutron and proton in the initial, intermediate and final states, respectively, and $\vec{\varkappa}$ is the momentum of the photon.

If we calculate all the matrix elements and sub-

stitute in (6), we get

$$H' = \frac{2e}{Mc}\{p_{0\epsilon}\to q_{25+1}\,[(\alpha-3\beta)V_{p_0+p} \tag{7}$$

$$+(2\beta-\gamma)V_{p_0+p}S(S+1)$$

$$+6\pi\gamma LS(S+1)-6\pi\gamma Nm_S^2]\,\delta_{m_1{}^0m_1{}'}\,\delta_{m_1{}'m_S}\,\delta_{1'S}\,\delta_{1''S}$$

$$+(2\beta-\gamma)V_{p_0+p}S''(S''+1)$$

$$-p_{\vec{\epsilon}}\,g_{25+1}\,[(\alpha-3\beta)V_{p_0+p}+6\pi\gamma LS''(S''+1)$$

$$-6\pi\gamma Nm_{S''}^2]\,\delta_{m_1{}^0m_{S^0}}\,\delta_{1^0S''}\,\delta_{m_1{}''m_S}\,\delta_{1''S}\}.$$

Here δ is the Kronecker delta and

$$L=\left\{\frac{2}{\hbar^{-2}|\mathbf{p}_0+\mathbf{p}|^2}\right.$$

$$\left.+\frac{\lambda}{\hbar^{-3}|\mathbf{p}_0+\mathbf{p}|^3}\arccos\frac{\lambda^2-\hbar^{-2}|\mathbf{p}_0+\mathbf{p}|^2}{\lambda^2+\hbar^{-2}|\mathbf{p}_0+\mathbf{p}|^2}\right\},$$

$$N=\left\{\frac{6\lambda^2+(4/\hbar^2)|\mathbf{p}_0+\mathbf{p}|^2}{\hbar^{-2}|\mathbf{p}_0+\mathbf{p}|^2(\lambda^2+\hbar^{-2}|\mathbf{p}_0+\mathbf{p}|^2)}\right.$$

$$\left.+\frac{3\lambda}{\hbar^{-3}|\mathbf{p}_0+\mathbf{p}|^3}\arccos\frac{\lambda^2-\hbar^{-2}|\mathbf{p}_0+\mathbf{p}|^2}{\lambda^2+\hbar^{-2}|\mathbf{p}_0+\mathbf{p}|^2}\right\},$$

$$V_{p_0+p}=2\pi/[\lambda^2+\hbar^{-2}|\mathbf{p}_0+\mathbf{p}|^2].$$

Summing H' over the values of total spin and spin projection in the intermediate states, squaring, summing over values of spin and spin projection in the final state, and then averaging over all initial spin states, we obtain, after some transformations, the differential effective cross section in the form:

$$d\sigma=\frac{e^2g_3^2}{64\pi^4\hbar^5}\frac{p}{p_0}\frac{1}{\omega_\varkappa^3}(\mathbf{p}_{0\vec{\epsilon}}-\mathbf{p}_{\vec{\epsilon}})^2\left\{3[(1-2\gamma)V_{p_0+p} \tag{8}\right.$$

$$+12\pi\gamma L]^2+72\pi^2\gamma^2N^2-24\pi\gamma N[(1-2\gamma)V_{p_0+p}$$

$$\left.+12\pi\gamma L]+(\alpha-3\beta)^2\frac{g_1^2}{g_3^2}V_{p_0+p}^2\right\}\varkappa^2\,d\varkappa\,d\Omega_\varkappa\,d\Omega_p.$$

Summing this expression over the two photon polarizations, and integrating over the angle of emergence of the photon and the azimuthal angle of the scattered particle, substituting the values of V_{p_0+p}, L and N, we find

$$d\sigma=2\frac{g_3^2}{p_0^2c^2}\frac{e^2}{\hbar c}\frac{p^2}{1-p^2}(\mathbf{n}_0-\mathbf{p})^2\left\{\frac{1}{\eta^2}[(1-2\gamma)^2\right.$$

$$+(g_1^2/3g_3^2)(\alpha-3\beta)^2+48\gamma^2+8\gamma(1-2\gamma)]$$

$$+\frac{96\gamma^2\lambda^2}{\xi^2\eta^2}+\frac{72\gamma^2\lambda^4}{\xi^4\eta^2}+\frac{24\gamma^2\lambda(3\lambda^2+2\xi^2)}{\xi^5\eta}\arccos\frac{\zeta}{\eta}$$

$$\left.+\frac{18\gamma^2\lambda^2}{\xi^6}\arccos^2\frac{\zeta}{\eta}\right\}dp\sin\theta\,d\theta. \tag{9}$$

We have introduced the symbols

$$\xi=(1/\hbar)|\mathbf{n}_0+\mathbf{p}|,\quad \eta=\lambda^2+\xi^2,\quad \zeta=\lambda^2-\xi^2;$$

$\mathbf{n}_0$ is a unit vector along $\mathbf{p}_0$, p is measured in units of p_0, λ in units of $p_0/\hbar$, and θ is the angle of scattering.

We note that if we set $\alpha=1$, $\beta=\gamma=0$ (the central forces), we get a formula for the differential cross section similar to that obtained in earlier papers.

Investigation of the differential cross section (9) shows that the inclusion of noncentral forces gives a sharper maximum of the radiation in the region of scattering angles close to π even for low photon energies.

In conclusion, it is a pleasant duty to express my thanks to L. N. Rozentsveig for suggesting the problem and for many valuable suggestions, and also to Prof. A. I. Akhiezer for his interest in the work.

[1] I. Pomeranchuk and I. Shmushkevich, Dokl. Akad. Nauk SSSR **64**, 499 (1949).

[2] I. Pomeranchuk and I. Shmushkevich, Dokl. Akad. Nauk SSSR 70, 33 (1950).

[3] J. Ashkin and R. Marshak, Phys. Rev. 76, 58 (1949).

[4] V. Fainberg and E. Feinberg, Dokl. Akad. Nauk SSSR 68, 45 (1949).

[5] G. Avak'iants, J. Exptl. Theoret. Phys. (U.S.S.R.) 20, 944 (1950).

[6] R. Bjorklund, W. Crandall, B. Moyer and H. York, Phys. Rev. 77, 213 (1950).

[7] H. A. Bethe, *Lectures on Nuclear Theory*, IIL, 1949 (Russian translation).

Translated by M. Hamermesh
181

Statistical Theory of the Atomic Nucleus. III

B. K. KERIMOV AND A. V. DZHAVADOE
Moscow State University

(Submitted to JETP editor March 13, 1955)
J. Exptl. Theoret. Phys. (U.S.S.R.) 30, 900-914 (May, 1956)

The statistical model of the nucleus is investigated for uniform and nonuniform density distributions of nucleons. It is shown that a two nucleon central interaction potential, which contains the ordinary nonexchange repulsive force along with the spin exchange force, leads to a saturation of the nuclear binding energy and nuclear density.

THE theoretical explanation of the saturation of nuclear in complicated nuclei (saturation of the nuclear density and the binding energy) is a basic problem of nuclear physics. Up to now this problem has not received a satisfactory solution because of the fact that a precise law of interaction for nucleons has not been established. The saturation properties of the forces puts a definite limit on the choice of interaction between two nucleons. For example, the possibility of explanation of the stability of a nucleus with the aid of a single Wigner force of attraction (in the form of a rectangular well and Yukawa potential[1,2]) is excluded. Some spin forces $\sim (\vec{\sigma}_1 \cdot \vec{\sigma}_2)$ also cannot guarantee stability of the nucleus.

In Refs. 3 and 4* it was shown that with the use of the statistical model a two nucleon central interaction potential, which contains the ordinary nonexchange repulsive force along with the spin force, permits us to obtain the saturation of the binding energy for normal density of nucleons which corresponds to the equilibrium nuclear radius $R_s = 1.48 \times 10^{-13} A^{1/3}$ cm. In this particular variant of the forces the general potential energy of the nucleus consists of the usual positive potential energy of repulsion V^0 and the negative exchange potential energy of attraction V^a of the nucleons. In Refs. 5 and 6, which are also devoted to the statistical calculation of the energy of the nucleus, and which take into account only the exchange forces of attraction of a different type of n-p and p-p interaction (with the force law and density functions different from those used in I, II) and excluding from consideration the potential energy V^0, that is determined by the usual density $\rho(r, r)$ of the nucleons.

In recently published works[7,8], the problem has also been investigated of the saturation of nuclear forces in complicated nuclei. It is pointed out in Ref. 7 that the repulsive forces between three nucleons, together with two nucleon forces in the pseudoscalar meson theory, give a satisfactory, qualitative explanation of nuclear saturation. In this case it is found that the saturation of the binding energy is approached for the equilibrium value of the nuclear radius $R_s = 1.61 \times 10^{-13} A^{1/3}$ cm. In Ref. 8 the authors show that consideration of the weak repulsion in the odd state (P state), in addition to the repulsive core (r_c) in the two nucleon potential of the pseudoscalar meson thoery permits us to obtain the saturation of the binding energy for the value of the nuclear radius. $R_s = 1.15 \times 10^{-13}/A^{1/3}$ cm without inclusion of the three nucleon repulsive forces. In these researches, as well as in Refs. 3 and 4, the statistical model of the nucleus with uniform density distribution of nucleons was employed.

Data on nuclear scattering of nucleons and electrons of high energy[9-14], on the shell structure of nuclei[15-19] and on x-ray emission of meson atoms[20,21] testify that a uniform density distribution of nucleons (and the Coulomb charge) in the nucleus cannot explain a series of experimental factors and force us to consider the possibility of use of a nuclear model based on the representation of a nonequilibrium distribution of particles (charges) inside the nucleus. In this connection, the investigation of the statistical model of the nucleus from the point of view of nonequilibrium density of nucleons is of considerable interest; it would permit better agreement of the ground state of the nucleus with the data on the shell structure of nuclei (empirical values of the mean square of the orbital momentum of nucleons, etc.).

The present paper is a development of our previous researches[3,4,22] for the case in which the density of the nucleons is characterized by a constant internal part (for $R < R_0$), and falls off on the boundary (for $r > R_0$) in exponential fashion. The role of the usual energy of repulsion of the nucleons is made clear in the investigation of

* We denote subsequent references to these works by I and II.

the problem of the saturation of forces in complicated nuclei. The energy of the nucleus is calculated as a function of the parameters of the nonuniform density distribution of the nucleons. It is shown that the saturation of the binding energy and the density of nucleons in the central portion of the nucleus is brought about by the presence of a repulsive force in the two nucleon potential and the Coulomb energy of the protons.

1. CALCULATION OF THE EXCHANGE AND ORDINARY POTENTIAL ENERGIES OF THE NUCLEUS

We assume that the interaction energy between two protons u_{12}^{pp}, between two neutrons u_{12}^{nn} and a proton and a neutron u_{12}^{np} is represented by the expression [see Eq. (1) in I]:

$$u_{12}^{pp} = u_{12}^{nn} = (g^2 + f^2 (\vec{\sigma}_1 \vec{\sigma}_2)) \frac{e^{-k_0 r}}{r}; \tag{1}$$

$$u_{12}^{np} = (g^2 + f^2 (\vec{\sigma}_1 \vec{\sigma}_2)) \frac{e^{-k_0 r}}{r} - (g^2 + f^2 (\vec{\sigma}_1 \vec{\sigma}_2)) \frac{e^{-k_0 r}}{r} Q_{\text{H}}, \tag{2}$$

where Q_{H} is the Heisenberg operator for the permutation of the space and spin coordinates of particles 1 and 2; g^2 and f^2 are constants of the interaction; $r = |\mathbf{r}_1 - \mathbf{r}_2|$ is the distance between the nucleons 1 and 2; $1/k_0$ is a certain constant determining the radius of action of the nuclear forces. For simplicity, in first approximation, we omit the Coulomb repulsion between the protons. The wave functions for the protons $\psi_k(\mathbf{r}, s)$ and for the neutrons $\varphi_k(\mathbf{r}, s)$ in the nonrelativistic approximation can be represented in the form of a product of coordinate and spin functions:

$$\psi_k(\mathbf{r}, s) = \psi_k(\mathbf{r})\, a_k(s); \quad \varphi_k(\mathbf{r}, s) = \varphi_k(\mathbf{r})\, b_k(s) \tag{3}$$

(k = propagation vector, s = nucleon spin). For the isolated proton and neutron, we choose the coordinated part of the wave function in the form of a plane wave

$$\psi_k(r) = V^{-1/2} \exp\{i\mathbf{k}_p \mathbf{r}\}; \quad \varphi_k(\mathbf{r}) = V^{-1/2} \exp\{i\mathbf{k}_n \mathbf{r}\}, \tag{4}$$

where $\mathbf{k}_p$ and $\mathbf{k}_n$ are the propagation vectors of the proton and the neutron; V is the volume of the nucleus. For the spin functions $a_k(s)$ and $b_k(s)$ we have the Eqs. (6) of I.

Applying the Hartree-Fock method and considering Eqs. (1) and (2) for the total energy E of a nucleus consisting of Z protons and N neutrons ($A = N + Z$ = mass number of the nucleus), we obtain

$$E = V_{pp}^0 + V_{nn}^0 + V_{pn}^0 + V_{pp}^a + V_{nn}^a + V_{pn}^a + T_k^p + T_k^n, \tag{5}$$

where (the index i denotes either p or n everywhere):

$$V_{ii}^0 = \frac{1}{2} g^2 \iint (d\mathbf{r}_1)\,(d\mathbf{r}_2)\, \frac{e^{-k_0 r}}{r} \rho_i(\mathbf{r}_1)\, \rho_i(\mathbf{r}_2); \tag{6}$$

$$V_{pn}^0 = g^2 \iint (d\mathbf{r}_1)\,(d\mathbf{r}_2)\, \frac{e^{-k_0 r}}{r} \rho_p(\mathbf{r}_1)\, \rho_n(\mathbf{r}_2); \tag{7}$$

$$V_{ii}^a = -\frac{1}{4} (g^2 + 3f^2) \iint (d\mathbf{r}_1)\,(d\mathbf{r}_2)\, \frac{e^{-k_0 r}}{r} |\rho_i(\mathbf{r}_1, \mathbf{r}_2)|^2; \tag{8}$$

$$V_{pn}^a = -\frac{1}{2} (g^2 + 3f^2) \iint (d\mathbf{r}_1) \times (d\mathbf{r}_2)\, \frac{e^{-k_0 r}}{r} \rho_p(\mathbf{r}_1, \mathbf{r}_2)\, \rho_n^*(\mathbf{r}_1, \mathbf{r}_2); \tag{9}$$

$$T_k^p = \frac{\hbar^2}{8\pi^2 M} \sum_{k=1}^{Z} \int \nabla\psi_k(\mathbf{r})\, \nabla\psi_k^*(\mathbf{r})\, (d\mathbf{r}_k), \tag{10}$$

$$T_k^n = \frac{\hbar^2}{8\pi^2 M} \sum_{k=1}^{N} \int \nabla\varphi_k(\mathbf{r})\, \nabla\varphi_k^*(\mathbf{r})\, (d\mathbf{r}_k).$$

Here V_{pp}^0, V_{nn}^0 and V_{pn}^0 are the ordinary parts of the total potential energy of interaction of the protons with protons, neutrons with neutrons and protons with neutrons: V_{pp}^a, V_{nn}^a and V_{pn}^a are the exchange parts of these same energies; T_k^p and T_k^n are the kinetic energies of the protons and neutrons. The ordinary and mixed densities of protons and neutrons in Eqs. (6)-(9) are determined by the expressions

$$\rho_p(\mathbf{r}_1) = \rho_p(\mathbf{r}_1, \mathbf{r}_1) = \sum_{k=1}^{Z} \psi_k^*(\mathbf{r}_1)\, \psi_k(\mathbf{r}_1); \tag{11}$$

$$\rho_p(\mathbf{r}_1, \mathbf{r}_2) = \sum_{k=1}^{Z} \psi_k^*(\mathbf{r}_1)\, \psi_k(\mathbf{r}_2)$$

and similarly for ρ_n with φ in place of ψ and summation over N.

With the help of Eq. (4) we obtain from Eq. (11) the following relation between the densities and the maximum wave numbers of the protons K_p and of the neutrons K_n:

$$K_i^3 = 3\pi^2\rho_i(r), \tag{12}$$

$$\rho_i(r_1, r_2) = (\sin K_i r - K_i r \cos K_i r)/\pi^2 r^3. \tag{13}$$

In this case we consider that each proton and neutron state is occupied by two protons and two neutrons, respectively, with antiparallel spins. Substituting the values (13) and (12) in Eqs. (8) and (9) and integrating, we obtain the exchange potential energies of the nucleons as functions of the densities $\rho_p(r)$, $\rho_n(r)$ in the form

$$V_{ii}^a = -(g^2 + 3f^2)(k_0^4/24\pi^3) V v(\rho_i), \tag{14}$$

$$V_{pn}^a = -(g^2 + 3f^2)(k_0^4/12\pi^3) V v(\rho_p, \rho_n), \tag{15}$$

where

$$v(\rho_i) = 6\alpha^4\rho_i^{4/3} - \alpha^2\rho_i^{2/3} - 8\alpha^3\rho_i \operatorname{arctg} 2\alpha\rho_i^{1/3} + {}^1/_4(1 + 12\alpha^2\rho_i^{2/3}) \ln(1 + 4\alpha^2\rho_i^{2/3}); \tag{16}$$

$$v(\rho_p, \rho_n) = 3\alpha^4(\rho_n\rho_p^{1/3} + \rho_n^{1/3}\rho_p) - \alpha^2\rho_n^{1/3}\rho_p^{1/3} + {}^1/_4[1 + 6\alpha^2(\rho_n^{2/3} + \rho_p^{2/3}) - 3\alpha^4(\rho_n^{2/3} - \rho_p^{2/3})^2] \ln \frac{1 + \alpha^2(\rho_n^{1/3} + \rho_p^{1/3})^2}{1 + \alpha^2(\rho_n^{1/3} - \rho_p^{1/3})^2} + 4\alpha^3(\rho_n - \rho_p)\operatorname{arctg}\alpha(\rho_n^{1/3} - \rho_p^{1/3}) - 4\alpha^3(\rho_n + \rho_p)\operatorname{arctg}\alpha(\rho_n^{1/3} + \rho_p^{1/3}). \tag{17}$$

Here $V = 4\pi/3R^3$ is the volume of the nucleus; $\alpha = (3\pi^2)^{1/3}k_0$.

Equations (14) and (15) are the exchange energies of the nucleons of the nucleus with constant density distributions of protons ρ_p and neutrons ρ_n. For nonuniform densities, Eqs. (14) and (15) change so that multiplication by V is replaced by integration over the nuclear volume. Here ρ_p and ρ_n are the densities of protons and neutrons in the volume element $d\tau$ of the nucleus, so normalized that

$$\int \rho_p d\tau = Z; \quad \int \rho_n d\tau = N. \tag{18}$$

For the ordinary potential energy of repulsion of the nucleons of the nucleus (in the case of constant densities ρ_p and ρ_n), we get from Eqs. (6) and (7) [see the derivation of Eq. (14) in II]

$$V_{ii}^0 = \frac{2\pi g^2}{k_0^2}\rho_i^2(r) V; \quad V_{pn}^0 = \frac{4\pi g^2}{k_0^2}\rho_p(r)\rho_n(r) V. \tag{19}$$

The total potential energy of the nucleus is composed of the total exchange potential energy of attraction and the total ordinary potential energy of repulsion and, in accord with Eqs. (14), (15) and (19), is equal to

$$W(\rho_n, \rho_p) = (V_{pp}^a + V_{nn}^a + V_{pn}^a) + (V_{pp}^0 + V_{nn}^0 + V_{pn}^0) = -\frac{(g^2 + 3f^2)k_0^4}{24\pi^3}[v(\rho_p) + v(\rho_n) + 2v(\rho_p, \rho_n)]V + \frac{2\pi g^2}{k_0^2}[\rho_p(r) + \rho_n(r)]^2 V \tag{20}$$

for the case of constant density of nucleons.

Taking into account Eqs. (4) and (12), we get from Eq. (10) the well-known expression for the kinetic energy of protons and neutrons:

$$T_k^i = (4\pi h^2/5M)(3\rho_i/8\pi)^{5/3} V; \tag{21}$$

M is the mean value of the masses of neutron and proton. For variable densities, multiplication by V in all formulas is replaced by integration over the volume. Thus we have obtained the exchange and ordinary parts of the total potential energy of the nucleus as a function of the density distribution of the particles and the parameters of the nuclear forces.

2. CASE OF A STATISTICAL NUCLEUS WITH $\rho_p(r) = \rho_n(r)$.

DETERMINATION OF THE PARAMETERS OF THE TWO NUCLEON POTENTIAL

Let us consider a simple case, assuming the density of protons and neutrons to be equal: $\rho_n(r) = \rho_p(r) = {}^1/_2\rho(r)$, where $\rho(r)$ is the total density of nucleons in the nucleus. Then the condition (18) takes the form

$$\int \rho(r) d\tau = A. \tag{22}$$

In accordance with Eq. (20), the total potential

energy of the nucleus as a function of the density $\rho(r)$ is equal to (we compute the formulas for constant ρ):

$$W(\rho) = V^a_{ii,\,pn}(\rho) + V^0_{ii,\,pn} = \tag{23}$$

$$-\frac{g^2+3f^2}{6\pi^3}k_0^4 V v_A(\rho) + \frac{2\pi g^2}{k_0^2}\rho^2(r)V.$$

Here,

$$v_A(\rho) = 6\alpha_1^4\rho^{4/3} - \alpha_1^2\rho^{2/3} - 8\alpha_1^3\rho\,\mathrm{arctg}\,2\alpha_1\rho^{1/3} \tag{24}$$

$$+\frac{1}{4}(1+12\alpha_1^2\rho^{2/3})\ln(1+4\alpha_1^2\rho^{2/3}),$$

$$\alpha_1 = (3\pi^2/2)^{1/3}/k_0.$$

With the help of Eq. (21) we will have for the Fermi kinetic energy of the nucleons:

$$T_k = T_k^p + T_k^n = (8\pi h^2/5M)(3\rho/16\pi)^{5/3}V. \tag{25}$$

For the determination of the parameters of the interaction potential (1) and (2), we limit ourselves to a consideration of the zeroth approximation, when we can consider the density $\rho(r)$ of the nucleons to be a constant in the volume V of the nucleus. It follows from Eq. (22) that $\rho = A/V = 3A/4\pi R^3$. Here R is the radius of the nucleus with constant particle density. Then, carrying out the substitution (18b) of II, we get the total energy E as a function of the radius R from Eqs. (23) and (25):

$$E = T_k(x) + V^0(x) + V^a_{(x)} \tag{26}$$

$$= \left\{\frac{a_2}{x^2} + \frac{a_3}{x^3} - a_1\Phi(\beta x)\right\}A,$$

where

$$a_1 = \frac{(9\pi)^{4/3}}{12\pi^2}\frac{\beta}{r_0}(g^2+3f^2); \tag{27}$$

$$a_2 = \left(\frac{3}{\pi}\right)^{4/3}\frac{3h^2}{160\,Mr_0^2}; \quad a_3 = \frac{3}{2}\frac{g^2}{\beta^2 r_0};$$

$$\Phi(\beta x) = \frac{1}{\beta x} - \frac{1}{6}\left(\frac{8}{9\pi}\right)^{2/3}\beta x$$

$$-\frac{4}{3}\left(\frac{8}{9\pi}\right)^{1/3}\mathrm{arctg}\,2\left(\frac{9\pi}{8}\right)^{1/3}\frac{1}{\beta x}$$

$$+\left[\frac{1}{2}\left(\frac{8}{9\pi}\right)^{2/3}\beta x + \frac{1}{4}\left(\frac{8}{9\pi}\right)^{4/3}\beta^3 x^3\right]$$

$$\times\ln\left[1+4\left(\frac{9\pi}{8}\right)^{2/3}\frac{1}{\beta^2 x^2}\right];$$

$$\beta = k_0 r_0; \quad x = R/r_0 A^{1/3}. \tag{28}$$

The quantity x determines the departure of the density ρ from its equilibrium value. For $x = 1$ we have the normal density, for which the energy ought to have a minimum, equal to the empirical value. With the help of Eq. (20) of II, which determines the stable state of the system of nucleons, and the empirical value of the binding energy

$$\{E(x)\}_{x=1} = -\alpha_0 A; \quad \alpha_0 \approx 14\ \text{mev} \tag{29}$$

we find g^2 and f^2 from Eq. (26) as functions of the quantities β and r_0:

$$g^2 = -\frac{\alpha_0\Phi'(\beta) + a_2[2\Phi(\beta)+\Phi'(\beta)]}{m_0[3\Phi(\beta)+\Phi'(\beta)]}; \tag{30}$$

$$f^2 = \frac{m_0 - n_0\Phi(\beta)}{3n_0\Phi(\beta)}g^2 + \frac{a_2+\alpha_0}{3n_0\Phi(\beta)}, \tag{31}$$

where

$$m_0 = 3/2\,\beta^2 r_0; \quad n_0 = (3/\pi)^{2/3}3\beta/4r_0.$$

$\Phi(\beta)$ and $\Phi'(\beta)$, $\Phi''(\beta)$ are the values of the function $\Phi(\beta x)$ and its derivatives for $x = 1$. The inequality which determines the upper limit of the value of the constant $\beta = k_0 r_0$ has the form:

$$6a_2 - 12\frac{(\alpha_0+a_2)\Phi'(\beta)+2a_2\Phi(\beta)}{3\Phi(\beta)+\Phi'(\beta)} \tag{32}$$

$$> \frac{3\alpha_0+a_2}{3\Phi(\beta)+\Phi'(\beta)}\Phi''(\beta).$$

For the determination of the upper limit of the value of β we make use of two different empirical values of the parameter r_0, for judgment on the accuracy of which we make reference to in the literature. The data on nuclear scattering of high energy electrons, on the isotopic shift, on mesoatoms lead to a value of the radius R of a nucleus with constant density, equal to [10,11,20,21,23]:

$$r_0 = RA^{-1/3} \approx 1.2\times10^{-13}\ \text{cm}. \tag{33}$$

On the other hand, it follows from the theory of α-decay, and the results of experiments on the scattering of fast neutrons, that [5,24,25]

$$r_0 = RA^{-1/3} \approx 1.48\times10^{-13}\ \text{cm and}\ 1.5\times10^{-13}\ \text{cm}. \tag{34}$$

For the value of r_0 from Eq. (33), we find from Eq. (33) that $\beta < 1.80$. We then obtain a limit for the value of the effective radius of action of the nuclear forces:

$$1/k_0 > 0.667 \times 10^{-13} \text{ cm}. \quad (35)$$

For the value of Eq. (34), it follows from Eq. (32) that equilibrium of the nucleus is possible if $\beta < 1.75$. We then obtain

$$1/k_0 > 0.846 \times 10^{-13} \text{ cm}. \quad (36)$$

It follows from Eqs. (30)-(32) that the usual potential energy of repulsion $V^0 \sim \alpha_3$ of the nucleons plays an essential role in the problem under consideration, since this energy determines the value of the limiting effective radius of action of nuclear forces. In accord with Eqs. (35) and (36) we take the effective radius of action of nuclear forces $1/k_0$ to be equal to the Compton wavelength of the π-meson:

$$1/k_0 = \hbar/m_\pi c = 1.4 \times 10^{-13} \text{ cm} \quad (m_\pi = 276\, m_e). \quad (37)$$

Substituting the values of Eqs. (33), (34) and (37) into Eqs. (30) and (31) we find

$$g^2/\hbar c = 0.051; \quad f^2/\hbar c = 0.340 \quad (38)$$

for $r_0 = 1.2 \times 10^{-13}$ cm,

$$g^2/\hbar c = 0.132; \quad f^2/\hbar c = 0.479 \quad (39)$$

for $r_0 = 1.48 \times 10^{-13}$ cm.

For the values of Eq. (38), the usual energy of repulsion, the exchange energy of attraction and the total potential energy per nucleon are, respectively, (for $x = 1$),

$$V^0/A = 17 \text{ mev}; \quad V^a/A = -51 \text{ mev}; \quad (40)$$

$$T/A = 20 \text{ mev};$$

$$W/A = V^0/A + V^a/A = -34 \text{ mev},$$

and for (39) we have

$$V^0/A = 23.6 \text{ mev}; \quad V^a/A = -50.8 \text{ mev}; \quad (41)$$

$$T/A = 13.2 \text{ mev};$$

$$W/A = -27.2 \text{ mev}.$$

The dependencies of all quantities on x, computed from Eq. (26), are shown graphically in Figs. 1 and 2. It is evident from these graphs that the total potential energy per nucleon has a minimum, equal to

$$W/A = -43.67 \text{ mev}$$

for $R_m = 0.7\, r_0 A^{1/3} = 0.840 \cdot 10^{-13} A^{1/3}$

for the case (38) and

$$W/A = -30.54 \text{ mev}$$

for $R_m = 0.8\, r_0 A^{1/3} = 1.184 \times 10^{-13} A^{1/3}$ cm

for case (39). Consideration of the kinetic energy leads to the result that the minimum mean energy E/A, equal to the empirical value ~ -14 mev, increases for $x = 1$, i.e., at the equilibrium, value of the nuclear radius R, it is somewhat larger

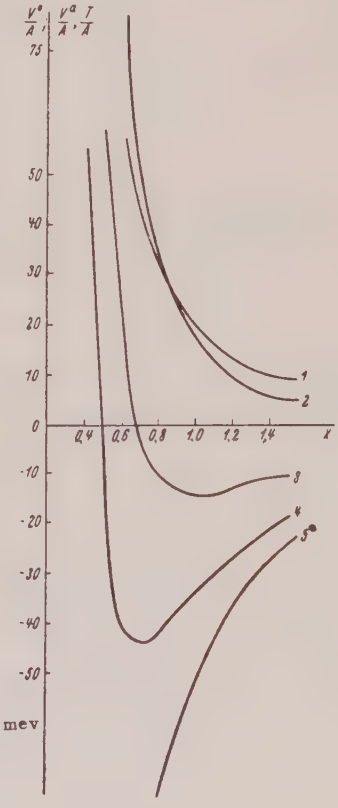

FIG. 1. Potential, kinetic and total energies per nucleon as functions of $x = R/r_0 A^{1/3}$ for values of the parameters from Eq. (38): $1 - T/A$, $2 - V^0/A$, $3 - E/A$, $4 - (V^0/A + V^a/A)$, $5 - V^a/A$.

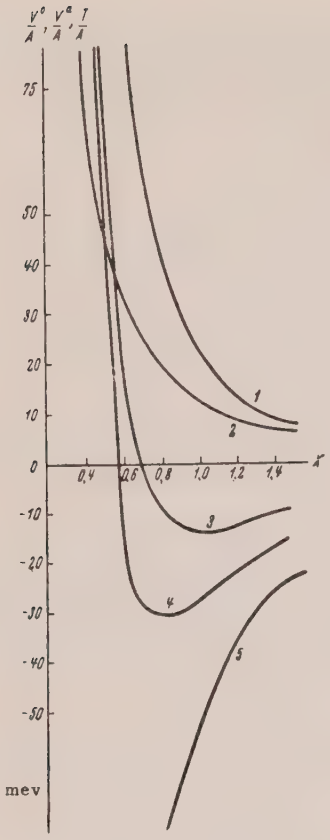

FIG. 2. Potential, kinetic and total energies per nucleon as functions of x for values of the parameters from Eq. (39). $1-V^0/A$, $2-T/A$, $3-E/A$, $4-(V^0/A+V^a/A)$, $5-V^a/A$.

than R_m. Thus, in the simplest case of the statistical model (constant density of particles), a two nucleon potential which contains both the exchange forces and the usual short range forces of repulsion, leads to a saturation of the binding energy which sets in for normal density ($x=1$).

3. CALCULATION OF THE BINDING ENERGY OF THE NUCLEUS WITH NONUNIFORM DENSITY DISTRIBUTION OF NUCLEONS

Taking into account the empirical facts that the mean binding energy per nucleon is almost constant and the nuclear volume is proportional to A, the density $\rho(r)$ of particle distribution in the nucleus can be taken equal to[22] (see also Refs. 26-28)

$$\rho(r)=\begin{cases}\rho_0 & \text{for } r\leqslant R_0,\\ \rho_0\cdot\exp\{-(r-R_0/a)\} & \text{for } r>R_0.\end{cases} \tag{42}$$

Here ρ_0 is the particle density (independent of r) in the central part of the nucleus; R_0 is the radius of the central part, a is the thickness of the surface layer, where the density falls off exponentially. For such a density choice, the nucleus has a dense interior part (core) and a diffuse periphery. More recently, Jastrow and Roberts[26] chose, for the explanation of the nuclear scattering of neutrons in the energy range 14-270 mev, a density of nuclear matter of the same for as in the work of one of us[22] [see Eq. (42)]. We note that the theoretical analysis of experimental data on nuclear scattering of nucleons and electrons of high energy shows that the nuclear model (42) gives better agreement with experiment than the model of Born and Yang[27,28].

We proceed to the calculation of the binding energy of the nucleus as a function of the variation parameters a, R_0 and ρ_0, with the help of the Ritz method. Carrying out integration over the volume of the nucleus, we obtain for the exchange and ordinary potential energies

$$V^a=-\frac{2}{9}(g^2+3f^2)\frac{k_0^4R_0^3}{\pi^2}\{B_0(q)+\varepsilon_0B_1(q)+\varepsilon_0^2B_2(q)+\varepsilon_0^3B_3(q)\}, \tag{43}$$

$$V^0=\frac{g^2k_0^4}{54\pi^2}q^6R_0^3\left\{1+\frac{3}{2}\varepsilon_0+\frac{3}{2}\varepsilon_0^2+\frac{3}{4}\varepsilon_0^3\right\}, \tag{44}$$

where

$$B_0(q)=\frac{3}{8}q^4-\frac{1}{4}q^2+\frac{1}{4}(1+3q^2)\ln(1+q^2)-q^3\operatorname{arctg}q; \tag{45}$$

$$B_1(q)=\frac{27}{32}q^4-3q^2+\frac{15}{8}\ln(1+q^2)+\frac{27}{8}q^2\ln(1+q^2)-3q^3\operatorname{arctg}q+\frac{9}{4}X_1(q);$$

$$B_2(q)=\frac{81}{64}q^4-\frac{129}{8}q^2+\frac{57}{8}\ln(1+q^2)+\frac{81}{8}q^2\ln(1+q^2)-6q^3\operatorname{arctg}q+\frac{45}{4}X_1(q)+\frac{27}{2}X_2(q);$$

$$B_3(q)=\frac{243}{256}q^4-\frac{291}{8}q^2+\frac{195}{16}\ln(1+q^2)+\frac{243}{16}q^2\ln(1+q^2)-6q^3\operatorname{arctg}q+\frac{171}{8}X_1(q)+\frac{135}{4}X_2(q)+\frac{81}{4}X_3(q);$$

$$X_1(q)=\int_0^\infty \ln(1+q^2e^{-2x})\,dx;$$

$$X_2(q)=\int_0^\infty x\ln(1+q^2e^{-2x})\,dx;$$

$$X_3(q)=\int_0^\infty x^2\ln(1+q^2e^{-2x})\,dx;$$

$$\varepsilon_0=a/R_0;\quad q=(12\pi^2)^{1/3}\rho_0^{1/3}/k_0.$$

For the kinetic energy we get

$$T_k=\frac{\hbar^2k_0^5q^5}{480\pi^3M}R_0^3\left\{1+\frac{9}{5}\varepsilon_0+\frac{54}{25}\varepsilon_0^2+\frac{162}{125}\varepsilon_0^3\right\}. \quad (46)$$

Making use of Eq. (45), we get from Eqs. (22) and (42) a single relation among the three parameters R_0, q and ϵ_0:

$$R_0=(9\pi)^{1/3}(k_0q)^{-1}A^{1/3}(1+3\varepsilon_0+6\varepsilon_0^2+6\varepsilon_0^3)^{-1/3}. \quad (47)$$

Eliminating R_0 from Eqs. (43), (44) and (46), we reduce the total energy of the nucleus to the following form, making use of Eq. (47):

$$\begin{aligned}E&=V^a+V^0+T_k\\&=\frac{A}{1+3\varepsilon_0+6\varepsilon_0^2+6\varepsilon_0^3}\left\{-b_0\left[\frac{B_0(q)}{q^3}+\varepsilon_0\frac{B_1(q)}{q^3}\right.\right.\\&\quad\left.+\varepsilon_0^2\frac{B_2(q)}{q^3}+\varepsilon_0^3\frac{B_3(q)}{q^3}\right]\\&\quad+b_1q^3\left[1+\tfrac{3}{2}\varepsilon_0+\tfrac{3}{2}\varepsilon_0^2+\tfrac{3}{4}\varepsilon_0^3\right]\\&\quad\left.+b_2q^2\left[1+\tfrac{9}{5}\varepsilon_0+\frac{54}{25}\varepsilon_0^2+\frac{162}{125}\varepsilon_0^3\right]\right\}. \quad (48)\end{aligned}$$

Here,

$$b_0=2k_0(g^2+3f^2)/\pi;\quad b_1=g^2k_0^2/6\pi;$$

$$b_2=3\hbar^2k_0^2/160\,\pi^2M.$$

The energy E depends on the two variation parameters g and ϵ_0. The parameter q characterizes the density ρ_0 of the central part of the nucleus, and ϵ_0 gives the ratio of the region of exponential decay to the linear dimension of the central part of the nucleus (which has constant density). From the condition of minimum energy $\partial E/\partial q=0$, we find the equation which connects the parameters q and ϵ_0:

$$\begin{aligned}\Phi_1(q,\varepsilon_0)&=-b_0[C_0(q)+\varepsilon_0C_1(q)\\&\quad+\varepsilon_0^2C_2(q)+\varepsilon_0^3C_3(q)]+3b_1q^2(1+\tfrac{3}{2}\varepsilon_0\\&\quad+\tfrac{3}{2}\varepsilon_0^2+\tfrac{3}{4}\varepsilon_0^3)\\&\quad+2b_2q\left(1+\frac{9}{5}\varepsilon_0+\frac{54}{25}\varepsilon_0^2+\frac{162}{125}\varepsilon_0^3\right)=0, \quad (49)\end{aligned}$$

where

$$C_j(q)=\frac{\partial}{\partial q}\left(\frac{B_j(q)}{q^3}\right);\quad j=0,1,2,3$$

$$X_1'(q)=\frac{\ln(1+q^2)}{q};\ X_2'(q)=\frac{X_1(q)}{q};$$

$$X_3'(q)=2\frac{X_2(q)}{q}.$$

For each chosen value of q in Eq. (49), we can find the corresponding ϵ_0 and thus establish the dependence of q on ϵ_0. For this purpose, we first determine the interval of possible values of the parameter q and consider two limiting cases of the density distribution (42). In the limiting case

$$R_0=0\quad\text{or}\quad\varepsilon_0\to\infty \quad (50)$$

Eq. (42) goes over to a density that falls off according to the simple exponential

$$\rho(r)=\rho_0\exp(-r/a). \quad (51)$$

With the aid of Eqs. (22) and (45), we find the dependence between the parameters q and a:

$$a=(3\pi/2)^{1/3}A^{1/3}/k_0q. \quad (52)$$

Setting $R=0$ in the general expression for the energy (48) (or $\epsilon_0\to\infty$) and considering Eq. (52), we get the binding energy E of the nucleus with density distribution (51) in the form

$$E=\left\{-\frac{b_0}{6}\frac{B_3(q)}{q^3}+\frac{b_1}{8}q^3+\frac{27}{125}b_2q^2\right\}A. \quad (53)$$

We get the equation defining q from the condition of minimum energy:

$$\begin{aligned}\Phi_2(q)&=-\frac{b_0}{6}\frac{\partial}{\partial q}\left(\frac{B_3(q)}{q^3}\right)\\&\quad+\frac{3}{8}b_1q^2+\frac{54}{125}b_2q=0. \quad (54)\end{aligned}$$

For the values (38) of the constants q^2, f^2, we find from Eq. (54) that $q = 6.2$ or, from Eq. (52),

$$a = 0.39 \times 10^{-13} A^{1/3} \text{ cm} \qquad (55)$$

for the values of Eq. (39), we get $q = 4.7$ from Eq. (54), or

$$a = 0.49 \times 10^{-13} A^{1/3} \text{ cm}. \qquad (56)$$

For these values of the parameter q or ρ_0, the mean binding energy per nucleon is, from Eq. (53), $E/A \approx -8.5$ mev.

It was shown in Ref. 13 that the charge density distribution in the nucleus of the type (51) gives better agreement with the experimental data on the nuclear scattering of fast electrons on beryllium, gold and lead (energy of the electrons $\sim$ 125 mev) and tantalum (energy $\sim$ 150 mev) for values of the parameter $a = 0.636 \times 10^{-13}$ cm for Be; $(2.3 \pm 0.3) \times 10^{-13}$ cm for Au; 2.36×10^{-13} cm for Pb and $(2.80 \pm 0.3) \times 10^{-13}$ cm for Ta. From our theoretical expressions (55) and (56) for a, we have, respectively, $a = 0.81 \times 10^{-13}$ cm for Be; 2.27×10^{-13} cm for Au; 2.31×10^{-13} cm for Pb, 2.21×10^{-13} cm for Ta and $a = 1.02 \times 10^{-13}$ cm for Be; 2.85×10^{-13} cm for Au; 2.90×10^{-13} cm for Pb; 285×10^{-13} cm for Ta.

In the other limiting case,

$$a = 0 \quad \text{or} \quad \varepsilon_0 = 0 \qquad (57)$$

the density relation (42) gives a constant density for the entire extent of the nucleus:

$$\rho(r) = \begin{cases} \rho_0 & \text{for} \quad r \leqslant R_0, \\ 0 & \text{for} \quad r > R_0. \end{cases} \qquad (58)$$

Taking into account Eqs. (45) and (57), we have the following relation between q and R_0 from (47):

$$R_0 = (9\pi)^{1/3} A^{1/3} / k_0 q. \qquad (59)$$

Substituting Eqs. (57) and (59) in (43), (44) and (46), we obtain the binding energy of a nucleus with constant particle density in the form of a function of $q (\sim \rho_0)$:

$$E = \left\{ -b_0 \frac{B_0(q)}{q^3} + b_1 q^3 + b_2 q^2 \right\} A. \qquad (60)$$

It follows from the condition $\partial E / \partial q = 0$ that: a) in the case (38), the binding energy per nucleon has a minimum with a value of ~ -14 mev for $q = 3.5$ or, in accord with Eq. (59), for $R_0 = 1.2 \times 10^{-13} A^{1/3}$ cm; b) for (39), the binding energy per nucleon has a minimum with value ~ -14 mev for the value $q = 2.8$ or for $R_0 = 1.48 \times 10^{-13} A^{1/3}$ cm. Thus, for ϵ_0, which changes from 0 to ∞, all the values of the parameter q, which are determined from the requirement of minimum energy, lie in the interval

$$3.5 \leq q \leq 6.2 \text{ for the value of (38)}, \qquad (61)$$

$$2.8 \leq q \leq 4.7 \text{ for the value of (39)}. \qquad (62)$$

The dependence of the parameter q on ϵ_0, computed from Eq. (49) in the case of Eqs. (61) and (62), is shown in Fig. 3, from which it is seen that in both cases the parameter q reaches its limiting value $q = 6.2$ and $q = 4.7$ for $\epsilon_0 \approx 13.798$. As is evident, in the approximation under consideration, when we neglected the Coulomb and surface energies, the density of the nucleons in the central part of the nucleus ρ_0 and the ratio a/R_0 are constant quantities which do not depend on the mass number A.

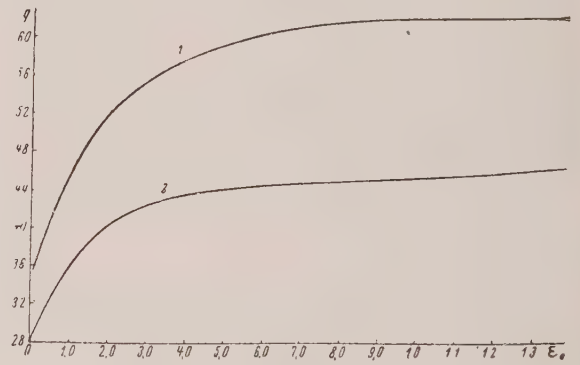

FIG. 3. Dependence of q upon ϵ_0. *1* – for values of the parameters from Eq. (38), *2* – for values of the parameters from Eq. (39).

According to Eqs. (45) and (47), the parameters R_0, a and $\bar{r}_0$ can be represented as functions of q and ϵ_0:

$$R_0 = R_0^*(q, \varepsilon_0) A^{1/3}; \quad a = a_0(q, \varepsilon_0) A^{1/3}; \qquad (63)$$

$$\bar{r}_0 = R_0 + a = r_0^*(q, \varepsilon_0) A^{1/3},$$

where the following notation is introduced:

$$R_0^*(q, \varepsilon_0) = (9\pi)^{1/3}(k_0 q)^{-1}(1 + 3\varepsilon_0 + 6\varepsilon_0^2 + 6\varepsilon_0^3)^{-1/3};$$

$$a_0(q, \varepsilon_0) = \varepsilon_0 R_0^*(q, \varepsilon_0);$$

$$r_0^*(q, \varepsilon_0) = R_0^*(q, \varepsilon_0) + a_0(q, \varepsilon_0).$$

For each pair of values of q and ϵ_0 we obtain from Fq. (63) the corresponding values of $R_0^*(q, \epsilon_0)$, $a_0(q, \epsilon_0)$ and $r_0^*(r, \epsilon_0)$. The results of the calculation are shown in Fig. 4, from which it follows that for a given A: a) the initial point of these curves with coordinates

$$R_0^*(q, \varepsilon_0) \approx 1.2 \times 10^{-13} \text{ cm}; \quad a_0(q, \varepsilon_0) = 0; \quad \rho_0 = 0.362\, k_0^3;$$

$$R_0^*(q, \varepsilon_0) \approx 1.48 \times 10^{-13} \text{ cm}; \quad a_0(q, \varepsilon_0) = 0; \quad \rho_0 = 0.185\, k_0^3$$

corresponds to a nuclear model with constant density of nucleons (58); b) the final point of the curves with coordinates

$$a_0(q, \varepsilon_0) \approx 0.39 \times 10^{-13} \text{ cm}; \quad R_0^*(q, \varepsilon_0) = 0; \quad \rho_0 = 2.012\, k_0^3;$$

$$a_0(q, \varepsilon_0) \approx 0.49 \times 10^{-13} \text{ cm}; \quad R_0^*(q, \varepsilon_0) = 0; \quad \rho_0 = 0.877\, k_0^3$$

corresponds to the nuclear model with variable density (51). The intervals $X_1(q)$, $X_2(q)$ and $X_3(q)$ were computed numerically.

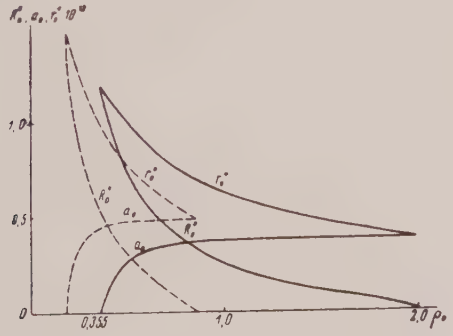

FIG. 4. Dependence of R_0^*, r_0^* and a_0 on ρ_0 (in units of k_0^3) for values of the parameters from Eq. (38) (Solid curves) and for values from Eq. (39) (broken curves).

4. CALCULATION OF THE ENERGY OF THE NUCLEUS AND THE DENSITY DISTRIBUTION OF NUCLEONS WITH CONSIDERATION OF COULOMB AND SURFACE EFFECTS

In Sec. 3 for the calculation of the density of nucleons in a nucleus, we took into account only the energy of the specific nuclear forces and neglected the Coulomb repulsion of the protons. Now we determine the parameters of the density (42), taking into account the Coulomb energy of the protons and the Weizsacker correction to the kinetic energy of the particles. In the Hartree-Fock approximation for the Coulomb energy of a nucleus with Z protons, we have

$$E_c = E_c^0 + E_c^a, \tag{64}$$

where

$$E_c^0 = \frac{1}{2}\int\int (d\mathbf{r}_1)(d\mathbf{r}_2)\frac{e^2}{r}\rho_p(\mathbf{r}_1)\rho_p(\mathbf{r}_2), \tag{65}$$

$$E_c^a = -\frac{1}{4}\int\int (d\mathbf{r}_1)(d\mathbf{r}_2)\frac{e^2}{r}|\rho_p(\mathbf{r}_1, \mathbf{r}_2)|^2. \tag{66}$$

The first term in (64) is the usual Coulomb energy, the second, the Coulomb exchange energy.

In the case of variable density $\rho_p(r)$, we get E_c^a from (66) with the help of Eqs. (12) and (13):

$$E_c^a = -\frac{3e^2}{4\pi}(3\pi^2)^{1/3}\int \rho_p^{4/3}(r)\, d\tau. \tag{67}$$

Substituting for ρ_p in Eqs. (65) and (67) the expression (42), and carrying out the integration, we find, in the notation of (45),

$$E_c^0 = \frac{e^2 k_0^6}{540\pi^2} R_0^5 q^6 \left[1 + \frac{15}{2}\varepsilon_0^2 + \frac{75}{4}\varepsilon_0^3 + \frac{75}{4}\varepsilon_0^4 + \frac{75}{8}\varepsilon_0^5\right], \tag{68}$$

$$E_c^a = -\frac{e^2 k_0^4}{48\pi^2} R_0^3 q^4 \left[1 + \frac{9}{4}\varepsilon_0 + \frac{27}{8}\varepsilon_0^2 + \frac{81}{32}\varepsilon_0^3\right]. \tag{69}$$

Making use of (47), we obtain the Coulomb energy of the nucleus as a function of the parameters ϵ_0 and q:

$$\begin{aligned} E_c &= E_c^0 + E_c^a \\ &= b_3 A^{4/3} q\left(1 + \frac{15}{2}\varepsilon_0^2 + \frac{75}{4}\varepsilon_0^3 + \frac{75}{4}\varepsilon_0^4 + \frac{75}{8}\varepsilon_0^5\right) \\ &\quad \times (1 + 3\varepsilon_0 + 6\varepsilon_0^2 + 6\varepsilon_0^3)^{-5/3} \\ &\quad - b_4 A q\left(1 + \frac{9}{4}\varepsilon_0 + \frac{27}{8}\varepsilon_0^2 + \frac{81}{32}\varepsilon_0^3\right) \\ &\quad \times (1 + 3\varepsilon_0 + 6\varepsilon_0^2 + 6\varepsilon_0^3)^{-1}. \end{aligned} \tag{70}$$

Here

$$b_3 = 9e^2k_0/60\,(9\pi)^{1/3}; \quad b_4 = 3e^2k_0/16\pi.$$

The kinetic energy associated with a nonuniform density of nucleons on the periphery of the nucleus is determined by the Weizsacker correction, which in our case has the form:

$$T_B = T_B^p + T_B^n = \frac{h^2}{32\pi^2 M}\int \frac{(\text{grad}\,\rho)^2}{\rho}\,d\tau. \quad (71)$$

Keeping (42) and (47) in mind, we get from (71) after integration,

$$T_B = b_5 A^{1/3} q^2 (2 + 2\varepsilon_0 + \varepsilon_0^{-1}) \quad (72)$$
$$\times (1 + 3\varepsilon_0 + 6\varepsilon_0^2 + 6\varepsilon_0^3)^{-1/3},$$

where

$$b_5 = \frac{(9\pi)^{1/3}}{96\pi^3}\,\frac{h^2k_0^2}{M}.$$

The total energy of the nucleus in this case will be equal to

$$E_n = E(q, \varepsilon_0) + E_c(q, \varepsilon_0) \quad (73)$$
$$+ T_B(q, \varepsilon_0) = E(q, \varepsilon_0)$$
$$+ \frac{A}{1 + 3\varepsilon_0 + 6\varepsilon_0^2 + 6\varepsilon_0^3}$$
$$\times\left\{b_3 A^{2/3} q\,\frac{1 + {}^{15}/_2\varepsilon_0^2 + {}^{75}/_4\varepsilon_0^3 + {}^{75}/_4\varepsilon_0^4 + {}^{75}/_8\varepsilon_0^5}{(1 + 3\varepsilon_0 + 6\varepsilon_0^2 + 6\varepsilon_0^3)^{2/3}}\right.$$
$$\left. - b_4 q\left(1 + \frac{9}{4}\varepsilon_0 + \frac{27}{8}\varepsilon_0^2 + \frac{81}{32}\varepsilon_0^3\right)\right.$$
$$+ b_5 q^2 A^{-2/3}(2 + 2\varepsilon_0 + \varepsilon_0^{-1})$$
$$\left.\times(1 + 3\varepsilon_0 + 6\varepsilon_0^2 + 6\varepsilon_0^3)^{2/3}\right\}.$$

Here $E(q, \epsilon_0)$ is the energy of the nucleus without consideration of the Coulomb and surface kinetic energy which is determined by Eq. (48).

The equation which relates q and ϵ_0,

$$\partial E_n/\partial q = F_1(q, \varepsilon_0, A) = 0, \quad (74)$$

was solved by us for ϵ_0 with q in the intervals (61) and (62) for the values $A = 40$, 60, 80, 120, 140, 180, 200 and 220. For each pair of values (q, ϵ_0) found from Eq. (74), we calculated [by means of Eq. (73)] the corersponding value of E/A. The dependence of E/A on ϵ_0 for certain A is given in Fig. 5. It is evident from these graphs that to each A there corresponds only one pair of values of the parameters (q, ϵ_0) for which the nucleus possesses minimum energies almost equal to the empirical values; these pairs of values (q, ϵ_0) are shown in Tables I and II. There are also plotted in these tables the values of the parameters R_0, a, $\overline{r}_0$ and ρ_0 with the aid of Eqs. (63) and (45), in which cases the Coulomb and surface energies have been taken into account.

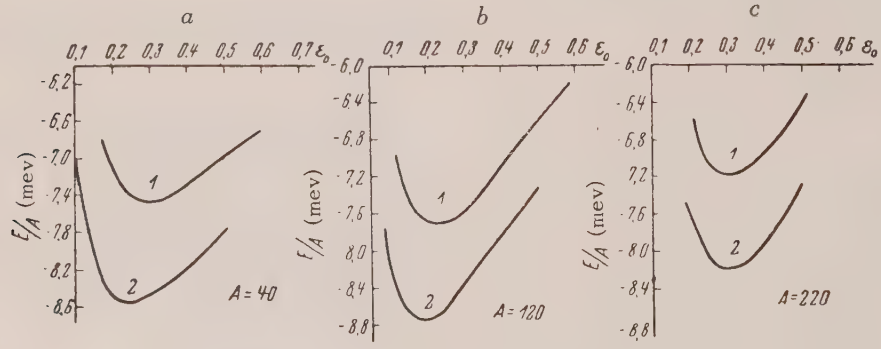

FIG. 5. Binding energy per nucleon E/A as functions of $\epsilon_0 = a/R_0$ for the values $A = 40$, 120, 220. *1* – for values of the parameters from Eq. (38), *2* – for values from Eq. (39).

TABLE I. For Values of the Parameters Used in Eq. (38)

A	q	$\varepsilon_0 = \frac{a}{R_0}$	$R_0 A^{-1/3} \times 10^{13}$	$a \cdot A^{-1/3} \times 10^{13}$	$\bar{r}_0 A^{-1/3} \times 10^{13}$	ρ_0 (в единицах k_0^3)
40	3.7	0.300	0.872	0.262	1.134	0.427
60	3.69	0.265	0.908	0.241	1.149	0.424
80	3.65	0.242	0.941	0.228	1.169	0.410
120	3.64	0.218	0.968	0.211	1.179	0.407
140	3.64	0.210	0.976	0.205	1.181	0.407
180	3.63	0.205	0.984	0.202	1.186	0.404
200	3.63	0.205	0.984	0.202	1.186	0.404
220	3.63	0.205	0.984	0.202	1.186	0.404

TABLE II. For Values of the Parameters Used in Eq. (39)

A	q	$\varepsilon_0 = \frac{a}{R_0}$	$R_0 A^{-1/3} \times 10^{13}$	$aA^{-1/3} \times 10^{13}$	$\bar{r}_0 A^{-1/3} \times 10^{13}$	ρ_0 (в единицах k_0^3)
40	3.0	0.233	1.155	0.269	1.424	0.228
60	3.0	0.215	1.178	0.253	1.431	0.228
80	3.0	0.204	1.192	0.243	1.435	0.228
120	3.0	0.195	1.204	0.235	1.439	0.228
140	3.0	0.195	1.204	0.235	1.439	0.228
180	3.0	0.195	1 204	0.235	1.439	0.228
200	3.0	0.195	1.204	0.235	1.439	0,228
220	3.0	0.195	1.204	0.235	1.439	0.228

It is evident from the tables and graphs that consideration of the Coulomb and surface kinetic energies leads to the following results. First, for each A, the parameters (q, ϵ_0) of the nuclear density (42) have only one pair of values, for which equilibrium of the nucleus is possible; this shows that the existence, in the medium and heavy nuclei, of a core (of radius R_0) with almost constant density is due to the effect of the usual repulsive force in the two nucleon potential and of Coulomb repulsion, without which the density of the distribution would be close to (51) for all A (see Sec. 3).

Second, the ratio $\epsilon_0 = a/R_0$ is a definite function of the mass number A of the nucleus (see Tables I, II); for $A \geq 120$, the ratio a/R_0 is practically independent of A: $\epsilon_0 \approx 0.2$.

Third, the value of the parameter q is virtually independent of A for $A > 50$, i.e., for medium and heavy nuclei, the density of nucleons in the core of the nucleus is constant. This conclusion is in agreement with the known empirical law, according to which, for medium and heavy nuclei, the density of nucleons inside the nucleus does not depend on the mass number A. We give here the values of the parameters R_0, a, ρ_0 and $\bar{r}_0$ – the particle distribution densities (42) for nuclei with $A \geq 120$ for two systems of values of the constants (38) and (39):

(75)

$$R_0 = 0.98 \times 10^{-13} A^{1/3}; \qquad a = 0.21 \times 10^{-13} A^{1/3};$$
$$\rho_0 = 0.41 k_0^3; \qquad \bar{r}_0 = 1.19 \times 10^{-13} A^{1/3};$$

(76)

$$R_0 = 1.20 \times 10^{-13} A^{1/3}; \qquad a = 0.24 \times 10^{-13} A^{1/3};$$
$$\rho_0 = 0.23 k_0^3; \qquad \bar{r}_0 = 1.44 \times 10^{-13} A^{1/3}.$$

The average energy per nucleon E/A, computed as a function of A, is shown graphically in Fig. 6. The dependence of E/A on A is in good agreement with the empirical curve of the binding energy, computed from the mass defect. Thus, for nuclei with $A \geq 120$, the parameters R_0 and a are obtained proportional to $a^{1/3}$. We note that a dependence of the form $a \sim A^{1/3}$, $R_0 \sim A^{1/3}$ follows from the connection between the structure of the nuclear shells and the density of the nucleons [16,17,27,28]. The density of $\rho(r)$ is shown in Fig. 7 as a function of r for various A

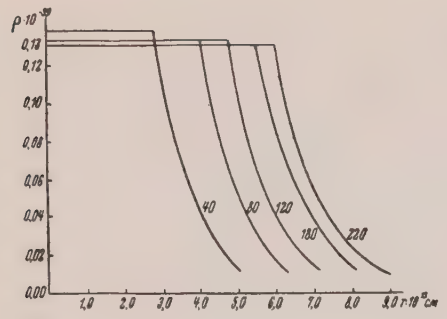

FIG. 6. Mean binding energy per nucleon E/A as a function of A for values of the parameters from Eq. (38). For values of the parameters from Eq. (39) for A=40-220, the quantity $E/A \approx -8.5$ mev.

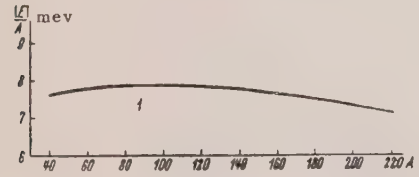

FIG. 7. Dependence of the density distribution $\rho(r)$ on r for A = 40, 80, 120, 180 and 220, and for values of the parameters from Eq. (39).

(see *Note added in proof* at end of paper).

In conclusion, we convey our deep gratitude to Prof. A. A. Sokolov for suggesting the theme and for discussions of the results. We also express our thanks to L. I. Morozovskii for help in the computations.

Note added in proof: We have the value

$$\sqrt{\langle r^2 \rangle} \approx 1.1 \times 10^{-13} A^{1/3} \text{ cm}$$

for the mean square of the nuclear radius from the density function (42).

[1] J. Blatt and V. Weisskopf, *Theoretical Nuclear Physics* (New York), 1952.

[2] W. J. Swiatecki, Proc. Phys. Soc. (London) **63A**, 1208 (2950).

[3] B. Kerimov, J. Exptl. Theoret. Phys. (U.S.S.R.) **24**, 299 (1953).

[4] A. A. Sokolov and B. K. Kerimov, J. Exptl. Theoret. Phys. (U.S.S.R.) **26**, 430 (1954).

[5] H. A. Bethe and R. F. Bacher, *Physics of the Nucleus*, Part I.

[6] P. Gombas, Usp. Fiz. Nauk **49**, 385 (1953).

[7] S. D. Drell and K. Huang, Phys. Rev. **91**, 1527 (1953).

[8] Brueckner, Levinson and Mahmond, Phys. Rev. **95**, 217 (1954).

[9] Lyman, Hanson and Scott, Phys. Rev. **84**, 626 (1951).

[10] K. M. Gatha and R. J. Riddell, Jr., Phys. Rev. **86**, 1035 (1952).

[11] A. L. Mathur and K. M. Gatha, Proc. Phys. Soc. (London) **66A**, 773 (1953).

[12] Pidd, Hammer and Raka, Phys. Rev. **92**, 436 (1953).

[13] Hofstadter, Fechter and McIntyre, Phys. Rev. **92**, 978 (1953).

[14] L. I. Schiff, Phys. Rev. **92**, 988 (1953).

[15] D. D. Ivanenko and V. Rodichev, Dokl. Akad. Nauk SSSR **70**, 605 (1950).

[16] M. Born and L. M. Yang, Nature **166**, 399 (1950).

[17] L. M. Yang, Proc. Phys. Soc. (London) **64A**, 632 (1951).

[18] J. H. D. Jensen and J. M. Luttinger, Phys. Rev. **86**, 907 (1952).

[19] N. N. Kolesnikov, Dokl. Akad. Nauk SSSR **103**, 57 (1955).

[20] V. L. Fitch and J. Rainwater, Phys. Rev. **92**, 789 (1953).

[21] L. N. Cooper and E. M. Henley, Phys. Rev. **92**, 801 (1953).

[22] B. Kerimov, Dissertation, Moscow State University, 1950.

[23] A. R. Bodmer, Proc. Phys. Soc. (London) **66A**, 1041 (1953).

[24] I. Perlman and T. J. Ypsilantis, Phys. Rev. **79**, 30 (1950).

[25] D. Hughes, Pile Neutron Research, Cambridge., Mass., 1953.

[26] R. Jastrow and J. E. Roberts, Phys. Rev. **85**, 757 (1952).

[27] A. L. Mathur and K. M. Gatha, Proc. Phys. Soc. (London) **66A**, 1075 (1953).

[28] Shah, Patel and Gatha, Proc. Phys. Soc. (London) **67A**, 92 (1954).

Translated by R. T. Beyer
184

On the Theory of Polaron Mobility

K. B. TOLPYGO AND Z. I. URITSKII
Kiev State University

(Submitted to JETP editor March 20, 1955)
J. Exptl. Theoret. Phys. (U.S.S.R.) 30, 929-937 (May, 1956)

The interaction of the translational motion of a polaron with the lattice vibrations and the associated energy loss of the polaron are investigated. Using a classical treatment, the energy transferred from one polaron to the vibrational degrees of greedom of the lattice is calculated. This type of excitation is possible for acoustic vibrations only if the polaron velocity exceeds the sound velocity in the crystal. It is thus analogous to the Cerenkov effect for an electron moving with a speed greater than that of light. The numerical results obtained for NaCl, KCl and KBr show that, although this mechmanim is not the main cause for slowing, nevertheless the interaction of the current carriers with the acoustical and transverse optical vibrations is by no means small for these crystals.

1. INTRODUCTION

THE theory of polaron mobility developed by Pekar on the basis of a macroscopic treatment of crystals[1,2] started from the picture of the scattering of polaron waves by the longitudinal optical vibrations of the lattice. The polarization of the crystal was split into two parts: a self-consistent part $\mathbf{P}_0(\mathbf{r}-\vec{\xi}) = (C/4\pi)\mathbf{D}(\mathbf{r}-\vec{\xi})$ [where $\mathbf{D}(\mathbf{r})$ is the average induction of the polaron, $C = (1/n^2) - 1/\epsilon$, ϵ and n are the dielectric constant and the index of refraction, $\vec{\xi}$ is the radius vector to the center of the polarization source] and a variable part $\mathbf{P}' = \sum_{\mathbf{K}} \mathbf{P}'_{\mathbf{K}} e^{i\mathbf{K}\mathbf{r}}$ describing the phonons.

On the assumption that the radius of the polaron state is large compared to the lattice constant, one can neglect the interaction of the polaron with short wavelength longitudinal optical vibrations as well as with the acoustic and transverse optical vibrations, which in this approximation have no longitudinal component of the dipole moment. Actually, for many materials (e.g., all alkali-halide crystals), the radius of the polaron state is only slightly greater than the lattice constant. It is therefore of interest to evaluate the magnitude of the interaction of a moving polaron with the acoustical and transverse vibrations of the crystal.

We shall limit our treatment to polarons whose radius is large enough for the results of Pekar's theory to be applicable as a zeroth approximation, and shall calculate the next approximation in which the energy of interaction of the electron with the transverse optical and acoustical vibrations can still be treated as a small quantity.

As in Pekar's first papers[3,4], we shall treat the electron motion quantum-mechanically and the oscillations of the ions classically. The constants characterizing the electron interaction with the crystal vibrations are taken from the data of one of the authors[5,6].

2. FORCED VIBRATIONS OF A CRYSTAL UNDER THE ACTION OF THE FIELD OF A MOVING POLARON

According to Pekar, the wave function of a moving polaron is

$$\psi(r,\ t) = \psi_0(|\mathbf{r} - \mathbf{v}t|),$$

where $\mathbf{v}$ is the translational velocity of the polaron, and $\psi_0(r)$ is the wave function for the polaron at rest. The wave function can be chosen to be Gaussian,

$$\psi_0 = (2/\pi)^{3/4}\alpha^{3/2} e^{-\alpha^2 r^2}, \qquad (1)$$

with an error of less than 1% compared to the function used by Pekar[1]. We denote the average electrical induction produced by the charge density $\rho = e|\psi_0|^2$ by

$$\mathbf{D}(\mathbf{r}) = -\nabla\varphi = -\nabla\int \frac{e|\psi_0(\mathbf{r}')|^2\, d\tau'}{|\mathbf{r}-\mathbf{r}'|}, \qquad (2)$$

and the "instantaneous" induction produced by an electron at the point $\mathbf{r}'$ by

$$\mathbf{D}(\mathbf{r},\ \mathbf{r}') = e(\mathbf{r}-\mathbf{r}')/|\mathbf{r}-\mathbf{r}'|^3. \qquad (2')$$

For a lattice made up of deformable ions, the ion displacements $\mathbf{u}_s^l$ and the associated dipole moments $\mathbf{p}_s^l = e_s\mathbf{u}_s^l$ (s numbers the ions and l the cells of the lattice) are determined by the average field $\mathbf{D}(r)$; according to the adiabatic approximation,

the dipole moments $\mathbf{P}_s^l$ of the electronic shells are determined[2] both by the momentary position of the electron [and consequently, by the field $\mathbf{D}(\mathbf{r}, \mathbf{r}')$] and the field resulting from the displacements $\mathbf{u}_s^l$. The equations describing the displacements and deformation of the ions can be written in the form[7]

$$m_s \ddot{p}_{sx}^l = -e_s^2 (\partial U^0 / \partial p_{sx}^l) + e_s^2 D_x (\mathbf{r}_s^l, \mathbf{r}'), \quad (3a)$$

$$0 = -(\partial U^0 / \partial P_{sx}^l) + D_x (\mathbf{r}_s^l, \mathbf{r}'), \quad (3b)$$

where U^0 is the potential energy of the crystal expressed as a function of $\mathbf{p}_s^l$ and $\mathbf{P}_s^l$. This function was given in Ref. 7 (with some differences in notation) as

$$U^0 = \frac{1}{2a^3} \sum \left(a_{ss'xy}^{l-l'} p_{sx}^l p_{s'y}^{l'} + 2 b_{ss'xy}^{l-l'} p_{s'x}^l P_{s'y}^{l'} + c_{ss'xy}^{l-l'} P_{sx}^l P_{s'y}^{l'} \right), \quad (4)$$

where the coefficients a, b, c depend only on the coordinate differences $\mathbf{r}_s^l - \mathbf{r}_s^{l'}$ and are dimensionless constants; the summation extends over all indices.

Since we are interested only in the vibrations of the ions, and not in the part $\check{\mathbf{P}}_s^l$ of the polarization which follows the electron motion without any lag, we can choose as the zero of energy of interaction of the electron with the crystal the state where $p_s^l = 0$ and the electron is at the bottom of the conduction band. In such a motion the inertialess part of the polarization, $\check{\mathbf{P}}_s^l$, remains the same as the case we are considering, where $\mathbf{p}_s^l \neq 0$. Then Eq. (3b) becomes

$$0 = -[\partial U^0 (0, \check{\mathbf{P}}_s^l) / \partial P_{sx}^l] + D_x (\mathbf{r}_s^l, \mathbf{r}'). \quad (5)$$

To eliminate the quantities $\check{\mathbf{P}}_s^l$, we subtract Eq. (5) from Eq. (3b) and get

$$0 = -\partial U^0 (\mathbf{p}_s^l, \mathbf{P}_s^l - \check{\mathbf{P}}_s^l) / \partial P_{sx}^l. \quad (6)$$

Thus the quantities $\tilde{\mathbf{P}}_s^l = \mathbf{P}_s^l - \check{\mathbf{P}}_s^l$ are determined only by the ion displacements $\mathbf{u}_s^l$ and do not depend on the instantaneous position of the electron. Consequently, they are equal to their quantum-mechanical average values, calculated with $|\psi(\mathbf{r}')|^2$. Averaging Eqs. (3) over $\mathbf{r}'$, we get

$$(m_s / e_s^2) \ddot{p}_{sx}^l = -(\partial U^0 (\mathbf{p}_s^l, \bar{\mathbf{P}}_s^l)) / \partial p_{sx}^l + D_x (\mathbf{r}_s^l); \quad (7a)$$

$$0 = -(\partial U^0 (\mathbf{p}_s^l, \bar{\mathbf{P}}_s^l) / \partial P_{sx}^l) + D_x (\mathbf{r}_s^l), \quad (7b)$$

where $\bar{\mathbf{P}}_s^l = \tilde{\mathbf{P}}_s^l + \bar{\check{\mathbf{P}}}_s^l$.

The potential energy of the electron interaction with the polarized crystals (measured from the bottom of the conduction band) will obviously be

$$U^l(r') = -\sum_{sl} \mathbf{D} (\mathbf{r}_s^l, \mathbf{r}') (\mathbf{p}_s^l + \tilde{\mathbf{P}}_s^l), \quad (8)$$

and since $\mathbf{p}_s^l + \tilde{\mathbf{P}}_s^l$ does not depend on the instantaneous position of the electron, the quantum-mechanical average of U^0 is

$$\overline{U^l} = -\sum_{sl} \mathbf{D} (\mathbf{r}_s^l, \mathbf{r}') \cdot (\mathbf{p}_s^l + \tilde{\mathbf{P}}_s^l) = -\sum_{s,l} \mathbf{D} (\mathbf{r}_s^l) (\mathbf{p}_s^l + \overline{\mathbf{P}_s^l} - \overline{\check{\mathbf{P}}_s^l}). \quad (9)$$

The quantities $\overline{\check{\mathbf{P}}_s^l}$ are found by averaging Eq. (5):

$$0 = -[\partial U^0 (0, \overline{\check{\mathbf{P}}_s^l}) / \partial P_{sx}^l] + D_x (\mathbf{r}_s^l). \quad (10)$$

We transform Eqs. (7) to normal coordinates by the substitutions

$$p_{sx}^l = \sum_{\mathbf{K}, \alpha} p_{sx}^\alpha (\mathbf{K}) \exp \{i \mathbf{K} \mathbf{r}_s^l\} \, q_{\alpha \mathbf{K}} (t); \quad (11)$$

$$P_{sx}^l = \sum_{\mathbf{K}} \left[\sum_\alpha P_{sx}^\alpha (\mathbf{K}) \, q_{\alpha \mathbf{K}} (t) + R_{sx} (\mathbf{K}, t) \right] e^{i \mathbf{K} \mathbf{r}_s^l},$$

where p_{sx}^α, P_{sx}^α are the normalized amplitudes of the free oscillations of the lattice, and satisfy the equations:

$$\mu_s p_{sx}^\alpha \Omega_{\alpha \mathbf{K}}^2 = \sum_{s'y} (A_{ss'xy} p_{s'y}^\alpha + B_{ss'xy} P_{s'y}^\alpha); \quad (12)$$

$$0 = \sum_{s'y} (B_{ss'yx}^* p_{s'y}^\alpha + C_{ss'xy} P_{s'y}^\alpha), \quad (13)$$

where

$$A_{ss'xy} = \sum_{l'} a_{ss'xy}^{l-l'} \exp \{-i \mathbf{K} (\mathbf{r}_s^l - \mathbf{r}_{s'}^{l'})\}$$

etc. (cf. Ref. 7),

$$\mu_s = m_s / \mu; \quad \mu = m_1 m_2 / (m_1 + m_2);$$

$$\Omega_{\alpha \mathbf{K}}^2 = (\mu a^3 / e^2) \, \omega_{\alpha \mathbf{K}}^2;$$

the $\omega_{\alpha\mathbf{K}}$ are the eigenfrequencies. Then (3) becomes

$$\frac{\mu a^3}{e^2}\ddot{q}_{\alpha\mathbf{K}} + \Omega^2_{\alpha\mathbf{K}} q_{\alpha\mathbf{K}} = a^3 \sum_{sx} p^{\alpha *}_{sx} \left\{ \frac{1}{N} \sum_l D_x(\mathbf{r}^l_s) \times \exp\{-i\mathbf{K}\mathbf{r}^l_s\} - \sum_{s'y} B_{ss'xy} R_{s'y} \right\}; \tag{14}$$

$$\sum_{s'y} C_{ss'xy} R_{s'y} = \frac{a^3}{N} \sum_l D_x(\mathbf{r}^l_s) e^{-i\mathbf{K}\mathbf{r}^l_s}, \tag{15}$$

where N is the number of cells in the fundamental domain of the crystal.

It is easy to see from a comparison of Eqs. (15) and (10) that the quantities $R_{s'y}$ are precisely the Fourier components of $\overline{\overline{P}}^l_s$. Solving Eq. (15) for the $R_{s'y}$ and substituting in (14), we get

$$\ddot{q}_{\alpha\mathbf{K}} + \omega^2_{\alpha\mathbf{K}} q_{\alpha\mathbf{K}} = Q_\alpha(\mathbf{K}, t) = \frac{e^2}{N\mu} \sum p^{\alpha *}_{sx} \exp\{-i\mathbf{K}\mathbf{r}^l_s\} \times [D_x(\mathbf{r}^l_s) - \sum_{\substack{s'y \\ s''yz}} B_{ss'xy} C^{-1}_{s's''yz} D_z(\mathbf{r}^l_{s''}) \exp\{i\mathbf{K}(\mathbf{r}_s - \mathbf{r}_{s''})\}]. \tag{16}$$

3. TRANSFER OF ENERGY FROM A MOVING POLARON TO THE CRYSTAL

In order to determine the time dependence of the generalized force $Q_\alpha(\mathbf{K}, t)$, we calculate the Fourier components of $\rho = e/|\psi(\mathbf{r}-\mathbf{v}t)|^2$ for an arbitrary point r:

$$\rho = \sum_{\mathbf{K}} \rho_{\mathbf{K}}(t) e^{i\mathbf{K}\mathbf{r}}, \tag{17}$$

$$\rho_{\mathbf{K}}(t) = \frac{e}{V}\int |\psi(\mathbf{r}-\mathbf{v}t)|^2 e^{-i\mathbf{K}\mathbf{r}} d\tau = \frac{e}{V} \exp\left\{-\frac{\mathbf{K}^2}{8\alpha^2} - i\mathbf{K}\mathbf{v}t\right\},$$

where V is the volume of the fundamental domain.

The Fourier transforms of the Poisson equation $\Delta\varphi = -4\pi\rho$ and the relation $\mathbf{D} = -\nabla\varphi$ are

$$\mathbf{D}(\mathbf{r}, t) = \sum \mathbf{D}(\mathbf{K}, t) e^{i\mathbf{K}\mathbf{r}}, \tag{18}$$

$$\mathbf{D}(\mathbf{K}, t) = -\frac{4\pi i e\,\mathbf{K}}{K^2} \exp\left\{-\frac{\mathbf{K}^2}{8\alpha^2} - i\,\mathbf{K}\mathbf{v}\,t\right\}.$$

Substituting (17) in (15) and noting that $\sum_l e^{i(\mathbf{K}-\mathbf{K}')\mathbf{r}^l_s} \neq 0$ only if $\mathbf{K}-\mathbf{K}' = 2\pi\mathbf{q}^m$ (where $\mathbf{q}^m$ is an arbitrary vector of the reciprocal lattice), we obtain a complicated expression for Q_α, consisting of a sum of terms with different frequencies $\mathbf{v}\cdot(\mathbf{K}+2\pi\mathbf{q}^m)$. However, in the macroscopic approximation where we consider polarons of large radius, only terms with wave vectors small compared to the vectors of the reciprocal lattice appear in the expansion of $\mathbf{D}(\mathbf{r})$. Therefore, since we are neglecting the components $\mathbf{D}(2\pi\mathbf{q}^m) \sim \exp\{-(2\pi q^m)^2/8\alpha^2\}$, it would be inconsistent to keep them in the expression for the external force. Thus, in the sum over m in the expression for Q_α, we should keep only the leading term with $m = 0$. Using (13) and (15), we can transform $Q_\alpha(\mathbf{K}, t)$ to the simpler form

$$Q_\alpha(\mathbf{K}, t) = e^{-i\mathbf{v}\mathbf{K}t}; \tag{19}$$

$$Q_\alpha(\mathbf{K}) = \frac{e^2}{\mu} \mathbf{D}(\mathbf{K}, t) \sum_s (\mathbf{p}^{\alpha *}_s t\, \mathbf{P}^{\alpha *}_s).$$

The solution of Eq. (16) can be put in the form

$$q_{\alpha\mathbf{K}} = \frac{Q_\alpha(\mathbf{K})}{\omega^2_{\alpha\mathbf{K}} - (\mathbf{K}\mathbf{v})^2}\{\cos\mathbf{K}\mathbf{v}\,t - \cos\omega_{\alpha\mathbf{K}}\,t - i\sin\mathbf{v}\mathbf{K}\,t + b_{\alpha\mathbf{K}}\sin(\omega_{\alpha\mathbf{K}}\,t + \beta_{\alpha\mathbf{K}})\}, \tag{20}$$

where $b_{\alpha\mathbf{K}}$ and $\beta_{\alpha\mathbf{k}}$ are arbitrary integration constants. If the crystal was not deformed at $t = 0$, then all the $\beta_{\alpha\mathbf{K}} = 0$.

From Eqs. (7a) and (7b), the work done on the crystal by the moving polaron during the time from 0 to t is

$$A = \int_0^t \frac{d}{dt}\left[\sum_{slx} \frac{1}{2} \frac{m_s}{e_s^2} \dot{p}^{l2}_{sx} + U^0(p^l_s, \overline{P}^l_s)\right] dt = \int_0^t \sum_{slx} \mathbf{D}_x(\mathbf{r}^l_s)(\dot{p}^l_{sx} + \dot{\overline{P}}^l_{sx})\, dt. \tag{21}$$

Taking Fourier transforms and using the relation

$$C^{-1}_{ss'xy} = C^{-1*}_{s'sy,x}, \tag{22}$$

we get, after simple transformations

$$A = \int_0^t \Big\{ \sum_{K\alpha} Q_{\alpha K}(t)\, \dot{q}_{\alpha K}(-K) + \sum_{ss'xyK} D_x(-K)\, C^{-1}_{ss'xy}\, \dot{D}_y(K) \Big\} N\mu/e^2\, dt. \tag{23}$$

The second term in the integral is identically zero, since the expression to be summed over K is an odd function of **K**. Integrating the first term in (23) with respect to t and dropping terms which go to zero or cancel one another when we sum over K, we find for sufficiently long times t

$$A = \frac{2\mu N}{e^2} \sum_{\alpha,K} \frac{|Q_\alpha(K)|^2\, \omega_{\alpha K}}{\omega_{\alpha K} + Kv} \frac{\sin^2 1/2\,(\omega_{\alpha K} - Kv)\, t}{(\omega_{\alpha K} - Kv)^2}. \tag{24}$$

As $t \to \infty$, A becomes proportional to t, and thus the special choice of solution with $q_{\alpha K}(t=0) = 0$, where A also includes the energy of formation of the polaron, has no significance.

4. COMPUTATION OF ENERGY LOSS OF A POLARON FOR SPECIFIC CRYSTALS

Further calculations in general form are not possible, so we shall limit ourselves to considering the simplest case of the motion of a polaron of relatively large radius in a cubic crystal. Numerical results will be obtained for crystals of NaCl, KCl and KBr.

We may assume that, for a polaron of large radius, $Q_\alpha(K)$ is significantly different from zero only for K's which are so small that the $\omega_{\alpha K}$ can be assumed to be equal to their limiting frequency in the case of optical waves, and proportional to $|K|$ in the case of acoustic waves.

For the optical branches $\omega_{1K} \approx \omega_\parallel$ (longitudinal waves), and $\omega_{2K} = \omega_{3K} = \omega_\perp$ (transverse waves), where $\omega_\parallel/\omega_\perp = \sqrt{\epsilon}/n$. Taking the z-axis along the direction of the velocity v and changing to polar coordinates, we can carry out the summation over the angle ϑ. Replacing the sum over K by an integral, we have

$$A_\alpha^{\cdot} = t\, \frac{VN}{16\pi^2} \frac{\mu}{e^2 |v|} \iint |Q(K, \vartheta_\alpha, \varphi)|^2\, K dK d\varphi, \tag{25}$$

where $\cos\vartheta_\alpha = \omega_\alpha/Kv$, 1,2, 3.

For the acoustic branches, we can set $\omega_{\alpha K} = KC_\alpha(\vartheta, \varphi)$. Then the integration over the angle ϑ gives the same formula (25), where $\vartheta^{\cdot}_\alpha$ is the "resonance" value of the angle ϑ, for which

$$C_i(\vartheta^{\cdot}_\alpha, \varphi) = v \cos\vartheta^{\cdot}_\alpha. \tag{26}$$

In a paper of one of the authors, solutions of the equations for the normal modes (12) were obtained including terms of order $k^2 = (aK)^2$, (where a is the separation of neighboring ions); numerical values of the amplitudes were found for the four crystals: LiF, NaCl, KCl and KBr[5].

For the longitudinal optical vibrations, the effect is already different from zero in the zeroth approximation with respect to k where, according to Ref. 5,

$$p_{sx} = k_x/k\mu_s; \qquad P_{sx} = (k_x/k)\,(c_s/a_0), \tag{27}$$

where the quantities μ_s and c_s/a_0 are numerical constants whose values for the crystals mentioned are given in Table I. Substituting (27) and (18) in (19) and (19) in (25) and integrating over φ we get

$$A_1 = t\, \frac{\pi e^4}{2\mu a^3 v} \left(1 + \frac{c_1 + c_2}{a_0}\right)^2 \int_{(\omega_\parallel/2\alpha v)^2}^{\infty} \frac{e^{-x}}{x} dx. \tag{28}$$

For low velocities v, when $\omega_\parallel/2\alpha v \gg 1$ and the asymptotic expansion of the exponential integral is applicable, we get for the approximate dependence of A_1/t on v

$$\frac{A_1}{t} = Bv \exp\{-(\omega_\parallel/2\alpha v)^2\} \times \left[1 - \left(\frac{2\alpha v}{\omega_\parallel}\right)^2 + 2! \left(\frac{2\alpha v}{\omega_\parallel}\right)^4 - \cdots\right], \tag{29}$$

$$B = \frac{\pi e^4}{\mu a^3} \frac{2\alpha^2}{\omega_\parallel^2} \left(1 + \frac{c_1 + c_2}{a_0}\right)^2. \tag{30}$$

Thus the energy loss is greater, the greater α, i.e., the smaller the radius of the polaron state, and increases exponentially with increasing velocity.

For the crystals NaCl, KCl and KBr, for which the parameter α in the polaron wave function is known, the result of computation with the exact formula (26) is given in Fig. 1.

For transverse optical vibrations the sum of $P_s + p_s$, which is parallel to the vector k, is given by the formula

TABLE I. Amplitudes of Dipole Moments of Optical Vibrations

Crystal	$1/\mu_1$	$1/\mu_2$	c_1/a_0	c_2/a_0	b
NaCl	0.6066	0.3934	—0.01485	—0.51755	0.084295
KCl	0,4756	0.5244	—0.05516	—0.43228	—0.042374
KBr	0.6715	0,3285	—0,04367	—0.48942	0.107363

$$\sum_{s=1}^{2} (\mathbf{P}_s + \mathbf{p}_s)_k = b\,\mathbf{k}/k\tau_{\pm}(k). \tag{31}$$

The value of the constant b depends on the properties of the crystal (values calculated from Ref. 5 are given in the last column of Table I), while $1/\tau_{\pm}(k)$ is a universal function and depends only on the direction of the vector k. Its expansion in spherical harmonics was found in Ref. 5. Approximately,

$$1/\tau_{\pm}(k) = \tau_{\pm}^{0} + \tau_{\pm}^{(4)} Y_4(\theta, \varphi) \tag{32}$$

$$+ \tau_{\pm}^{(6)} Y_6(\theta, \varphi) + \tau_{\pm}^{(8)} Y_8(\theta, \varphi) + \tau_{\pm}^{(10)} Y_{10}(\theta, \varphi);$$

where τ_q^0, $\tau_{\pm}^4$ etc. are numerical factors and the + and − refer to the two branches of the transverse optical vibrations. Because of the complicated dependence of $\tau_{\pm}$ on ϑ and φ, the energy loss of the polaron will be strongly dependent on the direction of the velocity v with respect to the crystal axes (ϑ and φ in formula (32) are the angles describing the vector k in a polar coordinate system fixed in the crystal). However, for a rough estimate of the energy loss, we can limit ourselves to the first term in (32). We then get

$$\frac{1}{t} A_{2,3} = \frac{8\pi b^2 a\alpha^4 e^4}{\mu} (\tau_{\pm}^0)^2 \frac{1}{v} \tag{33}$$

$$\times \exp\{-(\omega_{\perp}/2\alpha v)^2\} \left[1 + \left(\frac{\omega_1}{2\alpha v}\right)^2\right],$$

where $\tau_+^0 = 0.1481$; $\tau_-^0 = 0.0408$. Comparing (33) and (29), we see that for low velocities, where $\omega_{\perp}/2\,\alpha\, v \gg 1$, $A_{2,3}$ differs from A_1 by the factor

$$(\alpha a)^4 \left(\frac{2\omega_{\parallel}}{\alpha v}\right)^2 \exp\left\{\frac{\omega_{\parallel}^2 - \omega_{\perp}^2}{(2\alpha v)^2}\right\}$$

which comes from the quantity $(b\,\tau_{\pm}^0)^2$.

Thus as the velocity decreases, the importance of the transverse vibrations in the slowing down increases. Figure 2 shows the behavior of $A_{2,3}/t$ for the same three crystals.

We find the quantities $Q_{\alpha}(\mathrm{K}, t)$, $\alpha = 4, 5, 6$ for the acoustic vibrations from forumla (9), using the results of Ref. 5. In the zeroth approximation for k, $\mathbf{p}_1^{\alpha} = -\mathbf{p}_2^{\alpha}$, $\mathbf{P}_1^{\alpha} = \mathbf{P}_2^{\alpha} = 0$ for the acoustic vibrations. In second order in k, using formula (67′) of Ref. 5, the sum $\sum_{s=1}^{2} (\mathbf{p}_s^{\alpha} + \mathbf{P}_s^{\alpha}) \cdot \mathbf{k}/k$ gives

$$[n^0 + n^{(4)} Y_4(\theta, \varphi) + n^{(6)} Y_6(\theta, \varphi) \tag{34}$$

$$+ n^{(8)} Y_8(\theta, \varphi) + n^{(10)} Y_{10}(\theta, \varphi)]\, k^2;$$

the values of $n^{(0)}$, $n^{(4)}$, etc., are given in Table V of Ref. 5. Then

$$Q_{\alpha}(\mathrm{K}, t) = -\frac{4\pi i e^3 a^3 k}{\mu V} e^{-k^2/8(\alpha a)^2} \tag{35}$$

$$\times \{n^0 + n^{(4)} Y_4 + \ldots\}.$$

When substituting Q_{α} in formula (25) we must set the angle between k and v equal to the resonance value ϑ^*_{α} given by (26).

From Eq. (6) of Ref. 5, the sound velocity in the crystal is

$$C = \frac{\omega}{|K|} = \sqrt{\frac{e^2}{a\mu}}\, v^0 \{1 + v^{(4)} Y_4(\theta, \varphi) \tag{36}$$

$$+ v^{(6)} Y_6(\theta, \varphi) + \ldots\}.$$

The solution of Eq. (26) for ϑ^*_{α} is generally impossible for such a complicated dependence of C on the direction of k, so we shall replace the curly bracket by unity. From Table IV of Ref. 5 we see that all the $v^{(i)}$ ($i = 4, 6, \ldots, 10$) are small

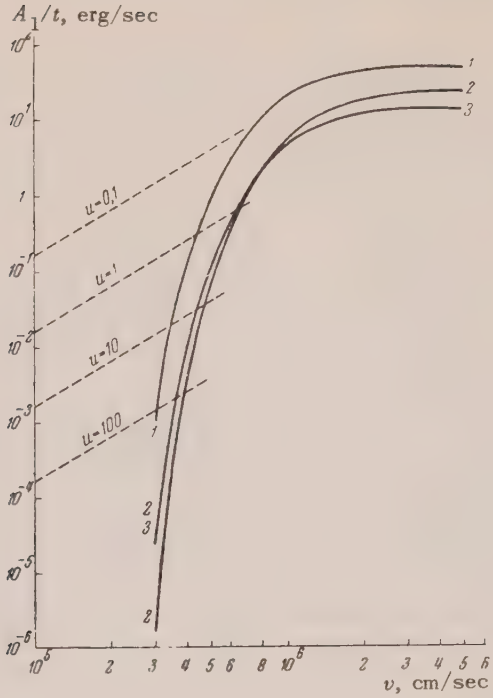

FIG. 1. Energy transferred from a polaron to the longitudinal optical vibrations of the lattice as a function of its velocity v: *1*-NaCl, *2*-KCl, *3*-KBr. The dotted lines shown the energy transferred to the lattice per second for various values of the mobility u, expressed in cm^2/volt sec and calculated according to the formula $W = eEv = ev^2/u$.

compared to one, so the resultant error is small.

With this simplification, Q_α no longer depends on the direction of $\mathbf{k}$, and integration of (25) gives

$$A_i/t = (\pi e^4/\mu a^3 v)(n_i^0)^2 (2\alpha a)^4, \qquad (37)$$

$$\alpha = 4, 5, 6.$$

Formula (37) is of course applicable only if $v \geq C$, since otherwise, Eq. (26) cannot be satisfied. In Table II the values of the constants in Eq. (37) are given for the various crystals and the various branches of acoustical vibrations. From a comparison of formulas (37), (33) and (29) it is clear that for low velocities, so long as $v \geq C$, most of the energy loss occurs via excitation of acoustical vibrations (except fo NaCl). The numerical values of the energy transfer are small for $v \sim C$ but of the same order of magnitude for all six branches. Thus we may expect that a quantum-mechanical calculation of the scattering will show an important contribution from interaction with the acoustical and transverse optical vibrations.

To estimate the role of the mechanism of energy loss which we are considering, we compare the quantity A_i/t with the power W from the external force $e\mathbf{E}$ which maintains the translational motion of the polaron at the fixed velocity $\mathbf{v} = u\mathbf{E}$, where u is the mobility of the polaron and $W = e\mathbf{E}\cdot\mathbf{v} = ev^2/u$. For a mobility $u \sim 1$-10 cm^2/volt sec, which is typical of alkali halide crystals, the line ev^2/u is above the curves of A_α/t. Only for polaron velocities $v \gtrsim 5 \times 10^5$ cm/sec does the energy loss to excitation of longitudinal optical vibrations become greater than W. This means that for such velocities the mobility of the polaron must decrease.

In conclusion, we note that the transfer of energy from a moving polaron to a crystal was calculated by Buckingham[8] on the basis of band theory, where the interaction of the electron with the vibrations was taken to be

$$\int c\rho \operatorname{div} \mathbf{u}\, d\tau \qquad (38)$$

where $\mathbf{u}$ is the displacement vector, and the crystal was treated macroscopically and the electron was

TABLE II. Constants of Formula (37) which Gives the Energy Transfer from the Polaron to the Acoustical Vibrations of the Lattice

Crystal	Branch No. α	$C_\alpha = v^0\sqrt{e^2/\mu a}$ in 10^5 cm/sec	$-n_\alpha^0 \cdot 10^3$	$\frac{A_{\max}}{t} = \frac{A_\alpha v}{tC}$ in 10^{-2} erg/sec
NaCl	4	2.53	0.694	0.277
	5	2.79	2.177	2.67
	6	4.65	1.003	0.276
KCl	4	2.01	1.061	0.120
	5	2.5	3.031	0.839
	6	4.1	12.48	8.36
KBr	4	1.6	1.176	0.0791
	5	2.1	3.155	0.433
	6	3.3	6.002	0.996

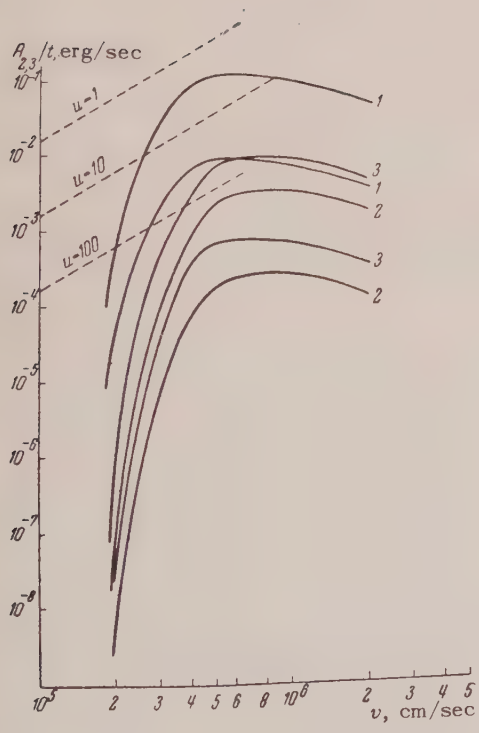

FIG. 2. Energy transferred from a polaron to the transverse optical vibrations of the lattice. The notation is the same as in Fig. 1. The upper curves show A_2/t, the lower curves A_3/t.

treated as a point: $\rho = e\,\delta(\mathbf{r} - \mathbf{v}t)$, c is a constant which cannot be calculated from the band theory. Such a calculation cannot possibly be correct, since a point electron obviously interacts not only with the longitudinal acoustic waves as given by formula (36), but with all other vibrations. Then the magnitude of the interaction turns out to be of the same order for both long and short wave vibrations. But the expression (38) is obviously not suitable for short wave oscillations. In addition, for $v \to C$ Buckingham's result diverges like $1/(v - C)$ (because the electron is treated as a point). As we see, all these difficulties are absent from the polaron theory.

[1] S. I. Pekar, J. Exptl. Theoret. Phys. (U.S.S.R.) 19, 796 (1949).

[2] S. I. Pekar, *Untersuchungen uber die Elektronentheorie der Kristalle*, Akademie-Verlag (Berlin), 1954.

[3] S. I. Pekar, J. Exptl. Theoret. Phys. (U.S.S.R.) 18, 105 (1948).

[4] L. D. Landau and S. I. Pekar, J. Exptl. Theoret. Phys. (U.S.S.R.) 18, 419 (1948).

[5] K. B. Tolpygo, Works (Trudy) Phys. Inst., Academy of Sciences, USSR 6, 102 (1954).

[6] K. B. Tolpygo, Works (Trudy) Phys. Inst., Academy of Sciences, USSR 5, 28 (1955).

[7] K. B. Tolpygo, Math. Reports, Kiev State University 5, 99 (1951).

[8] M. J. Bukcingham, Proc. Phys. Soc. (London) 66A, 601 (1953).

Translated by M. Hamermesh
186

The Relation between Stripping and Compound Nucleus Formation in Deuteron Reactions

Iu. A. Nemilov, K. I. Zherebetsova and B. L. Funshtein
Radium Institute, Academy of Sciences, USSR

(Submitted to JETP editor, August 29, 1955)
J. Exptl. Theoret. Phys. (U.S.S.R.) 30, 1013-1016 (June, 1956)

An estimate is made of the relative probability for stripping and compound nucleus formation in the Mg^{26} (d,p) Mg^{27} reaction, by comparing the yields of final nuclei formed as a result of d,p and d,α processes on Mg^{26}, and by n,p and n,α processes on Al^{27}.

We find that the ratio of the stripping cross section to the cross section for compound nucleus formation varies with deuteron energy and reaches a maximum value of 8-9 for deuteron energy 1-2 mev.

IT is well known that when deuterons interact with nuclei transformations of the type (d,p) and (d,n) can proceed in two ways: via the stripping reaction, in which only one of the nucleons which constitute the deuteron is absorbed by the nucleus, while the other goes on; or in the usual way in which the deuteron as a whole is absorbed by the nucleus and a compound nucleus is formed which upon decaying can emit one of the nucleons. The reaction products —final nucleus and emergent nucleon— can be the same for both mechanisms. Until now it has been possible to make only rough quantitative estimates of the relative probabilities of the two possible mechanisms from studies of the angular distributions of nucleons emitted in deuteron reactions. However this method cannot give sufficiently reliable results, since the angular distributions of nucleons produced as a result of stripping and compound nucleus breakup are known only approximately at present.

We have applied a different method in order to give a more precise quantitative estimate of the relative probability of the two mechanisms. Two reactions were selected (one with deuterons, the other with some other particles, for example neutrons) in which the same compound nucleus is formed. We shall denote by A_1 and A_2 the target nuclei which are subjected to bombardment, by C^* the excited compound nucleus, and by B_1 and B_2 the nuclei formed as a result of emission from the compound nucleus of a proton and an α-particle, respectively. We can then describe the processes considered in the following schematic form:

$$A_1 + D^2 \rightarrow C^* \begin{cases} \nearrow B_1 + p \\ \searrow B_2 + \alpha \end{cases},$$

$$A_2 + n \rightarrow C^* \begin{cases} \nearrow B_1 + p \\ \searrow B_2 + \alpha \end{cases}$$

If only one mechanism were possible for these reactions, via the formation of a compound nucleus, and if the energies of the deuterons and neutrons were chosen so that the excitation energy of the compound nucleus were the same in both cases, then for both reactions the ratio of the number of nuclei of type B_1 to the number of type B_2 would always have to be the same, since the mechanism of breakup of the compound nucleus does not depend on how it was formed. However, in the first reaction the process leading to emergence of a proton, (d,p), can proceed in two ways. Therefore in this case the number of final nuclei B_1 should be greater, and be proportional to the sum of the cross sections for stripping, compound nucleus formation, and a term F due to the interference between the two processes. Thus the number of final nuclei B_1 in the first process will be proportional to

$$\sigma(d,\ p) = \sigma(d,\ p)_{\text{st.}} + \sigma(d,\ p)_{\text{c.n.}} + F.$$

In all the other cases the number of final nuclei should be proportional to the cross sections for the corresponding processes which proceed via the formation of the compound nucleus.

We selected reactions which led to radioactive nuclei B_1 and B_2 with decay periods suitable for measurement. From the decay curves of the activities we determined the ratio of the numbers of radioactive nuclei B_1 and B_2 produced in the targets as a result of irradiation with deuterons and neutrons. We shall denote by N_1 the experimentally measured ratio of the number of final nuclei B_1 formed as a result of the (d,p) reaction to the number of nuclei of type B_2 formed as a result of (d,α) reaction, and by N_2 the ratio of the number of B_1 nuclei produced by (n,p) reaction to the number of B_2 nuclei produced by (n,α) reaction. Then we have:

$$\frac{\sigma(d,\ p)}{\sigma(d,\ \alpha)} = \frac{\sigma(d,\ p)_{c.n.} + \sigma(d,\ p)_{st.} + F}{\sigma(d,\ \alpha)} = N_1,$$

$$\frac{\sigma(n,\ p)}{\sigma(n,\ \alpha)} = N_2.$$

Since the mode of breakup of the compound nucleus is independent of how it was formed, we must have

$$\sigma(d,\ p)_{c.n.} / \sigma(d,\ \alpha) = \sigma(n,\ p) / \sigma(n,\ \alpha).$$

From these relations we find that

$$\frac{\sigma(d,\ p)_{st.} + F}{\sigma(d,\ p)_{c.n.}} = \frac{N_1 - N_2}{N_2}.$$

As already mentioned, this relation is valid if the compound nuclei formed as a result of capture of deuterons and neutrons have the same energy of excitation. However even if this condition is fulfilled we might anticipate some difference because of the fact that even if we have a sharply defined excitation energy, the states of the compound nucleus may be different if there are several wide overlapping levels in this region of excitation energy. In this case errors can arise only if the compound nucleus in different excited states has different probabilities for decay into the various channels and if the probabilities of formation of these states by deuterons and neutrons are not the same. In our experiments the energies of the particles producing the reactions were not strictly monochromatic, which should reduce such errors through an averaging over a series of levels. No resonance phenomena were observed, so that we can assume that errors associated with them were insignificant.

We chose the following two reactions:

$$Mg^{26} + D^2 \rightarrow \begin{cases} Mg^{27} + p \\ Na^{24} + \alpha \end{cases}, \quad Al^{27} + n \rightarrow \begin{cases} Mg^{27} + p \\ Na^{24} + \alpha \end{cases}.$$

These transformations lead to Mg^{27} with a half-life of 9.4 min and β-ray endpoints of 0.79 mev (20%) and 1.77 mev (80%), and to Na^{24} with a half-life of 15 hr with the end point of the β-spectrum at 1.39 mev. The radioactive products of other reactions and of reactions with other magnesium isotopes (the experiments were done with the normal mixture of Mg isotopes), have lifetimes very different from those used by us and did not disturb the measurements. In order to obtain the same excitation of the compound nucleus Al^{28} in these reactions, we had to use a neutron energy about 6 mev greater than the energy of the deuterons. The ratios of the numbers of radioactive nuclei produced by (d,p) and (d,α) processes on magnesium for different deuteron energies were found from curves of the decay of activity induced in the various layers of thin magnesium foils placed in the deuteron beam from the cyclotron. The activities were measured with a standard thin-walled Geiger-Muller counter and a scale-of-64 counting circuit. The ratios of activities as a function of deuteron energy E_d are shown as curve a in Fig. 1.

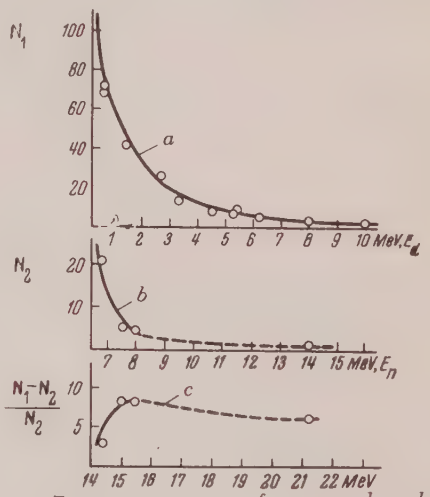

FIG. 1. a— ratio of d,p to d,α cross section; b— ratio of n,p to n,α cross section; c— ratio of stripping cross section to cross section for reaction going via compound nucleus formation.

The D–D reaction was used to obtain monochromatic beams of neutrons. The deuteron target was a layer of zirconium subjected to long irradiation with low energy deuterons (0.8 mev). The length of the preliminary deuteron irradiation of the foil was chosen to assure deposition of 1 C of deuteron ions per cm^2 of irradiated surface of the foil. According to published work,[1] under these conditions the neutron yield from the foil reaches saturation. It is well known that zirconium can adsorb hydrogen in relatively large quantities, so we may expect that all the D atoms impinging on the zirconium will be concentrated close to the surface in a layer of thickness no greater than a few microns. If we now irradiate the foil with faster deuterons, we may expect to obtain quite uniform energy neutrons. To test the degree of homogeneity of the neutrons thus obtained, experiments were

carried out to determine their energy spectrum by measuring ranges of proton recoils in thick-layered emulsions. To do this, the plate was placed in a special holder below the zirconium target inside the cyclotron chamber.

The results of one such series of measurements are shown in the histogram of Fig. 2. From the histogram it is apparent that in this experiment we had an intense neutron group with an energy somewhat less than 8 mev and a quite strong continuous background in the neutron energy region below 5 mev. The energy of the fast neutron group is in good agreement with the expected value. The

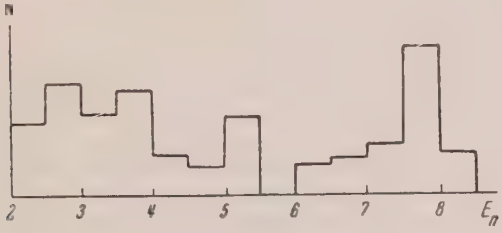

FIG. 2. Distribution in energy of number, N, of neutrons from D–D reaction on a zirconium target whose surface is saturated with deuterium.

background of slower neutrons apparently arises from the presence of deuterium all through the zirconium plate and from the zirconium itself, as well as from the beam striking parts of the cyclotron chamber and from collisions of the deuterons with gas in the chamber. The presence of quite large numbers of relatively slow neutrons should have no essential effect on the results of the experiment, since both of the reactions used by us are endothermic (for the Al^{27} (n,p) Mg^{27} reaction, Q_0=1.92 mev, while for Al^{27} (n,α) Na^{24}, $Q_0 = -3.17$ mev) and most of the slow neutron group is either below the threshold for these reactions or is in a region where the yield is small. To estimate the effect of the neutron background we carried out the following control experiment. First we measured the activity induced by the neutrons in aluminum when the zirconium target was saturated with deuterium, and then under the same conditions irradiated the aluminum target from a layer of zirconium without deuterium. It turned out that the activity of the target in the second experiment did not exceed 10% of the activity in the first experiment.

To determine the ratio N_2, we placed a piece of rolled aluminum foil below the Zr-D target and irradiated the latter in the cyclotron.

The experiments with the zirconium target were done for three deuteron energies, all below 5 mev, since at higher energies considerable numbers of neutrons appear from the reaction with zirconium. In addition we used 14 mev neutrons. Measurements of target activity were made under the same conditions as for the magnesium targets. The values obtained for the ratio N_2 as a function of neutron energy E_n are shown in Fig. 1b. The dashes show the assumed behavior of the curve in the neutron energy region where N_2 was not measured. The values of $(N_1 - N_2)/N_2$, which gives the ratio of the probabilities of the two possible mechanisms for deuteron interaction with nuclei, are given in Fig. 1c.

From the curves of Figure 1 we see that the yield of protons increases relative to the yield of α-particles as we decrease the deuteron energy, both for reactions with deuterons and with neutrons. This obviously arises from the fact that reactions yielding protons are more exothermic; in addition, for lower excitation energy of the compound nucleus, the effect of the potential barrier is greater in reactions in which α-particles are formed. The ratio $(\sigma_{st.} + F)/\sigma_{c.n.}$ is a maximum (within the range of deuteron energies for which the measurements were made) for deuteron energy 1–2 mev, and equals 8–9. We do not know the relative phase for these processes, so that we can say only that the actual value of the ratio $\sigma_{st.}/\sigma_{c.n.}$ lies within the limits 4 to 16. A decrease of $(\sigma_{st.} + F)/\sigma_{c.n.}$ when the deuteron energy is increased or decreased can arise either from a change in F or from a change in the ratio of the cross sections for the two interaction mechanisms. The sharp decrease of this quantity when we go to low deuteron energies cannot, it appears, be explained solely by changes in F, and is evidence that $\sigma_{st.}$ decreases faster than $\sigma_{c.n.}$. This is in contradiction with the ideas developed by Oppenheimer and Phillips,[2] but can be explained on the basis of stripping theory.[3] The capture by the nucleus of a neutron with large values l of angular momentum should be less probable for low deuteron energies. Therefore as the deuteron energy is lowered, only those states of the final nucleus should be formed which can occur for $l = 0$, and in many cases this may be associated with a decrease of the probability of the process.

[1] Campbell, Korsmeyer and Ralph, Phys. Rev. 94, 791 (1954).

[2] J. R. Oppenheimer and M. Phillips, Phys. Rev. 48, 500 (1935).

[3] S. T. Butler, Proc. Roy. Soc. (London) 208A, 559 (1951).

Translated by M. Hamermesh
214

Production of Slow π^+ Mesons in Photographic Emulsion Nuclei by 660 mev Protons*

V. V. Alpers,** L. M. Barkov, R. I. Gerasimova, I. I. Gurevich, A. P. Mishakova, K. N. Mukhin and B. A. Nikol'skii

(Submitted to JETP editor Feb. 11, 1956)
J. Exptl. Theoret. Phys. (U.S.S.R.) 30, 1034-1039 (June, 1956)

Production of slow mesons by 660 mev protons was studied with the aid of the emulsion camera. The method exployed permitted us to studyeffectivelythe stars formed by π^- mesons as well as the energy and angular spectra of the slow π^+ mesons formed in nuclei.

The present work is a continuation of the study of formation of π^+ and π^- mesons in the nuclei of photoemulsions by fast nucleons and contains results obtained with 660 mev protons. The camara used in this work was prepared with the photoemulsion NIKFI, type *R* (85% Ag Br), containing 45 layers each 300 μ thick and 42 mm in diameter and was irradiated with 600 $\pm$10 mev protons obtained from the synchrocyclotron of the Institute for Nuclear Problems, Academy of Sciences, USSR.

The greater thickness of the emulsion camera (15 mm) and the higher sensitivity of the emulsion used in this work permitted a more detailed analysis of the process of formation of slow π^- mesons in the photoemulsion nuclei.

1. ENERGY AND ANGULAR DISTRIBUTIONS OF THE FORMED π MESONS

TO obtain a correct picture of the different characteristics of the π^+ and π^- mesons in the photoemulsion we used the method of following each meson track from its end to the point of π meson production or its entrance into the camera. There were found by this method 95 cases of π^+ meson and 80 cases of π^- meson production. After making corrections for the end effect (as discussed in Ref. 1) there were obtained the angular distribution and energy spectrum of the produced π^+ and π^- mesons.

In Fig. 1 are shown the angular distributions of π^+ and π^- mesons produced by 600 mev protons in the photoemulsion nuclei. It is seen from Fig. 1 that the π meson production cross section depends slightly on the flight angle relative to the direction of the beam of the incident particles. The energy distribution of the π^+ and π^- mesons is shown in Fig. 2. It is seen from Fig. 2 that the difference between the spectra of π^+ and π^- mesons produced by protons is preserved at 660 mev although it is less pronounced than at 460 mev (Ref. 1) which is possibly connected with the increasing effect of the charge redistribution between the captured nucleon and the nucleus prior to the formation of the meson.

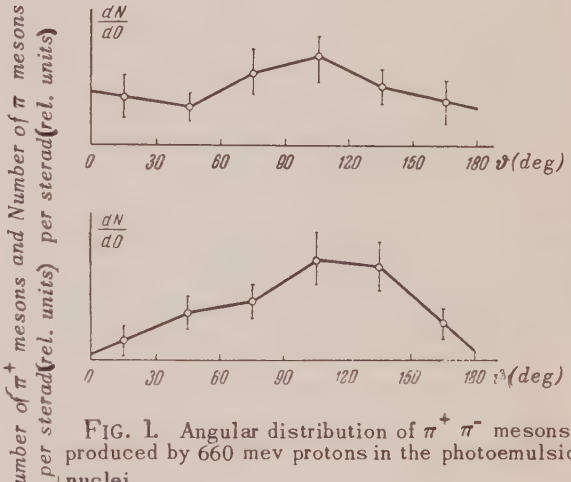

FIG. 1. Angular distribution of π^+ π^- mesons produced by 660 mev protons in the photoemulsion nuclei.

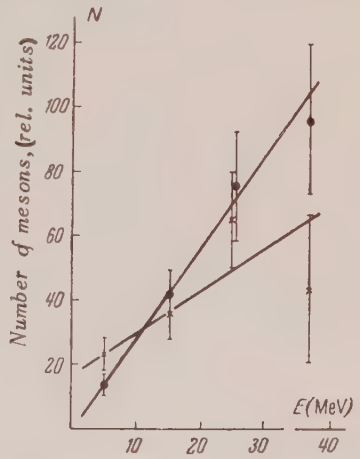

FIG. 2. Energy distribution of π^+ and π^- mesons produced by 660 mev protons in the photoemulsion nuclei ● — mesons; × — π^- mesons

*This communication is based on results obtained during 1954-55.

**Deceased

There was also computed the ratio of π^+ to π^- meson production which for mesons of $E_\pi > 40$ mev, after corrections for the end effect, turned out to be $\pi^+ / \pi^- = 1.6 \pm 0.4$. Allowance for the Coulomb displacement of 15 mev (Ref. 1) in the π^+ and π^- mesons energy spectra yields for the value of this ratio the quantity $\pi^+ / \pi^- = 2.3 \pm 0.5$ which coincides, within the limits of error, with the results obtained by irradiation of emulsions with 460 mev protons:

$$\pi^+/\pi^- = 2,5 \pm 0.6.$$

The production cross sections of π^+ and π^- mesons of energy $E_\pi < 40$ mev by 660 mev protons in photoemulsion nuclei was obtained from the number of produced π mesons in a definite volume of the emulsion and the density of the proton beam (Ref. 1). The cross sections were found to be: $\sigma_{\pi^-} = (2.8 \pm 1,0) \cdot 10^{-27}$ $см^2$; $\sigma_{\pi^+} = (4,4 \pm 1.5)$ 10^{-27} $см^2$; $\sigma_{(\pi^+ + \pi^-)} = (7.2 \pm 1.8) \times 10^{-27}$ $см^2$. These cross sections refer to mesons of the energy interval $0 < E_\pi < 40$ mev.

2. ANALYSIS OF STARS ACCOMPANYING PRODUCTION OF π MESONS

In the analysis of the stars accompanying production of π mesons, traces of the particles leaving the star were examined up to the point where they were stopped in the emulsion camera, or up to their emergence from it. In the first case the energy was determined from the curves $E = f(R)$ where R denotes the ionization path of the particle; in the second case, the energy was determined from the curves of energy dependence on the grain density $E = f(dN/dR)$. The curve $E = f(dN/dR)$ was obtained experimentally for π mesons and recomputed for protons according to the formula

$$\frac{dN}{dR}(E_p) = \frac{dN}{dR}\left(\frac{E_\pi M_p}{M_\pi}\right).$$

The application of this method permitted more reliable measurements of the energies of particles emitted from the stars compared with other investigations in which photographic plates were used for this purpose.

A total of 95 stars accompanied by production of π^+ mesons and 80 stars by production of π^- mesons were analyzed, and not a single case of formation of pairs of mesons was registered in all the 175 cases. In addition, we investigated 74 stars found in following tracks of protons not containing π mesons (see Sec. 3).

The distribution according to energy of the particles leaving the stars is shown in Fig. 3. The photographic emulsion used in the work did not permit effective identification of protons and α-particles of low energy ($E_\rho < 40$ mev); the particle energy in all cases was therefore determined from the curves $E = f(R)$ for protons. Numerical values for the energy distributions of the particles are shown in Table 1.

TABLE 1

Average star energy $\bar{E}$ (combined kinetic energy of charged particles) and average number of charged particles $\bar{N}$ in stars with and without production of mesons

Particle energy (in mev)		0—30	30—100	>100	All energies
$\bar{E}$	π^-	18±2	23±4	143±19	184±13
	π^-	28±2	54±7	163±22	246±17
	without π	28±2	36±5	296±34	360±20
$\bar{N}$	π^+	1.85±0.14	0.4 ±0.07	0.63±0.08	2.9 ±0.17
	π^-	3.2 ±0.2	0.9 ±0.1	0.71±0.09	4.85±0.25
	without π	2.5 ±0.2	0.62±0.09	1.0 ±0.1	4.2 ±0.2

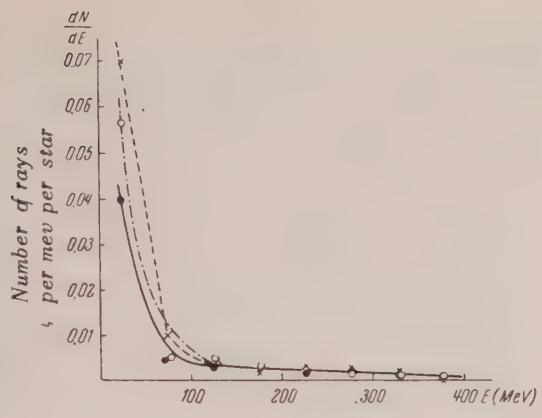

FIG. 3. Energy distribution of particles leaving the stars under the action of 660 mev protons. ● — denotes stars with production of π^+ mesons; × — stars with production of π^- mesons; O — stars without any mesons.

As shown in Table 1, the number of fast protons leaving the stars ($E > 100$ mev) is substantially the same for all cases of π^+ and π^- meson production, but there is a difference in the number of charged particles of low and medium energy. The independence of the number of fast protons of the sign of the produced meson is maintained also for the case when the meson is emitted forward. The latter characteristic , pointed out in the analysis of stars produced by 400-460 mev nucleons, indicates that the nuclei aretransparent to slow mesons ($E_\pi < 40$ mev) and that there exists a high probability of the nucleons recharging in the nucleus.

Stars which are not accompanied by π meson production are characterized by a relatively high number of charged particles and by high average value of star energy E. The difference in the number of charged particles of small and medium energies ($E < 100$ mev) corresponds to the change in the nuclear charge with the production of mesons of different signs.

In Figs. 4 and 5 are shown angular distributions of slow ($E < 30$ mev) and fast ($E > 100$ mev) particles leaving the stars. The corresponding numerical characteristics are shown in Table 2 where the anisotropy is determined as

$$[N(0\div 90^\circ) - N(90\div 180^\circ)]/[N(0\div 90^\circ) + N(90\div 180^\circ)].$$

It should be noted that the anisotropy of the angular distribution of particles leaving the stars is maintained down to particles of lowest energies. The corresponding results are shown in Fig. 6. It can be readily shown that the observed anisotropy cannot be explained by the motion of the nucleus as a whole.

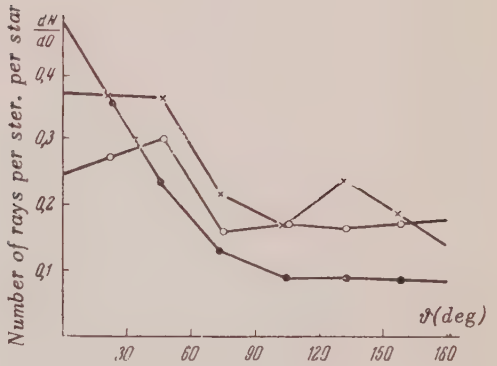

FIG. 4. Angular distribution of slow ($E < 30$ mev) particles leaving the stars under the action of 660 mev protons. ● — denotes stars with the production of π^+ mesons; × — stars with production of π^- mesons; O — stars without mesons.

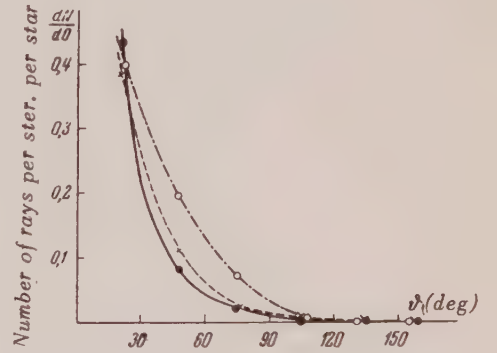

FIG. 5. Angular distribution of fast ($E > 100$ mev) particles leaving the stars under the action of 660 mev protons. ● — denotes stars with production of π^+ mesons; × — stars with production of π^- mesons; O — stars without mesons.

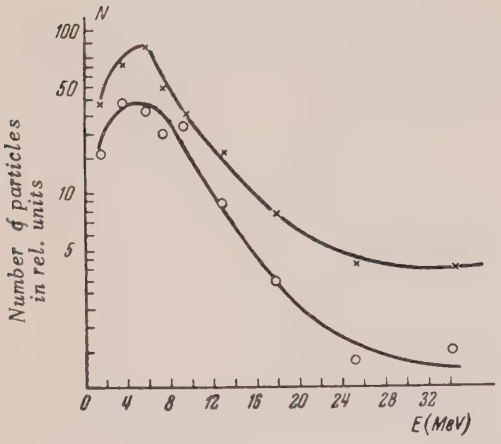

FIG. 6. Distribution by energy of slow particles ($E < 20$ mev) emitted forward ($\vartheta < 90°$) and backward ($\vartheta > 90°$) relative to the beam of the incident 660 mev protons. × — denotes particles emitted forward ($0° < \vartheta < 90°$) from stars with the production of π^+ and π^- mesons; O — particles emitted backward ($90° < \vartheta < 180°$) from stars with the production of π^+ and π^- mesons.

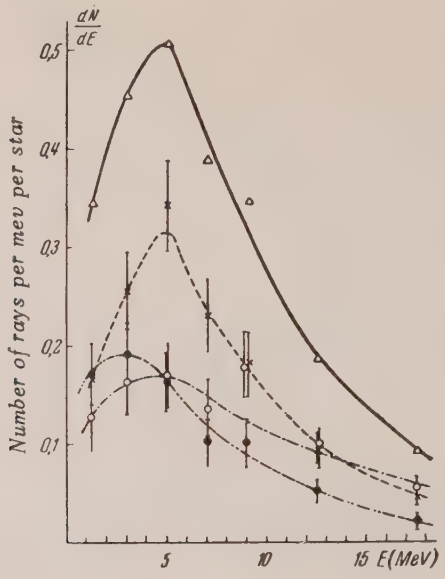

FIG. 7. Distribution by energy of slow particles ($E < 20$ mev) leaving the stars under the action of 660 mev protons. × — denotes stars with the production of π^+ mesons; O — stars without mesons; Δ — all the stars (in relative units). ● — stars with the production of π^+ mesons.

TABLE 2

Anisotropy value of particles leaving the stars within different energy intervals

Energy interval of the particles in mev	π^+	π^-	without π
0—30	0,39±0,08	0,22±0,06	0,15±0,07
> 30	0,82±0,06	0,81±0,05	0,82±0,05
>100	1,00±0,03	0,89±0,06	0,97±0,03

A comparison of the data in Table 2 with results of Ref. 1 shows that, with increase in energy of the incident protons from Ep = 460 mev to Ep= 660 mev, the anisotropy of slow particles leaving the stars decreases. In Fig. 7 are shown energy distribution curves for low energy ($E < 20$ mev) particles leaving the stars under the influence of 660 mev protons. The distribution shows that the energy spectrum includes a large number of slow particles. The number of stars containing particles of energy $E < 6$ mev comprises 70% in the case of π^- meson production and about 50% in the case of stars without mesons.

Considering the fact that nuclear interactions in the photoemulsion take place principally in the nuclei of silver and bromine for which the mean Coulomb potential is ~ 9 mev relative to protons, the number of stars containing slow particles appears to be too high to be explained by the action of light nuclei, presence of subbarrier particles or the decrease of the Coulomb barrier with nuclear excitation.[2,3] It should be noted that in emulsions which register particles of minimum ionization, it is impossible to determine effectively the mass and charge of low energy particles. Therefore, the path-energy relation

for protons was used in this work in determining the energy of particles of short paths. Thus, for example, α-particles of energy $8 < E_\alpha < 16$ mev fall into the energy interval of 2 to 4 mev. In this way, a considerable portion of the spectrum of the short path particles ($R > 40\ \mu$) could be explained by the presence of α-particles of energy $E_\alpha > 8$ mev. However, it can be seen from the distribution presented in Fig. 7 that, among the rays of the stars, there is a large number of particle traces of paths shorter than 40 μ which therefore must be related to particles with $Z > 2$.

3. THE MEAN FREE PATH IN THE PHOTOEMULSION OF 660 MEV PROTONS

There were also found in this work 127 cases of interactions between protons and nuclei, registered by the method of following the protons tracks. The total length of all the traces studied was 4362 cms. Four cases were related to the elastic scattering of protons by nuclei. Thus, the mean free path of the 660 mev protons in inelastic interactions with the emission nuclei was equal $\lambda = 35.4 \pm 3.1$ cm.

The theoretical estimate of the mean free path can be obtained from the formula

$$1/\lambda_{\text{theor}} = \sum N_i \pi R_i^2 (1 - p_i), \qquad (1)$$

where N_i denotes the concentration of nuclei in the ith component of the emulsion, $R_i = r_0 A_i^{1/3}$ — nuclear radius of the ith component, p_i the transparency of nuclei in the ith component. The transparency p_i was determined from the expression

$$p_i = \{1 - (1 + 2R_i/L) \times \exp(-2R_i/L)\} L^2/2R_i^2, \qquad (2)$$

where L denotes the mean free path of protons in the nuclear matter.

Computation of p_i was made for two values of parameter r_0 which determines the radii of the nuclei: $r_0 = 1.2 \times 10^{-13}$ cm and $r_0 = 1.37 \times 10^{-13}$ cm.

The cross section of the interaction between the proton and the nucleons was taken as $\sigma_{np} = \sigma_{pp} = 42 \times 10^{-27}$ cm^2.

Results of computations of λ_{theor} are given in Table 3. As seen from Table 3, λ_{theor}, obtained for two different values of r_0, does not differ much from λ_{exp}. It is readily shown that the dependence of λ_{theor} on σ_{np} and σ_{pp} is weaker than its dependence on r_0 [see Eq. (2)]. We can thus state that there is good agreement between the observed value of the proton mean free path in the photoemulsion and the computed value.

In conclusion we express our thanks to Prof. M. G. Meshcheriakov and Prof. V. P. Dzhelepev for the opportunity afforded us to conduct experiments with the syncrocyclotron of the Institute for Nuclear Problems, Academy of Sciences, USSR, to L. V. Surkova, O. L. Shchipakin and G. V. Kolganova for their assistance in this work.

TABLE 3

Comparison of λ_{theor} with λ_{exper} and λ_{geom}

$r_0 \cdot 10^{13}$, in cm.	λ_{theor}, in cm.	λ_{geom} in cm.	$\lambda_{\text{exp.}}$ in cm.
1.37	37.3	25.6	35.4±3.1
1.2	33.6	29.1	

[1] V. V. Alpers et al, J. Exptl. Theoret. Phys. (U.S.S.R.) 30, 1025 (1956).

[2] Le Couteur, Proc. Phys. Soc. (London) 63A, 259 (1950).

[3] E. Bagge, Ann. d. Phys. 33, 389 (1938).

Translated by J. L. Herson
217

Nuclear Levels in Li^6

Iu. L. Sokolov, M. M. Sulkovskaia, E. I. Karpushkina and E. A. Albitskaia

(Submitted to JETP editor December 26, 1955)
J. Exptl. Theoret. Phys. (U.S.S.R.) 30, 1007-1012 (June, 1956)

With the aid of the photographic detection method, reactions with emergence of several particles were studied, which arise as a result of interaction of fast deuterons (with energies up to 13.8 mev) with nuclei of Li^6 and Li^7. The following reactions were detected: $Li^6(d; 2d)He^4$, $Li^6(d; d', p, n)He^4$ and $Li^7(d; t, d')He^4$, which lead to the formation of excited Li^6 nuclei. The following levels of the Li^6 nucleus were found (with $T = 0$): $E_1^* = 2.2$ mev, $E_2^* \approx 4.5$ mev and $E_3^* \approx 7.5$ mev.

FROM the point of view of the shell model, $(1s)^4(1p)^2$ is the probable configuration of the ground state of Li^6. This configuration corresponds to the assumption that the four nucleons in the $(1s)$ state form a system similar to the α-particle, in whose field the other two nucleons occupy places in the p-shell. Since there is every reason to think that the excitation of the α-particle does not appear before energies ~ 15 mev[1,2], it follows that the first levels of the Li^6 nucleus must correspond to different states of the two nucleons in the field of the α-particle. Therefore, an experimental investigation of the properties of the Li^6 nucleus is of considerable interest, since it makes it possible to draw a number of conclusions concerning the character of the neutron-proton interaction as well as concerning their interaction with the group of four nucleons in the $(1s)$ state.

1. In the present investigation, the interaction of fast deuterons with the nuclei of Li^6 and Li^7 was studied. The registration of the reaction which took place was made by means of the photographic method; lithium was introduced into the emulsion layer of the plate, which was then irradiated with deuterons in such a way that their tracks were completely within the emulsion. Under such conditions, because of the continuous decrease of the energy of the deuterons as they were slowed down, the disintegrations of the lithium nuclei could be caused by deuterons of different energies.

We used plates of type E-1 (Ilford) with layer thickness of 100μ. Emulsion of type E-1 was chosen because, under proper conditions of developing, it makes it possible to obtain tracks of singly charged particles, α-particles, and other, heavier nuclei, which differ markedly in their external appearance (grain dimensions and density). These properties of the E-1 emulsion greatly facilitate the identification of tracks in analyzing the stars belonging to various reactions.

The introduction of lithium in the emulsion layer was accomplished by saturation in a solution of lithium acetate; the concentration of lithium atoms was then determined, as well as the uniformity of its distribution in depth and area of the emulsion layer.

The plates saturated with lithium were irradiated in a cyclotron with deuterons of $13.8 \pm .2$ mev energy. The maximum density of deuteron tracks with which, in the majority of cases, it was still possible to determine with certainty the point of entry into the emulsion of the deuteron causing the reaction in question, was 5×10^5 deuterons per sq. cm of plate surface. It should be noted that the handling of plates with such density of tracks was only possible with the aid of a special stereomicroscope.

General inspection of the irradiated and developed plates for the purpose of finding stars belonging to different reactions, was carried out with a magnification of 450×.

We have investigated plates saturated with an acetate of the natural mixture of lithium isotopes, as well as plates which contained lithium enriched with the isotope Li^6. On equal areas of plates of both kinds were found approximately equal numbers of various stars consisting of two, three and four rays (not counting numerous cases of d-p scattering). Among them were a number of stars consisting (besides the deuteron track causing the disintegration) of one track of an α-particle and two tracks of singly-charged particles.

Energetically possible reactions with $Q \geq -5$ mev, which could give stars of this type, are the following:

TABLE 1

Type of reaction	Q (mev)
$Li^6(d, t, p)He^4$	+ 2.5
$Li^6(d, 2d)He^4$	— 1.5
$Li^6(d, d', p, n)He^4$	— 3.7
$Li^6(d, p, p)He^6$	— 5.0
$Li^7(d, d', t)He^4$	— 2.5
$Li^7(d, t, p, n)He^4$	— 4.7

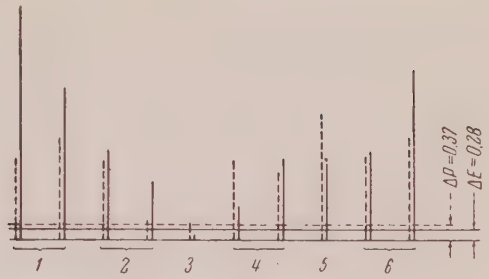

FIG. 1. Values of the differences: Continuous lines $\Sigma\epsilon_i - (\epsilon_d + Q)$ and dotted lines $P_d - \Sigma P_i$ found on the supposition that the star pictured in Fig. 2 belongs to the various possible reactions. For *1*--$Li^6(d, t, p)He^4$ the sign of the difference is minus; for the other reactions: *2*--$Li^7(d, d', t)He^4$, *3*--$Li^6(d, 2d)He^4$, *4*--$Li^6(d, d', p, n)He^4$, *5*--$Li^6(d, 2p)He^6$, *6*--$Li^7(d, t, p, n)He^4$, the sign of the difference is plus.

Identification of the stars was made on the basis of the laws of conservation of energy and momentum. The necessary measurements of track lengths, angles between them and projection of tracks on a vertical axis[*] were made with MBI-8 microscopes.

In identifying each star, it was assumed successively that it belongs to one of the reactions listed above. Then, from the measured lengths of the tracks, the kinetic energies ϵ_i and momenta $\mathbf{p}_i$ of the emerging particles[**] were determined, and on the basis of the equalities $\epsilon_d + Q = \Sigma\epsilon_i$ and $\mathbf{p}_d = \Sigma\mathbf{p}_i$ it was determined to what reaction the star in question belonged[***]. Figure 1 gives graphically the results of this analysis in the case of the star pictured in Figure 2. Here vertical lines represent the values of the differences $|(\epsilon_d + Q) - \Sigma\epsilon_i|$ (continuous lines) and the values of the differences $|\mathbf{p}_d - \Sigma\mathbf{p}_i|$ (dotted lines) for reactions of the various types indicated on the axis of abscissas.

The conditions $|(\epsilon_d + Q) - \Sigma\epsilon_i| = 0$ and $|\mathbf{p}_d - \Sigma\mathbf{p}_i| = 0$ were fulfilled for the reactions studied within limits of error which were, on the average, ±0.25 mev for total energy and ± 0.5 momentum units form momentum[*].

This method of identification is sufficiently reliable, since the difference in Q-values for the reactions in question is substantially greater than the error in the determination of total energy.

[*] The coefficient of shrinkage was 2.5 for all of the plates examined.

[**] For unit of momentum the momentum of a nucleon with energy of 0.5 mev was taken.

[***] For those reactions as a result of which, besides the α-particle, two different singly-charged particles appeared, for instance a proton and a triton, each of the tracks in turn was assumed to be the track of one of these particles.

[*] Maximum possible errors in the determination of the total energy and momentum were calculated separately for each star.

2. As a result of the processing of the plates described above, it was found that the overwhelming majority of three-ray stars consisting of two tracks of single charge particles and one α-particle track, belong to the following reactions:

$$Li^6(d; 2d)He^4, \quad Li^6(d; d', p, n)He^4,$$

$$Li^7(d; t, d')He^4.$$

1) *Reaction* $Li^6(d, 2d)He^4$. This reaction was the most numerous among the reactions mentioned; as far as is known to us, this reaction has not been previously observed. This was probably due to the use of other methods of registration in the corresponding experiments.

Figure 2 shows a microphotograph of a star pertaining to this reaction.

If one regards the deuteron and the α-particle in the Li^6 nucleus as more or less independent formations, it may be assumed that such a reaction consists in the pulling out by the incident deuterons of a deuteron comparatively weakly bound to the α particle in the Li^6 nucleus. Obviously, in this case the kinetic energy sums of the α-particles and the deuterons (determined in the corresponding center-of-mass system), must have a continuous distribution in the entire interval of possible values.

On the other hand, it may be assumed that the reaction under consideration takes place in two

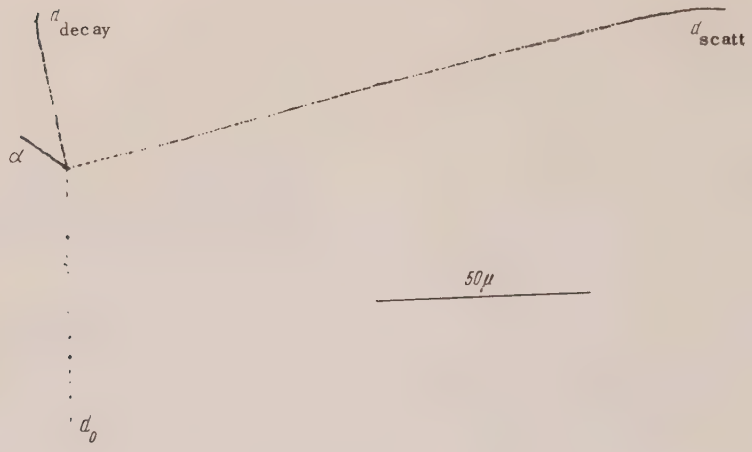

FIG. 2. Microphotograph of a star belonging to the reaction $Li^6(d, 2d)He^4$.

stages; the incident deuteron, undergoing inelastic scattering, excites the Li^6 nucleus to a definite level from which it then decays into a deuteron and an α-particle. In this case the sum of the kinetic energies of the α-particle and the deuteron (in the center-of-mass system of the Li^6 nucleus), plus the binding energy must equal the excitation energy of the level in question.

This hypothesis may be checked by the construction of the corresponding vector diagrams, from which it is possible, first, to find the momentum received by the Li^6 nucleus in the center-of-mass system of Li^6 and the incident deuteron, and, second, to determine the momenta (energies) of the α-particle and the second deuteron in the center-of-mass system of the excited Li^6 nucleus. The energy of the level is in this case determined by

$$E^* = \varepsilon_d + \varepsilon_\alpha + |Q| .$$

The energy of the Li^6 level may also be found by means of the following relation:

$$E^* = {}^2/_3 [E - 2E' + \sqrt{EE'}\cos\vartheta], \qquad (1)$$

where E is the energy of the incident deuteron, E' is the energy of the scattered deuteron and ϑ is the scattering angle (all in the laboratory coordinate system).

It is necessary to note, however, that in both cases the analysis of the stars is made more difficult by the circumstance that it is not known in advance which of the two deuterons present in the star is the inelastically scattered one and which is the one which appears as a result of decay of Li^6. Hence, during the processing it was necessary to assume successively each one of the deuterons to be scattered and the other appearing as a result of decay; hence, obtaining two values of E^* for each star. It should be noted that reduction with Eq. (1) is rather cumbersome because the determination of the true value of angle ϑ is complicated.

The graphical method turned out to be simpler. For each star two vector diagrams were constructed (with the above assumptions concerning the two deuterons), with the aid of which two values of the sum $\epsilon_\alpha + \epsilon_d$ (in the center-of-mass system of the excited Li^6 nucleus) were obtained.

On of these sums, $E_1 = \epsilon_{d_{scatt}} + \epsilon_\alpha$, obtained in the case when the scattered deuteron is taken for the one resulting from decay, is obviously not connected with the positions of the levels of the Li^6 nucleus. Since the energy $\epsilon_{d_{scatt}}$ may assume any values lying in the allowed limits, the sum E_1 will have a continuous distribution.

The second sum is $E_2 = \epsilon_{d_2} + \epsilon_\alpha$. If the process mentioned above takes place, in which the incident deuteron pulls out the deuteron d_2 from the Li^6 nucleus, the energies ϵ_{d_2} and ϵ_α will also have any values in the allowed intervals. In this case the sum E_2, like the sum E_1, will have a

continuous distribution, If, however, excitation of the Li^6 nucleus to definite levels takes place, with subsequent disintegration into α-particle and deuteron, the sum $E_2 = \epsilon_d + \epsilon_\alpha$ must have discrete values equal to $E^* - |Q|$ where E^* is the excitation energy corresponding to the level in question. Therefore, in order to determine whether the disintegration of the excited Li^6 nucleus from the various levels is taking place, it is necessary to ascertain whether in the sequence of pairs of sums E_1 and E_2 there are groups of neighboring values belonging to definite levels.

Upon analysis of the vector diagrams it was found that one of such paired sums in the majority of cases is markedly different from the other. Among the smaller sums there were many values near to 0.7 mev which, in a sum with reaction energy $|Q| = 1.5$ mev gives a value equal to 2.2 mev which coincides exactly with the known energy of the first excited state of the Li^6 nucleus[3]. Figure 3 shows the distribution of the quantity $E^* = \epsilon_d + \epsilon_\alpha + |Q|$ for $(d; 2d)$-stars constructed using the most frequently occurring values of the sums. The graphs shows a distinct maximum at the energy $E^* = 2.2$ mev.

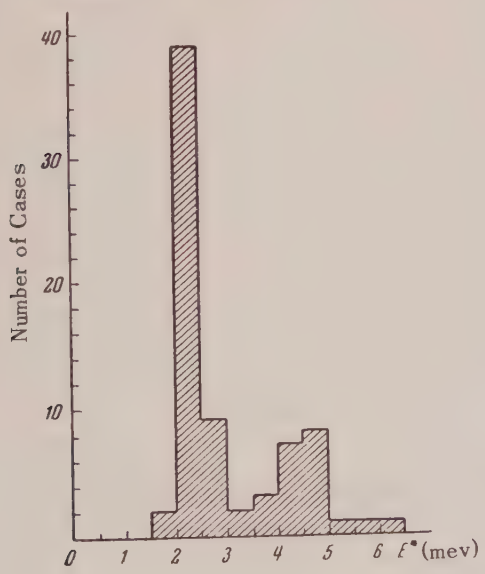

FIG. 3. Distribution of the quantity $E^* = \epsilon_d + \epsilon_\alpha + |Q|$.

It may, therefore, be regarded as established that the decay of the excited nucleus of Li^6 during the reaction $(d, 2d)$ takes place in the majority of cases from the level at 2.2 mev. This level, as was to be expected, has isotopic spin zero, since the decay products in this case are an α-particle and a deuteron (which have isotopic spins zero).

Besides the group of stars corresponding to the level at 2.2 mev, there is a certain number of stars for which the quantity E^* lies within the limits ~3.5 to ~5 mev. It was not possible to determine, because of their small number, the origin of these stars with sufficient definiteness. They could, for instance, correspond to the process, mentioned above, in which a deuteron is pulled out from the lithium nucleus or to the decay of the excited Li^6 nucleus from higher levels. The character of the histogram shown in Fig. 4 speaks in favor of the last supposition, since a sufficiently definite maximum at $E^* \approx 4.5$ mev is observed which confirms the available indications of the existence of a level of Li^6 at ~4.5 mev[4]. This level as well as the level at 2.2 mev should have isotopic spin $T = 0$.

We have not found any $(d, 2d)$ stars corresponding to higher levels of the Li^6 nucleus.

2) *Reactions* $Li^6(d, d', p, n)He^4$ and $Li^7(d; t, d')He^4$. Besides stars belonging to the reaction $Li^6(d; 2d)He^4$, we found stars corresponding to reactions $Li^6(d; d', p, n)He^4$ and $Li^7(d; t, d')He^4$

The value of Q for the reaction $Li^6(d; d', p, n)He^4$ is −3.7 mev; hence the decay of the excited Li^6 nucleus formed during the inelastic scattering of a deuteron cannot take place in this case from the level at 2.2 mev. The next level which can be excited by an inelastically scattered deuteron is the level at ~4.5 mev. However, all of the stars observed by us which belong to the reaction $Li^6(d; d', p, n)He^4$ correspond to a previously unobserved level whose energy turned out to be 7.6 ± .3 mev. We have not found any stars corresponding to the level at 4.5 mev.

Figure 4 shows a microphotograph of a star corresponding to the reaction $Li^7(d; t, d')He^4$ which can, apparently take place in two ways[*]:

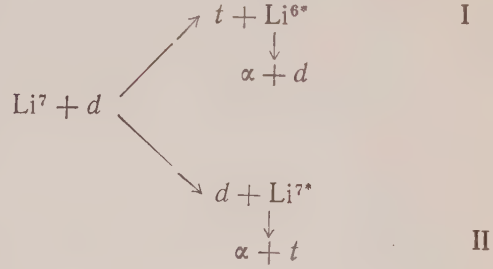

[*] We have also found a small number of stars corresponding to the reaction $Li^7(d; t, p, n)He^4$.

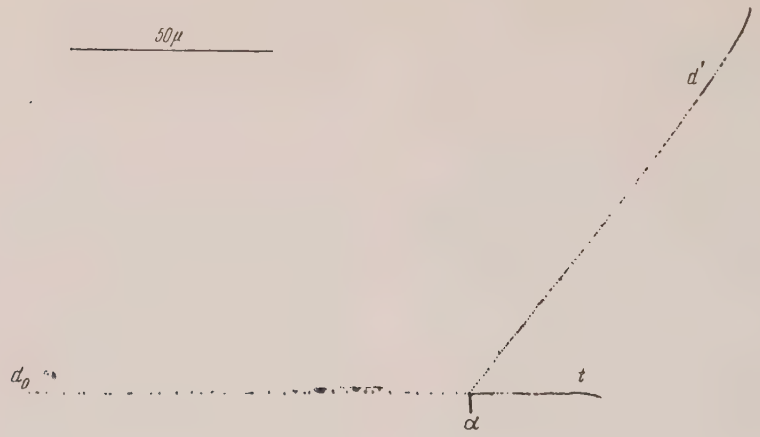

FIG. 4. Microphotograph of a star belonging to the reaction $Li^7(d, t, d')He^4$.

The reaction

$$Li^7 + d \rightarrow t + Li^{6*} \downarrow \alpha + d$$

allows, obviously, to determine the position of certain levels of the Li^6 nucleus.

As a result of the analysis of stars belonging to this reaction, we have found levels at 2.2 and ~4.5 mev, as well as the level, mentioned above, at ~7.5 mev[*], which was found in studying the reaction $Li^6(d; d', p, n)He^4$. The appearance of levels at 2.2 and ~4.5 mev, belonging to the Li^6 nucleus, is confirmation of the fact that the reaction $Li^7(d; t, d')He^4$ may take place in the manner indicated.

Besides the stars for which the values of E^* are 2.2 ~ 4.5 and 7.5 mev, we found a comparatively small number of stars which cannot be attributed to any of the known levels of the Li^6 nucleus. One may assume that these stars correspond to unknown levels of the Li^6 nucleus or to the second course of the $Li^7(d; t, d')He^4$ reaction. However, the small number of such stars made it impossible to make any definite conclusions in this regard.

In the literature there are indications of the existence of a level of the Li^6 nucleus with isotopic spin $T = 0$ at ~5.4 mev[4]. However, the data obtained by us concerning the reactions $Li^6(d;2d)He^4$, $Li^6(d; d', p, n)He^4$ and $Li^7(d; d, t')He^4$, do not confirm so far the existence of this level.

In conclusion, the authors express their deep gratitude to Prof. I. I. Gurevich for discussion of the results and general assistance in carrying out the present work; to Prof. Ia. A. Smorodinskii and A. I. Baz' for discussion of a number of problems; to Z. M. Kudriasheva, Mi. I. Ovskiannikova and V. S. Balova for examination of the plates; as well as to the staff of the Cyclotron Laboratory for help in irradiating the plates.

[*] An indication of the existence of this level (private communication) appeared recently in the review of Ajzenberg and Lauritsen, e.g., see Rev. Mod. Phys. 27, 77 (1955).

[1] N. A. Vlasov, S. P. Kalinin, et al., J. Exptl. Theoret. Phys. (U.S.S.R.) 28, 639 (1955); Soviet Phys. JETP 1, 500 (1955).

[2] Willard, Bair and Kington, Phys. Rev. 90, 865 (1953).

[3] F. Ajzenberg and T. Lauritsen, Rev. Mod. Phys. 24, 321 (1952).

[4] A. Galonsky and M. T. McEllistrem, Phys. Rev. 96, 826 (1954).

Translated by A. V. Bushkovich
213

Inelastic Scattering of 0.3, 0.77 and 1.0 mev Photoneutrons*

KH. R. POZE AND N. P. GLAZKOV

(Submitted to JETP editor December 2, 1955)
J. Exptl. Theoret. Phys. (U.S.S.R.) 30, 1017-1024 (June, 1956)

We have measured the cross section for inelastic scattering of neutrons of three energies: 0.3, 0.77 and 1.0 mev by the nuclei of 13 elements: uranium, bismuth, lead, mercury, wolfram, antimony, tin, cadmium, copper, nickel, iron, aluminum and sodium. For heavy nonmagic nuclei (uranium, mercury and wolfram), the cross section for inelastic scattering of neutrons with energies 0.8 and 1 mev was found to be 1-2 barns. For light and magic nuclei the cross section for these same neutrons was found to be small, of order 0.1-0.2 barns. In addition, for incident neutrons with $E_0 = 1$ mev, an estimate was made of the average energy of the inelastically scattered neutrons, and the energy levels excited were determined for some nuclei.

1. INTRODUCTION

THE investigation of the inelastic scattering of neutrons in the 0.3-1 mev energy region from nuclei of various elements has great theoretical and practical interest. Measurements of the inelastic effect are especially important for those elements which are structural materials for reactors. In addition, data from such measurements are a test of existing theoretical descriptions of nuclear structure. Unfortunately, the great experimental difficulties associated with such measurements are an obstacle to any complete investigation of the effect. Thus, up to now, too little effort has been devoted to the study of inelastic scattering, while the published results are usually very crude and often insufficiently reliable. The investigation of inelastic scattering of neutrons of energy 1 mev and below is especially difficult. For these energies there are no published data at present. The present work deals with just this energy region.

2. METHOD AND MEASURING TECHNIQUE

As sources, we used photoneutrons from Na-Be, La-Be and Na-D_2O (see Fig. 1). The inelastic effect was measured in experiments using spherical geometry, from the change in the initial neutron spectrum in the materials under study; the materials were in the form of spheres (for convenience, they consisted of two hemispheres) with diameter $D = 230$ mm, having a small cavity at the center, of diameter 50 mm for the neutron sources.

The neutrons were recorded by using nuclear recoils in a spherical ionization chamber filled with hydrogen or helium. The type of chamber used depended on the neutron energy: for La-Be and Na-Be neutrons the measurements were made with a helium chamber (volume 4 liters, pressure 3 atm), for the Na-D_2O neutrons they were done with a hydrogen chamber (volume 4 liters, pressure 1 atm). The experiments consisted in measuring the initial spectrum (from the source without scatterer) and the secondary spectrum (from the source placed at the center of the scatterer), reduced to the same time and source distance from the ionization chamber. Individual pulses from the ionization chamber were amplified in a type ULZD proportional amplifier and recorded by a twenty channel

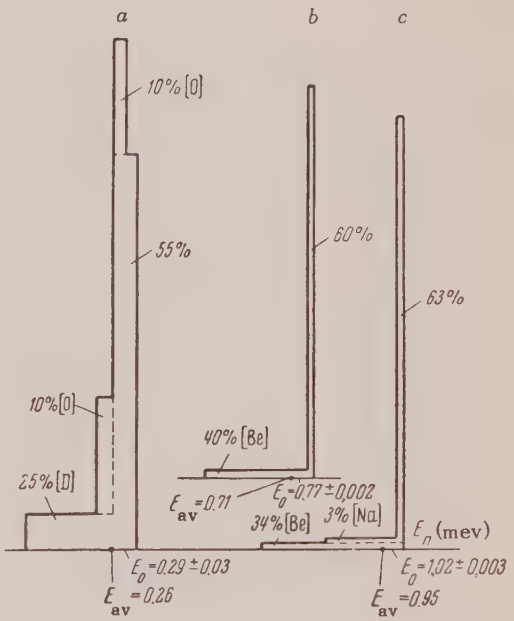

FIG. 1. Neutron spectrum from spherical sources: *a*--Na-D_2O, *b*--La-Be, *c*--Na-Be, used in the present work. The last two sources are especially monochromatic. We give, in percent, the fraction of the neutrons which suffer a single elastic scattering in the source itself, for each of the source materials.

* This work was completed in 1953-1954. The results were reported at the Geneva International Conference on Peaceful Uses of Atomic Energy.

analyzer. The duration of each measurement was 30-60 minutes, during which time we obtained 900-1000 pulses per channel.

To reduce the results to the initial activity, additional time was added to the duration of each successive measurement to correct for the decay of the source, using the fact that the half life for Na^{24} is 14.8 hr, for La^{140}, 42 hr. The difficulties in measurement arose mainly from the strong γ-radiation accompanying the neutrons, since the number of γ-quanta was approximately 10^5 times the number of neutrons. Therefore, the copiously formed secondary electrons which enter the gas from the walls of the chamber give rise to a large background, whose superposition on the neutron pulses causes a statistical spread in their amplitudes.

To shield the chamber from γ-radiation we placed over the scatterer and auxiliary lead shield of spherical shape and wall thickness 100 mm (which produced 100-fold attenuation).

It was shown by separate experiments that there is no inelastic scattering in lead in the energy region from 0.3 to 0.9 mev (cf. below). Therefore, the use of lead as a shield does not introduce errors into the measurements, and the spectrum of the source surrounded by only the lead shield may be taken to be the primary spectrum. Another method which was used to separate the neutron pulses from the background of secondary electrons was the introduction into the amplifier circuit of a differentiating network with low RC, equal to 3 microseconds.

3. CONSTRUCTION AND OPERATION OF THE SPHERICAL IONIZATION CHAMBER

A spherical chamber filled with pure hydrogen or helium is most effective for recording photoneutrons. Especially simple in construction is the glass spherical chamber, silvered on the inside and coated with a layer of electrolytic copper on the outside for withstanding high pressures. The advantages of the spherical chamber over other types are:

1) small capacity of the collecting electrode, of order 5-10 cm;

2) efficiency independent of the direction of incidence of neutrons;

3) optimal ratio of chamber wall surface to working volume, and consequent lower background from γ-radiation producing secondary electrons in the walls of the chamber;

4) small inductive effect, of the order of 5%, from positive ions;

5) constant effective time for electron collection, independent of place of formation of charges in the chamber.

These advantages as well as proper operation of the spherical chamber are possible only when it is filled with pure gases with 100% electron collection. Even small impurities of oxygen and water vapor lead to electron attachment which in general distorts the spectrum to be measured. For this reason, commercial hydrogen and helium were purified by passing over copper turnings heated to 300°, and tested for purity by filling a chamber and observing pulses from polonium α-particles. Only in pure gases are the amplitude and the leading edge of pulses determined by electron collection. In addition, the effective electron collection time is the same, about 10 microseconds, independent of the amount or place of formation of charge; pulses of different amplitude then differ from one another only in the slope of their leading edge. This fact enabled us to introduce into the amplifier a differentiating circuit with $RC = 3$ microseconds, a time constant which is smaller than the effective collection time for electrons. Such a network produces almost complete discrimination of pulses from background. The pulse shape is altered and the amplitude decreased, but pulses at the output of the circuit are still proportional to the input pulses.

The shape of the overall spectrum (spectrum of recoil nuclei) depends on the chamber filling. We know that the spectrum of recoils in hydrogen is uniform in energy for monochromatic incident neutrons. Unlike the case of hydrogen, the scattering of neutrons in helium is anisotropic[1,2] and preferentially fore and aft, so that the recoil spectrum rises toward the low and high energy sides. From an analysis of the spectrum of recoils in a helium chamber for various neutron energies, we were able to show that in the 0.3-1.0 mev region the distributions of recoil nuclei have a common, approximately straight portion independent of the energy of the incident neutrons. Thus, for incident neutrons with energy E_0 and scattered neutrons with energy $E < E_0$, the recoil spectra can be described in general as:

$$N_1(E) \approx (A + BE)\, n(E_0), \qquad (1)$$

$$N_2(E) \approx (A + BE) \int_E^{E_0} n(E)\, dE, \qquad (2)$$

where A and B are parameters which can be eliminated by dividing:

$$\frac{N_2}{N_1} = \int_{E}^{E_0} n(E)\, dE. \qquad (3)$$

The spectrum of scattered neutrons is obtained by differentiating Eq. (3):

$$n(E) = -\frac{d}{dE}(N_2 / N_1). \qquad (4)$$

One can see from Figs. 2 and 3 that the anisotropy of scattering in helium is especially large for energy $E_0 \approx 1$ mev, for which the ratio of maximum to minimum in the recoil spectrum amounts to 2:1 and the effect to be measured is, as a result, more strongly emphasized. On the other hand, in the low energy region $E_0 = 0.2$-0.3 mev the helium chamber does not have these advantages, and it is therefore more convenient to use a hydrogen chamber as neutron detector.

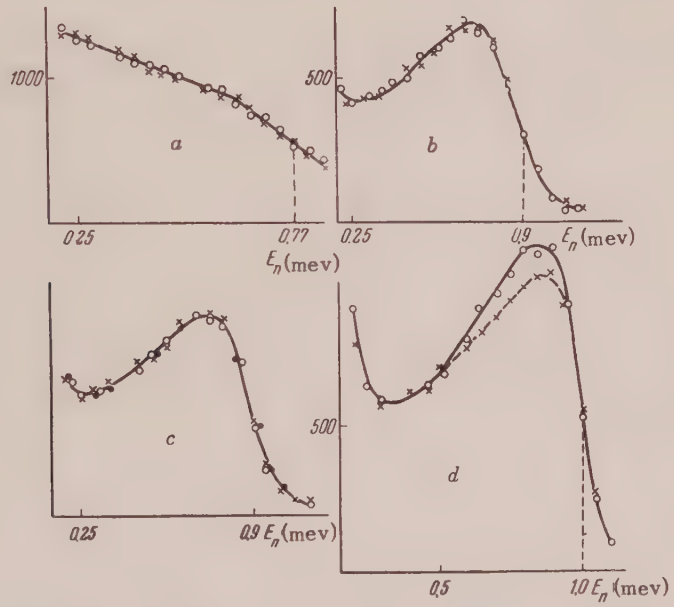

FIG. 2. Spectra of lead and bismuth. a--H_2-chamber, b,c,d--He-chamber; curves a,b,d taken with Pb (crosses) and Bi (circles); curve c taken only with Pb for varying thicknesses: 150, 190, 230 mm. In the region above 0.9 mev we observe inelastic scattering in lead corresponding to an energy level $E = 550 \pm 50$ kev.

4. CHARACTERISTICS OF THE PHOTONEUTRON SOURCES

The energy of the photoneutrons is determined by the energy of the γ-ray and by the threshold energy as follows:

$$E = \frac{A-1}{A}(E_\gamma - Q) + \delta. \qquad (5)$$

Here δ is the small spread in neutron energies depending on the angle between the directions of the neutron and γ-ray

$$\delta = E_\gamma(\cos\theta)\left[\frac{2(A-1)(E_\gamma - Q)}{931A^3}\right]^{1/2} \approx (0.1-1\%)\, E_\gamma. \qquad (6)$$

In principle, one can obtain neutrons which are almost homogeneous in energy, with a small spread $\delta = \pm(0.1$-$1\%)E_\gamma$. If we assume[3] $E_\gamma(\mathrm{Na}) = 276$ mev, $E_\gamma(\mathrm{La}) = 2.49$ mev, $Q(\mathrm{Be}) = 1.63$ mev and $Q(\mathrm{D}) = 2.18$ mev, then the maximum energies of photoneutrons as given by Eqs. (5) and (6) for each source are, respectively, equal to the quantities given in Table I. However, because of the slowing down of the neutrons in the sources themselves, the spread in energy, Δ, can reach several percent. For a spherical (Na-Be)-source, made up of two concentric spheres--the inner one 30 mm in diameter containing 13 gm of sodium, and the outer one a hollow sphere of beryllium with wall thickness 10 mm, it can be shown that 34% of all the neutrons are scattered once in the beryllium,

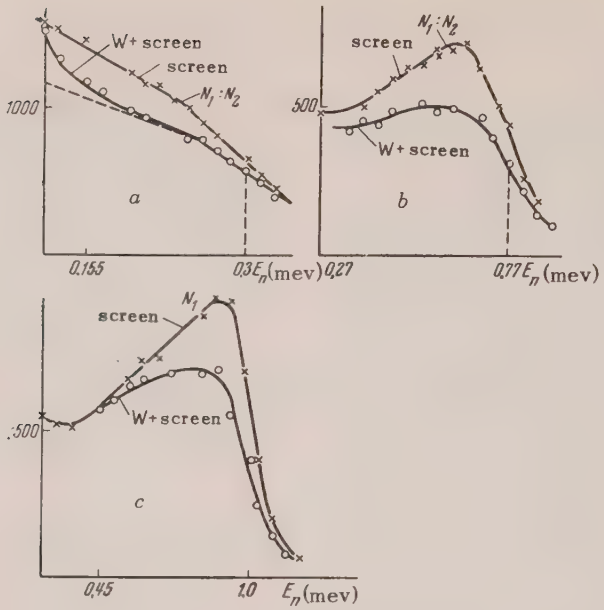

FIG. 3. Wolfram spectrum. *a*--H_2-chamber, *b* and *c*--He-chamber. *a*--Na-D_2O, *b*--La-Be, *c*--Na-Be. Inelastic scattering is observed at all energies. In particular, for $E = 0.3$ mev only the first level at 145 ± 20 kev is excited.

TABLE I

Source	E_0 in mev	Spherical		Cylindrical	
		E_{av} in mev	Δ in %	E_{av} in mev	Δ in %
Na — Be	1.02±0.003	0.95	5	0.80	20
La — Be	0.77±0.002	0.71	8	0.62	20
Na — D_2O	0.29±0.03	0.26	10	0.22	33

and 3% in the sodium, while the remaining 63% of the primary neutrons with energy $E_0 = 1$ mev emerge without being scattered. From these data, we can construct the neutron spectrum, and obtain from it the average neutron energy E_{av} (cf. Fig. 1). Table I gives the characteristics of the spherical sources used in the present work, and includes, for comparison, the characteristics of the cylindrical sources with which Wattenberg and Hughes worked[3,4]. As one sees, the spherical sources are more monochromatic. Moreover, for the first two sources, Na-Be and La-Be, the homogeneity is so great that we can, for practical purposes, take as the effective energy the maximum energy E_0 which is 1.0 mev for the Na-Be source and 0.77 mev for the La-Be source.

5. RESULTS OF MEASUREMENTS AND CALCULATION OF σ_{in}

Assuming that because of inelastic scattering the number of neutrons with the initial energy E_0 decreases exponentially (to be more precise, in cases where the inelastic effect is large as in uranium, mercury and wolfram, we must correct l for the inelastic scattering itself),

$$N_2(E_0) = N_1(E_0)\, e^{-nl\sigma}, \tag{7}$$

from which we can obtain a formula for computing σ_{in}

$$\sigma_{in} = (1/nl) \ln (N_1/N_2), \tag{8}$$

where N_1/N_2 is the ratio of the number of pulses in the primary and secondary recoil spectra, respectively, with energy E_0, and l is the mean distance traversed by the neutrons in the scatterer, calculated in the diffusion approximation (where we neglect the volume of the cavity in which the neutron source is located),

$$l = \frac{R_1^2}{2\lambda_1} + \frac{R_1^2}{\lambda_2} - \frac{R_1^3}{\lambda_2 (R_2 + 0.7\lambda_2)}. \quad (9)$$

R_1 and λ_1 are the scatterer radius and the transport mean free path in the scatterer, R_2 and λ_2 are the radius of the lead shield and the transport free path in lead.

The errors which are introduced into σ_{in} because of the use of the diffusion approximation for computing the mean distance traversed and because of the assumption of exponential attenuation of the primary spectrum are relatively small. The errors in σ_{in} because of the corrections for neutron absorption in the scatterer[4] and inelastic scattering in the lead shield are also small.

The significant errors in σ_{in} will depend mainly on the accuracy (5%) with which the primary and secondary spectra are measured, and on the accuracy (10-15%) of the published[5] values of λ. The combined errors are included in Table II.

TABLE II. Inelastic Scattering Cross Section σ_{in} in Barns

Neutron Energy, E_n	0.3 mev	0.77 mev	1.0 mev
Uranium	0.4±0.1	0.9±0.3	1.6±0.5
Bismuth	0	0	< 0.1
Lead	0	< 0.1	0.2±0.1
Mercury	0.1±0.06	0.8±0.2	1.5±0.4
Wolfram	0.4±0.2	1.3±0.4	2.6±0.8
Antimony	0	0.4±0.2	0.7±0.3
Tin	0	<0.1	0.4±0.2
Cadmium	< 0.1	0.6±0.2	1.0±0.2
Copper	0	0	0.2±0.1
Nickel	0	0	< 0.1
Iron	0	0	0.3±0.1
Aluminum	0	< 0.1	0.2±0.1
Sodium	0	< 0.2	0.4±0.2

In addition to the cross sections, whenever it was possible, we determined from the spectrum of recoils from the scattered neutrons the energies of the individual levels which were excited or the average energy of the inelastically scattered neutrons (see Table III). The determination of these energies can be done very roughly, in the most favorable case with an accuracy of 1½ channels out of 20, which amounts to 5-7% of the energy of the incident neutrons. The energies of some of the excited levels are given in the summary table, with this resolution. We determined much more poorly the mean energy of the inelastically scattered neutrons, whose spectra are not measured directly in the present experiments, but can be gotten only by graphical differentiation of the recoil spectra [in accordance with Eq. (4)], which gives a qualitative rather than a quantitative result. The low energy end of the spectrum of inelastically scattered neutrons is determined especially poorly, so that we used the convention of setting the average energy equal to the "median", i.e., the energy above and below which half the recoils occur.

For example, in Fig. 2 are given the results of measurements made with lead and bismuth. It is apparent that for three of the energies--0.3, 0.77 and 0.9 mev, the recoil spectra for lead and bismuth coincide completely within the limits of error of the experiments, so that we may assume that absorption and inelastic scattering of neutrons with energy below 0.9 mev does not exceed 0.1 barns. In the region above 0.9 mev (for neutron energy 1 mev) appreciable inelastic scattering is observed in lead: the lead spectrum runs lower over the whole interval from $E_0 = 1$ mev to $E = 0.45$ mev. Thus, we observe a drop in energy equal to 550 ± 50 kev, which agrees well with the known energy[6] 0.6 mev of the first level in Pb^{207}. The ratio

TABLE III

Neutron Energy, E_n	0.3 mev	0.77 mev	1.0 mev
Uranium	—	$E_{av} = 350$	$E_{av} = 500$
Bismuth	—	—	—
Lead	—	—	$E = 550 \pm 50$
Mercury	$E > 200$	$E_{av} = 300$	$E_{av} = 400$
Wolfram	$E = 145 \pm 20$	$E_{av} = 400$	$E_{av} = 550$
Antimony	—	$E_{av} = 430$	$E_{av} = 450$
Tin	—	—	$E > 800$
Cadmium	—	$E_{av} = 300$	$E_{av} = 400$
Copper	—	—	$E > 800$
Nickel	—	—	—
Iron	—	—	$E = 800$
Aluminum	—	—	$E = 400 \pm 50$
Sodium	—	—	$E = 440 \pm 50$

Note: E is the energy, in kev, of individual levels excited by inelastic scattering of neutrons; E_{av} is the average energy, in kev, of the inelastically scattered neutrons.

$N_1/N_2 = 1.1$ is determined directly from the curves. Then, neglecting the absorption ($\sigma_c = 20$ millibarns), we get

$$\sigma_{in} = \frac{1}{nl} \ln 1.1 = 0.2 \pm 0.1 \text{ barn},$$

where $n = 0.33 \times 10^{24}$ nuclei/cm^3 and $\overline{l} = 14.7$ cm.

As another example, Fig. 3 gives the results for wolfram. The scatterer consisted of two hemispheres with $D = 220$ mm, filled with powdered wolfram having a density $\rho = 5.47$ gm/cm^3. It is apparent that for incident neutrons with $E_0 = 0.3$ mev the primary and secondary spectra from the hydrogen chamber differ considerably. About 25% of the secondary spectrum is shifted by more than 100 kev, i.e., some of the neutrons have suffered an inelastic energy loss in the wolfram. A rough estimate shows that only one level, the first excited state with energy $E = 145 \pm 20$ kev, has been excited.

The ratio $N_1/N_2 = 1.25$ was found. Then, eliminating the absorption ($\sigma = 0.09$ barns), we get

$$\sigma_{in} = \frac{1}{nl} \ln 1.25 - 0.09 = 0.4 \pm 0.2 \text{ barn},$$

where $n = 0.018 \times 10^{24}$ nuclei/cm^3 and $l = 24$ cm.

The measurements for incident neutrons with $E_0 = 0.77$ mev were carried out with a helium chamber. The ratio $N_1/N_2 = 1.45$ was found. Neglecting absorption ($\sigma_c = 10$ millibarns), and correcting l for inelastic scattering, we find

$$\sigma_{in} = \frac{1}{nl} \ln 1.45 = 1.3 \pm 0.4 \text{ barn}$$

where $n = 0.018 \times 10^{24}$ nuclei/cm^3 and $\overline{l} = 16$ cm. An estimate of the average energy of the inelastically scattered neutrons gives $E_{av} \approx 400$ kev. The measurements for incident neutrons with $E_0 = 1$ mev were also done with a helium chamber. The ratio N_1/N_2 was 1.4. A factor of 1.1 must be applied to this ratio to correct for inelastic scattering in the shield ($\sigma_{in} \approx 200$ millibarns). Then, neglecting absorption and correcting l for inelastic scattering we get

$$\sigma_{in} = \frac{1}{nl} \ln 1.4 \cdot 1.1 = 2.6 \pm 0.8 \text{ barn}$$

where $l = 11$ cm. A rough estimate of the average energy gives $E_{av} = 550$ kev.

In conclusion, the authors thank A. I. Leipunskii for general guidance and interest in the work.

[1] T. A. Hall and P. G. Koontz, Phys. Rev. **72**, 196 (1947).

[2] R. K. Adair, Phys. Rev. **86**, 155 (1952).

[3] Elliott, Deutsch and Roberts, Phys. Rev. **63**, 386 (1943); A. Wattenberg, Phys. Rev. **71**, 497 (1947).

[4] D. J. Hughes and C. Eggler, Phys. Rev. 72, 902 (1947).

[5] Barschall, Manley and Weisskopf, Phys. Rev. 72, 875 (1947); H. Feshbach and V. Weisskopf, Phys. Rev. 76, 1550 (1949); M. Walt and H. Barschall, Phys. Rev. 93, 1062 (1954).

[6] J. A. Harvey, Phys. Rev. 81, 353 (1951).

Translated by M. Hamermesh
215

Letters to the Editor

The Two-Dimensional Schrödinger Equation and Representations of the Group of Plane Motions

E. L. KONSTANTINOVA AND G. A. SOKOLIK
P. N. Lebedev Physical Insitute, Academy of Sciences, USSR
(Submitted to JETP editor July 8, 1955)
J. Exptl. Theoret. Phys. (U.S.S.R.) 30, 430-431 (February, 1956)

WE have found the irreducible unitary infinite-dimensional representations of the group of plane motions. The infinitesimal operators of the representations, $H_+ = iA_1 - A_2$, $H_- = iA_1 + A_2$, $H_3 = iA_3$ satisfy the commutation relations

$$[H_+H_-] = 0;\ [H_\pm H_3] = -H_\pm,\ [H_-H_3] = H_- \quad (1)$$

where

$$A_1 = -\partial/\partial x,\ A_2 = -\partial/\partial y,\ A_3 = -x\partial/\partial y + y\partial/\partial x.$$

In the infinite basis of the normalized eigenvectors f_m of H_3 the operators H_+, H_-, H_3 are given by matrices of the following form:

$$H_+ = \begin{pmatrix} \ddots & \ddots & \ddots & \ddots \\ \ddots & 0 & 0 & \ddots \\ \ddots & \beta & 0 & \ddots \\ \ddots & 0 & \beta & \ddots \\ \ddots & \ddots & \ddots & \ddots \end{pmatrix}$$

$$H_- = \begin{pmatrix} \ddots & \ddots & \ddots & \ddots \\ \ddots & \beta & 0 & \ddots \\ \ddots & 0 & \beta & \ddots \\ \ddots & \ddots & \ddots & \ddots \end{pmatrix} \quad (2)$$

$$H_3 = \begin{pmatrix} \ddots & \ddots & \ddots & \ddots \\ \ddots & m-1 & 0 & \ddots \\ \ddots & 0 & m & \ddots \\ \ddots & \ddots & 0 & \ddots \\ \ddots & \ddots & \ddots & \ddots \end{pmatrix}$$

The weight β of the representation is given by an equation of second order

$$\Delta f_m^\beta + \beta^2 f_m^\beta = 0, \quad (3)$$

where Δ is the scalar operator of the group (Laplace operator) commuting with all operators of the representations.

We realize the representation we have obtained in function space. For this purpose we write H_+, H_-, and H_3 in polar coordinates:

$$H_+ = e^{i\varphi}\left\{-i\frac{\partial}{\partial r} + \frac{1}{r}\frac{\partial}{\partial\varphi}\right\};$$

$$H_- = e^{-i\varphi}\left\{-i\frac{\partial}{\partial r} - \frac{1}{r}\frac{\partial}{\partial\varphi}\right\};\ H_3 = -i\frac{\partial}{\partial\varphi}.$$

Then Eq. (2) takes the form:

$$\frac{\partial^2 f_m^\beta}{\partial r^2} + \frac{1}{r^2}\frac{\partial^2 f_m^\beta}{\partial\varphi^2} + \frac{1}{r}\frac{\partial f_m^\beta}{\partial r} + \beta^2 f_m^\beta = 0. \quad (4)$$

From Eqs. (2) and (4) it follows that $f_m^\beta(r,\varphi) = e^{im\varphi}R_m^\beta(r)$, where R_m^β satisfies Bessel's equation

$$\left[\frac{1}{r}\frac{d}{dr}\left(r\frac{d}{dr}\right) + \left(\beta^2 - \frac{m^2}{r^2}\right)\right]R_m^\beta(r) = 0. \quad (5)$$

From the form of the matrices (2) one can obtain the well-known recurrence relations for Bessel functions[1].

Thus if the representations of the rotation group are realized in the space of spherical functions[2], then the representations of the group of plane motions are realized in the space of Bessel functions. It is easy to see that in the representations we have obtained maximal vectors are absent, in consequence of which the weight β of a representation is not connected with m. An analogous situation occurs in the theory of the representations of the Lorentz group, in the case of the unitary representations. In the latter case of the two numbers giving a representation, that one k_1 which for finite-dimensional representations gives the maximum value of the moment k is not connected with k in the infinite-dimensional case[3]. The problem of decomposing the Kronecker product $R_{\beta_1} \times R_{\beta_2}$ of irreducible representations of the group of plane motions into irreducible representations is solved by the reduction to diagonal form of the operator Δ, written in the basis $f_{m_1} g_{m_2}$[4].

The results obtained are of interest in the investigation of the isotropy of a quantum-mechnical Hamiltonian in the plane

$$\hat{H} = -(\hbar^2/2\mu)(\partial^2/\partial x^2 + \partial^2/\partial y^2) + U(x, y).$$

The condition of isotropy can be written in the form $[A_i, H] = 0$. We note that the components of the quantum-mechanical angular momentum coincide with A_i for $Z = \text{const}$. Using Eqs. (2) and (4), one can carry out a classification of the quantum states of a two-dimensional system according to the representations of the group of plane motions, by expanding the Ψ-function in terms of Bessel functions. Since all of the representations we have found are irreducible, the quantum states of the system turn out to be nondegenerate. Thus β appears as a new quantum number, giving the state of a two-dimensional quantum-mechanical system.

In conclusion, we regard it as our pleasant duty to express gratitude to M. L. Tsetlin and F. A. Ermakov for fruitful discussions.

[1] E. Jahnke and F. Emde, *Tables of Functions.*

[2] I. M. Gel'fand and Z. Ia. Shapiro, Usp. Matemat. Nauk 7, 3 (1952).

[3] I. M. Gel'fand and A. M. Iaglom, J. Exptl. Theoret. Phys. (U.S.S.R.) 18, 703 (1948).

[4] G. A Sokolik, J. Exptl. Theoret. Phys. (U.S.S.R.) 28, 13 (1955); Soviet Phys. JETP 1, 9 (1955).

Translated by W. H. Furry
85

Radiographic Study of X-Ray Photoelectric Emission

S. KARAL'NIK, N. NAKHODKIN AND L. MELESKO
Kiev State University

(Submitted to JETP editor January 24, 1955)
J. Exptl. Theoret. Phys. (U.S.S.R.) 30, 780-781
(April, 1956)

A RADIOGRAPHIC method has been applied to the study of the dependence of x-ray photoelectric emission on the atomic number of an element. We used a variant of the "reflection" method[1,2] in the arrangement described below. Samples of various substances were carefully ground and polished. Then a few chosen samples were spread out on a glass plate and paraffin was poured over them. When the paraffin had cooled, the glass plate was removed. This procedure gave a block of samples, the upper surfaces of which were located in a single plane. This block was then pressed against the light-sensitive surface of a photographic plate, placed in an aluminum cassette and the entire system was placed in a beam of hard x-rays (~200 kv) in such a way that the x-rays passed through the photographic plate and fell on the surfaces of the samples which were pressed against the photographic emulsion. Due to the great penetrability of hard x-rays, short exposures do not produce appreciable blackening of the emulsion. On the other hand, the photoelectrons and the secondary electrons ("reflected") connected with them produce a significant blackening, which is especially noticeable when electron-sensitive photographic plates are used.

The blackening of the photographic plate was comparatored (on a microphotometer of type MF-2) at various places in the neighborhood of each of the impressed samples, and the previously measured background blackening was subtracted. Graphs indicated that the blackening of the photographic plate approached the straight line region of the blackening curve.

The following combinations of substances were studied:

1) Cr, Mn, Fe, Co, Ni, Cu, Zn, Ga, Ge, Se;
2) Mo, Pd, Ag, Cd, Sn, Sb;
3) Ta, W, Pt, Au, Hg, Pb, Bi;
4) Cu, Ag, Au;
5) Zn, Cd;
6) Si, Sn, Pb;
7) Cr, Se, Mo, W;
8) Ni, Pd, Pt.

1)-3) are "horizontal" groups, while 4)-8) are "vertical" groups. In other words, in the first case the block of specimens is made up of elements which increase in atomic number as one goes along a period of the Mendeleev chart, while in the second case the block is made up of elements from a single group of the periodic system. Some of the results of the measurements are given in the accompanying figures (the atomic number of the radiator-element is plotted as abscissa and the blackening, in relative units, is plotted as ordinate.

It is clear from Fig. 1 that the blackening, which characterizes the intensity of emission of photoelectrons and secondary electrons, increases almost linearly with increase in atomic number, as has already been pointed out in the literature[1,2] Figure 2 shows that there is a sharp decrease in the intensity of the electron emission when one passes from the elements of the first group to those of the second. This result occurs for a transition from copper to zinc, from silver to cadmium, etc., that is, for elements such that

the outer shell of electrons becomes filled (transition from $3d^{10}4s^1$ in copper to $3d^{10}4s^2$ in zinc, and so forth).

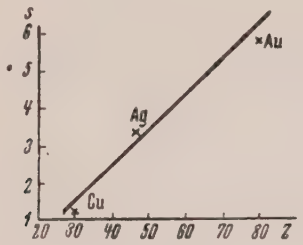

FIG. 1

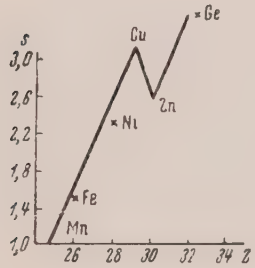

FIG. 2

The experiments performed allow us to draw some conclusions as to the mechanism of the phenomenon. X-ray quanta with an energy of the order of 200 kev knock electrons from the K-shells of the various atoms and give them high energies. The appearance of secondary electrons is due to the fast electrons. Actually it is difficult to picture to oneself how the filling of the external electron shells could play any part in the x-ray photoeffect for quantum energies of about 200 kev, whereas the structure of the external shells plays an essential role in secondary emission[3,4]; when the external shell of the atom is filled, the probability of ionization of the atom is decreased (Fig. 2). This is supoorted by the fact that the blackening of the photographic plate grows almost linearly with increase in atomic number, and is not proportional to Z^5, as might have been expected from the fact that the effective cross section for absorption of x-rays and production of photoelectrons is proportional[5,6] to Z^5.

[1] A. K. Trapeznikov, Zavodskaia Lab. 8 (1947).

[2] Jean-Jacques Trillat, J. Appl. Phys. 19, 844 (1948).

[3] E. J. Sternglass, Phys. Rev. 95, 345 (1954).

[4] N. G. Nakhodkin, *Theses of the Report of the Tenth Scientific Conference of the Kiev State University*, Kiev, 1953.

[5] M. A. Blokhin, *Physics of X-Rays*, 1953.

[6] W. Heitler, *The Quantum Theory of Radiation*, Oxford.

Translated by M. Gibbons
153

The θ-Meson and the Fermi-Yang Hypothesis

V. I. KARPMAN
Minsk Institute

(Submitted to JETP editor January 30, 1956)
J. Exptl. Theoret. Phys. (U.S.S.R.) **30**, 781-782
(April, 1956)

IN the literature one meets with suggestions that the θ-meson can be considered, in the light of the Fermi-Yang hypothesis,[1] as a composite particle consisting of a nucleon and anti-hyperon (or hyperon and anti-nucleon) in the bound state[2,3]. A few considerations in connection with this concept are set forth below.

1. What spin should the θ-meson possess for this representation? Let us consider the θ-meson as consisting of a nucleon and a $[\Lambda^0]$ particle (the brackets here and henceforth indicate the anti-particle).

Experiments made in the course of studying the correlation between the planes of production and of decay of the hyperons[4,5] indicate that the spin of the hyperon, in all probability, is not less than 3/2. Let us assume that the Λ^0-particle has a spin of 3/2. If one now considers a system of two particles with spin 1/2 and 3/2 existing in a bound state, as pictured by Fermi and Yang[1], then one can show that the normal state of this system has the form $^3S_1$ and has a total angular momentum of 1, that is, the θ-meson appears as a vector particle. This is in complete accord with the decay scheme: $\theta \to 2\pi$ (see, for example, Ref. 6).

If we allow the spin of the Λ^0-particle to be greater than 3/2, then the spin of the θ-meson can be greater than 1. To date no angular correlations have been obtained which would confirm a greater spin for the θ-meson; however, the statistics of these experiments are quite inadequate[4].

As for the isotopic spin of the θ-particle, the model under consideration predicts a half-integral value, consistent with an isotopic spin of 0 for the Λ^0-particle[4]. In addition, the anti-particles

$[\theta^0] = ([n] + \Lambda^0)$ and $[\theta^+] = ([p] + \Lambda^0)$ correspond to the doublet $\theta^0 = (n + [\Lambda^0])$ and $\theta^+ = (p + [\Lambda^0])$ [2].

2. At present, in addition to the Λ^0 hyperon, there exist the hyperon $\Sigma^{\pm}$ and, to all appearances, Σ^0 [4,7] with a mass $\sim 2370\, m_e$, all of which decay into a nucleon and a π-meson. It is natural to consider them as forming an isotopic triplet*. Assuming that these hyperons are excited nucleons, it is natural, in the light of the Fermi-Yang hypothesis, to permit the existence of heavy mesons, each consisting of a system of a nucleon and a $[\Sigma]$. We shall label these hypothetical particles as θ_1. The isotopic spin of the θ_1 particle can be 1/2 or 3/2.

If the difference in mass between the θ_1- and θ-particle exceeds the π-meson mass, then the interaction in which the isotopic spin is directly conserved and which is strong, according to the Gell-Mann scheme [2], leads to the decay $\theta_1 \to \theta + \pi$ with an extremely small lifetime ($\sim 10^{-22}$ sec). (We assume that no "unexpected" exclusion rules exist here.)

If the difference in mass between θ_1 and θ is smaller than the π-meson mass, then an electromagnetic interaction which conserves the Z component of the isotopic spin induces, practically instantaneously, a decay of the form $\theta_1 \to \theta + \gamma$ (analogous to the decay $\Sigma^0 \to \Lambda^0 + \gamma$ [4,7]). Only the θ^{++}-particle may be "stable" (in the case that the isotopic spin of θ_1 equals 3/2 and the emission of a π-meson is forbidden by the energetics).

Note added in proof: After the communication of this letter, the author learned that M.A. Markov[8] considered particles analogous to the θ_1-particle.

* We are not considering the "cascade" hyperon $^-\Xi(\Xi^- \to \Lambda^0 + \pi^-)$ since at present there are no experimental data which permit one to make definite conclusions concerning the isotopic spin of Ξ.

[1] E. Fermi and C. Yang, Phys. Rev. **76**, 1739 (1949).

[2] M. Gell-Mann, Phys. Rev. **92**, 833 (1953).

[3] M. A. Markov, Dokl. Akad. Nauk SSSR **101**, 451 (1955).

[4] W. B. Fowler, R. P. Shutt, et al., Phys. Rev. **98**, 121 (1955).

[5] J. Ballam, A. L. Hodson et al., Phys. Rev. **97**, 245 (1955).

[6] I. C. Shapiro, J. Exptl. Theoret. Phys. (U.S.S.R.) **27**, 257 (1954).

[7] W. Walker, Phys. Rev. **98**, 1407 (1955).

[8] M. A. Markov, *The Systematics of Elementary Particles*, Academy of Sciences Press, Moscow, 1955.

Translated by A. Skumanich
154

Production of a Nuclear Star and π-Meson by a Gamma Photon

IU. A. VDOVIN
Physico-Engineering Institute, Moscow
(Submitted to JETP editor November 26, 1955)
J. Exptl. Theoret. Phys. (U.S.S.R.) 30, 782-783
(April, 1956)

POMERANCHUK has considered [1] the production of a π-meson pair by a collision between a γ-photon and a nucleus where, in the final state, there was a π-meson pair while the nucleus suffered only a slight recoil. In the present work a process is considered in which one of the mesons of the resulting π-meson pair is absorbed within the struck nucleus and produces a nuclear "star". Thus, one has an unusual mechanism for the creation of nuclear "stars" by γ-photons where, in the final state, one also has a fast π-meson which carries off energy of the order of the total energy of the star. All considerations are ultra-relativistic and only the small angles between the γ-photon momentum and the emitted π-meson momentum play an essential role. For these conditions on the indicated process, distances greater than the dimensions of the nucleus play the same role as in the formation of a free π-meson pair [1,2]. This follows from a consideration of the corresponding integrals and is tied in with the small longitudinal transfer of momentum to the nucleus in the process of pair formation (from the uncertainty relation $\Delta r_{\parallel} \simeq h/\Delta p_{\parallel}$).

The intense interaction of the π-mesons with nuclei implies that the nucleus can be considered, in the first approximation, as "absolutely black" as regards π-mesons.

In this process the absorbed meson exists in the same condition as in the process of γ-photon emission where a meson is absorbed by a nucleus. This process was studied by Landau and Pomeranchuk [3] by a suitably constructed Green's function and by an approximate solution of the corresponding wave equation. An analysis of their resulting expressions indicated, however, that the process can be studied with the aid of a radiation

transition matrix element in which the absorbed meson is represented as a spherical wave converging on an arbitrary point of the nucleus and the square of the modulus of the matrix element must be integrated across the nucleus cross section. Consequently, we shall represent the meson absorbed in our process by a converging spherical wave.

The matrix element has the form

$$M = \frac{e}{i}\sqrt{\frac{2\pi}{\omega}}\int [\psi_1^*(j\nabla)\,\psi_2^* - \psi_2^*(j\nabla)\,\psi_1^*]\,e^{i\vec{\omega}\mathbf{r}}dr \quad (1)$$

($\hbar = c = 1$) where ω is the γ-photon frequency and j is its polarization. Let us apply index 2 to the free meson which we describe by a plane wave plus a converging wave diffracted by the "absolutely black" nucleus[1]

$$\psi_2 = \frac{1}{\sqrt{2E_2}}\left[e^{ip_2\mathbf{r}} + \frac{p_2}{2\pi i}\int\frac{e^{-ip_2|\mathbf{r}-\mathbf{s}_2|}}{|\mathbf{r}-\mathbf{s}_2|}d\mathbf{s}_2\right], \quad (2)$$

where E_2 and $\mathbf{p}_2$ represent the energy and momentum of the escaping meson, $E \gg \mu$. The integration over $\mathbf{s}^2$ is carried over a circle of radius R perpendicular to $\mathbf{p}_2$ and passing through the nucleus center; πR^2 is the cross section for all inelastic collisions between the π-meson and the nucleus. Furthermore,

$$\psi_1 = \frac{\sqrt{p_1}}{4\pi^{3/2}}\frac{e^{-ip_1|\mathbf{r}-\mathbf{s}|}}{|\mathbf{r}-\mathbf{s}|} = \frac{\sqrt{p_1}}{8\pi^{7/2}}\int\frac{e^{-i(\mathbf{q},\,\mathbf{r}-\mathbf{s})}}{q^2 - p_1^2 + i\varepsilon}\,d\mathbf{q}, \quad (3)$$

$$\varepsilon \to 0$$

where the normalization is so chosen that the differential cross section for the process has the form

$$d\sigma_j(p_2, \mathbf{k}_2) = 2\pi\int |M|^2\,d\mathbf{s}\,|F|^2(2\pi)^{-3}dp_2 d\mathbf{k}_2. \quad (4)$$

Here $\mathbf{k}_2$ is the transverse momentum of the escaping π-meson, $\omega\cdot\mathbf{k}_2 = 0$ and F is a constant (form-factor) which allows for the possibility of a nonlocal interaction of the π-particles with the nuclear background[1-3]. Comparison of the theoretical conclusions with experimental facts will permit one to specify this constant, which is of great interest to the theory.

Thus, the outlined method is based on a very strong interaction between the mesons and the nucleons while the interaction with the electromagnetic field is considered in the first approximation of perturbation theory. It has proved possible to carry out the calculation for heavy nuclei, i.e., $\mu R \gg 1$, where μ is the rest mass of the meson. For the differential cross section we have,

$$d\sigma_j(p_2, \mathbf{k}_2)$$

$$= \frac{e^2}{2\pi^2}\frac{E_2(\omega - E_2)}{\omega^3}R\frac{1}{\mu\eta^2\sqrt{1+\eta^2}}\left\{E(\varepsilon)\left(\frac{\cos^2\varphi}{1+\eta^2} - \sin^2\varphi\right)\right.$$

$$\left. + K(\varepsilon)\left(\frac{\eta^2-1}{\eta^2+1}\cos^2\varphi + \sin^2\varphi\right)\right\}|F|^2\,dE_2 d\vec{\eta}, \quad (5)$$

where $\vec{\eta} = k_2/\mu$; $\epsilon^2 = \eta^2/(1+\eta^2)$; $\mathbf{k}_2 = k_2\cos\varphi$; $d\vec{\eta} = \eta d\eta d\varphi_\eta$; K and E are the complete elliptical integrals of the first and second kind, respectively.

Averaging of the polarization of the γ-photon we obtain

$$d\sigma(E_2, \mathbf{k}_2) = \frac{e^2}{4\pi^2}\frac{E_2(\omega - E_2)}{\omega^3}R\frac{1}{\mu(1+\eta^2)^{3/2}} \quad (6)$$

$$\times\,(2K(\varepsilon) - E(\varepsilon))\,|F|^2\,d\vec{\eta}dE_2.$$

From Eq. (6) it is evident that the effective $\eta \sim 1$, i.e., the effective angles $\theta \sim \mu/E_2$. The form-factor F can be determined by comparing Eq. (6) with experimental data.

We note that, even though the total cross section appears small compared to the nucleus, the differential cross section for small angles has larger values for greater E_2. Thus for $\eta = 1$, the differential cross section equals

$$d\sigma/d\vartheta dE_2 = e^2E_2(\omega - E_2)\,\omega^{-3}(E_2^2/\mu^2)(R/\mu). \quad (7)$$

For larger values of E_2 the factor E_2^2/μ^2 can compensate for the small factor e^2.

One can integrate, if one sets $F = 1$, Eq. (6) over E_2 and η. Performing the integration with η varying from 0 to some $\eta_{max} \sim 1$, we obtain

$$\sigma = (e^2/12\pi)(R/\mu)\,\Phi(\eta_{max}); \quad (8)$$

$$\times\Phi(\eta_{max}) = \int_0^{\eta_{max}}\left[2K\left(\frac{\eta}{\sqrt{1+\eta^2}}\right)\right.$$

$$\left. - E\left(\frac{\eta}{\sqrt{1+\eta^2}}\right)\right]\frac{\eta d\eta}{(1+\eta^2)^{3/2}}. \quad (9)$$

The value of η_{max} is defined by the fact that we have neglected the form-factor and also by the fact that all considerations are applicable for small angles.

The total cross section does not depend upon the photon energy and is proportional to R/μ rather than R^2, i.e., the periphery of the nucleus with a

width of $1/\mu$ enters into the cross section. This circumstance is due to the wave properties of the π-mesons. Actually, in the region effective for the process (in front of the nucleus) the ψ-function of the escaping meson has a shadow and the entire process is determined within the region of the penumbra.

If we set $\eta_{max} = \infty$, then

$$\sigma = (\pi/32) e^2 R/\mu \sim 10^{-28} \text{ cm}^2. \quad (10)$$

The preceding considerations were based on a specific model of the nucleus, viz., an "absolutely black" sphere of radius R. Employing a method developed in Ref. 2, one can generalize the problem to any arbitrary law of interaction between π-mesons and nucleons. The correction for semi-transparency which occurs for the case of strong absorption by heavy nuclei is of the order of $1/\mu R$ to the cross section for "black" nuclei.

The author expresses his sincere gratitute to I. Ia. Pomeranchuk for his valuable advice and continuing interest in this work.

[1] I. Ia. Pomeranchuk, Dokl. Akad. Nauk SSSR 96, 265, 481 (1954).

[2] Iu. A. Vdovin, Dokl. Akad. Nauk SSSR 105, 947 (1955).

[3] L. D. Landau and I. Ia. Pomeranchuk, J. Exptl. Theoret. Phys. (U.S.S.R.) 24, 505 (1953).

Translated by A. Skumanich
155

Contribution to the Theory of Reactions Involving Polarized Particles

A. M. Baldin and M. I. Shirokov
P. N. Lebedev Physical Institute, Academy of Sciences, USSR

(Submitted to JETP editor December 6, 1955)
J. Exptl. Theoret. Phys. (U.S.S.R.) 30, 784-785 (April, 1956)

THE general theory of the correlation phenomena which depend on the law of conservation of the total angular momentum has been considerably developed in Refs. 1-3.

We have obtained the tensor momenta (see the determination below) for the two body problem in the most general case, when the incident and scattered particles and the particles of the target are in arbitrary spin states (for example, polarized).

The diagonality of the S-matrix with respect to the total impulse, total energy E, total angular momentum J and its projection M is made use of, and the transformation theory of Dirac[4] is applied systematically. The advantage of such an approach lies in the fact that it establishes a direct connection between its results and the conservation laws, allows errors and inexactitudes to be avoided more easily than in other approaches[2-5] and allows a direct generalization to the case of reactions involving more than two particles.

The reaction $a + b \to \Lambda + \theta$ was considered. Particles Λ and θ are in general different from a and b. All the particles have spins and rest masses not equal to zero (they could be either nuclei or "elementary" particles).

All the investigations are carried out in the center of mass system; hence, the indices of the total impulse and the diagonality with respect to them are not shown expressly.

The elements of the S-matrix have the form:

$$(i_\Lambda i_\theta s' l' \alpha' | S^{JE} | i_a i_b s l \alpha) \delta_{JJ'} \delta_{MM'} \delta(E' - E) \quad (1)$$

where the symbols are as follows: i_Λ, i_θ are the particle spins, s and s' are the total orbital angular momenta of the two particles relative to the center of mass before and after the reaction, respectively, α and α' are the remaining variables which are not specified here (for example, variables connected with the internal state of the particles). Equation (1) is an expression of the conservation laws.

Since the magnitudes expressly shown above are not directly measured, but instead the directions of motion and the projections of the spins are measured, we must obtain the elements of an S-matrix corresponding to experiment from the elements of (1). In order to do this we must first of all go from the $s'l'JM$ representation to the $s'\nu'l'\mu'$ representation (the corresponding unitary transformation is the matrix of the Clebsch-Gordan coefficients $C^{JM}_{s'\nu' l'\mu'}$), and then with the help of the transformation

$$i^l Y^*_{l'\mu'}(\vartheta_\Lambda \varphi_\Lambda) C^{s'\nu'}_{i_\Lambda \lambda i_\theta n} \quad [1]$$

go from the $l'\mu's'\nu'$ representation to the $\vartheta_\Lambda \varphi_\Lambda \lambda' n$ representation ($\vartheta_\Lambda \varphi_\Lambda$ are the spherical angles of

the vector impulse of the particle Λ in the chosen system). The right side of (1) is transformed analogously.

The initial and final states in the problems under consideration must be assigned not to wave functions but to density matrices[6] (for example, an unpolarized beam of particles must be assigned to the density matrix $\delta_{mm'}$). The density matrices of the initial and final states are connected by means of the S-matrix

$$\rho_f = S\rho_i S^+. \tag{2}$$

The average value of the operator $\hat{A}$, which operates on the spin variables, in the form of a density matrix $(m_1|\rho|m_2)$ as just described, is given by the formula

$$\overline{A} = \mathrm{Sp}\,\rho A = \sum_{m_1 m_2} (m_1 \mid \rho \mid m_2)(m_2 \mid \hat{A} \mid m_1). \tag{3}$$

If we use the Wigner-Eckart theorem[7], Eq. (3) transforms to

$$A^{q\varkappa} = (i \parallel \hat{A} \parallel i)\frac{(-1)^q}{\sqrt{2q+1}} T^q_{\varkappa}, \tag{4}$$

where

$$T^q_{\varkappa} = \sqrt{2i+1} \sum_{m_1 m_2} (-1)^{-i+m_1} C^{q\varkappa}_{i-m_1;\, i m_2} (m_1 \mid \rho \mid m_2), \tag{5}$$

so that in order to find $A^q_{\varkappa}$ directly, the magnitude of $T^q_{\varkappa}$ rather than the density matrix is needed.

The assignment of magnitudes $T^q_{\varkappa}$ completely determines the density matrix, and conversely. Equation (5) may be considered as the transformation of the density matrix from the $m_1 m_2$ representation to the q, $\varkappa$ representation.

We call the magnitudes $T^q_{\varkappa}$ the tensor momenta (compare Refs. 1 and 3).

In this new representation the corresponding transformation of the spin operator matrices takes the form

$$\hat{A}_{JM} = \frac{1}{\sqrt{2i+1}} \times \sum_{m_1 m_2} (-1)^{i+m} C^{JM}_{i-m_1;\, i m_2} (m_2 \mid \hat{A} \mid m_1). \tag{6}$$

Using Eq. (2) and carrying out the corresponding unitary transformation, we obtain from $T^{q_a q_b}_{\varkappa_a \varkappa_b}$. The magnitudes of $T^{q\Lambda q\theta}_{\varkappa\lambda\,\varkappa\theta}$ are determined in terms of

$$[(2i_\Lambda+1)(2i_\theta+1)]^{1/2} \times \sum_{m_\Lambda m'_\Lambda} (-1)^{-i_\Lambda - m_\Lambda - i_\theta - m_\theta} C^{q_\Lambda \varkappa_\Lambda}_{i_\Lambda - m_\Lambda\, i_\Lambda m'_\Lambda} \times C^{q_\theta \varkappa_\theta}_{i_\theta - m_\theta\, i_\theta m'_\theta} (\mathfrak{n}_\Lambda E_\Lambda m_\Lambda m_\theta \alpha \mid \rho \mid \mathfrak{n}_\Lambda E_\Lambda m'_\Lambda m'_\theta \alpha) \Big],$$

the matrix elements (1), the Clebsch-Gordan coefficients and the spherical harmonics, a somewhat cumbersome expression for $T^{q\Lambda q\theta}_{\varkappa\Lambda\,\varkappa\theta}$.

After simplifications, the final formula takes the form:

$$T^{q_\Lambda q_\theta}_{\varkappa_\Lambda \varkappa_\theta}(\mathfrak{n}_\Lambda, E_\Lambda, \alpha') = \sum_{q'\varkappa'} C^{q'\varkappa'}_{q_\Lambda \varkappa_\Lambda q_\theta \varkappa_\theta} \times \sum_{s_1 s_2'} [(2q_\Lambda+1)(2q_\theta+1)(2s'_1+1)(2s'_2+1)]^{1/2} \times X(i_\Lambda q_\Lambda i_\Lambda; s'_1 q' s'_2; i_\theta q_\theta i_\theta)\, T^{q'}_{\varkappa'}(\mathfrak{n}_\Lambda, E_\Lambda s'_1 s'_2 \alpha'), \tag{7}$$

where

$$T^{q'}_{\varkappa'} = \frac{\lambda_a^2}{4}[(2i_\Lambda+1)(2i_\theta+1)]^{1/2} [(2i_a+1)(2i_b+1)]^{-1/2} \sum (-1)^{q'+q+\varkappa'+\varkappa} \times [(2s_1+1)(2s_2+1)(2s'_1+1)(2s'_2+1)]^{1/2} G_{\varkappa'} \times (J_1 l'_1 s'_1; Jq; J_2 l'_2 s'_2) \times G^*_{\varkappa}(J_1 l_1 s_1; Jq; J_2 l_2 s_2)(i_\Lambda i_\theta s'_1 l'_1 \alpha \mid R^{J_1}(E) \mid i_a i_b s_1 l_1 \alpha) \times (i_\Lambda i_\theta s'_2 l'_2 \alpha' \mid R^{J_2}(E) \mid i_a l_b s_2 l_2 \alpha) D^J_{\varkappa\varkappa'}(\varphi_\Lambda, \vartheta_\Lambda, 0)\, T^q_{\varkappa}; \tag{8}$$

$$T^q_{\varkappa}(\mathfrak{n}_a, E_a, s_1, s_2, \alpha) = \sum_{q_a q_b} [(2q_a+1)(2q_b+1)(2s_1+1)(2s_2+1)]^{1/2} \times X(i_a q_a i_a; s_1 q s_2; i_b q_b i_b) \times \sum_{\varkappa_a \varkappa_b} C^{q\varkappa}_{q_a \varkappa_a q_b \varkappa_b} T^{q_a q_b}_{\varkappa_a \varkappa_b}(\mathfrak{n}_a, E_a, \alpha) \tag{9}$$

The summation Σ in Eq. (8) is to be taken over $J_1 J_2 : l'_1 l'_2 l_1 l_2 s_1 s_2 J_q$ and over $\varkappa$.

The coefficients $G_{\varkappa}$, X are determined in Refs. 3 and 8. $D^J_{\varkappa\varkappa'}(\varphi_\Lambda, \vartheta_\Lambda, 0)$ is the matrix element corresponding to the irreducible representation of the group of rotations of weight J.

The connection of our tensor momenta with the density matrix is different from the connection between the density matrix and the tensor momenta which were derived by Simon (see the corrections to Refs. 2 and 3), but when normalized they are the same. In the particular case when $q_\theta = 0$ and $q_b = 0$ our expression yields a formula which differs from Eq. (3.2) of Ref. 3 by several factors. The distinction basically depends on the difference in the definition of the tensor momenta. This distinction does not affect the final results, as compared with experiment, since a change in the definition of the tensor momenta must be accompanied by a corresponding change in the derived matrix element.

An essential factor which is needed under the summation sign Σ, as compared with Eq. (3.2) of Ref. 3, is $(-1)^{\varkappa}$.

In conclusion, we express our gratitude to Prof. M. A. Markov for his constant interest in the work. We also thank L. G. Zastavenko for his advice on a number of questions concerning the theory of representations of rotation groups.

* As has been pointed out in Ref. 5, spherical harmonics must be preceded by i^l, otherwise the result of the action of the inverse time operator will not be invariant with respect to complex angular momenta.

[1] J. M. Blatt and L. C. Biedenharn, Rev. Mod. Phys. **24**, 258 (1952)

[2] A. Simon and T. A. Welton, Phys. Rev. **90**, 1036 (1953); **93**, 1435 (1954).(errata).

[3] A. Simon, Phys. Rev. **92**, 1050 (1953); Phys. Rev. **93**, 1435 (1954) (errata).

[4] P. A. M. Dirac, *The Principles of Quantum Mechanics*, Oxford.

[5] R. Huby, Proc. Phys. Soc. (London) **A67**, 1103 (1954).

[6] D. I. Blokhintsev, *Fundamentals of Quantum Mechanics*, GTTI, 1949.

[7] G. Racah, Phys. Rev. **62**, 438 (1942).

[8] A. Arima, H. Horie and Y. Tanabe, Progr. Theoret. Phys. **11**, 143 (1954).

Translated by M. G. Gibbons
156

Scattering of Fast Neutrons by Nonspherical Nuclei. III

S. I. Drozdov

(Submitted to JETP editor December 26, 1955)
J. Exptl. Theoret. Phys. (U.S.S.R.) **30**, 786-788
(April, 1956)

In a previous communication[1] an effective cross section was calculated for the scattering of fast neutrons by a "black" nucleus having the form of an ellipse of rotation and a zero spin (even-even nucleus). In the present note these calculations are generalized to nuclei with spins different from zero (odd nuclei). In the adiabatic approximation the effective cross section is determined by the matrix element

$$f_{n'n}(\Omega) = \int d\omega \varphi^*_{n'}(\omega) f(\omega, \Omega) \varphi_n(\omega). \qquad (1)$$

The amplitude for the scattering of a neutron by a stationary nucleus is:

$$f(\omega, \Omega) = i \frac{(kb)^2}{k} \xi(\mu) \frac{J_1(t)}{t}; \qquad (2)$$

$$t = kb\theta [\xi^2(\mu) \cos^2(\Phi - \varphi) + \sin^2(\Phi - \varphi)]^{1/2},$$

where $\xi(\mu) = [z^2 + (1 + z^2)\mu^2]^{1/2}$, $z = a/b$. The quantity b is the radius of the largest circular cross section of the ellipsoid and $2a$ is the length of the axis of symmetry. The spherical angles ϑ and φ specify the direction of the axis of symmetry ω and the angles θ, Φ, the direction of scattering Ω. The polar axis of the external coordinate system is chosen to lie in the direction of the incident beam. We shall assume a strong coupling between the motion of the nucleons in the nucleus and the motion of the nuclear surface[2]. In this case the wave functions for the rotational states of the nucleus $\varphi_n(\omega)$ can be represented by the proper functions of the symmetric top*,

$$\varphi_n(\omega) = \sqrt{(2I + 1)/8\pi^2} D^I_{MK}(\omega), \qquad (3)$$

where I is the total nuclear moment, M and K are the projections onto the external axis and axis of nuclear symmetry, repsectively, and $\omega = (\varphi_1, \theta, \varphi_2)$ represents the Eulerian angles which describe the orientation of the nucleus relative to the external coordinate system. The rotational states of the nucleus are given by

$$\varepsilon_{IK} = (\hbar^2/2J)\{I(I+1) - K(K+1)\}; \quad (4)$$

$$I = K, K+1, \ldots$$

To determine the cross section for the excitation of different rotational states n' one must compute the corresponding matrix element (1). Employing Eq. (1) through (3) along with the known relation for $D^J_{MK}(\omega)$ we obtain

$$f_{n'n}(\Omega) \equiv f^{I'M'K}_{IMK}(\Omega)$$

$$= i(-1)^{M-K} e^{i(M-M')\Phi} \frac{(kb)^2}{4\pi k} \sqrt{(2I'+1)(2I+1)}$$

$$\times \sum_{\varkappa} C^{\varkappa M-M'}_{I'-M'M} C^{\varkappa 0}_{I'-KIK} \sqrt{\frac{(\varkappa - M' + M)!}{(\varkappa + M' - M)!}}$$

$$\times \int_{-1}^{1} d\mu \xi^{-}_{\varkappa}(\mu) P^{M'-M}_{\varkappa}(\mu)$$

$$\times \int_{0}^{2\pi} d\varphi \cos(M'-M)\varphi \frac{J_1(t)}{t};$$

$$t = kb\theta \sqrt{\xi^2(\mu)\cos^2\varphi + \sin^2\varphi}. \quad (5)$$

Here $C^{JM}_{jmj'm'}$ is the Clebsch-Gordan coefficient and $P^m_{\varkappa}(\mu)$ is the associated Legendre polynomial. The external axis of quantization is chosen to be in the direction of the incident beam.

The differential cross section for the excitation of the rotational state ϵ_{IK} is given by

$$\sigma^{I'K}_{IK}(\theta) = \frac{1}{2I+1} \sum_{M,M'} |f^{I'M'K'}_{IMK}(\Omega)|^2.$$

Hence, inserting Eq. (5) into this expression and employing the known relations for the Clebsch-Gordan coefficients we find

$$\sigma^{I'K}_{IK}(\theta) = \frac{4(kb)^4}{\pi^2 k^2} \sum_{\varkappa,m} \frac{2I'+1}{2\varkappa+1} (C^{\varkappa 0}_{I'KI-K})^2 I^2_{\varkappa m}(\theta); \quad (6)$$

$$I_{\varkappa m}(\theta) = \frac{1}{8} \sqrt{(2\varkappa+1)\frac{(\varkappa-m)!}{(\varkappa+m)!}}$$

$$\times \int_{-1}^{1} d\mu \xi(\mu) P^m_{\varkappa}(\mu) \int_{0}^{2\pi} d\varphi \cos m\varphi \frac{J_1(t)}{t}.$$

The functions $I^{\bullet}_{\varkappa m}(\theta)$ were investigated in Ref. 1 in the study of scattering for even-even nuclei. Because of the symmetry of the nucleus they are different from zero only for even $\varkappa$, m in which case, $I_{\varkappa m} = -I_{\varkappa,-m}$. The functions $I_{\varkappa m}(\theta)$ oscillate, roughly speaking, like the function $J_1(kR\theta)/(kR\theta)$ wherein the value of θ for which $I_{\varkappa m}(\theta) = 0$ depends upon $\varkappa$ and m.

For $I' = I$ Eq. (6) becomes the differential cross section for scattering without an energy exchange, viz.,

$$\sigma^{IK}_{IK}(\theta) = \frac{4(kb)^4}{\pi^2 k^2} \sum_{\varkappa,m} \frac{2I+1}{2\varkappa+1} (C^{\varkappa 0}_{IKI-K})^2 I^2_{\varkappa m}(\theta). \quad (7)$$

We see that this differential elastic cross section for neutron scattering by nonspherical nuclei with spin different from zero ($K \neq 0$) does not pass through zero for scattering angles $\theta < 1$. This is understandable since the cross section given by Eq. (7) is represented by a sum of cross sections which correspond to transitions between states with different projections of I, i.e., M before, M' after scattering. On the other hand, there is the exceptional case of an even-even nucleus with $I = K = 0$ where the angular distribution for elastic scattering has a zero similar to the cross section for elastic scattering by the diffraction of fast neutrons by a spherical nucleus. Actually, for $I = K = 0$ Eq. (6) shows that the cross section for exciting the state $\epsilon_{I'}$ of an even-even nucleus is

$$\sigma_{I'}(\theta) = \frac{4(kb)^4}{\pi^2 k^2} \sum_{m=-I'}^{I'} I^2_{I'm}(\theta),$$

in agreement with the result of Ref. 1. From this equation we see that the cross section for elastic scattering is

$$\sigma_0(\theta) = \frac{4(kb)^4}{\pi^2 k^2} I^2_{00}(\theta).$$

The differential cross section for scattering into the direction Ω with the excitation of different nuclear rotational states is given by

$$\sigma^{IK}_{s}(\theta) = \frac{1}{2I+1} \sum_{I',M',K} |f^{I'M'K}_{IMK}(\Omega)|^2.$$

It is convenient to represent this cross section in another form (see Ref. 1):

$$\sigma^{IK}_{s}(\theta) = \frac{1}{2I+1} \sum_{M} \int d\omega |f(\omega,\Omega)\varphi_n(\omega)|^2.$$

Employing this equation with Eqs. (2) and (3) we find

$$\sigma^{IK}_{s}(\theta)$$

$$= \frac{1}{8\pi^2} \sum_{\varkappa,M} (-)^{M-K} C^{\varkappa 0}_{I-MIM} C^{\varkappa 0}_{I-KIK} \int d\omega D^{\varkappa}_{00}(\omega) |f(\omega,\Omega)|^2.$$

Furthermore, it is easily seen that,

$$\sum_{\varkappa, M} (-)^{M-K} C^{\varkappa 0}_{I-MIM} C^{\varkappa 0}_{I-KIK} D^{\varkappa}_{00}(\omega) = 1, \qquad (8)$$

hence,

$$\sigma_s^{IK}(\theta) = \frac{2}{\pi} \frac{(kb)^4}{k^2} \int_0^1 d\mu \xi^2(\mu) \int_0^{\frac{\pi}{2}} d\varphi \left[\frac{J_1(t)}{t}\right]^2 = \sigma_s(\theta). \qquad (9)$$

Thus, the differential scattering cross section $\sigma_s(\theta)$ does not depend on the initial state of the nucleus, i.e., on the index I, K. Graphs of the function $\sigma_s(\theta)$ for different degrees of nuclear deformation and different neutron energies have been published[1].

The integrated cross section $\sigma_s = \int d\Omega \sigma_s(\theta)$, does not depend on the energy (in agreement with the results of Ref. 1) and has the form

$$\sigma_s = \pi b^2 \int_0^1 d\mu \xi(\mu).$$

The dependence of σ_s on the degree of nuclear deformation was considered in Ref. 1.

The total cross section for all scattering processes is specified by the imaginary part of the amplitude for elastic scattering evaluated at $\theta = 0$, i.e.,

$$\sigma_t^{IK} = \frac{4\pi}{K} \frac{1}{2I+1} \sum_M \operatorname{Im} f^{IMK}_{IMK}(\Omega) \Big|_{\theta=0}.$$

This reduces with the use of Eq. (5) to the total cross section $\sigma_t^{IK} = \sigma_t = 2\pi b^2 \int_0^1 d\mu \xi(\mu) = 2\sigma_s$. The cross section for capture is $\sigma_c = \sigma_t - \sigma_s = \sigma_s$. Thus, the total neutron scattering cross section and absorption cross section do not depend on the initial state of the nucleus either.

It is easy to see that for the case of spherical nuclei the above formulas reduce to the formulas given by the diffraction of neutrons by "black" spherical nuclei.

The author expresses his gratitude to B. T. Geilikman and V. M. Strutinski for many valuable discussions.

* Because of the reflection symmetry of the nucleus, the wave function (3) has to be symmetrized correspondingly[2]. However, for our purposes we can use the nonsymmetric expression.

[1] S. I. Drozdov, J. Exptl. Theoret. Phys. (U.S.S.R.) 28, 734, 736 (1955); Soviet Phys. JETP 1, 588, 591 (1955).

[2] A. Bohr and B. Mottelson, K. Danske. Vidensk Selsk. Mat.-fys. Medd., 27, No. 16 (1953).

Translated by A. Skumanich
157

Concerning the Radiative Correction to the μ-Meson Magnetic Moment

V. B. Berestetskii, O. N. Krokhin
AND
A. K. Khlebnikov

(Submitted to JETP editor January 7, 1956)
J. Exptl. Theoret. Phys. (U.S.S.R.) 30, 788-789
(April, 1956)

ANALYSIS of the structure of the present quantum theory of fields indicates its inapplicability to distances of the order of $\hbar/\lambda_0 \sim 10^{-13} - 10^{-14}$ cm[1]. Consequently, for those quantum-electrodynamic processes where momenta (real or virtual) of the order of λ_0 play a role, deviations from the usual formulas are to be expected. For the evaluation of these deviations in the integrals which appear in the determination of radiative corrections (integrals over virtual momenta) one can restrict the upper limit of integration to λ_0. Since these integrals converge for momenta $\sim m$, then the deviations should be of the order of m^2/λ_0^2, where m is the mass of the charged particle. This is why the deviations for the magnetic moment of the electron appear only in the third order radiative correction, viz., α^3 ($\alpha = e^2/\hbar c$) [2]. In the case of the heavier μ-meson, the finiteness of λ_0 affects the first radiation correction ($\sim \alpha$) and one expects a different value than predicted by Schwinger's formula. If one assumes that the μ-meson is devoid of any specific interactions which are greater than the electromagnetic one, then the problem can be treated as one in pure electrodynamics.

For the determination of the magnitude of the change in the radiative correction to the magnetic moment of the μ-meson (a change which is dependent upon the finiteness of λ_0) we shall consider, as is customary[3,4], the vertex portion of the scattering matrix of the third order Λ_3. The

linear term of its expansion in wave vectors of the external field $q/\hbar$ has the following form [$\hat{q} = q_\alpha \gamma_\alpha$; $q \tilde{-} (q; iq_0)$]:

$$\Lambda_i = (\pi^2/2m) F (\gamma_i \hat{q} - \hat{q}\gamma_i). \quad (1)$$

The coefficient F serves to specify the radiative correction to the magnetic moment, i.e.,

$$\Delta\mu/\mu = (\alpha/2\pi) F. \quad (2)$$

For $|\lambda_0| = \infty$, we have $F = 1$, and Eq. (2) is just the Schwinger formula. For finite λ_0, we can write $F = 1 - \delta F(\lambda_0)$, and hence

$$\Delta\mu/\mu = (\alpha/2\pi)[1 - \delta F(\lambda_0)]. \quad (3)$$

F is expressed by integrals in momentum space of the form

$$J = \int \frac{d^4k\,[1; k_\sigma; k_\sigma k_\tau]}{(k^2 - 2p_1k)(k^2 - 2p_2k)k^2}$$

(p_1 and p_2 are the initial and final momenta of the meson and $p_2 - p_1 = q$). Instead of integrating over a finite region one can retain the infinite integration limits and introduce Feynman's[3] truncating factor $\lambda_0^2/\lambda_0^2 + k^2$. Then

$$J(\lambda_0) = J(\infty) - \delta J(\lambda_0),$$

where

$$\delta J(\lambda_0) = \int \frac{d^4k\,[1; k_\sigma; k_\sigma k_\tau]\cdot}{(k^2 - 2p_1k)(k^2 - 2p_2k)(k^2 + \lambda^2)}.$$

Continuing the calculation in the usual manner[3,4], we obtain for the apex the following expression

$$\Lambda_i(\lambda_0) = \Lambda_i(\infty) - \delta\Lambda_i(\lambda_0);$$

$$\delta\Lambda_i(\lambda_0) = \int_0^1 2x\,dx \int_0^1 dy\,\{(1 - y - xy)\hat{q}\gamma_i - (1 - x + xy)\gamma_i\hat{q}\} \times \frac{\pi^2 mx}{x^2p_y^2 - (1-x)\lambda_0^2}, \quad (4)$$

where

$$p_y = yp_1 + (1 - y)p_2.$$

Let us first perform the integration over y. Since we are only interested in terms linear in q, we can substitute $p^2 = -m^2$ for p_y^2 in the integrand. Then Eq. (4) assumes the form of Eq. (1), viz.,

$$\delta\Lambda_i = (\pi^2/2m)(\gamma_i\hat{q} - \hat{q}\gamma_i)\,\delta F(\lambda_0),$$

where

$$\delta F(\lambda_0) = 2\int_0^1 \frac{(1-x)x^2}{x^2 + (\lambda_0/m)^2(1-x)}\,dx \quad (5)$$

$$= 1 + 2\gamma - \gamma(\gamma+2)\ln\frac{1}{\gamma} - \frac{\gamma^2 + 4\gamma + 2}{\sqrt{1+4/\gamma}}\ln\frac{1+\sqrt{1+4/\gamma}}{1-\sqrt{1+4/\gamma}}$$

($\gamma = \lambda_0^2/m^2$). With $\gamma \gg 1$, the value of the integral is

$$\delta F(\lambda_0) = 2m^2/3\lambda_0^2. \quad (6)$$

---

[1] L. Landau and I. Pomeranchuk, Dokl. Akad. Nauk SSSR **102**, 489 (1955); I. Pomeranchuk, Dokl. Akad. Nauk SSSR **103**, 1005 (1955); Dokl. Akad. Nauk SSSR **104**, 51 (1955).

[2] G. Gandel'man and Ia. Zel'dovich, Dokl. Akad. Nauk SSSR 105, 445 (1955).

[3] R. Feynman, Phys. Rev. **76**, 769 (1949).

[4] A. Akhiezer and V. Berestetskii, *Quantum Electrodynamics*, Moscow, 1953.

Translated by A. Skumanich
158

Charged Particle Green's Function in the "Infrared Catastrophe" Region

L. P. Gor'kov
Institute for Physical Problems
Academy of Sciences, USSR

(Submitted to JETP editor January 3, 1956)
J. Exptl. Theoret. Phys. (U.S.S.R.) **30**, 790-791
(April, 1956)

In the electrodynamics of the electron Abrikosov[1] has shown that the interaction with the electric field leads to the appearance in the Green's function of the electron in the infrared region ($|p^2 - m^2| \ll m^2$) of the additional singularity

$$\left(\frac{m^2}{p^2 - m^2}\right)^{(e^2/2\pi)[3 - d_l(0)]} \quad (1)$$

as compared with the simple pole for the Green's function of the free electron. An analogous investigation in the electrodynamics of spin zero[2]

shows that the same singularity arises in the Green's function of a charged scalar particle, where the result obtained coincides exactly with (1). Hence, it seems worthwhile to present a result from which this effect would follow independently of the nature (spin) of the charged particle. The present letter is devoted to this question.

The Green's function of the particle is defined in the usual way:

$$G(x, x') = \langle (\psi(x), \bar{\psi}(x'))_+ \rangle_0$$

The brackets indicate a time-ordered average over the vacuum, $\psi(x)$ is the particle field operator, $\bar{\psi}(x)$ is the adjoint operator. The operations of conversion between ψ and $\bar{\psi}$ are evidently Hermitian conjugates.

The Fourier components of $G(x, x')$ in the region $p^2 \sim m^2$ are determined by the matrix element $\langle 0 | \psi(x) | p \rangle$, where $p^2 \sim m^2$. In other words, in the Fourier expansion of the operator $\psi(x)$, it is sufficient to determine only the part of the spectrum of $\psi(p)$ where $p^2 \sim m^2$. In the state in which $p^2 \sim m^2$, there is a single particle interacting with the electric field, and the magnitude $\Delta = |p^2 - m^2| m^{-2}$ is a measure of the energy of the photons which this particle may emit or absorb. We make the assumption, justified below, that for the effect under consideration only a connection with the low frequency part of the electromagnetic field is necessary. Choosing a system of reference in which the motion of the particle is nonrelativistic, we may write the nonrelativistic Schrödinger equation

$$i \frac{\partial \psi(x)}{\partial t} = \left\{ m + eA_0(x) + \frac{1}{2m} (\hat{\mathbf{p}} - e\mathbf{A}(x))^2 \right\} \psi(x), \quad (2)$$

where $\hat{\mathbf{p}} = -i \nabla$. This equation is correct for the description of the interaction of the "free" part of the Fourier expansion of $\psi(x)$ ($p^2 \sim m^2$) with the low frequency part of the electromagnetic field. Neglecting terms quadratic in the field, since, as may be shown, they give rise to a higher order contribution in the final result, we substitute into Eq. (2)

$$\psi(\mathbf{x}, t) = P_\tau \exp\left\{ -i \int^t j_\mu A_\mu(\mathbf{x}, \tau)\, d\tau \right\} \psi_0(\mathbf{x}, t), \quad (3)$$

where P_τ is the time-ordering operator and $j_\mu = \{e, e\mathbf{v}\}^*$. The operator $\psi_0(\mathbf{x}, t)$ satisfies the free particle equation

$$i \partial \psi_0 / \partial t = (m + \mathbf{p}^2 / 2m)\, \psi_0.$$

In the approximation $e^2 \ll 1$ we may consider $A_\mu(\mathbf{x}, \tau)$ in Eq. (3) as the free-field operator; hence, ψ_0 and A_μ commute. For the Green's function $G(x, x')$ (more exactly, for the "free" part $p^2 \sim m^2$ in the Fourier expansion) we obtain

$$G(x, x') = G_0(x, x') \left\langle P_\tau P_{\tau'} \left(\exp\left\{ -i \int^t j_\mu A_\mu(\mathbf{x}, \tau)\, d\tau \right\} \times \exp\left\{ i \int^t j_\nu A_\nu(\mathbf{x}', \tau')\, d\tau' \right\} \right)_+ \right\rangle_0,$$

where $G_0(x, x')$ is the free particle Green's function.

Using the formula

$$\exp(A + B) = \exp(A) \cdot \exp(B) \cdot \exp\left(-\frac{1}{2} [A, B] \right),$$

which is correct when there exists a number $[A, B]$, and taking an average over the photonic vacuum, we obtain the following simple transformations:

$$G(x, x') = G_0(x, x') \quad (4)$$

$$\times \exp\left\{ -\frac{1}{2} \left[\int^t \int^t \langle (A_\mu(\mathbf{x}, \tau),\ A_\nu(\mathbf{x}, \tau')_+ \rangle_0\, j_\mu j_\nu d\tau\, d\tau' + \int^{t'} \int^{t'} \langle (A_\mu(\mathbf{x}', \tau),\ A_\nu(\mathbf{x}', \tau'))_+ \rangle_0 j_\mu j_\nu d\tau\, d\tau' \right] + \int^t \int^{t'} \langle (A_\mu(\mathbf{x}, \tau),\ A_\nu(\mathbf{x}', \tau'))_+ \rangle_0 j_\mu j_\nu\, d\tau\, d\tau' + I(t, t') \right\},$$

where

$$I(t, t') = \begin{cases} \int^t \int^{t'} \theta(\tau' - \tau) [A_\mu(\mathbf{x}, \tau),\ A_\nu(\mathbf{x}', \tau')]\, j_\nu j_\mu d\tau\, d\tau'; & t > t', \\ -\int^t \int^{t'} \theta(\tau - \tau') [A_\mu(\mathbf{x}, \tau),\ A_\nu(\mathbf{x}', \tau')]\, j_\nu j_\mu d\tau\, d\tau'; & t < t'. \end{cases} \quad (5)$$

$$[A_\mu(x),\ A_\nu(x')] = -4\pi i \delta_{\mu\nu} D(x - x'); \qquad \langle (A_\mu(x),\ A_\nu(x'))_+ \rangle_0 = 4\pi D_{f\mu\nu}(x - x').$$

The assumption of adiabatic cessation of the interaction

$$e = e(t) = \begin{cases} e, & t > T_0 \\ e \exp \alpha t, & t < T_0 \end{cases} \quad (T_0 \to -\infty)$$

allows us to neglect the values of all the integrals taken at the lower limit. In particular, Eq. (5) depends only on the lower limit, and hence is equal to zero. Carrying out the integration with respect to $d\tau$ and $d\tau'$ in Eq. (4) in the indicated manner, and varying Eq. (4) with respect to δe^2, we take the Fourier component of the resulting relation in the momentum region $|p^2 - m^2| \ll m^2$ which is of interest to us. We find

$$\delta G(p) = \frac{i\delta e^2}{\pi} \left\{ \int [G(p) - G(p-k)] \left[\left(v^2 - \frac{(vk)^2}{k^2} \right) + \frac{(vk)^2}{k^2} d_l(k^2) \right] \frac{d^4k}{\omega^2 (k^2 + i\varepsilon)} \right\}. \quad (6)$$

The calculation is most simply carried out in the system of reference in which the velocity of the particle $v = p/m$ is equal to zero. Then

$$\delta G(p) = \frac{i\delta e^2}{\pi} \left\{ \int [G(p) - G(p-k)] \left[\left(1 - \frac{\omega^2}{k^2} \right) + \frac{\omega^2}{k^2} d_l(k^2) \right] \frac{d^4k}{\omega^2 (k^2 + i\varepsilon)} \right\}.$$

Carrying out the integration with respect to $d\omega$ according to the usual rules of contouring[3], we find that the terms sought are obtained by taking a calculation at the point $k^2 = 0$:

$$\delta G(p) = \frac{\delta e^2}{2\pi} \left\{ \int [G(p) - G(p-k)] \frac{d|k|}{|k|} \right\} [3 - d_l(0)]; \quad (\omega = +|k|). \quad (7)$$

The essential logarithmic region of interaction in this integral is $|p^2 - m^2|/m \ll k \ll m$. The region of high frequencies leads to renormalization effects, which, naturally, cannot be correctly taken into account in this technique. Carrying out the integration in (7) for low frequencies, we obtain

$$\delta G(p) = G(p) \left(\frac{\delta e^2}{2\pi} \right) [3 - d_l(0)] \ln \left(\frac{m^2}{p^2 - m^2} \right)$$

or

$$G(p) = G_0(p) \left(\frac{m^2}{p^2 - m^2} \right)^{(e^2/2\pi)[3 - d_l(0)]}$$

where $G_0(p)$ differs from the Green's function of a free particle by the renormalization factors. Thus, the appearance of the additional singularity (1) in the Green's function of a particle interacting with an electromagnetic field is connected only with the classical properties of the electric current being produced by the particle in its uniform motion.

In conclusion, I wish to express my deep gratitude to A. A. Abrikosov and I. M. Khalatnikov for discussions of this work.

* Designations are those used in Ref. 3.

[1] A. A. Abrikosov, Dissertation, Institute for Physical Problems, Academy of Sciences, USSR, 1955.

[2] L. P. Gor'kov, Dissertation, Institute for Physical Problems, Academy of Sciences, USSR, 1955.

[3] R. Feynman, Phys. Rev. 76, 749, 769 (1949).

Translated by M. G. Gibbons
159

Transformation of Positive Helium Ions Colliding with Inert Gas Atoms into Negative Ions

V. M. Dukel'skii, V. V. Afrosimov
and
N. V. Fedorenko
Leningrad Physico-technical Institute, Academy of Sciences, USSR

(Submitted to JETP editor January 14, 1956)
J. Exptl. Theoret. Phys. (U.S.S.R.) 30, 792-793 (April, 1956)

In studying the processes which take place during the passage of He^+ ions through rarefied gases, we noted that negative ions He^- occurred in the beam after it had passed through the gas.

The experiments were carried out in the double mass spectrometer arrangement described in Ref. 1. A beam of He^+ ions of given energy was separated by the magnetic mass-monochromator, after which it entered the gas-filled collision chamber. For a gas pressure of $\sim 3 \times 10^{-4}$ mm Hg in the chamber, we can keep the pressure in the remaining parts of the apparatus at a level $< 1 \times 10^{-5}$ mm Hg. The composition of the beam which has passed through the collision chamber is investigated by means of a magnetic mass analyzer.

If we admit a beam of He^+ ions into the collision chamber and select a suitable intensity of magnetic field in the mass analyzer, we can pass through it He^+ ions which will retain their charge and their velocity after the passage. On reversing the direction of the magnetic field in the mass

analyzer, we discovered the presence of negative ions in the beam coming from the collision chamber. These ions passed through the mass analyzer for the same value of magnetic intensity as did the He^+ ions. It is obvious that they were He^- ions which had been formed from the He^+ ions and which had kept their velocity.

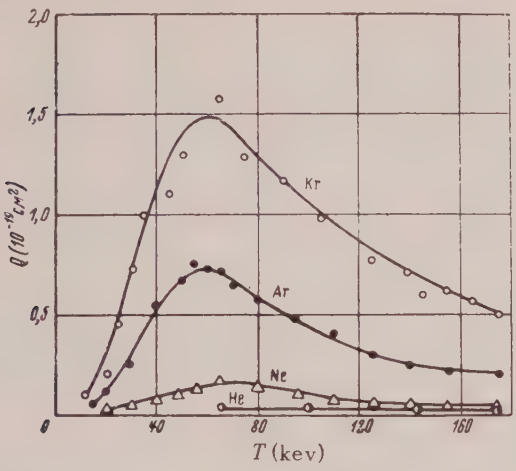

Dependence of the effective cross section for the conversion process $He^+ \rightarrow He^-$ in He, Ne, Ar, Kr on the energy of the He^+ ions.

The formation of the He^- ions was established for the He^+ ion energy interval from 15 to 175 kev in four inert gases: Kr, Ar, Ne, He. We are convinced that in the case of Kr, Ar and Ne the effect is proportional to the pressure of the gas in the collision chamber right down to a pressure of 5×10^{-4} mm Hg, that is, the process $He^+ \rightarrow He^-$ occurred during *single* collisions of He^+ ions with the atoms of the gas. This shows that in interacting with the atom the He^+ ion must have simultaneously taken two electrons from it. In order to show the magnitude of the observed effect, we adduce an example. For a He^+ ion energy of 80 kev and a pressure of 2.5×10^{-4} mm Hg of argon in the collision chamber (16 cm path length of the ions in the gas), the current of secondary He^- ions was equal to 1.4×10^{-12} amp when the current of primary He^+ ions was equal to 3.3×10^{-7} amp.

On the basis of the measurements performed, we carried out an approximate determination of the effective cross sections for the process $He^+ \rightarrow He^-$. In order to do this, it was necessary to know the transmission coefficient k_- of the mass analyzer for the secondary ions He^-. We measured the coefficient k_+ for the primary ions He^+, scattered in the gas, and used its value in calculating the effective cross sections for the process $He^+ \rightarrow He^-$. In the energy interval which we used, the value of k_+ changed only slightly and was equal to 0.4-0.5. It was also verified that the angular distribution of the He^- ions was only slightly different from that of the primary He^+ ions after going through the collision chamber.

Our results are given in the figure in the form of curves showing the dependence of the effective cross section Q for the conversion process $He^+ \rightarrow He^-$ on the energy T of the He^+ ions. The curves for neon, argon and krypton have a maximum for an energy of 60-70 kev. As the atomic number of the gas atoms decreases, the curves become lower, keeping the same general shape. For krypton the magnitude of Q corresponding to the maximum of the curve is 1.5×10^{-19} cm^2. In the case of helium the conversion effect is very small (Q of the order of 10^{-21} cm^2), and hence we were not able to determine the form of the $Q(T)$ curve.

The formation of negative ions on the collision of positive ions with gas molecules was first observed for protons[2,3], and later for oxygen ions[4]. The $He^+ \rightarrow He^-$ process which we have observed is of special interest in view of the fact that the very possibility of the formation of the He^- ions is unexpected. As was shown in Ref. 5, the energy of an He^- ion in its normal state $(1s^2 2s)^2 s$ (similar to the ground state of the lithium atom) should exceed the energy of the normal state of a helium atom; hence, such an ion should not exist. In a recently published work[6] it was pointed out that a highly excited state of the negative ion He^- was possible, which, if it existed, would have to be metastable (with respect to the process of auto-ionization) and possess an average lifetime τ of the order of 10^{-13} sec. This theoretical result coincides with the results of Ref. 7, in which an analysis of the composition of canal rays showed a weak He^- line.

On the basis of our experiments we cannot judge whether the He^- ions which we have observed are stable or metastable. The He^- ions travel a path of 70 cm in our apparatus; for an energy of 60 kev the time of flight is 4×10^{-7} sec. If the He^- ions which we observed were metastable, with $\tau = 10^{-3}$ sec, then the fraction 4×10^{-4} of them should disintegrate by spontaneous emission of an electron while going along the path from the point of collision to the receiver. Such an insignificant decrease in the number of He^- ions because of their disintegration in the apparatus could not be detected in the results of our experiments, in particular, in the form of the $Q(T)$ curves which we obtained.

[1] D. M. Kaminker and N. V. Fedorenko, J. Tech. Phys. (U.S.S.R.) 25, 1843 (1955).

[2] A. C. Whittier, Can. J. Phys. 32, 275 (1954).

[3] Ia. M. Fogel', L. I. Krupnik and B. G. Safronov, J. Exptl. Theoret. Phys. (U.S.S.R.) 28, 589 (1955); Soviet Phys. JETP 1, 415 (1955).

[4] Ia. M. Fogel' and L. I. Krupnik, J. Exptl. Theoret. Phys. (U.S.S.R.) 29, 209 (1955); Soviet Phys. JETP 2, 252 (1956).

[5] Ta-You Wu, Phil. Mag. 22, 837 (1936).

[6] E. Holøien and J. Midtal, Proc. Phys. Soc. (London) A68, 815 (1955).

[7] J. W. Hiby, Ann. Physik 34, 473 (1939).

Translated by M. G. Gibbons
160

Concerning a Certain Generalization of a Renormalization Group

A. A. Logunov
Moscow State University

(Submitted to JETP editor January 24, 1956)
J. Exptl. Theoret. Phys. (U.S.S.R.) 30, 793-795
(April, 1956)

THE basic goal of the present note is the generalization of the Lie equations for the Green functions for the case of an arbitrary longitudinal coupling of photons.

1. We shall work with finite Green functions and shall assume that all divergences which exist in the theory have been eliminated by means of the subtraction formalism[2]. However, there still remain, even after the elimination of the infinites, final ambiguities which are associated with the finite counter-terms introduced into the Lagrangian of the same operator which occurs in the elimination of the divergences[2]. In the case where the zeroth coupling of the photon contains an admixture of an arbitrary longitudinal coupling,

$$\mathfrak{G}^0_{mn}\, d(k^2) = \frac{i}{k^2}\left(g^{mn} - \frac{k_m k_n}{k^2}\right) + \frac{i}{k^2}\frac{k_m k_n}{k^2}\,\omega^2 d_l(k^2),$$

the calculation of the introduced counter-terms introduces a multiplicative renormalization factor for the transverse part of the photon coupling but does not change its longitudinal part. Insofar as the introduced finite counter-terms (for the transverse photon coupling) led to a renormalization of the Green function and of the electron charge, then, in the present problem, because of the circumstance shown above regarding the "incomplete renormalization" of the zeroth coupling, we shall work with the following transformation group:

$$G_1 \to G_2 = Z_2 G_1;\quad \mathfrak{G}_1 \to \mathfrak{G}_2 = Z_3 \mathfrak{G}_1;\quad \Gamma_1 \to \Gamma_2 = Z_1^{-1}\Gamma_1;$$

$$e_1^2 \to e_2^2 = Z_3^{-1} e_1^2;\quad \omega_1^2 \to \omega_2^2 = Z_3 \omega_1^2;\quad Z_1 = Z_2. \quad (1)$$

This transformation group is a generalization of the transformation group[1] for the case of an arbitrary longitudinal photon coupling. The significance of these transformations is that the set of quantities $(G_1, \mathfrak{G}_1, \Gamma_1, e_1, \omega_1)$ and $(G_2, \mathfrak{G}_2, \Gamma_2, e_2, \omega_2)$ can be used in the same form for the specification of particles with their mass and charge equal to the experimental values.

2. The transformation group obtained above permits one to derive the equations for the Green functions. If we represent the Green functions in the form

$$G(k) = i\,\frac{\hat{k}a(k^2) + mb(k^2)}{k^2 - m^2}, \quad (2)$$

$$\mathfrak{G}_{mn}(k) = \frac{i}{k^2}\left(g^{mn} - \frac{k_m k_n}{k^2}\right) d(k^2) + \frac{i}{k^2}\frac{k_m k_n}{k^2}\,\omega^2 d_l(k^2)$$

and if we reason as in Ref. 1, we obtain with no difficulty the following functional equations,

$$d(x, y, e^2) = d(-t, y, e^2)\, d(x\ \ t, y/t, e^2 d(-t, y, e^2)),$$

$$t > 0. \quad (3)$$

$$s'(x, y, \omega^2, e^2) = \frac{s'(x/t,\ y/t,\ \omega^2 d^{-1},\ e^2 d(-t, y, e^2))}{s'(-1/t, y/t, \omega^2 d^{-1},\ e^2 d(-t, y, e^2))},$$

where

$$k^2\ \lambda_2^2 = x,\quad m^2/\lambda_2^2 = y,$$

$$s'(x, y, \omega^2, e^2) = s(x, y, \omega^2, e^2)\, s^{-1}(-1, y, \omega^2, e^2).$$

The first of these equations agrees with the analogous equation for d in Ref. 2, insofar as the transverse part of the zeroth coupling.

Differentiating each of the above equations with respect to x and setting $t = -x$, we obtain,

$$\frac{\partial}{\partial x}\ln d(x, y, e^2) \quad (4)$$

$$= -\frac{1}{x}\left[\frac{\partial}{\partial \xi}\, d\left(\xi - \frac{y}{x},\ e^2 d(x, y, e^2)\right)\right]_{\xi=-1},\quad x < 0,$$

$$\frac{\partial}{\partial x}\ln s'(x, y, \omega^2 e^2)$$

$$= -\frac{1}{x}\left[\frac{\partial}{\partial \xi}\, s'\left(\xi, -\frac{y}{x},\ \omega^2 d^{-1},\ e^2 d(x, y, e^2)\right)\right]_{\xi=-1}.$$

The functions $s'(x, y, \omega^2, e^2)$ and $d(x, y, e^2)$ are real in the region $x < 0$. In order that we deal only with real functions in the region $x > 0$, we can write the Lie equations separately for the real and imaginary parts of the Green functions:

$$\frac{\partial}{\partial x} \ln d_R(x, y, e^2) = \frac{1}{x}\left[\frac{\partial}{\partial \xi} \ln d_R\left(\xi, \frac{y}{x}, e^2 d(-x, y, e^2)\right)\right]_{\xi=1}, \tag{5}$$

$$\frac{\partial}{\partial x} \ln d_J(x, y, e^2) = \frac{1}{x}\left[\frac{\partial}{\partial \xi} \ln d_J\left(\xi, \frac{y}{x}, e^2 d(-x, y, e^2)\right)\right]_{\xi=1},$$

$$\frac{\partial}{\partial x} \ln s'_R(x, y, \omega^2, e^2) = \frac{1}{x}\left[\frac{\partial}{\partial \xi} \ln s'_R\left(\xi, \frac{y}{x}, \omega^2 d^{-1}, e^2 d(-x, y, e^2)\right)\right]_{\xi=1},$$

$$\frac{\partial}{\partial x} \ln s'_J(x_1, y, \omega^2, e^2) = \frac{1}{x}\left[\frac{\partial}{\partial \xi} \ln s'_J\left(\xi, \frac{y}{x}, \omega^2 d^{-1}, e^2 d(-x, y, e^2)\right)\right]_{\xi=1},$$

where $d = d_R + id_J$; $s' = s'_R + is'_J$.

3. Let us consider the asymptotic region of large momenta, i.e., for $m^2 \ll |k^2|$. According to excitation theory we find:

$$a_c\left(\frac{k^2}{m^2}, \omega_0^2, e_0^2\right) = 1 - \frac{e_0^2\omega_0^2}{4\pi} \int_{\ln(-k^2/m^2)}^{\infty} d_l(z)\, dz, \tag{6}$$

$$b_c\left(\frac{k^2}{m^2}, \omega_0^2, e_0^2\right) = 1 - \frac{e_0^2}{4\pi}\left[3\ln\left(-\frac{k^2}{m^2}\right) + \omega_0^2 \int_{\ln(-k^2/m^2)}^{\infty} d_l(z)\, dz\right],$$

where $d_l(z)$ is a slowly varying function of z and, a_c and b_c are counterparts of the real electron Green function. If we consider the obvious relation between the function $s(x, y, \omega^2, e^2)$ and the real electron function $s_c(x/y, \omega_0^2, e_0^2)$

$$s'(x, y, \omega^2, e^2) = \frac{s_c(x/y, \omega_0^2, e_0^2)}{s_c(-1/y, \omega_0^2, e_0^2)}, \tag{7}$$

$$\omega^2 = \omega_0^2 d_c^{-1}\left(-\frac{1}{y}, e_0^2\right), \quad e^2 = e_0^2 d_c\left(-\frac{1}{y}, e_0^2\right),$$

then we obtain

$$a'(x, y, \omega^2, e^2) = 1 - \frac{e^2\omega^2}{4\pi} \int_{\ln(-x/y)}^{-\ln y} d_l(z)\, dz, \tag{8}$$

$$b'(x, y, \omega^2, e^2) = 1 - \frac{e^2}{4\pi}\left[3\ln(-x) + \omega^2 \int_{\ln(-x/y)}^{-\ln y} d_l(z)\, dz\right].$$

If we insert these expressions into Eq. (4), we have

$$a'(x, y, \omega^2, e^2) = \exp\left[-\frac{e^2\omega^2}{4\pi} \int_{\ln(-x/y)}^{-\ln y} d_l(z)\, dz\right], \tag{9}$$

$$b'(x, y, \omega^2, e^2) = \left[1 - \frac{e^2}{3\pi}\ln(-x)\right]^{1/4} \exp\left[-\frac{e^2\omega^2}{4\pi} \int_{\ln(-x/y)}^{-\ln y} d_l(z)\, dz\right].$$

Let us consider the region $k^2 \sim m^2$, where the functions a' and b' possess an "infrared characteristic."

If we represent s' in the form

$$s'\left(\frac{k^2}{\lambda^2}, \frac{m^2}{\lambda^2}, \omega^2, e^2\right) = S'\left(-\frac{m^2 - k^2}{m^2 + \lambda^2}, -\frac{m^2 + \lambda^2}{m^2}, \omega^2, e^2\right), \tag{10}$$

we can transform Eq. (4) to

$$\ln s'(x, y, \omega^2, e^2) = \int_{-1}^{x} \frac{dx}{x - y}\left[\frac{\partial}{\partial \eta} S'\left(\eta, \frac{x}{y} - 1, \omega^2 d^{-1}, e^2 d(x, y, e^2)\right)\right]_{\eta=-1},$$

from which, by means of the formulas of excitation theory,

$$\frac{\partial A'(\eta, x - 1, \omega^2, e^2)}{d\eta}\bigg|_{\eta=-1} = -\frac{e^2}{4\pi}\left[-\frac{6 + \omega^2 d_l^0}{x} + \frac{2\omega^2 d_l^0}{x^2} + \frac{(1 - x)(2\omega^2 d_l^0 - 6)\ln(1 - x)}{x^3} + \omega^2 d_l^0\right], \tag{11}$$

$$\frac{\partial B'(\eta, x - 1, \omega^2, e^2)}{\partial \eta}\bigg|_{\eta=-1} = \frac{e^2}{4\pi}(3 - \omega^2 d_l^0)\left[\frac{1 - x}{x}\ln(1 - x) + \frac{x + 1}{x}\right],$$

we obtain

$$a' \sim a'_0 \left(1 - \frac{k^2}{m^2}\right)^{-(e^2/2\pi)(3-d_l^0)}, \qquad (12)$$

$$b' \sim b'_0 \left(1 - \frac{k^2}{m^2}\right)^{-(e^2/2\pi)(3-d_l^0)}.$$

Equations (9) and (12) which we have obtained as a qualitative illustration of the method of renormalization groups agrees with those results obtained earlier[3] by means of a summation of a series of Feynman "primary diagrams."

In conclusion, I wish to express my deepest thanks to Academician N. N. Bogoliubov under whose guidance this work was completed and, in addition, to D. V. Shirokov for discussion of this work.

[1] N. N. Bogoliubov and D. V. Shirkov, Dokl. Akad. Nauk SSSR 103, 203, 391 (1955).

[2] N. N. Bogoliubov and D. V. Shirkov, Usp. Fiz. Nauk 57, 87 (1955).

[3] L. D. Landau, A. A. Abrikosov and I. M. Khalatnikov, Dokl. Akad. Nauk SSSR 95, 497, 773 (1954); Dokl. Akad. Nauk SSSR 96, 261 (1954).

Translated by A. Skumanich
161

On the Mass of the Photon in Quantum Electrodynamics

D. A. KIRZHNITS
P. N. Lebedev Physical Institute, Academy of Sciences, USSR

(Submitted to JETP editor January 18, 1956)
J. Exptl. Theoret. Phys. (U.S.S.R.) 30, 796-797 (April, 1956)

IN the present quantum theory of fields, point (local) interaction is often considered as the limit of smeared (nonlocal) interaction[1,2]; this permits one to operate with finite expressions in the intermediate calculations. For this purpose a scalar smearing function F, a form-factor which contains a cut-off parameter Λ, is introduced into the interaction Lagrangian. This factor converges to unity when $\Lambda \to \infty$. In this point of view the interaction has the form

$$S \sim e_1 \int F(p, k, p-k, \Lambda)\, \bar{\psi}(p)\, \hat{A}(k)\, \psi(p-k)\, d^4p d^4k + \text{charge interaction}. \qquad (1)$$

In order that the smearing function does not lead to a violation of physical reality (i.e., the Hermitian character of the Lagrangian) it must satisfy the condition[3,4]

$$F(p, k, p-k) = F^*(p-k, k, p). \qquad (2)$$

To each node in the Feynman diagram (or to each operator of the vertex portion) there will correspond a factor in F which depends on the momentum associated with the node.

It is known that the use of the simplest square-form smearing functions* leads to a violation of the gradient invariance; a violation which appears in the form of a nonzero photon mass. In this connection in Ref. 1, where a square-smearing function was used, the photon mass was eliminated by subtraction. In addition to this it was expressed by these authors (whose larger goal was the elimination of the divergences without the use of a subtractive procedure) that the assumption about the existence of such a smearing function leads automatically with its use to the falling-out of the photon mass. This note is devoted to a consideration of this question.

The mass of the photon corresponds to the value of the polarization operator at $k = 0$ (the symbolism of Ref. 1 is used here):

$$P_{\mu\nu}(0) = \frac{e_1^2}{\pi i} \operatorname{Sp} \int G(p)\, \Gamma_\mu(p, p, 0)\, G(p)\, \gamma_\nu\, |F(p, 0, p, \Lambda)|^2\, d^4p. \qquad (3)$$

The appearance of the square of the modulus of F is associated with the Hermitian character of the Lagrangian [Eq. (2)]; it specifies the presence of two vertex parts in the diagram of the polarization operator for which the momenta differ only in direction**.

To study Eq. (3) we shall use the asymptotic expression[1,5]

$$\tilde{G}(p) = \hat{p}^{-1}, \tilde{\Gamma}_\mu(p, p, 0) = \gamma_\mu, \qquad (4)$$

which means we will consider the case where the longitudinal part of the photonic Green's function d_l is equal to zero. With the help of Eq. (4), we find

$$P_{\mu\nu}(0) = \tilde{P}_{\mu\nu}(0) + [P_{\mu\nu}(0) - \tilde{P}_{\mu\nu}(0)],$$
$$\tilde{P}_{\mu\nu}(0) = \frac{e_1^2}{\pi i} \int \operatorname{Sp}\left(\frac{1}{\hat{p}} \gamma_\mu \frac{1}{\hat{p}} \gamma_\nu\right) |F|^2\, d^4p. \qquad (5)$$

If, as is customary (see Ref. 2), $F(p, 0, p, \Lambda) = f(p^2/\Lambda^2)$, then

$$\tilde{P}_{\mu\nu}(0) = \frac{e_1^2}{\pi i} \Lambda^2 \delta_{\mu\nu} \int_0^\infty |f(x)|^2 dx. \quad (6)$$

The eliminated part of Eq. (5) was of the order of $\ln(\Lambda^2)$. An analogous evaluation occurs in the more general case of $F(p, \Lambda) = f(p^2/\Lambda^2, p^2)$; at the same time, of course, one assumes that $F \to 1$ as $\Lambda \to \infty$.

In this fashion the problem of dealing with the elimination of the photon mass for any sufficiently large Λ by means of the selection of a suitable form for the smearing function rests, in all cases, upon the necessity of reducing Eq. (6) to zero. This leads to the condition

$$\int_0^\infty |f(x)|^2 dx = 0, \quad (7)$$

which cannot be satisfied because of the essential positive definite form for the integrand.

It may be remarked that the elimination of the photon mass by the Pauli-Villars method[6] is possible because the method does not depend on the smearing of the Lagrangian; therefore, the form-factor.

$$\int_{\lambda_0}^\infty \frac{\lambda^4 G(\lambda)}{(p^2 + \lambda^2)^2} d\lambda$$

with $\lambda_0 \gg m$, which corresponds to $|F(p, \Lambda)|^2$ in the present method, is an oscillating quantity. Eq. (7) assumes the well-known form $\int_{\lambda_0}^\infty \lambda^2 G(\lambda) d\lambda = 0$, then the condition can be satisfied.

For the case of a nonzero longitudinal Green's function d_l, $P_{\mu\nu}(0)$ becomes an explicit function of d_l inasmuch as the phase factors in G and Γ [1] which depend on d_l cannot be completely reduced in expression (3). Consequently if, indeed, one could eliminate $P_{\mu\nu}(0)$ with the aid of smearing, then the corresponding function F should depend explicitly on the arbitrary and abstract (i.e., without direct physical meaning) quantity d_l.

In this exceptional case the use of a square-smearing function allows one to calculate the magnitude of $P_{\mu\nu}(0)$ exactly. Transforming Eq. (3) with the help of Warden's equality

$$\Gamma_\mu(p, p, 0) = \partial G^{-1}(p) \quad \partial p_\mu,$$

we obtain the expression***

$$P_{\mu\nu}(0) = -\frac{e_1^2}{\pi i} \int_0^\Lambda \frac{\partial}{\partial p_\mu} \mathrm{Sp}(G\gamma_\nu) d^4p, \quad (8)$$

to which the Gauss theorem can be applied. At the same time, the surface integral around the point $p^2 = m^2$ disappears in view of the proximity of a series of poles of G at this point[7]. As a result, it appears that $P_{\mu\nu}(0)$, like its value in the second order perturbation theory, is cut off at the momentum Λ. This is associated with the fact that over the surface of radius Λ nonexcited functions must be inserted in Eq. (3). In the exceptional case investigated it appears that $P_{\mu\nu}(0)$ does not depend on d_l because the region $p^2 < \Lambda^2$, where the phase factors are different from unity, does not contribute to Eq. (8).

Thus, in the elimination of the photon mass by means of a smeared (nonlocal) interaction through the use of a scalar form factor F one meets with a serious difficulty; in view of this fact one cannot possibly avoid the use of one or another form of the subtraction process.

My deepest gratitude to Academician I. E. Tamm for his interest in the work and for valuable advice and to E. S. Fradkin for detailed discussions.

Note added in Proof: Academician L. D. Landau has graciously directed my attention to the possibility of eliminating the mass of the photon by a method which is tied in with the use of a spinor F-function together with the customarily used (see the quote references) scalar F-function. The analysis of this question, however, is difficult in view of the absence of an aymptotic theory for such a smearing function.

* A square-shaped smearing function ($F(p, \Lambda) = 0$ for $p^2 > \Lambda^2$ and $F(p, \Lambda) = 1$ for $p^2 < \Lambda^2$) corresponds to the customary cut-off for integrals in momentum space.

** The question of possibly using a non-Hermitian smearing requires special study.

*** In the derivation of Eq. (8) the smearing function is essentially constant for $p^2 < \Lambda^2$ (and equal to unity).

[1] L. D. Landau, A. A. Abrikosov and I. M. Khalatnikov, Dokl. Akad. Nauk SSSR 95,497, 773, 1177 (1954).

[2] A. A. Abrikosov and I. M. Khalatnikov, Dokl. Akad. Nauk SSSR 103, 993 (1955); I. Ia. Pomeranchuk, Dokl. Akad. Nauk SSSR 103, 1003 (1955).

[3] P. Kriestensen and C. Moller, Det. Kgl. Danske. 27, 7 (1952).

[4] B. V. Medvedev, Dokl. Akad. Nauk SSSR 100, 3, 433 (1955).

[5] E. S. Fradkin, J. Exptl. Theoret. Phys. (U.S.S.R.) 28, 750 (1955); Soviet Phys. JETP 1, 604 (1955).

[6] W. Pauli and F. Villars, Rev. Mod. Phys. 21, 434 (1949).

[7] A. A. Abrikosov, Dissertation Int. Fiz. Problem, AN SSSR (1955); N. N. Bogoliubov and D. V. Shirkov, Dokl. Akad. Nauk SSSR **104**, 1391 (1955).

Translated by A. Skumanich
162

Effect of the Rate of Flow of a He II Film on Its Thickness

V. M. KONTOROVICH
Physico-Technical Institute,
Academy of Sciences, Ukrainian SSR
(Submitted to JETP editor January 27, 1956)
J. Exptl. Theoret. Phys. (U.S.S.R.) **30**, 805 (April, 1956)

IT is well known that below the λ-temperature point the wall of a container of liquid helium becomes covered with a thin ($\sim 3 \times 10^{-16}$ cm), rapidly creeping film which moves (under isothermal conditions) in the direction of a lower level[1-4] (i.e., toward a lower gravitational potential). It is of interest to ascertain how the motion influences the thickness of the film. The fact that some influence is expected follows from the dependence of the thermodynamic potential of He II on the rate of relative motion of the superfluid and the normal component[5,6].

We shall consider the leaking of a film over a vertical wall. The rate of overflow of the film, i.e., the volume of fluid Q, transported by the film in unit time and across a unit perimeter, shall be considered as a known quantity. The hydrodynamic equations of motion in a constant potential field are obtained in the customary manner from the conservational laws and the requirement of the existence of a velocity potential for the superfluid motion[5,6]. The equations of motion for the superfluid component prove to be

$$\mathbf{v}_s + \nabla \{ {}^1/_2 v_s^2 + \tilde{\mu} + U \} = 0. \tag{1}$$

Here $\tilde{\mu}$ is the chemical potential of helium per unit mass in the absence of a field, U is the potential energy per unit mass of fluid. For the problem under consideration, U equals $\beta y^{-3} + gz$, where β is a constant specifying the Van der Wall's interaction with the wall. The y-axis is directed along the normal to the wall and lies in the plane that contains the horizontal surface of the helium in the container.

We shall consider the motion quasi-stationary. In view of the extremely small film thickness we can neglect the motion of the normal component in comparison to the superfluid: $v_n = 0$. If we insert $\tilde{\mu} = \mu(P, T) - (\rho_n / 2\rho) v_s^2$ into Eq. (1) and integrate over the free surface of the film, we find that

$$(\rho_s / 2\rho) v_s^2 + \mu(P, T) + gz - \beta\delta^{-3} = \mu(P_0, T_0), \tag{2}$$

where δ is the thickness of the film at height z and P_0, T_0 is the pressure and temperature, respectively, at the horizontal surface. We shall consider the flow isothermal. Then

$$\mu(P, T) - \mu(P_0, T_0) = (P - P_0) / \rho. \tag{3}$$

The boundary condition at the free surface requires

$$P_\sigma + P = P_0, \tag{4}$$

where P_σ is the pressure associated with the curved surface. The change in the pressure of helium vapor with height is neglected. If we consider a z sufficiently large in comparison with the capillary constant of helium so that the film can be considered plane-parallel, then we obtain from Eq. (2) through (4)

$$(\rho_s / 2\rho) v_s^2 + gz - \beta\delta^{-3} = 0. \tag{5}$$

In this part of the film the flow rate is

$$Q \equiv \frac{\rho_s}{\rho} \int_0^\delta v_{sz}\, dy \approx v_s \delta \frac{\rho_s}{\rho}.$$

Expressing v_s in terms of Q and allowing for the fact that

$$(\rho / 6\rho_s)\, (Q^2/\beta)\, (\beta / gz)^{1/3} \equiv q \ll 1,$$

we find from Eq. (5) that

$$\delta = (\beta / gz)^{1/3} (1 - q). \tag{6}$$

For observed values of Q we find that $q \sim 10^{-1}$ to 10^{-2} [1,2]. For $Q = 0$ we obtain the usual equation for thin stationary helium films[7]. We note that the form of the first term in Eq. (5) is specified by the dependence of the chemical potential on the relative rate of flow.

I use this opportunity to express my sincere gratitude to Prof. I. M. Lifshitz for detailed discussions on the problems considered in this note.

[1] V. Keezom, *Helium, with "Supplement"* by I. M. Lifshitz and E. L. Andronikashvili, IIL, 1949.

[2] B. N. Esel'son and B. G. Lazarev, J. Exptl. Theoret. Phys. (U.S.S.R.) **23**, 552 (1952).

[3] K. R. Atkins, Proc. Roy. Soc. (London) **A203**, 119, 240 (1950).

[4] G. S. Picus, Phys. Rev. **94**, 1459 (1954).

[5] I. M. Khalatnikov, J. Exptl. Theoret. Phys. (U.S.S.R.) 23, 169 (1952).

[6] L. D. Landau and E. M. Lifshitz, *Mechanics of Continuous Media*, Ch. 7, 1953.

[7] Ia. I. Frenkel', J. Exptl. Theoret. Phys. (U.S.S.R.) 10, 650 (1940).

Translated by A. Skumanich
167

Specific Heat of Solid Oxygen between 20° and 4° K

M. O. KOSTRIUKOVA
Moscow State University

(Submitted to JETP editor March 22, 1956)
J. Exptl. Theoret. Phys. (U.S.S.R.) 30, 1162-1164 (June, 1956)

WE have previously reported measurements of the heat capacity of solid oxygen below 4° K [1]. These were undertaken to clarify the question of the character of the magnetic anomalies in solid oxygen. The absence (in the expression for the heat capacity) of a term which depends linearly on the temperature suggested that, at liquid helium temperatures, solid oxygen is in an antiferromagnetic state. It was surmised that a transition of the oxygen to an antiferromagnetic state took place in the temperature interval between 4° and 10° K. In order to verify this surmise, measurements of the heat capacity of solid oxygen have been carried out between 4° and 20° K in the present work.

A calorimeter similar to that described in Ref. 2 was used for the measurement of the heat capacity [2]. A high vacuum was produced in the container as a result of the adsorption by activated charcoal of heat-exchanging helium or hydrogen introduced therein. The temperature scale in these experiments was established with the aid of a carbon resistance thermometer, which was calibrated before each experiment in terms of the vapor pressure of helium and hydrogen*.

TABLE

First series of measurements		Second series of measurements		Third series of measurements	
T° K	C cal/mole-degree	T° K	C cal/mole-degree	T° K	C cal/mole-degree
4.325	0.0343	4.275	0.0361	12.50	1.06
4.387	0.0372	4.32	0.0367	13.06	1.16
4.723	0.0481	4.66	0.0463	13.15	1.21
4.89	0.0544	4.685	0.0485	13.93	1.43
4.947	0.0556	4.727	0.0481	14.02	1.36
5.235	0.0686	5.01	0.0592	14.09	1.51
5.282	0.0756	5.12	0.0575	14.17	1.42
5.47	0.0788	5.67	0.0840	14.26	1.48
5.52	0.0798	5.71	0.0883	14.73	1.61
5.76	0.0937	6.49	0.140	14.8	1.62
5.81	0.0961	6.55	0.140	14.89	1.60
6.32	0.118	7.41	0.213	14.97	1.69
6.37	0.132	7.46	0.215	15.06	1.66
6.95	0.167	8.14	0.285	15.39	1.80
7.67	0.227	8.19	0.304	15.47	1.83
7.78	0.236	8.25	0.296	15.95	2.03
8.70	0.346	8.43	0.312	16.04	2.01
8.75	0.350	8.63	0.350	16.13	1.98
9.25	0.424	8.68	0.343	16.78	2.28
9.72	0.470	8.76	0.359	16.88	2.15
—	—	8.82	0.364	16.97	2.25
—	—	8.97	0.397	17.68	2.59
—	—	10.38	0.599	17.77	2.58
—	—	—	—	18.52	2.74
—	—	—	—	18.61	2.82
—	—	—	—	19.25	3.03
—	—	—	—	19.35	3.08

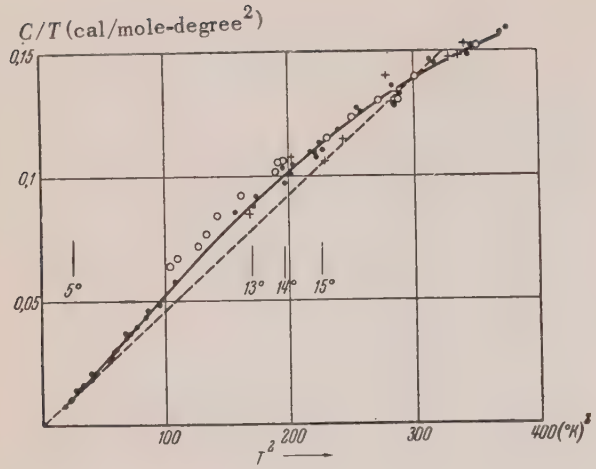

●-Data of author, O-Data of Clusius, +-Data of Giauque and Johnston.

The results of three series of measurements of the heat capacity of solid oxygen between 20° and 4° K are given in the Table. These same results are plotted in the graph (which gives C/T as a function of T^2) and are compared with the results of the measurements of Clusius[3] and Giauque and Johnston[4] which extend, respectively, to 10° and 13° K. The dotted line in the drawing represents an extrapolation of the cubic temperature dependence of the heat capacity of oxygen, found in measurements between 4° and 1.6° K [1]. It is evident from these results that the heat capacity of solid oxygen increases smoothly for the temperature range 4°-20° K, while, beginning at 5°K, the departure from the cubic law of change of heat capacity with temperature increases. The smooth character of the change in the heat capacity between 4° and 10° K bears witness to the absence of any antiferromagnetic transformation in solid oxygen in the temperature range investigated.

The measurements were carried out at the Institute for Physical Problems of the Academy of Sciences, USSR.

* A thermometer made from a radio resistor was kindly lent by B. N. Samoilov.

[1] M. O. Kostriukova and P. G. Strelkov, Dokl. Akad. Nauk SSSR **90**, 525 (1953).

[2] M. O. Kostriukova, Dokl. Akad. Nauk SSSR 96, 959 (1954).

[3] K. Clusius, Z. Phys. Chem. 3, 41 (1929).

[4] W. F. Giauque and H. L. Johnston, J. Am. Chem. Soc. 51, 2300 (1929).

Translated by R. T. Beyer
245

The Theory of Cyclotron Resonance In Metals

M. Ia. Azbel and E. A. Kaner
Physico-Technical Institute, Academy of Sciences, Ukrainian SSR

(Submitted to JETP editor January 31, 1956)
J. Exptl. Theoret. Phys. (U.S.S.R.) 30, 811 (1956)

THE present work predicts and studies theoretically a new form of resonance in metals, which differs fundamentally from diamagnetic resonance.[1] In metals close to resonance, the skin-depth δ is much less than the radius r of the orbit in the magnetic field.* Thus in a constant magnetic field $H(H_x=H,\ H_y=H_z=0)$, parallel to the surface of the metal $z=0$, an electron which moves in a helical orbit through a number of revolutions ($l/2\pi r >> 1$ where l is the mean free path) will return several times into the layer of thickness $\delta << r$ where the electric field is large. Thus the motion is similar to that of an electron in a cyclotron with a single dec, so that for a value of ω which is a multiple of the 'cyclotron' frequency $\Omega_0 = eH/mc$ ($\omega = q\Omega_0$, $q = 1, 2, \ldots$) we shall have resonance. This resonance in metals we shall call cyclotron resonance (as distinct from diamagnetic resonance,** which occurs only in semiconductors, for $\omega = \Omega_0$).

If the magnetic field is not parallel to the surface of the metal, the electrons will pass through the layer once only, and resonance will be absent since the impedance does not depend on the magnetic field.

The condition for cyclotron resonance $\delta << r << l$ corresponds to the anomalous skin effect, so that the system is governed by Maxwell's equations together with the kinetic equation for $f_1(z, E, p, \tau)$, the perturbation to the Fermi distribution function (E – energy, p – momentum, $\tau = (eH/m_0 c)t$, t – periodic time of electron in orbit[2], m_0 – effective mass of electron). The role of boundary condition on f_1 is played by the requirement that f_1 shall be periodic with respect to τ with period $\theta = m_0^{-1} dS/dE$, together with the condition of diffuse reflection at the surface.[3] The problem is solved under the most general conditions of the electron theory of metals – for arbitrary energy dependence $E = E(p)$ and arbitrary collision term $(df_1/dT)_{coll.}$. It turns out that in the anomalous skin effect region, because of the particular form of f_1, the collision

integral can be put in the form $f_1/t_0(p)$ (in the zero approximation where $\delta/l \ll 1$.

Omitting all calculations, we give the final equation for the surface impedance $Z_j = R_j + iX_j$ $\times (j = x', y')$ close to resonance, where

$$\omega \sim \frac{|e|H}{m_0 c}, \qquad (1)$$

$$\frac{m_0 c}{|e|t_0} \ll H \ll v\sqrt{2\pi m_0 n}; \quad \frac{|\omega - q\Omega_0|}{\omega} \ll 1.$$

Under these conditions

$$Z_j \equiv -\frac{4\pi i\omega}{c^2}\frac{E_j(0)}{E_j'(0)} = 2I\left(\frac{\sqrt{3}\pi\omega^2}{c^4 B_j}\right)^{1/3} e^{i\pi/3}; \quad I \approx 1, \qquad (2)$$

where x', y' are the principal axes, and B_j is the principal (diagonal) value of the tensor B_{ik} ***,

$$B_{ik} = \frac{16e^2 m_0}{3h^3}\int \frac{v_i(\tau_1)\,v_k(\tau_1)}{|v_z'(\tau_1)|} \times \left[1 - \exp\left\{-\frac{2\pi}{\Omega}\overline{\left(\frac{1}{t_0}\right)} - 2\pi i\frac{\omega}{\Omega}\right\}\right]^{-1}_{\varepsilon=\varepsilon_0} dp_x; \qquad (3)$$

$$\Omega = \frac{2\pi|e|H}{c\,|\partial S/\partial\varepsilon|}; \quad v_z(\varepsilon_0, p_x, \tau_1) = 0;$$

$$p_y(\varepsilon_0, p_x, \tau_1) > 0; \quad \overline{\left(\frac{1}{t_0}\right)} = \frac{1}{\theta}\int_0^\theta \frac{d\tau}{t_0};$$

S – cross-sectional area of Fermi surface $E(p) = E_0$ by the plane $p_x = \text{const.}$, (assuming the Fermi surface is closed; if the orbit is open, resonance is absent) ****

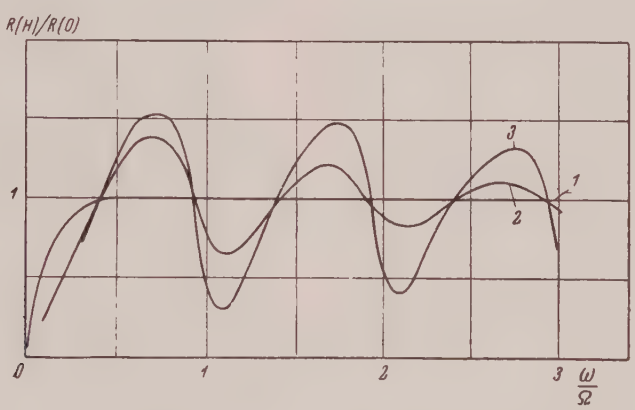

$1 - \omega t_0 = 1$; $2 - \omega t_0 = 10$; $3 - \omega t_0 = 50$

If $\Omega >> 1/t_0$, and Ω is not close to a resonance ω/q ($q = 1, 2, \ldots$) the denominator of the integrand in Eq. (3) is near unity, and Z does not depend on the collision integral. For $\Omega \approx /q$, the denominator becomes small, and for

$$\Omega_{res} \equiv \frac{2\pi|e|H_{res}}{c\,|\partial S/\partial\varepsilon|_{ext}} = \frac{\omega}{q}(1 + \Delta); \qquad (4)$$

$$|\Delta| \ll 1; \quad q = 1, 2, \ldots \ll \frac{1}{2\pi}\left(\frac{r}{\delta}\right)^{2/3}$$

we have resonance. The relative heights of resonance, R_{res}/R_0 and X_{res}/X_0, are determined by $K = 1/\omega t_{00}$ and differ considerably in the following cases:

1. If the surface $E(p) = E_0$ is an ellipsoid, dS/dE is independent of p_x;

$$R_{res}/R_0 \sim \varkappa^{2/3}, \quad X_{res}/X_0 \sim \varkappa^{1/3}. \qquad (5)$$

2. If $E(p) = E_0$ is not an ellipsoid, and the extremum of dS/dE is a minimum;

$$R_{res}/R_0 \sim \varkappa^{4/5}, \quad X_{res}/X_0 \sim \varkappa^{1/5}. \qquad (6)$$

If the extremum of dS/dE is a maximum:

$$R_{res}/R_0 \sim \varkappa^{1/5}, \quad X_{res}/X_0 \sim \varkappa^{1/5}. \qquad (7)$$

Here Z_0 is the surface impedance in zero magnetic field; $1/t_\infty$ is the value of $1/t_0$ for $p_x = p_0$; p_0 is the value of p_x at which dS/dE has its extreme value.

The relative shift of resonant frequency Δ [cf. Eq. (4)] differs for R and X. The shift of order K which occurs for X in all cases and for R in case (7) is connected with the growth of the number of revolutions of the electron between collisions with increase of H. A shift of order $K^{1/2}$ (for R in cases (5), (6)), although it leads to a phase change of π in the electric field after $(2q|\Delta|)^{-1}$ revolutions of the electron, also turns out to be profitable, since it is equivalent to a small change in phase of the electric field in the layer $\delta (X >> R)$.

The character of the resonance can be seen in the sketch, where is shown $R(H)/R_0$ versus $\omega/\Omega = mc\,\omega/eH$ for various ratios of ω to $1/t_0$, in the simplest case of an ellipsoidal Fermi surface with l/t_0 independent of p_x.

The conclusions reached above are also valid when several zones are present. An experimental study would in principle allow one : (a) to find out, from the existence or not of the resonance, whether the surface $E(p)=E_0$ is closed, (b) to determine the degree of filling of the zones, i. e. how far the Fermi surface differed from ellipsoidal shape; (c) to establish the speed of electrons at the Fermi surface (4), by determining from H_{res} the value of $(dS/dE)_{ext}$. In the presence of several surfaces, we can determine the speed on each in turn; in equation (4) only $(dS/dE)_{ext}$ enters. Note that here we discuss only the main surfaces, not the anomalously small zones.[5]

The authors thank I. M. Lifshitz, L. D. Landau and M. I. Kaganov for discussions.

---

* $\delta/r \sim Hm^{1/3}\hbar^{-1}n^{-2/3} \sim 10^{-6}$ $H \ll 1$. In semiconductors, where diamagnetic resonance is observed, $\delta/r \gg cm(|e|t_0)^{-1}(nkT)^{-1/2} \gtrsim 1$ (t_0 – time of free path, n – density of electrons, $\omega t_0 >> 1$, ω – angular frequency of electromagnetic field, T – temperature).

**Unfortunately, diamagnetic resonance has often been called cyclotron resonance in the literature. The present nomenclature seems more appropriate.

*** It turns out that near resonance, for a non-quadratic law of dispersion the complex tensor B_{ik} can be reduced to principal axes. For a quadratic law of dispersion $E(p)=\frac{1}{2}\mu_{ik}p_ip_k$ and $1/t_0$ independent of p_x, this is possible for all ω and H, and equation (2) is valid for $\delta \ll \tau \ll l$ and becomes an interpolation formula for all $H \ll v\sqrt{2\pi m_0 n} \sim 10^6$ G.

**** The derivation of these equations, and detailed discussion of some further points, will be the subject of a separate article.

Note added in proof: Quite recently a paper has appeared[6] on a resonance in bismuth: this is to be distinguished from the resonance discussed here, since the latter (1) occurs at multiple frequencies, (2) occurs independently of the sign of the magnetic field, (3) occurs only for magnetic fields exactly parallel to the surface of the specimen (the angle ϕ must satisfy $\phi > (\delta/r)^{2/5}$). In particular, condition (3) is not fulfilled in the work referred to.

[1] Ia. G. Dorfman, Dokl. Akad. Nauk SSSR 81, 765 (1951); R. B. Dingle, Proc. Roy. Soc. (London) A212, 38 (1952); Dresselhaus, Kip and Kittel, Phys. Rev. 98, 368 (1955).

[2] Lifshitz, Azbel and Kaganov, J. Exptl. Theoret. Phys (U.S.S.R.) 30, 220, 1956; Soviet Phys. JETP 3, 143 (1956).

[3] K. Fuchs. Proc. Camb. Phil. Soc. 34, 100 (1938).

[4] I. M. Lifshitz and A. B. Pogorelov, Dokl. Akad. Nauk SSSR 96, 1143 (1954).

[5] I. M. Lifshitz and A. M. Kosevitch, Dokl. Akad. Nauk SSSR 96, 963 (1954).

[6] Galt, Yager, Merritt, Cetlin and Dail, Phys. Rev. 100, 748 (1955); R. N. Dexter and B. Lax, Phys. Rev. 100, 1216 (1955).

Translated by D. Shoenberg
171

Quantum Theory of Electrical Conduction in a Magnetic Field

I. M. LIFSHITZ
Physico-Technical Institute, Acadmey of Sciences, Ukrainian SSR

(Submitted to JETP editor January 24, 1956)
J. Exptl. Theoret. Phys. (U.S.S.R.) 30, 814 (1956)

IN a previous paper we have developed a theory of galvanomagnetic phenomena in strong magnetic fields, treating the electrons classically as Fermi-particles with a general dispersion law $E=E(p)$.[1] There, however, we did not treat certain specific phenomena connected with the quantisation of the electronic energy levels (for example, the oscillations in resistance as the magnetic field changes). Such effects are observed experimentally[2], but previous theoretical investigations[3] are not entirely satisfactory. In the present paper we shall construct a consistent quantum-mechanical theory of metallic conduction in a magnetic field.

1. In quasi-classical approximation, the spacing of levels in a magnetic field in the z direction is given by[4]

$$\Delta\varepsilon_n = \varepsilon_{n+1} - \varepsilon_n = \mu^* H; \qquad (1)$$

$$\mu^* = \frac{e\hbar}{m^* c}; \quad 2\pi m^* = \frac{\partial S}{\partial \varepsilon},$$

where $S=S(E,p_z)$ is the area cut by the surface $E(p)=E$ in the plane p_z = constant. Thus the essentially quantum-mechanical effects appear when $\mu^* H \sim kT$.

The Hamiltonian $\mathcal{H}$ of an electron in a magnetic field $H_z=H$ and an electric field E may be written

$$\hat{\mathcal{H}} = \hat{\mathcal{H}}^0 + \hat{U}; \quad \hat{U} = -e\mathbf{E}\mathbf{r}, \tag{2}$$

where $\hat{H}^0$ is the kinetic energy operator of an electron in the magnetic field. This is obtained (at least in the quasi-classical approximation) from $E(p_x, p_y, p_z)$ by substituting for the momentum components of the kinetic momentum operator satisfying $[\hat{p}_x, \hat{p}_y] = eH/c$, suitably symmetrized. The exact significance of this need not be discussed in this approximation.

According to the quantum theory the electronic state is described by the density matrix $\hat{f}$. In the absence of an electric field, $\hat{f} = \hat{f}^0$ is the equilibrium Fermi distribution.

$$\hat{f}^0 = f^0(\hat{\mathcal{H}}^0); \quad f^0(z) = (1 + e^{(z-\zeta)/kT})^{-1}.$$

When the electric field is present, we put $\hat{f} = \hat{f}^0 + \hat{f}^1$. The kinetic equation for $\hat{f}^1$ is given by

$$[\hat{f}^1, \hat{\mathcal{H}}] + [\hat{f}^0, \hat{\mathcal{H}}] + \tilde{W}\hat{f}^1/t_0 = 0$$

or including only terms linear in E

$$[\hat{f}^1, \hat{\mathcal{H}}_0] + \tilde{W}\hat{f}^1/t_0 = -[\hat{f}^0, \hat{U}] \tag{3}$$

where $\tilde{W}/t_0$ is a certain linear transformation, corresponding to the collision integral, and t_0 has the nature of a relaxation time. The operator f^1 is diagonal with respect to p_z but not with respect to n. Equation (3) when written in terms of matrix elements becomes

$$\frac{i}{\hbar}(\varepsilon_{n'} - \varepsilon_n) f^1_{n,n'} + (\tilde{W}f^1)_{n,n'} \frac{1}{t_0}$$

$$= -e\mathbf{E}\mathbf{v}_{n,n'} \frac{f^0_{n'} - f^0_n}{\varepsilon_{n'} - \varepsilon_n},$$

where $\mathbf{v}_{n,n'}$ is the matrix element of the velocity which corresponds to the classical quantity $\mathbf{v} = d\mathbf{E}/d\mathbf{p}$. From equation (1) we have $E_{n'} - E_n = (n' - n)\mu^* H$. Thus assuming that $f^1 = -et_0 \mathbf{E}\vec{\psi}$, we get after some transformation

$$ik\vec{\Psi}_k + \gamma W_{k,k'}\vec{\Psi}_{k'} = \gamma g_k \mathbf{v}_k; \tag{4}$$

$$\gamma = H_0^*/H; \quad H_0^* = m^* c/et_0;$$

$$\vec{\Psi}_{n,n+k} \equiv \Psi_k(\varepsilon_n); \quad \mathbf{v}_{n,n+k} \equiv \mathbf{v}_k(\varepsilon_n);$$

$$g_k = [f^0(\varepsilon_n + k\mu^* H) - f^0(\varepsilon_n)]/k\mu^* H$$

$$k \neq 0; \quad g_0 = \partial f^0/\partial\varepsilon.$$

In the quasi-classical approximation, the matrix elements $\mathbf{v}_k$ are the Fourier components of the classical velocity vector $\mathbf{v}$ expanded in terms of $e^{ik\phi}$, where ϕ is the angle variable around the orbit in momentum space

$$\mathbf{v}(\varepsilon, p_z, \varphi) = \sum \mathbf{v}_k e^{ik\varphi};$$

$$\varphi = 2\pi \int \frac{dl}{v_\perp} \Big/ \oint \frac{dl}{v_\perp}; \quad dl = |d\mathbf{p}|,$$

$v_\perp = \sqrt{v_x^2 + v_y^2}$. In the limit $h \to 0, (\mu^* H \to 0)$ we have $g_k \to df^0/dE$, and equation (4) becomes the classical equation for the Fourier components of the distribution function $\vec{\psi}$. The quantities $W_{k,k'}$ in this case become the Fourier components of the collision operator. At low temperatures where impurity scattering is predominant, $W_{k,k'}$ in (4) coincides with its classical analogue. Similar substitution is not however permissible for the quantity g_k when $\mu^* H \sim kT$.

The expressions for the current $\mathbf{j}$ and the conductivity $\sigma^{xx'}$ are given by the formulas

$$\mathbf{j} = e\,\mathrm{Sp}\,\hat{f}^1\hat{\mathbf{v}}; \quad \sigma^{x,x'} = -e^2 t_0\,\mathrm{Sp}\,\hat{v}^x\hat{\Psi}^{x'} \tag{5}$$

$$= \frac{e^2 t_0}{h^3} \sum_n \int \left\{ v_0^x \Psi_0^{x'} + 2\mathrm{Re} \sum_{k=1}^{\infty} v_{-k}^x \Psi_k^{x'} \right\} dp_z\, m^* \Delta\varepsilon_n.$$

In the limit $\hbar \to 0$ the expression (5) also tends to the corresponding classical formula.

2. The connection established above between the quantum-kinetic Eq. (4) and its classical analogue allows us to find an expression for the quantum effects by means of the solutions of the classical equations investigated earlier [1], and in particular to clarify the connection between the quantum oscillations of conductivity and their mean values, and also the oscillations in susceptibility (de Haas-van Alphen effect). Omitting all calculation and discussion (which is rather lengthy) we shall give here only the results obtained.

Let us write the expression for the classical conductivity tensor in terms of the 'mobility tensor' $q^{x,x'} = q^{x,x'}(E, p_z, H)$ (the value of $q^{x,x'}$ is obtained from the solution of the classical problem):

$$\sigma^{xx'} = h^{-3}\int\int f^0 q^{x,x'} m^* \, d\varepsilon \, dp_z = N^0 \overline{q^{x,x'}}. \qquad (6)$$

Here N^0 is the number of electrons in the conduction zone, and $q^{x,x'}$ is the mean value of the mobility, taken with the weighting factos f^0. Then the expression for the oscillating part $\Delta\sigma^{x,x'}$ (for $x,x' \neq z,z$) may be written in terms of the independent variables H, ζ as

$$(\Delta\sigma^{x,x'})_{H,\zeta} = q_m^{x,x'} H (\partial \ln S / \partial\varepsilon)_m \Delta M^z, \qquad (7)$$

where ΔM^z denotes the oscillatory part of the moment M^z in the de Haas-van Alphen effect and the values $q_m^{x,x'}$ and $(d \ln S / dE)_m$ are taken at the extreme cross-section of the Fermi surface $E(p) = \zeta$ by the planes $p_z = \text{const}$. An analogous expression for $\Delta\sigma^{xz}$, not given here, contains $\Delta\sigma^{zz}$ and also $d\Delta M^z / dH$.

As is known[4] each zone (or more precisely, each extreme section of the Fermi surface) gives a separate contribution to ΔM^z, and in fields $\sim 10^4$ G only anomalously small zones show themselves.[4] Note that in $\sigma^{x,x'}$ the major contribution is from 'normal' zones, which complicates comparison of Eqs. (6) and (7).

In comparing with experiment, we must also take account of the oscillations in the chemical potential $\zeta = \zeta(H)$, which are determined by the conditions that the total number of electrons in all zones remain constant. Taking account of the additional term $\Delta\sigma_1^{x,x'} = (\partial\sigma^{x,x'} / \partial\zeta)\Delta\zeta$, we obtain finally for the case where several conduction zones are present.

$$\Delta\sigma^{x,x'} = \sum_i \left\{ q_{mi}^{x,x'} - \sum_k \frac{\partial N_k^0 \overline{q_k^{x,x'}}}{\partial\zeta} \Big/ \sum_k \frac{\partial N_k^0}{\partial\zeta} \right\} H \left(\frac{\partial \ln S_i}{\partial\varepsilon}\right)_m \Delta M_i^z \qquad (8)$$

(the summation to be taken over all zones).

Thus, for example, for a single zone with a small number of electrons and an isotropic dispersion law $E = p^2/2m$, $q^{xy} = ec/H(1+\gamma^2)$, and we have:

$$\frac{\Delta\sigma^{xy}}{\sigma^{xy}} = {}^4/_3\,\gamma^2 \frac{\partial \ln t_0}{\partial\zeta} \cdot H \frac{\Delta M^z}{N^0}; \quad t_0 = t_0(\zeta).$$

The presentation of other results and also the mathematical treatment will be the subject of a detailed communication later.

The author is grateful to L. D. Landau for valuable discussions.

[1] Lifshitz, Azbel and Kaganov, J. Exptl. Theoret. Phys. (U.S.S.R.) **30**, 220 (1956); de Haas and Sohubnikov, Leid. Comm. **297**, 210 (1930).

[2] Lazarev, Makhimovitch and Parfenova, J. Exptl. Theoret. Phys. (U.S.S.R.) **9**, 1169 (1939); Borovik, Dokl. Akad. Nauk SSSR **69**, 769 (1949).

[3] A. I. Akhiezer, Dokl. Akad. Nauk SSSR **25**, 872 (1939); B. I. Davydov and I. Ia. Pomeranchuk, J. Exptl. Theoret. Phys. (U.S.S.R.) **9**, 1294 (1940); Zilberman, J. Exptl. Theoret. Phys. (U.S.S.R.) **29**, 762 (1955); Soviet Phys. JETP **2**, 650 (1956).

[4] I. M. Lifshitz and A. M. Kosevitch, Dokl. Akad. Nauk SSSR **96**, 963 (1954). J. Exptl. Theoret. Phys. (U.S.S.R.) **29**, 730 (1955); Soviet Phys. JETP **2**, 636 (1956).

Translated by D. Shoenberg
172

Concerning the Choice of Physically Acceptable Solutions of the Schrödinger Equation for the Hydrogen Atom

T. TITS
Torun' University, Poland

(Submitted to JETP editor January 15, 1955)
J. Exptl. Theoret Phys. (U.S.S.R.) 30, 948-949
(May, 1956)

IN a calculation of the stationary states of hydrogen atoms a representation of the wave function in the form

$$\Psi(r, \vartheta, \varphi) = R(r) P_l^m(\cos\vartheta) e^{\pm im\varphi} \tag{1}$$

leads to the following differential equation for R and $E < 0$ (in atomic units):

$$\frac{d^2R}{dr^2} + \frac{2}{r}\frac{dR}{dr} + \left(2E + \frac{2Z}{r} - \frac{l(l+1)}{r^2}\right)R = 0, \tag{2}$$

The characteristic equation corresponding to the differential equation (2) has two roots l and $-(l+1)$ at the point $r = 0$. Consequently, the expansions of the particular solutions R_1 and R_2 begin with the term r^l or $r^{-(l+1)}$, respectively. The eigenfunction R_2, which behaves in the expansion as $r^{-(l+1)}$, is discarded for $l \geq 1$ since the condition of quadratic integrability cannot be satisfied. For $l = 0$ Sommerfeld and Kramers[1] and Rellich[2] proposed that there is no basis for discarding the second eigensolution, since all eigensolutions are normalizable. Subsequently, Falk and Marschall[3] showed that the second particular solution R_2 still should be discarded because of the normalization condition, and the problem appeared to be clarified.

The proposals of Sommerfeld, Kramers and Rellich are indeed incorrect. However, the proof of Falk and Marschall is applicable only for the case $1 - 2z/\varkappa = -n$, $n = 0, 1, 2\ldots$ and therefore, it tacitly assumes the continuity of the solution at $r = 0$. The purpose of the present letter is to show that for the case $l = 0$ there is only one solution which can be normalized. It will also be shown below that it is necessary to impose some local condition at the point $r = 0$ in order to obtain the correct spectrum of eigenvalues.

For $l = 0$ we have the following independent eigensolutions:

$$R_1 = e^{-\rho/2}\,{}_1F_1\left(1 - \frac{2Z}{\varkappa}, 2, \rho\right), \tag{3}$$

$$R_2 = e^{-\rho/2}\,\Phi\left(1 - \frac{2Z}{\varkappa}, 2, \rho\right).$$

The following abbreviations were introduced in Eq. (3):

$$2E = -\varkappa^2/4;\ \varkappa r = \rho > 0. \tag{4}$$

${}_1F_1$ denotes the confluent hypergeometric series, and Φ is the second independent solution of the confluent hypergeometric differential equation.

As is well known[4], Φ may be written

$$\Phi(a, b, x) = \frac{\Gamma(1-a)}{2\pi i} e^{-a\pi i} \times \int_{\infty \cdot e^{i\varphi}}^{(0+)} e^{-xt} t^{a-1}(1+t)^{b-a-1}\,dt, \tag{5}$$

$$-\pi/2 \leqslant \varphi < \pi/2.$$

The asymptotic form of this function for $x \to +\infty$ is

$$\Phi(a, b, x) = x^{-a}[1 + 0(1/x)]. \tag{6}$$

Therefore, our second solution R_2 has the following form for $\rho \to +\infty$:

$$R_2 = e^{-\rho/2}\rho^{-[1-(2Z/\varkappa)]}[1 + 0(1/\rho)]. \tag{7}$$

This formula shows that the second eigenfunction R_2 can be normalized for large r. For small r the relation

$$\lim_{x \to +0} x^{b-1}\Phi(a, b, x) = \Gamma(b-1)/\Gamma(a);\ b > 1 \tag{8}$$

shows that R_2 approaches in the limit of $\rho \to +0$ the expression

$$\lim_{\rho \to +0} R_2 = \frac{e^{-\rho/2}}{\Gamma[1-(2Z/\varkappa)]}\frac{1}{\rho}. \tag{9}$$

Equations (7) and (9) show that R_2 can be normalized for all eigenvalues $E < 0$. Thus there always exists a solution that can be normalized. Further-

more, we note that the normalization conditions are not sufficient to obtain the correct spectrum of eigenvalues. This deficiency can be overcome by imposing an additional regional condition, namely, the condition that the function be regular at the origin. If we demand that $1-(2Z/\varkappa) = -n$, $n = 0, 1, 2\ldots$, then Φ goes into the Laguerre polynomial, and consequently, the function R_2 is regular at $r = 0$. For $1-(2Z/\varkappa) = -n$ the functions R_1 and R_2 are lineraly dependent and for $1-(2Z/\varkappa) \neq -n$ they are linearly independent. In conclusion, we note that for $l = 0$ the theory of Weyl also demands some regional condition. In the present case the demand that the solution be regular corresponds to the choice of some fully determined boundary condition of Weyl for $r = 0$. In this way the demand of regularity guarantees the physical correctness of the spectrum of eigenvalues. It is also possible to substantiate the regional condition at $r = 0$ by making a use of the Hermiticity conditions[5].

[1] A. Sommerfeld, *Atombau und Spektrallinien*, 2 Auf. 2 Bd., Braunschweig, 1944; H. A. Kramers, *Quantentheorie des Elektrons und der Strahlung*, Leipzig, 1938.

[2] F. Rellich, Math. Z. 49, 719 (1943-1944).

[3] G. Falk u. H. Marschall, Z. Phys. 131, 269 (1952).

[4] F. G. Tricomi, Math. Z. 52, 668 (1950).

[5] T. Tietz, Ann. Physik 15, 79 (1954).

Translated by M. J. Stevenson
189

Nuclear Capture of Neutrons with an Energy of Several MEV

V. L. GUREVICH
Leningrad State University

(Submitted to JETP editor January 4, 1956)
J. Exptl. Theoret. Phys. (U.S.S.R.) 30, 961-962 (May, 1956)

THE object of the present note is to calculate the cross section for neutron capture by excitation of the nuclear volume vibrations.

The incident neutron, interacting with the vibrational motion, gives up its energy and goes into a bound state in the nucleus. We consider the excitation of the first radial vibration, the frequency of which ω_0 corresponds to an energy of the order 10 mev.[1] The corresponding level has an appreciable width γ as a result of dissipation. However, such a mechanism of capture makes sense if the width of the level is not too large compared with the vibrational energy.

The Schrödinger equation of the system, nucleus + neutron, is

$$[-(\hbar^2/2M)\nabla^2 + U_0(r) + U(\mathbf{r}, Q) + T + W]\Psi = E\Psi, \quad (1)$$

where $\mathbf{r}$ is the radius vector of the neutron, U_0 is a spherically symmetrical potential well of depth V_0 and radius R; $U(\mathbf{r}, Q)$ is the potential arising from the nuclear density vibrations described by coordinates Q; T and W are the kinetic and potential energies of vibration. According to Ref. 1, for a two-fluid compressible model of the nucleus

$$W = \frac{1}{2}\int (a\delta\rho_p^2 + 2b\delta\rho_p\delta\rho_n + a\delta\rho_n^2)\, d\tau, \quad (2)$$

where $\delta\rho_p$ and $\delta\rho_n$ are the deviations of neutron and proton densities from their static values and $\delta\rho_{n,p} = f_{n,p}(\mathbf{r})\, Q$;

$$f_p(r) = D_{1p}j_0(q_1r) + D_{2p}j_0(q_2r); \quad (3)$$

$$f_n(r) = D_{1n}j_0(q_1r) + D_{2n}j_0(q_2r).$$

Here the constants D and q depend only on the number of neutrons and protons in the nucleus; j_l is the spherical Bessel function of order l.

In zero order

$$\Psi = \psi(\mathbf{r})\varphi(Q);$$

$$-\frac{\hbar^2}{2M}\nabla^2\psi + U_0\psi = E^{(0)}\Psi; \quad (T+W)\varphi = \varepsilon\varphi.$$

Bearing in mind the short range of nuclear force, we consider that the interaction energy of the neutron with the vibrations is proportional to the density deviation $\delta\rho = \delta\rho_n + \delta\rho_p$ at that point where the neutron is located. We define the coefficient of proportionality such that the interaction with a single-fluid static distribution of charge could be described by a potential U_0.

After summation over all final states of the captured neutron, the cross section is, to first approximation in perturbation theory;

$$\sigma = \sum_{nl}\sigma_{nl} = (2\pi/\hbar)\sum_{nl}|U_{nl}|^2, \quad (4)$$

where l is the angular momentum of the captured neutron, n is the quantum number of the bound state with momentum l;

$$U_{nl} = -\frac{4\pi r_0^3 V_0}{3M}\int \psi_{nl}\varphi(Q)\,\delta\rho\psi_k h_0(Q)\,d\tau\,dQ, \quad (5)$$

where $R = r_0 A^{1/3}$, $\psi_{n,l}$ and ψ_k are the wave functions of the captured and incident neutron, $h_0(Q)$ is the wave function of the oscillator ground state. Because of the rapid fall off of the latter, in the integration indicated in Eq. (5) small Q are important and therefore the wave function of an excited level of width γ is [2]

$$\varphi(Q) = \{\gamma/\pi[(\varepsilon-\varepsilon_0)^2+\gamma^2]\}^{1/2} h_1(Q), \quad (6)$$

where $h_l(Q)$ is the wave function of the first excited state of the oscillator.

Carrying out the integration in Eq. (5) and using Eq. (2), we obtain

$$\sigma_{nl} = \frac{4\pi^4(2l+1)r_0^4 V_0^2}{9A^{2/3}a\hbar^2 MkK^2} \quad (7)$$

$$\times \frac{\cos\eta_l j_l(kR) + (-1)^l \sin\eta_l j_{-l-1}(kR)}{j_l(KR)}$$

$$\times \frac{\hbar\omega_0\gamma}{(E_k^{(0)} - E_{nl}^{(0)} - \hbar\omega_0)^2+\gamma^2} F_{nl}^2(k),$$

where $\hbar k = \sqrt{2ME_k^{(0)}}$; $\hbar K = \sqrt{2M(E_k^{(0)}+V_0)}$; η_l is the lth phase shift from the potential U_0^3;

$$F_{nl}(k) = F_{nl}^{(1)}(k) + F_{nl}^{(2)}(k), \quad F_{nl}^{(i)}(k) \quad (8)$$

$$= \alpha_i\left[P_l\left(\frac{K^2+\varkappa_{nl}^2-q_i^2}{2K\varkappa_{nl}}\right) - \frac{\cos(q_i+\varkappa_{nl}-K)R}{\pi(q_i+\varkappa_{nl}-K)R}\right],$$

$$\hbar\varkappa_{nl} = \sqrt{2M(E_{nl}^{(0)}+V_0)},$$

where P_l is the Legendre polynomial of order l, α_i is a dimensionless constant of order unity, which can be expressed in terms of D and q and, consequently, depends only on the number of neutrons and protons in the nucleus. In carrying out the integration of Eq. (5) we use the relation [4]

$$\int_0^\infty j_0(qr)\,j_l(Kr)\,j_l(\varkappa r)\,r^2\,dr = \frac{\pi}{4K\varkappa q} P_l\left(\frac{K^2+\varkappa^2-q^2}{2K\varkappa}\right), \quad (9)$$

valid for $K-\varkappa < q < K+\varkappa$; $q_i R$ is the order of several units; if [5] $V_0 = 40$ mev, the inequality is satisfied. The formula (7) is valid only for $l \ll \varkappa R$, which is also satisfied, in so far as in Eq. (4) only those terms are important for which $E_k^{(0)} - E_{nl}^{(0)} - \hbar\omega_0 \sim \gamma$ and so far as for large l there are no bound states.

Taking [1] $a = 3.4\times10^5$ cm^5 gm^{-1} sec^{-2} and considering the order of several mev, we obtain a cross section of order 10^{-26} cm^2.

The author expresses his deep gratitude to K. A. Ter-Martirosian for valuable advice and discussion of the problem.

[1] J. M. Araujo, Nuovo Cimento 12, 700 (1954).

[2] V. A. Fock, *Summary of Lectures on Quantum Mechanics*, delivered in 1936-1937 at Leningrad University, duplicated, Leningrad State University, 1937.

[3] N. Mott and H. Massey, *Theory of Atomic Collisions*.

[4] G. Watson, *Theory of Bessel Functions*.

[5] R. K. Adair, Phys. Rev. 94, 737 (1954).

Translated by G. E. Brown
196

Characteristics of the Levels of Nonspherical Even-Even Nuclei

I. S. SHAPIRO
Moscow State University

(Submitted to JETP editor February 12, 1956)
J. Exptl. Theoret. Phys. (U.S.S.R.) 30, 975-977 (May, 1956)

IN the adiabatic approximation the state of motion of external nucleons in a nonspherical nucleus which possesses an axis and center of symmetry is defined by quantum numbers that are completely analogous to the quantum characteristics of electronic terms for a diatomic molecule containing identical nuclei. [1] In this case the sum Ω of the projections w_i of the nucleonic spins on the axis of symmetry of the nucleus and the parity of the state $P = \pm 1$ are integrals of the motion.

In the present note we consider the characteristics of levels with $\Omega = 0$. Analogous to the Σ terms of a diatomic molecule, in the case of $\Omega = 0$ there is an additional quantum number $\eta = \pm 1$ which characterizes the behavior of the wave function under reflection with respect to a plane passing through the nuclear axis of symmetry,

i.e., for the transformation $r \to r$, $\vartheta \to \vartheta$, $\varphi \to 2\Phi - \varphi$, where r, ϑ, φ are the polar coordinates of a point and Φ is the azimuthal angle of the plane with respect to which the reflection is performed. This transforms the wave function $\psi_{\Omega P}$ into $\hat{I}_\Phi \psi_{\Omega P} = \psi_{\Omega P}$. Since the Hamiltonian of the system (neglecting rotation of the nucleus) is invariant with respect to the above reflection because of the axial symmetry of the entire problem, each term will be doubly degenerate in Ω. For $\Omega = 0$

$$\hat{I}_\Phi \psi_{0P\eta} = \eta \psi_{0P\eta}, \ \eta = \pm 1, \qquad (1)$$

so that instead of the degeneracy there can be two levels with different values of η.*

The states with $\Omega = 0$ can exist in nuclei with even A. Particularly in even-even nuclei (even Z, even A) levels with $\Omega = 0$ surely are to be found. These include, for example, the ground state (total spin $J = 0$, $P = \pm 1$) and the first excited level ($J = 2$, $P = +1$) which is of rotational origin. The ground and first excited levels of even-even nuclei will be characterized by identical values of η [see (2), below] . The same refers to all levels which differ only in excitation of collective degrees of freedom. Levels which differ in the states of external nucleons can in principle have either identical or different η.

The following selection rule for radiative transitions is associated with η: transitions between levels with identical η can only be of an electric multipole type, whereas transitions accompanied by a change of the sign of η can only have magnetic character.

Since we are actually considering transitions between levels with $\Omega = 0$ the projection w_r of the angular momentum of the quantum on the nuclear axis of symmetry must also be 0. The wave function of the quantum will therefore be the eigenfunction of the operator $\hat{I}_\Phi$ with eigenvalues $\eta_r = \pm 1$. On the other hand, it is easily shown that in the most general case

$$\eta = (-1)^J P. \qquad (2)$$

When we apply (2) to electric and magnetic 2^l-pole radiation we obtain

$$P_E = (-1)^l, \ \eta_E = +1;$$
$$P_M = (-1)^{l-1}, \ \eta_M = -1. \qquad (3)$$

Since η is an integral of the motion the following relationship must be in effect between the quantum numbers η_i, η_t of the initial and final nuclear states:

$$\eta_i = \eta_r \eta_f. \qquad (4)$$

From Eqs. (3) and (4) it follows that $\eta_i = \pm \eta_t$ for electric (+) and magnetic (−) transitions, respectively.

The above-mentioned selection rules have several interesting consequences. Let us, for example, consider two levels: i, f with $\Omega = 0$ and $|\Delta J| \lesssim l - 1$, $P_i = (-1)^l P_f$ (we assume that $J_i \neq 0$ and $J_f \neq 0$). In this case electric 2^l-pole and magnetic 2^{l-1} - pole transitions are allowed simultaneously by the parity and spin selection rules. If, however, they are not specially forbidden, the magnetic transitions should predominate, as the ratio of the squares of the matrix elements of an electric 2^l-pole and a magnetic 2^{l-1}-pole transition is equal (in order of magnitude) to $[(l^2 - 1)/l(2l+1)](R/\lambda)^2/\beta^2$, where R is the nuclear radius, λ is the radiation wave length divided by 2π and β is the ratio of nucleon velocity in the nucleus to the velocity of light. When the transition energy is of the order of a few hundred kev for a nucleus with $A = 100 - 200$, this ratio will be much below 1. The above selection rules for η can change the situation; for example, the matrix element of a magnetic transition between levels with $\eta_i = \eta_f$ can have a considerably reduced value. Strong forbiddenness of the magnetic transitions is, of course, not to be expected, as Ω and η are good quantum numbers only in the adiabatic approximation, which can be assumed to be valid for nuclei which are markedly nonspherical. When the nonsphericality is small we can expect only a certain reduction of magnetic transition probabilities leading to mixed radiation [$E(l) + M(l-1)$] .

In view of the above it is interesting to examine the experimental data for even-even nuclei. Among these are nuclei whose first two excited levels are characterized by $J = 2$, $P = +1$ (expressed briefly as 2^+)[3-5] for which the $2^+ \to 2^+$ transition is usually mixed ($E2 + M1$). An important point is that the farther the numbers Z and $N = A - Z$ are from the magic numbers the smaller the $M1$ contribution (see the table). Since the nonsphericality of nuclei increases with the number of nuclei outside closed shells the data of the table clearly show that the probability of $E2$ radiation from the $2^+ \to 2^+$ transition in even-even nuclei is augmented as the nucleus becomes less spherical. This is also supported by the position of the first excited (rotational) level, which is lowered with greater nonsphericality. Among the nuclei included in the table the lowest of the first excited levels is found in the isotopes of Pt, for which

the $M1$ fraction in the $2^+ \rightarrow 2^+$ transition is also smallest. For Pt nuclei, in addition, $|N-N_{mag}| \geq 8$, $|Z-Z_{mag}| \geq 4$, whereas for the other nuclei in the table $|N-N_{mag}| \geq 2$, $|Z-Z_{mag}| \geq 2$. This fact can be explained by the selection rules which were referred to above. If, indeed, it is assumed that for the states being considered $\Omega = 0$, then by (3) $\eta_i = \eta_f = +1$, so that magnetic radiation will be forbidden.

$2^+ \rightarrow 2^+$ transitions in even-even nuclei

Nucleus	$N-N_{mag}$ / $Z-Z_{mag}$	% $M1$ in transition	transition energy in kev	Position of first excited level in kev
$^{76}Se_{34}^{42}$	+2 / −6	20—66	650	560
$^{122}Te_{52}^{70}$	−12 / + 2	20	680	560
$^{114}Cd_{48}^{66}$	+16 / − 2	95,6	710	530
$^{194}Pt_{78}^{116}$	− 8 / − 4	5—6	330	360
$^{196}Pt_{78}^{118}$	−10 / − 4	2	1480	330
$^{198}Hg_{80}^{118}$	− 8 / − 2	30—50	680	410

In connection with these considerations it would be desirable to obtain the following experimental data: a) a comparison of the nonsphericality of the nuclei in the table through observation of the Coulomb excitation (at present data exist for Cd [114] [6-7]); b) more accurate information concerning the multipolarity of the $2^+ \rightarrow 2^+$ transition in Os^{186} (at present we have only a reference to a private communication by the author of reference [5]); c) a study of the level schemes and transition multipolarities of strongly nonspherical even-even nuclei of rare earths and heavy elements (in the majority of cases only the characteristics of the first excited levels are known at present; see Ref. 5).

*This is completely analogous to the Σ^+ and Σ^- terms of a diatomic molecule (see Ref. 2).

[1] A. Bohr, Dansk Mat.-Fys. Medd. 26, 14 (1952); A. Bohr and B. R. Mottelson, ibid, 27, 16 (1953).

[2] L. D. Landau and E. M. Lifshitz, *Quantum Mechanics*, GITTL, 1948.

[3] G. Scharff-Goldhaber and J. Weneser, Phys. Rev. 98, 212 (1955).

[4] G. Scharff-Goldhaber, Phys. Rev. 90, 587 (1953).

[5] J. J. Kraushaar and M. Goldhaber, Phys. Rev. 89, 1081 (1953).

[6] Mark, McClelland and Goodman, Phys. Rev. 98, 1245 (1955).

[7] Temmer and Heydenburg, Phys. Rev. 98, 1308 (1955).

Translated by I. Emin
203

Concerning the Correlation Function for Quantum Systems

Iu. L. Klimontovich
Moscow State University

(Submitted to JETP editor February 13, 1956)
J. Exptl. Theoret. Phys. (U.S.S.R.) 30, 977-979 (May, 1956)

THE correlation function for a classical system of weakly interacting particles can be determined by an approximate solution of the equation for the binomial distribution function.[1] In this method the distribution function f_3 in the set of equations is approximately expressed in terms of the binomial distribution function f_2.

The method of Bogoliubov is used in the present letter to determine the correlation function of a quantum system of interacting particles. Instead of a set of classical equations for the distribution function used by Bogoliubov[1] we use a set of [2] equations for the quantum distribution function. The approximation of the quantum distribution function f_3 by a binomial quantum distribution

function is made excluding the exchange effects. For the correlation function the following expression is obtained:

$$g(|q|) = g_{id} + (2\pi)^{-3}\int \frac{\nu(k)F(k)}{1-\nu(k)F(k)} e^{ikq}\,dk, \quad (1)$$

where

$$g_{id} = 1 \pm \int f_0(p')\, f_0(p'')\, e^{iq(p'-p'')}\,dp'\,dp'' \quad (2)$$

is the quantum correlation function of an ideal gas.[3] This correlation function of ideal gas, dependent on exchange effects, was first considered by V. S. Fursov and A. D. Galanin. In Eq. (2)

$$f_0 = 1/(2\pi\hbar)^3 n_0 [A\exp(p^2/2mkT \mp 1)] \quad (3)$$

is the momentum distribution function of particles distributed uniformly in space. The minus and plus signs apply to particles obeying Bose-Einstein and Fermi-Dirac statistics respectively.

The second term in Eq (1) is determined by the interaction of the particles. The functions $F(k)$ and $\nu(k)$ entering into it are evaluated in the following way

$$F(k) = \hbar^{-1}\int \frac{f_0(p+\hbar k/2) - f_0(p-\hbar k/2)}{pk/m}\,dp, \quad (4)$$

$$\nu(k) = \int \Phi(|q|)\, e^{-ikq}\,dq, \quad (5)$$

where $\Phi(|q|)$ is the potential energy of interaction of a pair of particles.

For $h = 0$ Eq. (1) goes over into the expression for a correlation function of a classical system.

$$g(|q|) = 1 - (2\pi)^{-3}\int \frac{\nu(k)}{n_0\nu(k) + kT}\, e^{ikq}\,dk, \quad (6)$$

obtained by Zubarev.[4] For completely ionized gas and $h = 0$ one obtains the Debye correlation function[1] from Eq. (1).

We shall consider several particular examples. For a completely degenerate Bose gas, Eq. (1) assumes the form

$$g(|q|) = g_{id} - (2\pi)^{-3}\int \frac{\nu(k)}{\nu(k)\, n_0 + \hbar^2k^2/2m}\, e^{ikq}\,dk. \quad (7)$$

For small momenta we may set $\nu(k) = \nu(0)$. Then we obtain from Eq. (4)

$$g(|q|) = g_{id} - (1/4)\pi n_0 r_c^2 |q| \exp(-|q|/r_c), \quad (8)$$

where $r_c = h/2mc$ is the correlation radius, $c = \sqrt{\nu(0)\, n_0/m}$ is the velocity of sound in the gas. For helium $r_c = 10^{-8}$ cm. Equation (7) for the correlation function agrees with the expression that can be obtained from the work of Bogoliubov and Zubarev[5] and Zubarev[6]. From Eq. (7) we can also obtain the correlation function for charged Bose gas.

For a completely degenerate system obeying Fermi-Dirac statistics

$$F(k) = -\frac{3m}{2p_0^2} + \frac{3m}{4p_0^3\hbar k}\left[\left(\frac{\hbar k}{2}\right)^2 - p_0^2\right]\ln\left(\frac{p_0 + \hbar k/2}{p_0 - \hbar k/2}\right) \quad (9)$$

for $\hbar k \ll p_0$ $F(k) = -3m/p_0^2$. If the considered system is plasma, then we obtain for $\hbar k \ll p_0$ the following expression for the correlation function of electrons

$$g(|q|) = g_{id} - (1/4)\pi n_0 r_d^2 |q| \exp(-|q|/r_d), \quad (10)$$

where

$$r_d = (p_0^2/12\pi e^2 n_0)^{1/4}. \quad (11)$$

is the Debye radius for degenerate Fermi gas. This determination of the correlation function of Fermi gas is for the case in which the average interaction energy is less than the limiting energy of the Fermi distribution.

In the above approximation for completely ionized gas it is possible to disregard the set of equations for quantum distribution function and one may limit oneself to a solution for the quantum distribution function[2] of the kinetic energy equation with self-consistent field. Indeed to compute the thermodynamic functions of completely ionized gas one must know the magnitude of the energy in excess of the energy of ideal gas.[3] The magnitude of this additional energy is determined by the distribution of the potential U around an arbitrary ion.

To find the equation for the potential U of a quantum system we shal use the kinetic equation with self-consistent field for quantum distribution function, which can be written for electron-ion plasma in the form[2]

$$\frac{\partial f}{\partial t} + \frac{p}{m}\frac{\partial f}{\partial q} = i\frac{e}{\hbar}\int\left[U\left(q - \frac{\hbar\vec{\tau}}{2}\right) - U\left(q + \frac{\hbar\vec{\tau}}{2}\right)\right] \times f(\vec{\eta}, p)\exp[i\vec{\tau}(\vec{\eta} - p)]\,d\vec{\tau}d\vec{\eta}; \quad (12)$$

$$\Delta U = -4\pi e\left\{\int f(q, p)\,dp - n_i\right\}.$$

From Eq. (12) we obtain the relation for U assuming that the deviation of the distribution function from f_0 is small, i.e.

$$f(q, p) = f_0(p) + f''(q, p);\ f''(q, p) \ll f_0(p). \quad (13)$$

Substituting Eq. (13) into Eq. (12) and retaining only the first order terms, we obtain for $\partial t/\partial t = 0$ the following equation for the potential

$$\Delta U = -4\pi e^2 \int F(k)\, e^{ik(q-q')}\, U(q')\, dk dq'. \quad (14)$$

In Eq. (14) the function $F(k)$ is given by Eq. (4). For $\hbar = 0$ Eq. (14) turns into the expression derived by the Debye theory. For $\hbar k \ll p_0$ we obtain for the potential of a quantum system the equation

$$\Delta U = r_d^{-2} U, \quad (15)$$

which agrees with the relation obtained in the Debye theory, except that it is for a different correlation radius. For a completely degenerate Fermi gas, the correlation radius is determined by Eq. (11). This result agrees with the results of Landau and Lifshitz.[3]

The expressions obtained for the correlation function are therefore correct in the case of weak interactions both for classical and quantum systems of particles with central interactions at arbitrary temperatures.

[1]N. N. Bogliubov, *Problems of the Dynamic Theory in Statistical Physics*, State Publishing Co., 1946.

[2]Iu. L. Klimontovich and V. P. Silin, J. Exptl. Theoret. Phys. (U.S.S.R.) 23, 151 (1952).

[3]L. D. Landau and E. M. Lifshitz, *Statistical Physics* GITTL, Moscow, 1951.

[4]D. N. Zubarev, Dissertation, Moscow State University, 1953.

[5]N. N. Bogoliubov and D. N. Zubarev, J. Exptl. Theoret. Phys. (U.S.S.R.) 28, 129 (1955); Soviet Phys. JETP 1, 83 (1955).

[6]D. N. Zubarev, J. Exptl. Theoret. Phys. (U.S.S.R.) 29, 881 (1955); Soviet Phys. JETP 2, 745 (1956).

Translated by M. J. Stevenson
204

Interaction of π^--Mesons with Protons at 4.5 BEV

A. I. NIKISHOV

(Submitted to JETP editor February 16, 1956)
J. Exptl. Theoret. Phys. (U.S.S.R.) 30, 990-991
(May, 1956)

THE experimental data on the n-p interaction at 1.7 bev and the π^--p interaction at 1.37 bev do not contradict the statistical theory which takes into account the isobaric states of nuclei[1,2]. We have carried the calculation for the π^--p interaction, the energy of the incident meson being equal to 4.5 bev in the laboratory system.

In the calculation of the final state density, we have taken into account the conservation of momentum and the indistinguishability of mesons, as well as the exact nucleonic mass (or the isobaric state). We have, however, neglected the mass of the meson. The last approximation is justified by the fact that, as we shall see, in the most important processes there are no more than four particles in the final (or the intermediate isobaric) state. Even in the worst case (process $3N'$) the kinetic energy per particle amounts to 0.365 bev (total energy in the center-of-mass stystem 3.1 bev). If every one of the four mesons, created in the process of annihilation of a nucleon and an antinucleon, possessed such an energy, the correction factor to the meson mass would amount to 0.7 (according to I. L. Rozental' and V. M. Maksimenko). We take exactly into account only one (the heaviest) mass and the correction, therefore, will be even smaller. Only the processes $4N'$ and $5N$ may substantially depend on it, but their role is small at such high energies.

We shall use the following notation[1,2]: N--nucleon, N'--isobaric state; nN--state with n pions and one nucleon, nN'--state with n pions and one isobar. The statistical weights of the processes under consideration are given in Table I.

As usual, we take $R = 1.4 \times 10^{-13}$ (R is the parameter determining the nonshortened interaction volume $V_0 = 4/3\ \pi R^3$).

Table II gives the division of the charge states for all processes.

Some of the implications of our calculations can be already compared with preliminary experimental results on the $\pi^- - p$ interaction at 4.5 bev[3]. In Ref. 3 the relative proabilities are given of elastic nondiffractive collisions and of inelastic collisions producing two-, four- and six-prong stars.

TABLE I

Number of Pions	Type of process	Statistical weight
1	1 N	1.17
2	2 N	13.0
	1 N'	2.10
3	3 N	21.67
	2 N'	19.2
4	4 N	9.72
	3 N'	23.4
5	5 N	1.75
	4 N	7.96

TABLE II

Number of pions n	Products of the Reaction	Distribution of nN	Distribution of $(n-1)$ N'
1	$p-$	0.555	
	n 0	0.445	
2	$p-0$	0.378	0.274
	n 0 0	0.155	0.163
	$n+-$	0.467	0.563
3	$p+--$	0.276	0.248
	$p-$ 0 0	0.200	0.174
	$n+-0$	0.462	0.508
	n 0 0 0	0.062	0.070
4	$p+--0$	0.358	0.326
	$n++--$	0.209	0.229
	$p-$ 0 0 0	0.096	0.086
	$n+-$ 0 0	0.316	0.338
	n 0 0 0 0	0.021	0.021
5	$p++---$	0.129	0.121
	$p+--$ 0 0	0.302	0.282
	$n++--0$	0.337	0.357
	$n+-$ 0 0 0	0.182	0.192
	$p-$ 0 0 0 0	0.042	0.039
	n 0 0 0 0 0	0.008	0.009

The experimental and the theoretical values of the relative probability of the processes are compared in Table III. As it can be seen, the agreement is satisfactory.

I wish to express my gratitude to Prof. S. Z. Belenkii for interesting discussions and his constant attention to the present work.

TABLE III

	Experimental data	Statistical Calculation	
		isobaric states accounted for	isobaric states neglected
Elastic nondiffractive scattering	2	1	2
2-prong stars	44	49	56
4-prong stars	28	24.5	17
6-prong stars	1	0.5	0.1

[1] S. Z. Belenkii and A. I. Nikishov, J. Exptl. Theoret. Phys. (U.S.S.R.) 28, 744 (1955); Soviet Phys. JETP 1, 593 (1955).

[2] A. I. Nikishov, J. Exptl. Theoret. Phys. (U.S.S.R.) 30, 601 (1956); Soviet Phys. JETP 3, 634 (1956).

[3] Maenchen, Powell, Saphir and Wright, Phys. Rev. 99, 1619 (1955).

Translated by H. Kasha
210

"Smoothing Out" of Charge Density in Polaron Theory

M. SH. GITERMAN
Moscow State Pedagogical Institute, Saransk
(Submitted to JETP editor February 21, 1956)
J. Exptl. Theoret. Phys. (U.S.S.R.) 30, 991-992
(May, 1956)

IF the effective mass method (E.M.M.) is used in the polaron theory[1], one must solve an auxiliary equation for a "smoothed out" wave function

$$\left(-\frac{\hbar^2}{2\mu}\Delta + W\right)\varphi = E\varphi; \qquad \varphi = \sum_{\mathbf{k}} a_{\mathbf{k}} e^{i\mathbf{k}\mathbf{r}}, \quad (1)$$

where μ is the effective mass of an electron. The polarization potential $W(\mathbf{r})$ in Eq. (1) is not computed from the exact wave function (the so-called detailed wave function) of the polaron $\psi(\mathbf{r}) = \Sigma a_{\mathbf{k}}\psi_{\mathbf{k}}(\mathbf{r})$ ($\psi_{\mathbf{k}}$ is the Bloch wave function), i.e., not as $W_{|\psi|} = -e^2 c \int \frac{|\psi(\mathbf{r}')|^2}{|\mathbf{r}-\mathbf{r}'|}\, d\tau'$ but from a "smoothed out" function $\varphi(\mathbf{r})$. Such smoothing out of potential which brings Eq. (1) into a self-consistent form, introduces a definite error into the value of the computed energy. The purpose of the present letter is to evaluate the error committed when the criterion of applicability of E.M.M. $r_p \gg a$ (r_p is the polarization radius, a is the separation between neighboring ions) is barely met. Such is the case for the majority of the alkali-halide crystals.

Applying perturbation theory, we obtain for this error

$$E_1 = \int (W_{[\psi]} - W_{[\varphi]})\,|\varphi|^2\, d\tau \qquad (2)$$

$$= -e^2 c \int \frac{|\psi(\mathbf{r}')|^2\,|\varphi(\mathbf{r})|^2}{|\mathbf{r}-\mathbf{r}'|}\, d\tau\, d\tau'$$

$$+ e^2 c \int \frac{|\varphi(\mathbf{r})|^2\,|\varphi(\mathbf{r}')|^2}{|\mathbf{r}-\mathbf{r}'|}\, d\tau\, d\tau'.$$

We neglect here the dispersion of the crystal and the dependence of its polarization on the wave length, assuming $c = 1/n^2 - 1/\epsilon = \text{const}$. Because of considerations discussed by Tolpyg[2] we shall start from the approximation of strongly bounded electrons, according to which

$$\psi_k = \sum_{\mathbf{n}} e^{ik\mathbf{n}} \psi_a(|\mathbf{r}-\mathbf{n}|),$$

where $\mathbf{n}$ is the radius vector to the center of a cell coinciding with the nucleus of the positively charged ion. Pekar[1] used a variation principle to replace the integration of Eq. (1) and, as an approximation, the following function may be used:

$$\varphi(r) = \frac{\alpha^{3/2}}{\sqrt{55\pi}}\left(1 + \alpha r + \frac{(\alpha r)^2}{2!} + \frac{(\alpha r)^3}{3!}\right) e^{-\alpha r},$$

where α is determined by minimizing the corresponding potential which yields

$$\alpha = 0.821\,(\mu/m)\, c/a_0,$$

where a_0 is the Bohr radius.

The second term of Eq. (2) is integrated directly after the substitution of $\varphi(\mathbf{r})$. The result is $0.2613\, e^2 c\, \alpha$ and, after substituting $\psi(\mathbf{r}) = \sum_{\mathbf{k}} a_{\mathbf{k}}\psi_{\mathbf{k}}(\mathbf{r})$, the first term of Eq. (2) has the form

$$\int W_{[\psi]}\,|\varphi|^2\, d\tau \qquad (3)$$

$$= \Delta \sum_{\mathbf{n},\mathbf{n}'} \varphi(\mathbf{n})\,\varphi^*(\mathbf{n}')$$

$$\times \int \psi_a^*(|\mathbf{r}'-\mathbf{n}'|)\,\psi_a(|\mathbf{r}'-\mathbf{n}|)\; W_{[\varphi]}(\mathbf{r}')\, d\tau',$$

where Δ is the volume of the elementary cell.

We further demand (analogously to Tolpyg[2]) that $W(\mathbf{r})$ be expandable in a series of $(\mathbf{r}-\mathbf{n})$ within the boundaries of each cell. After substituting such expressions into Eq. (3) we obtain for the case $n = n'$

$$\sum_{\mathbf{n}} |\varphi(\mathbf{n})|^2 \left[\psi^0 W_{(n)} + \frac{\psi^{(2)}}{3!}\nabla^2 W_{(n)} + \frac{\psi^{(4)}}{5!}\nabla^4 W_{(n)} + \cdots\right],$$

$$\psi^{(2n)} = \int \psi_a(|\mathbf{r}-\mathbf{n}'|)\, r^{2n}\, d\tau.$$

The last expression is computed by passing from a sum over $\mathbf{n}$ to an integral. The terms with $n \neq n'$ in Eq. (3) are computed on the assumption that the maximum value of the integrand in the overlap integral lies midway between the lattice points, which follows from symmetry consideration. $W(\mathbf{r})$ is expanded in orders of $|\mathbf{r} - \frac{1}{2}(\mathbf{n}+\mathbf{n}')|$. The numerical calculation was carried out for the sodium salts. The function ψ_a was approximated

with sufficient accuracy from the data of Fock and Petrashen[3].

$$\psi_a(r) = 0.727\,(4\pi a_0^3)^{-1/2}\,(r/a_0 - 1)\,e^{-0.71r/a_B}.$$

The result is

$$E_1 = (0.01873\cdot 10^{-16}\alpha^2 + 0.07221\times 10^{-32}\,\alpha^4 + \cdots)\,e^2 c\alpha.$$

For example, for the crystal NaCl $\alpha = 1.109 \times 10^8$ and the error in Pekar's[1] energy evaluation due to smoothing out of the potential is about 15%, which lowers the computed energy value after Eq. (1) is brought to a self-consistent form. We note, however, that using the approximation of strongly bound electrons increases somewhat the estimate of the energy error, and in reality this error is only about 10-12% for NaCl.

Tolpyg[2] considered higher order terms in the E.M.M. and showed that the E.M.M. of Pekar overstates the energy values, for NaCl in particular by 12-13%. Thus, the above errors are approximately equal and in opposite directions, which verifies the applicability of E.M.M. for calculation of energies, even when r_p is greater than a by a factor of 2 or 3.

The author expresses a deep gratitude to K. B. Tolpyg for his help in carrying out the present work.

---

[1] S. I. Pekar, *Investigations of the Electron Theory of Crystals*, State Publishing House, 1951.

[2] K. B. Tolpyg, J. Exptl. Theoret. Phys. (U.S.S.R.) 21, 443 (1951).

[3] V. A. Fock and M. Petrashen, Physik Z. d Sowjetunion 6, 369 (1934).

Translated by M. J. Stevenson
211

On Annihilation of Antiprotons with Star Formation

S. Z. Belen'kii and I. S. Rozental'
P. N. Lebedev Physical Institute, Academy of Sciences, USSR

(Submitted to JETP editor November 29, 1955)
J. Exptl. Theoret. Phys. (U.S.S.R.) 30, 595-596 (March, 1956)

COLLISION of the antiproton with the proton and the annihilation of both particles results in the liberation of not less than 1.8×10^9 ev (if the velocities of both particles are small). This energy is sufficient for the formation of 13 π-mesons. It seems natural to apply to the investigation of stars of such high energy the statistical theory of multiple particle formation (see Refs. 1 and 2). The theory of thermodynamic variants leads to the following formula for the complete number of the formed particles[2,3].

$$N = k\,(E/Mc^2), \tag{1}$$

where M denotes the mass of the nucleon and k is a coefficient determined from experiment. For large energies ($E \geq 10^{12}$ ev) $k \sim 2$. If this value of k is used with the energies of interest, $N \sim 2$. For such a small value of N the application of thermodynamics is not justified and we, therefore, turn to a variation of statistical theory suggested by Fermi[1] for the investigation of stars with the formation of not too many particles.

We shall start with the following formula (see Refs. 1, 4 and 5):

$$S(n) = f_{n,T}\,[\Omega/8\pi^3\hbar^3]^{n-1}\,W_n(E_0). \tag{2}$$

The value of $S(n)$ determines the probability of meson formation, Ω the effective volume in which the energy of the colliding nucleons is concentrated and where the formation of particles takes place, E_0 the full energy of star formation, $W_n(E_0) = dQ_n(E_0)/dE_0$, $Q_n(E)$ the volume of the momentum space corresponding to the energy E_0, $f_{n,T}$ a factor accounting for the conservation of isotopic spin and the equivalence of particles (see Refs. 4 and 5), T the isotopic spin of the system. The effective volume was taken as $(4\pi/3)(\hbar/\mu c)^3$, where μ is the mass of the π^--meson. Justification for this selection was the fact that similar computations for multiple formation of particles for p-n and π^--p collisions result in a satisfactory agreement with experiment when the same expression is used for the evaluation of the effective volume[6]. It should be noted that the energy E_0 in these cases ~ 1 bev, i.e., not strongly different from the energy ~ 2 bev under consideration.

The magnitude of $W_n(E_0)$ has been computed in Ref. 7 with consideration for conservation of energy and momentum but on the assumption that the formed particles are ultrarelativistic. As it will be shown further this assumption is approxi-

mately correct in our case. The formula for $W_n(E_0)$ is given as:

$$W_n(E_0) = \frac{\pi^{n-1}}{2^{n-1}} \frac{(4n-4)!\,(2n-1)}{[(2n-1)!]^2\,(3n-4)!} E_0^{3n-4}. \qquad (3)$$

The factor $f_{n,T}$, accounting for the preservation of isotopic spin and the identity of particles is given by the following formula (see Ref. 8): $f_{n,T} = g_n(T)/n!$, where

$$g_n(T) = (2T+1) \sum_i \frac{(-1)^{n+i}}{2i+1} \binom{n}{i} \binom{2i+1}{i-T}. \qquad (4)$$

Values of $g_n(T)$ for different d and T are computed in Ref. 8.

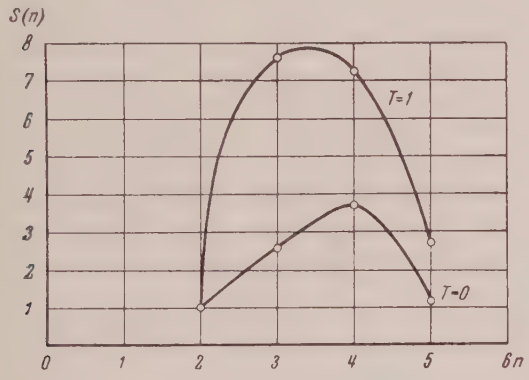

In the collision of two particles, proton and antiproton, the values of the isotopic spin may be equal only to 1 or 0. Indeed, the eigenfunctions $(p\tilde{p})$ (p--proton, $\tilde{p}$--antiproton), (nn) (n--neutron and n--antineutron), (np) and (pn) can be expressed in the following manner through the eigenfunctions of states with a given value of T (upper index) and its z component T_z (lower index):

$$(p\tilde{p}) = \Phi_1^1; \quad (p\tilde{n}) = \Phi_{-1}^1; \qquad (5)$$
$$(pp) = 2^{-1/2}\,(\Phi_0^0 + \Phi_0^1);$$
$$(n\tilde{n}) = 2^{-1/2}\,(\Phi_0^1 - \Phi_0^0).$$

In the Figure are shown the probability $S(n)$ for the distribution of the n-meson formation for values of isotopic spin $T = 0$ and $T = 1$. It is seen from the presented data that on the average four particles are formed, thereby making the energy per particle of the order of 0.5×10^9 ev. This justifies the assumption made that the particles are relativistic*. It is also of interest to investigate the distribution of the formed mesons according to charge. For the case of 2 and 3 meson formation this type of investigation was carried out by others (see Refs. 9 and 10).

In conclusion, we express our thanks to Messrs. M.I. Podgoretski and I.E. Tamm for their participation in the discussions of questions pertaining to this work.

* Computation of the statistical weight by the exact formula for the case when two particles are in the final state (see Ref. 11) showed that Eq. (3) gives values different from the exact values by about 1%.

[1] E. Fermi, Progr. Theor. Phys. 5, 570 (1950).

[2] L. Landau, Izv. Akad. Nauk SSSR, 17, 51 (1953).

[3] S. Z. Belen'kii and L.D. Landau, Usp. Fiz. Nauk 56, 309 (1955).

[4] E. Fermi, Phys. Rev. 92, 452 (1953).

[5] E. Fermi, Phys. Rev. 93, 143 (1954).

[6] S.Z. Belen'kii and A.I. Nikishov, J. Exptl. Theoret. Phys. (U.S.S.R.) 28, 744 (1955); Soviet Phys. JETP 1, 593(1955).

[7] I.L. Rozental', J. Exptl. Theoret. Phys. (U.S.S.R.) 28, 118 (1955); Soviet Phys. JETP 1, 166 (1955), G.V. Lepore and R.N. Stuart, Phys. Rev. 94, 1724 (1954).

[8] V. Veivin and de Shalit, Nuovo Cim. 1, 1146(1955).

[9] I. Kobzarev and I. Shmushkevich, Dokl. Akad. Nauk SSSR 102, 929 (1955); I. Shmushkevitch, Doklad. Akad. Nauk SSSR 103, 235 (1955).

[10] D. Amati and B. Vitale, Nuovo Cim. 11, 4, 719 (1955).

[11] M.I. Podgoretskĭ and I.L. Rozental', J. Exptl. Theoret. Phys. (U.S.S.R.) 27, 129 (1954).

Translated by J.L. Herson
115

Concerning Papers of S. E. Khaikin, S. V. Lebedev and L. N. Borodovskaia Published in the J. Exptl. Theoret. Phys. (U.S.S.R.) in 1954-1955

I. F. KVARTSKHAVA

(Submitted to JETP editor June 15, 1955)
J. Exptl. Theoret. Phys. (U.S.S.R.) 30, 621-622 (March, 1956)

IN the works of S. E. Khaikin, S. V. Lebedev and L. N. Borodovskaia, a presentation was given of the results of experiments in which processes occurring in metallic wires during the passage through them of large impulsive currents were studied. From an analysis of the results obtained, the authors came to two conclusions of significance in the physics of metals:

1. With an impulsive current density of 10^6-10^7 A/cm^2, the substance of the wire passes into an abnormal nonmetallic state, differing "by a sharp change of the character of the dependence of the resistance R of the wire on the energy E introduced into it."

2. In a series of experiments conducted on tungsten and iron wire in vacuum, an "abnormally high electronic emission" from the surface of the wire was discovered, accompanied "by the violation of the law of Boguslovskii-Langmuir" and associated, in the opinion of the authors, with the transition of matter into an abnormal state.

In the first three articles[1-3], the character of the abnormal state of matter was not made precise. In succeeding articles[4,5], it was surmised that this state bears a purely electronic character. Characterizing this new state, Lebedev asserts[4] that "the existing theory of metals not only did not predict the results of our experiments, but apparently cannot generally explain them without adding a new physical hypothesis to the theory."

Careful scrutiny of the above-mentioned works leads us to the conclusion that the evidence put forward by the authors is not sufficiently convincing.

The first conclusion of the authors (concerning an abnormal state of matter) is based on the fact that the amount of energy introduced into the wire during various durations of passage of the impulsive current, calculated on the basis of oscillographic data, appeared to be greater than the wire could take up, while being in the usual state for metals. For example, according to the authors' calculations, the wire, maintaining a solid state during the impulsive heating, can take up an amount of energy considerably greater than the energy of fusion.

Similar experiments were conducted by a group of co-workers together with the author of this letter, in order to study the properties of the substance of a wire during the passage through it of impulsive currents of great power[6,7]. The experimental method was similar to the method used in the works under discussion here, the only difference being that simultaneously with oscillography, shadow photographs were taken of the wire in various stages of explosion, and particular attention was paid to decreasing to a minimum the inductive distortion of the oscillograms. The current impulses were shorter, and accordingly, the current densities achieved were greater than in Refs. 1-5. As a result of these experiments, it was possible to show that Ohm's law for the solid state is maintained up to current densities $\sim 10^7$ A/cm^2.

With relatively low voltages on the condenser (< 5 kv), within the accuracy of the measurements, no particular abnormalities in the behavior of the substance of the wire was observed, and up to the first current maximum the energy introduced completely corresponded to the resistance of the wire. The contradictory results obtained in Refs. 1-3 can be explained, apparently, by the fact that the oscillograms from which the authors calculated the energy reveal considerable inductive distortion. In Ref. 1, in the calculation of the energy introduced into the wire according to Eq. (2), no correction to the magnitudes of the voltages V_R and V_r were made for the inductive fall of the voltage, amounting to several tens of percent of their maximum value (see, for example, the oscillograms in Fig. 7). Since the product of V_R and V_r occurs under the integral sign in Eq. (2), exaggerated values are found for the energy. The apparent surpluses of energy are greater, the greater the derivative of current with respect to time, i.e., the greater the amplitude of the impulsive currents. Similar inaccuracies occur also in Ref. 8, which is referred to by the authors as a work confirming their results. But as regards the calculation of the resistance of the wires according to Eq. (1)[1], sufficiently correct values are given, since in this equation the ratio of V_R and V_r enters, and their percents of inductive distortion are approximately the same.

Also considered in Ref. 1 is the question of the abnormal trend of the dependence of the resistance R of the wire on the amount of energy E introduced into it. According to the data of our experiments, such a dependence always occurs only at the end of the region of impulsive current before its so-called pause, and is associated with the intensive motion of matter arising as a result of the rapid thermal expansion of the wire, the strong compression of separate parts of it in a radial direction (caused by the action of the magnetic field of the current), the very rapid evaporation of these parts, etc. In this region, the wire is capable of taking up a considerably greater amount of energy than is necessary for its complete evaporation. Thus, that state of matter which the authors call abnormal, in actuality evidently represents the beginning of the stormy process of destruction of the wire. In the epxeriments in vacuum with refractory wire, in view of thermoelectronic emission from the surface of the wire, particularly from its superheated parts, and the associated shunting discharge, the wire may not obtain sufficient energy for explosion or even for fusion. Therefore, during the impulsive regime of heating in vacuum, the wire frequently remains unmelted.

The second conclusion of the authors (regarding abnormal electronic emission from the surface of refractory wires) is based on the fact that during heating by a large impulsive current, and in the presence of a certain anode voltage, the anode current is hundreds of times greater than the emission current of the wire at its fusion temperature in a stationary regime of heating, while the same wire here frequently remains unmelted. The authors make numerous attempts to prove that the abnormal increase of emitted current is not associated with some manifestation of a discharge in the gas or other secondary currents. Resting on these proofs, they concluded that the abnormal emission is due to an abnormal state of the substance of the wire. It should be noted that here, no account is taken of two circumstances which might be essential for the correct understanding of the appearance of abnormal electronic emission:

1. During impulsive heating almost to the temperature of fusion, occluded gases and part of the substance of the wire are evaporated from its surface. The mean thermal velocities of molecules and atoms at the temperature of fusion, for example, of tungsten ($\sim 3400°$) is of the order of 10^5 cm/sec. Therefore, during several microseconds (duration of the impulse for the greatest currents) the majority of them are able to fly only several millimeters from the surface of the wire. In view of this, in distinction to a stationary regime of heating, in the regime of impulsive heating a nonuniform distribution of gas pressure arises between the anode and cathode, with maximum pressure on the surface of the wire. With such a pressure distribution, in the presence of a sufficiently great electric field along the wire (several hundred volts per centimeter) and a magnetic field perpendicular to it, there exist, evidently, suitable conditions for the occurrence of discharges with large currents shunting the wire. In experiments on the explosion of wire in vacuum we visually observed that with a tungsten wire with a diameter of 0.1 mm and with a current of several thousand amperes, the visible diameter of the discharge does not exceed 4-5 mm, which evidently indicates the presence of a pressure gradient in the direction of the radius. Moreover, in this case the untwining of the discharge is also possible, caused by the action of the current's own magnetic field. Hence, it follows that in the comparison of the results of experiments in the impulsive and in the stationary regimes, disregarding the above-mentioned statements may lead to incorrect conclusions.

2. Certain deviations from the law of Boguslovskii-Langmuir in the initial part of diode characteristics are known, caused by the action of the magnetic field of the current of the incandescent cathode on the motion of the electrons. Here, there exists a critical value of anode voltage U_{kp}, below which the electrons in general do not strike the anode. In the case of a cylindrical anode with a coaxial wire cathode, U_{kp} is associated with a heating current i by the relation (see Ref. 9, p. 125):

$$U_{кр} = 188 \cdot 10^{-4} i^2 \left(\lg \frac{r_a}{r_к}\right)^2 ,$$

where U_{kp} is expressed in volts, i in amperes and r_a and r_k are the radii of the anode and cathode. Under the conditions of the experiments considered herein, $i \sim 10^3 A$, $r_k \leq 0.05$ mm, the anode is plane with area ~ 1 cm^2 and is at a distance of 1 cm from the cathode. If a cylindrical anode is taken in place of a plane, the magnitude of U_{kp} is evidently not decreased. Therefore, a magnitude of 1 cm may be assumed for r_a. Then the above equation gives $U_{kp} \sim 100$ kv, and with a current of $i \sim 10^2 A$, $U_{kp} \sim 1$ kv. Thus, in the experiments considered, the authors would not have obtained electron currents differing from zero had the emission been normal, since the anode voltage in these experiments did not exceed 1 kv. In that case, in order to explain the abnormal emission, it is necessary to assume the existence of initial velocities of thermoelectrons sufficiently large to surmount the magnetic field of the current. A calculation of electron trajectories under the condition considered indicates that an initial electron energy < 10 ev is insufficient to surmount the magnetic field of the current. The assumption of significantly higher energies is not physically justifiable; therefore, evidently, it is fitting to acknowledge the basic role of a discharge shunting the wire. The abnormal electron emission could be easily understood if it were assumed that in the process of the impulsive regime of heating, an increase in the emitting surface occurs with a simultaneous decrease in the magnetic field on this surface. Both of these conditions are satisfied if a shunting discharge with a large shunting current develops along the wire. Here, the emitting surface is increased, and simultaneously the magnetic field of the current is decreased because of the decreased current density. From this, evidently, there is also associated the possibility of drawing off large electron currents

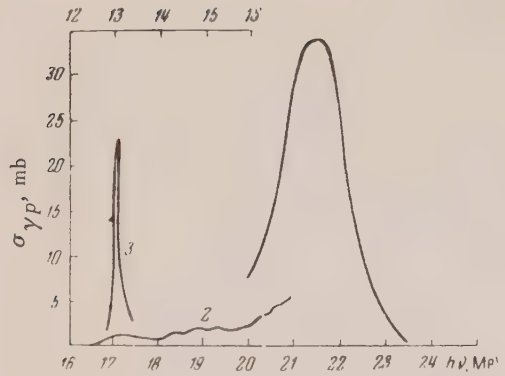

FIG. 1. (γ, p) excitation function for C^{12} and O^{16}. *1*--$C^{12}(\gamma, p)B^{11}$--"giant" resonance (see Ref. 12), $\sigma_{int} = 63$ mev mb; *2*--$C^{12}(\gamma, p)B^{11}$ (see Refs. 5, 9 and 10), $Q = 15.95$ mev, $\sigma_{int} = 8.2$ mev mb; *3*--$O^{16}(\gamma,p)N^{15}$ (see Ref. 13), $Q = 12.11$ mev, $\sigma_{int} = 4.4$ mev mb. Lower scale for *1* and *2*; upper scale for *3*.

photo nuclear studies, which are, as a rule, carried out over broad spectral ranges of the γ-rays. It would be of particular interest to study such reactions in the "giant" resonance region.

An anlysis of the data on (p, γ) reactions without cascade emission of γ-rays enables us to draw definite conclusions as to the predominance (although it is not overwhelming) of $E1$ γ-ray absorption in this energy region. In some instances such data also provide definite information concerning the cross sections for anisotropic proton emission in (γ, p) reactions. For example, the integral cross section for levels 3, 5 and 6 in the $S^{32}(\gamma, p)P^{31}$ reaction, which levels correspond to the emission of protons in the p-state, is $\sigma_{int} = 4.5$ mev mb. One must keep in mind the contributions of individual levels to the anisotropic emission of photonucleons in comparing the spectrum and angular distribution of these nucleons with calculations from statistical theory.

TABLE

Reaction	Threshold in mev	Energy interval $\Delta h\nu$ in mev	Levels and type of gamma absorption	σ_{int} in mev mb	References to the literature
$B^{10}(\gamma p)Be^9$	6.58	6.58 -- 11	6.89($M2$) 7.48($E1$) 8.89($M1$) 10.83(?)	~1.1 0.3 1.4	5-8
$C^{12}(\gamma p)B^{11}$	15.95	15.95 — 21	16.10($E2$) 16.57($M2$) 17.22($E1$) 18.39($E2$) 18.86(?) 19.25(?) 20.25(?) 20.49(?)	8.2	5,9,10
$N^{14}(\gamma p)C^{13}$	7.54	7.54 -- 9,2	8.06($E1$) 8.62($M1$) 8.70($E1$) 9.18($E1$)	~0,6 2	5,11
$S^{32}(\gamma p)P^{31}$	8.85	8.85 —11,2	9.65($M1, E1$) 9.93($M1, E1$) 10.68($E1$) 10.77($E1, M1$) 10.81($E1$) 10.90($E1$) 11.10($M1, E1$) 11.12($M1, E1$)	0,003 0.01 2.3 0.8 1.8 0.4 1.3 3.5 10,3	14,16

In conclusion, I wish to thank Iu. K. Khokhlov and E. M. Leikin for discussions of the problem treated in this note.

[1] A. B. Migdal, J. Exptl. Theoret. Phys. (U.S.S.R.) 15, 81 (1945).

[2] Haslam, Katz, Horsley, Cameron and Montalbetti, Phys. Rev. 87, 196 (1952).

[3] Katz, Haslam, Horsley, Cameron and Montalbetti, Phys. Rev. 95, 464 (1954).

[4] J. Goldemberg and L. Katz, Phys. Rev. 95, 471 (1954).

during the explosion of a wire in vacuum. The ionic currents drawn off from such a discharge must be hundreds of times smaller than the electronic currents, because the ratio of these currents with the same anode voltage is determined by the square root of the inverse ratio of the masses bearing the charges, which is also confirmed in the works considered.

[1] S. V. Lebedev and S. E. Khaikin, J. Exptl. Theoret. Phys. (U.S.S.R.) 26, 629 (1954).

[2] S. V. Lebedev and S. E. Khaikin, J. Exptl. Theoret. Phys. (U.S.S.R.) 26, 723 (1954).

[3] S. V. Lebedev, J. Exptl. Theoret. Phys. (U.S.S.R.) 27, 487 (1954).

[4] S. V. Lebedev, J. Exptl. Theoret. Phys. (U.S.S.R.) 27, 605 (1954).

[5] L. N. Borodovskaia and S. V. Lebedev, J. Exptl. Theoret. Phys. (U.S.S.R.) (no page no., n.d.).

[6] Bondarenko, Kvartskhava, Pliutto and Chernov, J. Exptl. Theoret. Phys. (U.S.S.R.) 28, 191 (1955); Soviet Phys. JETP 1, 221 (1955).

[7] Kvartskhava, Pliutto, Chernov and Bondarenko, J. Exptl. Theoret. Phys. (U.S.S.R.) 30, 42 (1956).

[8] J. Wrana, Arch. f. Elecktrotechn. 33, 656 (1939).

[9] F. Vlasov, *Electro-vacuum systems*, Sviaz'izdat, Moscow, Leningrad, 1949.

Translated by D. Lieberman and M. Mestchersky
130

(γ, p) Reactions Associated with the Formation of Ground State Nuclei

V. I. GOL' DANSKII
P. N. Lebedev Institute of Physics
Academy of Sciences, USSR

(Submitted to JETP editor January 30, 1956)
J. Exptl. Theoret. Phys. (U.S.S.R.) 30, 969-971 (May, 1956)

DURING the last few years a great deal of confirmation has been obtained for the existence of the so-called "giant" resonance in photonuclear reactions [such as (γ,n) and (γ,p) reactions] which is caused by the location between 15 and 25 mev of the center of gravity of dipole levels excited through nuclear absorption of $E1$ γ-quanta.[1] Beginning in 1952, a group of Canadian physicists[2-4] have distinguished an entire series of separate resonance levels in the "giant" (γ, n) resonance of a few light nuclei (Li^7, C^{12}, O^{16}, F^{19}). The study of the photonuclear excitation function fine structure is of decided interest both for nuclear spectroscopy and for the determination of the character of γ-ray absorption by nuclei. In connection with the latter question it is especially important not only to determine the contribution of any of the individual levels to the observed yield but also to reveal the nature of the final nuclear state [which is not usually done in the study of (γ, p) and (γ, n) reactions] as well as the angular distribution of the emitted particles.

In the present note we wish to estimate the contribution of individual levels to photonuclear (γ, p) reactions, which can be obtained from experimental data regarding the cross sections of reverse (p, γ) reactions that take place without cascade emission of γ-rays ($\sigma_{p\gamma}$). The cross sections $0_{\gamma, p}$) reactions connected with the formation of ground states in the final nuclei are related to the (p, γ) cross sections by the simple relationships of detailed balancing; for example, in the case of O^{16} (γ, p) N^{15} we have:

$$\sigma_{\gamma 0} = \sigma_{pN} 2 \frac{16}{15} \frac{mc^2 (h\nu - Q)}{(h\nu)^2} \frac{2I_N + 1}{2I_O + 1}.$$

Here $I_N (= 1/2)$ and $I_O (= 0)$ are the spins of N^{15} and N^{16}, m is the proton mass, $Q (= 12.11$ mev) is the energy released by the reaction, $h\nu$ is the energy of a γ-quantum associated with the proton energy (E_p) in the (p, γ) reaction by the relationship $h\nu = Q + (15/16) E_p$. From an analysis of the data in the literature, considerable information can be obtained concerning (γ, p) reactions associated with the formation of ground state final nuclei in the case of five light nuclei: B^{10}, C^{12}, N^{14}, O^{16} and S^{32}. The results are summarized in the Table and Figure.

As can be seen from the Table and Figure, the maximum cross sections for (γ, p) reactions connected with the formation of ground state final nuclei associated with individual levels, sometimes exceed by a large factor the maximum cross sections in "giant" resonance. The integral cross sections of such reactions which are associated with individual levels amount to about 10% of the integral cross sections in "giant" resonance, which encompass all possible states of the final nuclei. Consideration of this fact leads to some increase in the experimental values of the gamma absorption cross sections (σ_γ) and to reduction of the difference between the theoretical and experimental values of $\sigma_{\gamma\,\mathrm{int}}$ for light nuclei as has been noted in Ref. 15, for example. It will be necessary to use extensive experimental data concerning (p, γ) and (n, γ) reactions in order to make an independent check of the results from

[5] F. Ajzenberg and T. Lauritsen, Revs. Mod. Phys. 27, 77 (1955).

[6] S. Hunt, Phys. Rev. 87, 902 (1952).

[7] W. F. Hornyak and T. Coor, Phys. Rev. 92, 675 (1953).

[8] Hahn, Snyder, Willard, Bair, Klema, Kington and Green, Phys. Rev. 85, 934 (1952).

[9] T. Huusa and R.B. Day, Phys. Rev. 91, 599 (1953).

[10] Bair, Kington and Willard, Phys. Rev. 100, 21 (1955).

[11] J. Seagrave, Phys. Rev. 85, 197 (1952).

[12] A. K. Mann and J. Halpern, Phys. Rev. 83, 370 (1951).

[13] Schardt, Fowler and Lauritsen, Phys. Rev. 86,527 (1952).

[14] Paul, Gove, Litherland and Bartholomew, Phys. Rev. 99, 1339 (1955).

[15] Iu. K. Khokhlov, Dokl. Akad. Nauk SSSR 97, 239 (1954).

[16] G. R. Grove and J.N. Cooper, Phys. Rev. 82, 505 (1951).

Translated by I. Emin
200

Capture of K^--Mesons by Deuterium and Hyperon-Nucleon Interaction

L. B. Okun' and M. I. Shmushkevich
Academy of Sciences, USSR

(Submitted to JETP editor February 14, 1956)
J. Exptl. Theoret. Phys. (U.S.S.R.) 30, 979-981
(May, 1956)

THE study of K-meson capture in hydrogen and deuterium can provide valuable information not only concerning the properties of K-mesons but also concerning the interactions between hyperons and nucleons. In particular, it may be possible to answer the question about the existence of bound states of a hyperon-nucleon system. Examples of such reactions (occurring with conservation of "strangeness"[1] and, consequently, possessing large cross sections) are

1) $K^- + d \to \Lambda + n + \pi^0$, 1′) $K^- + p \to \Lambda + \pi^0$,
2) $K^- + d \to \Lambda + p + \pi^-$, 2′) $K^- + n \to \Lambda + \pi^-$,
3) $K^- + d \to \Sigma^- + n + \pi^+$, 3′) $K^- + p \to \Sigma^- + \pi^+$,
4) $K^- + d \to \Sigma^+ + n + \pi^-$, 4′) $K^- + p \to \Sigma^+ + \pi^-$,
5) $K^- + d \to \Sigma^0 + n + \pi^0$, 5′) $K^- + p \to \Sigma^0 + \pi^0$,
6) $K^- + d \to \Sigma^0 + p + \pi^-$, 6′) $K^- + n \to \Sigma^0 + \pi^-$,
7) $K^- + d \to \Sigma^- + p + \pi^0$, 7′) $K^- + n \to \Sigma^- + \pi^0$.

As definite examples we shall consider reactions 3 and 3′.

Assuming that the hyperon has spin 1/2, the amplitude of reaction 3′ will in general be of the form

$$A = a + \mathbf{b}\vec{\sigma}, \tag{1}$$

where a and $\mathbf{b}$ are functions of the K- and π-meson momenta; of k and p and of the spin of the K-meson, if this amplitude exists. The differential cross section of this reaction, averaged over the spins of the heavy particles, is

$$d\sigma = (|a|^2 + |b|^2)\, d\Omega. \tag{2}$$

If we consider the formation of π^+-mesons near the upper limit of their energy spectrum in reaction (3) we have for the corresponding cross section in the momentum approximation[2]

$$d\sigma = \left| \int \psi_f^*(\vec{\rho}) \exp\{i\vec{\varkappa}\vec{\rho}\}\ \psi_0(\vec{\rho})\, d\vec{\rho} \right|^2 \frac{df}{(2\pi)^3}\, d\Omega, \tag{3}$$

$$\vec{\varkappa} = \frac{M_1}{M_1 + M_2}(\mathbf{k} - \mathbf{p}).$$

Here M_1 and M_2 are the nucleon and hyperon masses and f is their relative momentum. Averaging over the spins of the baryons, we obtain

$$d\sigma = \{|a|^2 + {}^2/_3 |b|^2) |I_t|^2 + {}^1/_3 |b|^2 |I_s|^2\} (2\pi)^{-3} f^2\, df\, d\Omega_f\, d\Omega. \tag{4}$$

Here

$$I_{t,s} = \int \varphi_f^{(t,s)*}(\vec{\rho}) \exp\{i\vec{\varkappa}\vec{\rho}\}\, \varphi_0(\vec{\rho})\, d\vec{\rho}.$$

Taking

$$\varphi_0 = \sqrt{\alpha/2\pi}\ \frac{e^{-\alpha\rho}}{\rho}, \tag{5}$$

$$\varphi_f^{(t,s)} = \exp\{i\vec{f}\vec{\rho}\} - (e^{-2i\delta_{t,s}} - 1)\frac{e^{-if\rho}}{2if\rho},$$

where $\delta_{t,s}$ is the S-phase in the triplet and singlet states of the hyperon-nucleon system, we obtain (after integrating over all directions)

$$\int |I_{t,s}|^2\, d\Omega_f = 8\pi\alpha \left\{ \frac{4\pi}{[\alpha^2 + (\varkappa - f)^2][\alpha^2 + (\varkappa + f)^2]} + \frac{\pi}{2(\varkappa f)^2} \ln \frac{\alpha^2 + (\varkappa - f)^2}{\alpha^2 + (\varkappa + f)^2} \right.$$
$$\times \left[\sin 2\delta_{t,s} \left(\operatorname{arctg} \frac{\varkappa + f}{\alpha} + \operatorname{arctg} \frac{\varkappa - f}{\alpha} \right) - \sin^2\delta_{t,s} \ln \frac{\alpha^2 + (f + \varkappa)^2}{\alpha^2 + (f - \varkappa)^2} \right] \tag{6}$$
$$\left. + \frac{\pi}{(\varkappa f)^2} \sin^2\delta_{t,s} \left[\left(\operatorname{arctg} \frac{\varkappa + f}{\alpha} + \operatorname{arctg} \frac{\varkappa - f}{\alpha} \right)^2 + \frac{1}{4} \left(\ln \frac{\alpha^2 + (\varkappa + f)^2}{\alpha^2 + (\varkappa - f)^2} \right)^2 \right] \right\}.$$

When we make use of the relationship

$$E_0 = \sqrt{\mu^2 + k^2} - (M_2 - M_1) \qquad (7)$$

$$= \sqrt{m^2 + p^2} + \frac{(\mathbf{p} - \mathbf{k})^2}{2(M_1 + M_2)} + \frac{M_1 + M_2}{2M_1M_2} f^2,$$

Eqs.(4) and (6) give the pion distribution near the upper limit of the spectrum. Assuming $\cot\delta_{t,s} = -\beta_{t,s/f}$ and considering mesons whose energy differs from the upper limit by an amount of the order β^2/M, we obtain

$$d\sigma = \frac{\alpha}{\pi\varkappa_m^2}\left[\frac{M_1M_2}{2(M_1+M^2)}\right]^{1/2}\left(1+\frac{w_m}{M_1+M_2}\right) \qquad (8)$$

$$\times\left\{\frac{|a|^2 + {}^2/_3|b|^2}{\varepsilon_t + [E_0 - w - (w^2 - m^2)/2(M_1+M_2)]}\right.$$

$$\left. + \frac{{}^1/_3|b|^2}{\varepsilon_s + [E_0 - w - (w^2 - m^2)/2(M_1+M_2)]}\right\}$$

$$\times\sqrt{E_0 - w - \frac{w^2 - m^2}{2(M_1+M_2)}}\, dw.$$

Here $\epsilon_{t,s} = \beta^2_{t,s}(M_1 + M_2)/2M_1M_2$ and $\varkappa_m$ and w_m are the limiting values of $\varkappa$ and $w = \sqrt{m^2 + p^2}$ (for $f = 0$). According to (8), the pion energy distribution near the upper limit of the spectrum has two sharp peaks whose position and width is determined by ϵ_t and ϵ_s. An experimental investigation of this process in hydrogen and in deuterium would enable us to determine these important quantities as $|a|$ and $|b|$.

If bound states of the nucleons and hyperons exist there will be discrete lines in addition to the continuous portion of the pion energy spectrum. We obtain as the corresponding cross sections

$$d\sigma_t = \left(|a|^2 + \frac{2}{3}|b|^2\right) 2\frac{\sqrt{\alpha\beta_t}}{\varkappa}\,\mathrm{arctg}\,\frac{\varkappa}{\alpha+\beta}, \qquad (9)$$

$$d\sigma_s = \frac{1}{3}|b|^2 2\frac{\sqrt{\alpha\beta_s}}{\varkappa}\,\mathrm{arctg}\,\frac{\varkappa}{\alpha+\beta_s}.$$

In connection with the capture of a K^-–meson from the K-shell or from the continuous spectrum, but with emission of a pion at a small angle with relation to the K-meson momentum, certain conclusions can be reached regarding the magnitudes of a and b (see the Table). Here P_K and S_K are the parity and spin of the K-meson; P_Y is the parity of the hyperon relative to the nucleon.

For the study of the interactions between Ξ-particles and nucleons we can use the reactions

$$K^- + d \to K^+ + \Xi^- + n, \quad K^- + d \to K^\circ + \Xi^- + p$$

along with the corresponding reactions with protons. These reactions are impossible in connection with the capture of K^--mesons from the K-shell because of the energy threshold.

P_Y \ S_k, P_k	0^+	0^-	1^+	1^-
+1	$a=0$	$b=0$	$a\neq 0$, $b\neq 0$	$a=0$
−1	$b=0$	$a=0$	$a=0$	$a\neq 0$, $b\neq 0$

We note in conclusion that the interaction between nucleons and hyperons could also be studied by investigating the energy spectrum of K-mesons in reactions such as[3]

$$p + p \to \begin{cases} p + \Lambda + K^+ \\ p + \Sigma^+ + K^\circ \end{cases} \text{ или } p + n \to \begin{cases} n + \Lambda + K^+ \\ n + \Sigma^+ + K^\circ \\ p + \Sigma^- + K^+ \end{cases}$$

[1] M. Gell-Mann, Paper at the Pisa Conference on Elementary Particles.

[2] I. Ia. Pomeranchuk, Dokl. Akad. Nauk SSSR **80**, 47 (1951); V. B. Berestetskii and I. Ia. Pomeranchuk, Dokl. Akad. Nauk SSSR **81**, 1019 (1951); B. L. Ioffe and I. M. Shmushkevich, Dokl. Akad. Nauk SSSR **82**, 869 (1952).

[3] A. B. Migdal, J. Exptl. Theoret. Phys. (U.S.S.R.) **28**, 10 (1955); Soviet Phys. JETP **1**, 7 (1955).

Translated by I. Emin
205

Spectra of Neutrons Produced by Bombarding Light Nuclei with 14 mev Deuterons

G.F. Bogdanov, N.A. Vlasov, S.P. Kalinin, B.V. Rybakov and V.A. Sidorov

(Submitted to JETP editor February 15, 1956)
J. Exptl. Theoret. Phys. (U.S.S.R.) **30**, 981-983 (May, 1956)

IN the previous work of our laboratory[1] it was found that the spectra of neutrons, produced by bombarding tritium and deuterium with 14 mev deuterons, are not monchromatic. Besides the neutron groups, corresponding to the production of

the He^4 and He^3 nuclei in the ground state, other groups of slower neutrons were observed. The work was continued with other light-element targets in order to explain the mechanism of neutron production in these reactions. The experimental setup used analyzed the time of flight of the neutrons for the 2.85 m distancebetween the target and the counter. The details of the experiment are given in Ref. 2.

Two types of targets were used: gaseous H, He^3 and He^4, and solid-T (in zirconium), Li, Be, B, C and Cu. The gaseous targets were 4 cm thick and at the pressure of 2 atmospheres (in the case of He^3, 0.8 atmospheres). The entrance window of the targets, 30 mm in diameter, was covered by platinum foil 30 μ thick. The back wall, upon which the beam was falling after passing through the gas, was covered by a thick layer of lead. The solid targets, about 0.5 mev thick (for 14 mev neutrons) were set up on a thick lead base. Since comparatively few neutrons are produced in the lead during the bombardment, the difference of the results obtained with the target and with the empty holder only could be could only be regarded as caused by the element under examination.

The obtained neutron spectra are shown in Figs. 1-3. The measurements were carried out at the angle of 0°. The neutron energy was in the case of solid targets equal to 14.4 mev, in the case of gases, 13.0 mev.

The curves shown are the averages obtained from several series of measurements having a spread up to ±20%. This spread is basically due to the phase instability in the cyclotron.

The resolving power of our apparatus can be characterized by the width of the γ-peak, shown in the Figures. In the case of a solid target another 0.5 mev should be added to this width in order to account for the thickness of the target. The resulting resolving power permits the observation of separate levels of the final nucleus in the case of bombardment of H and He isotopes only. In all other cases, the spectra should appear to be continuous.

If the secondary groups of slower neutrons in the $T + d$ and $D + d$ reactions were produced in the result of the deuteron stripping without any change in the bombarded nucleus, we could expect a similar effect in the case of other light nuclei. The neutron spectrum and the effective production cross section should, consequently, depend smoothly on the number of the nucleons in the nucleus. In reality, neither the spectrum nor the cross section change smoothly. When the reaction has a large positive value of Q, the upper limit of the spectra exceeds the maximum energy of a neutron produced by deuteron stripping, without any change in the bombarded nucleus. In consequence, the state of the final nucleus has a marked influence upon the neutron spectrum being investigated.

The comparison of the neutron spectra obtained by bombarding T and He^3 targets is of special interest (see Fig. 1). These nuclei differ only in

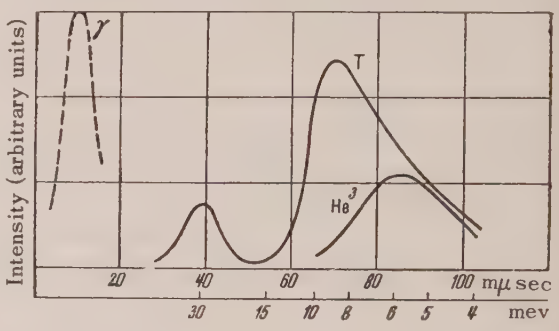

FIG. 1. Neutron spectra obtained by bombarding T and He^3 with 14.4 mev and 13.0 mev deuterons, respectively. The γ-peak is shown.

their charge, which should not greatly influence the stripping cross section for incident deuterons, since the energy of these is much larger than the Coulomb energy. Nonetheless, the neutron production cross section is almost twice as large in the $T + d$ reaction as in the He^3 reaction. The mean neutron energy in the both cases differs also, by approximately 3 mev. The cross section difference is partly due to the reaction $(d, 2n)$ reaction nor by a possible nonuniformity of the energies of the incident deuterons. This difference is evidently due to the production of the He^4 nucleus in an excited state which was discovered previously investigating the $T(p,n)He^3$ reaction [3,4].

The results of Henkel, Percy and Smith[5], who studied the neutron yield bombarding the H and He isotopes with deuterons of energies close to the stripping threshold, are also in agreement with our deduction. As it can be seen from the graphs, the production cross section for neutrons emitted at the angle 0° is several times larger for the T target than for the He^3 target. This difference can be explained by taking into account the existence of an excited state of the He^4 nucleus, since the reaction $(d, 2n)$ has a 1.2 mev higher threshold than the deuteron stripping.

Comparison of the production cross sections and of the neutron spectra in the reactions $T + d$ and $He^3 + d$ confirms, therefore, the existence of the excited state of He^4 with the excitation energy

equal to about 22 mev, and also indicates the absence of a similar state for the Li^4 nucleus. It should be expected that H^4, similarly to Li^4, does not exist in such a state. This confirms the assumption made by Smorodinski and Baz'[6] that the isotopic spin of the 22 mev excited state equals zero. If the isotopic spin of He^3 in this state were equal to 1, similar states would exist for Li^4 and for H^4, and the neutron spectrum of the $He^3 + d$ reaction would be analogous to the neutron spectrum of the $T + d$ reaction.

The neutron spectrum obtained by bombardment of He^4 is of equal interest. The final nucleus obtained in this case for the (d, n) reaction is Li^5. For this nucleus the existence of a 2.5 mev excited state is currently assumed[7], besides the unstable ground state. It is well known that the energy difference between the two states of Li^5 (or He^5) represents the very important spin-orbit splitting constant. It should be noted, however, that the data indicating the existence of the excited state are so far not convincing[7]. The neutron spectrum obtained by bombarding He^4 with 13.0 mev deuterons is shown in Fig. 2. The arrows indicate

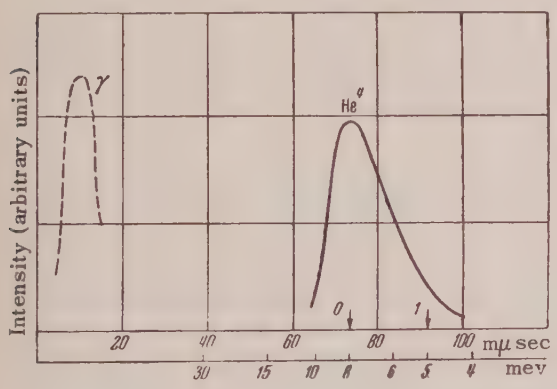

FIG. 2. Neutron spectra obtained by bombarding He^4 with 13.0 mev deuterons. Arrows indicate neutron energies corresponding to the ground state (0) and the supposed excited state (1) of Li^5. The γ-peak is shown.

the position of the centers of the energy groups which should correspond to the ground state (left) and to the excited state (right) of Li^5. It can be seen that in the neutron spectrum of the $He^4 + d$ reaction the excited state of Li^5 does not show up markedly, which is in accord with works denying the existence of a similar state for the mirror nucleus He^5.

We have estimated, for various elements, the effective production cross sections for neutrons emitted at the angle 0° to the direction of the incident deuteron beam. For all light elements investigated, with the exception of tritium, the cross section equals about 50 mbarn/sterad per nucleon, i.e., is roughly proportional to the number of nucleons in the nucleus A. For heavier elements the cross section diminishes; for Cu it is equal to 200 mbarn/sterad only.

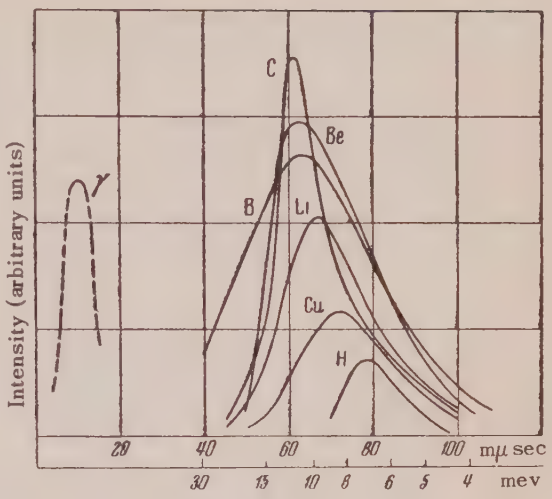

FIG. 3. Neutron spectra obtained by bombarding H and He^4 with 13.0 mev neuteron, and Li, Be, B, C and Cu with 14.4 mev deuterons. The γ-peak is shown.

The authors express their thanks to the staff of the Cyclotron Laboratory of the Academy of Sciences, USSR, who enabled the successful accomplishment of the present work.

[1] Bogdanov, Vlasov, Kalinin, Rybakov and Sidorov, J. Exptl. Theoret. Phys. (U.S.S.R.) **30**, 185 (1956).

[2] Bogdanov, Kurashev and Sidorov, Atomnaia Energiia **1**, 66 (1956).

[3] Vlasov, Kalinin, Ogloblin, Samoilov, Sidorov and Chuev, J. Exptl. Theoret. Phys. (U.S.S.R.) **28**, 639 (1955); Soviet Phys. JETP **1**, 500 (1955).

[4] Willard, Baira and Kington, Phys. Rev. **90**, 865 (1953).

[5] Henkel, Perry and Smith, Phys. Rev. **99**, 1050 (1955).

[6] A.I. Baz' and Y. A. Smorodinskii, J. Exptl. Theoret. Phys. (U.S.S.R.) **27**, 382 (1954).

[7] F. Ajzenberg and T. Lauritsen, Rev. Mod. Phys. **27**, 77 (1955).

Translated by H. Kasha
206

Magnitude of the Nuclear Spin-Orbit Interaction

I. I. LEVINTOV
Institute of Chemical Physics, Academy of Sciences, USSR
(Submitted to JETP editor February 16, 1956)
J. Exptl. Theoret. Phys. (U.S.S.R.) 30, 987-989 (May, 1956)

A WIDE group of interaction phenomena of nucleons with nuclei is at present sufficiently well described by a central potential with added spin-orbit term

$$A_1\rho(r) + A_2(\vec{l},\vec{\sigma})\, d\rho/r\, dr, \qquad (1)$$

where $\rho(r)$ is a function representing the density distribution of nucleons in the nucleus. Polarization effects in elastic scattering of medium and high energy nucleons as well as the spin-orbit splitting of single particle levels belong to this group of phenomena. In the case of polarization and scattering the $A_{1,2}$ are complex, $A_{1,2} = V_{1,2}e^{i\alpha_{1,2}}$ and, besides, there is a basis for the assumption that Eq. (1) describes the scattering processes adequately in the case of not too large angles only[1]. In the case of single particle levels the $A_{1,2}$ are real ($\alpha_{1,2} = 0$), Eq. (1) being applicable, however, only in the case of nuclei with strongly closed kernel (nuclei of the type of He^5, O^{17}, etc.). In these cases the kernel is only little deformed by the external nucleon, the criterion of which is closeness of the values of the magnetic moments of such nuclei to their Schmidt values.

In this note we intend to present the relative values of the moduli V_2/V_1, the ratio of the central and of the spin-orbit potentials, based on all data available to the author.

1. The ratio V_2/V_1 can be obtained from the polarization data at high energies (100-300 mev). It is not necessary to determine the function $\rho(r)$ if we assume that the added spin-orbit term (so) in Eq. (1) has only a small influence upon the phases ($\delta_l^{s.o} \ll 1$) while the phase shift caused by the central part of the potential may be arbitrarily large. This approximation is correct for all nuclei and leads to an expression for the neutron polarization similar to the well-known Fermi formula[2], obtained by him, however, under the assumption of small phase shift

$$P(\theta) = 2\theta k^2 |V_2/V_1| \sin(\alpha_1 - \alpha_2) / [1 + k^4 |V_2/V_1|^2 \theta^2]. \qquad (2)$$

(for details, see Ref. 3). It follows from (2) that $V_1/V_2 = k^2\theta_m$ and $\sin(\alpha_1 - \alpha_2) = P_m$, where θ_m is the angle of the maximum polarization P_m. Since the angle θ_m is not very small (12°-25°) we can obtain the value of V_2/V_1 from (2) with the help of well-known data[1] on the proton scattering polarization (see Table below). The mean value obtained for V_2/V_1 is 3.5×10^{-27} cm^2.

2. The estimation of the ratio V_2/V_1 from the low-energy scattering data on nuclear levels and shells requires the determination of the function $\rho(r)$. The evaluation is, however, correct in several cases:

1) Levels of He^5 and Li^5. The well-measured phase dependence of $P_{1/2}$ and $P_{3/2}$ levels in 1 to 15 mev nucleon scattering by He^4 can be exactly calculated assuming $\rho(r) \approx \exp(-r^2/a^2)$. Best agreement with experiment is obtained in Ref. 4 for the potential:

$$\left[1 - \beta(\vec{l},\vec{\sigma})\frac{d}{r\,dr}\right] A \exp[-r^2/a^2],$$

where $a = 2.3 \times 10^{-13}$ cm, $A = 47.32$ mev, $\beta = 7.4\,(\hbar^2/Mc^2)$ (M is the nucleonic mass). We then obtain the value of $V_2/V_1 = 3.3 \times 10^{-27}$ cm^2.

2) Single particle doublet levels of O^{17} and Pb^{209}. The estimation of the absolute value of V_2 in Eq. (1) was done by Blin-Stoyle[5] for the levels of Pb^{209}, for the case of an infinitely deep well. We have obtained a more exact result, solving the Schrödinger equation for a finite potential well with flat bottom and diffuse walls, making use of Airy functions. The expression for V_2/V_1 in the first approximation of the perturbation theory is:

$$\frac{V_2}{V_1} = \frac{\Delta E_{co}}{V_1}\frac{R_0^2}{2l+1}\,\frac{(\hbar^2/4mR_0^2E_{co})[(E_l+1/2)^2 - (l+1/2)^2] + (E_l+1/2)\delta + 1/2E_l^2\delta^2}{(1+E_l\delta+1/3E_l^2\delta^2)(1+1/2\delta)}, \qquad (3)$$

where ΔE_{co} is the value of the doublet splitting, E_{co} is the center-of-mass energy of the doublet (defined as the binding energy of the lower doublet component $+\frac{l+1}{2l+1}\Delta E_{co}$), R_0 is the total radius of the nucleus (taking the diffusion into account): $R_0 = (1.33\,A^{1/3} + 1.3) \times 10^{-13}$ cm, δ is the relative value of the diffusion*, given by:

$$-E_l = \frac{R_0}{\hbar}\sqrt{2mE_{co}}\,\frac{K'_{l+1/2}(R_0\hbar^{-1}\sqrt{2mE_{co}})}{K_{l+1/2}(R_0\hbar^{-1}\sqrt{2mE_{co}})} + \frac{1}{2},$$

Data on V_2/V_1

Source	Nucleus	Energy in mev	$(V_2/V_1)\times 10^{27}$ cm^2
Polarization of high-energy protons	He	315	3.3
	C	290	3.4
	C	130	3.5
	Be	315	4
	Be	130	3.5
	Al	290	3.5—4.5
	Al	130	4.5
	Fe	130	3.5
	Cd	130	4
	Jn	130	3
	Bi	130	3.5
	U	130	3.5
Scattering	$He^4 - p$	1 — 10	3.9
	$He^4 - n$	1 — 18	3.3
Single-particle levels	O^{17}	$1D_{5/2-3/2}$	3.9
	Pb^{209}	$3D_{5/2-3/2}$	3.0
	Pb^{209}	$2G_{9/2-7/2}$	3.3
Shells	—	—	4.

where $K_{l+1/2}$ is the modified Bessel function. The values of V_1 for $\delta \ll 1$ are determined from the logarithmic derivative condition:

$$F_l^{-1}\{R_0(1-\delta)\hbar^{-1}\sqrt{2m(V_1 - E_{co})}\} - E_l^{-1}\{R_0\hbar^{-1}\sqrt{2mE_{co}}\} = \delta.$$

E_l and F_l are tabulated in Ref. 7. We obtain from the above V_1 (Pb^{209}) = 54 mev for $\delta = 0.29$.

There exist two single particle doublets in the case of Pb^{209} [8]:

$3D_{5/2-7/2}$ ($\Delta E_{co} = 0.98$ mev, $E_{co} = 1.91$ mev),
$2G_{9/2-7/2}$ ($\Delta E_{co} = 2.03$ mev, $E_{co} = 2.9$ mev).

In the case of O^{17}, one doublet[9]:

$1D_{5/2-3/2}$ ($E_{co} = 1.81$ mev, $\Delta E_{co} = 5.08$ mev).

In general, the values of V_2/V_1 and δ can be determined for the case of Pb^{209} in a unique way with the help of Eq. (3). However, the simultaneous solution of Eq. (3) for the both doublets gives a much too low value of $\delta(\sim 0.08)$. This fact is evidently connected with a substantial deformation of the kernel of the Pb^{209} nucleus. We have, therefore, for the estimation of the ratio V_2/V_1, chosen the values of δ and V_1 according to the potential of Ref. 9: The values of V_2/V_1 in the Table are calculated for $\delta = 0.57$ (O^{17}), $\delta = 0$ (Pb^{209}) and $V_1 = 50$ mev.

3. The sequence of level filling in shells, calculated using potential of a form in-between the oscillatory and the square-well potentials, gives the value of $V_2/V_1 = 4 \times 10^{-27}$ cm^2. [10]

The relative value of the spin-orbit potential is therefore constant for wide variations of nucleon energies and of the size of the nucleus being equal approximately to 3.5×10^{-27} cm^2. This fact can be interpreted as an indication that the effective nuclear potential is the mean potential of the nucleons forming the nucleus. It is essental that, averaging over closed shells, forces depending on the products of spins of the external and the nuclear nucleons (e.g., tensor forces) do not appear in the first approximation. The forces leading to

the desired interaction are of the form $V(r)\{1(\vec{\sigma}_i + \vec{\sigma}_j)\}$[5]. The existence of a strong spin-orbit interaction is an indication of the presence of such forces, and the interaction constant expresses their magnitude in relation to central forces in the nucleon-nucleon interaction.

I wish to express my thanks to L. D. Landau and A. S. Kompaneits for discussion and advice.

* R_0 and δ are chosen according to the potential of Woods and Saxon[6] $V(r) = V_0(1 + i\xi)\{1 + \exp \times[(r - r_0)/a]\}^{-1}$, $r_0 = 1.33\, A^{1/3} \times 10^{-13}$ cm, $a = 0.49 \times 10^{-13}$ cm. In our case this potential can be approximated by a trapezium-shaped well with $R_0 = (1.33\, A^{1/3} + 1.3) \times 10^{-13}$ cm, $\delta = 4.3\ a/R_0$, $V_0 = 50$ mev, $\xi = 0$.

[1] Fernback, Heckrotte and Lepore, Phys. Rev. 97, 1057 (1955).

[2] Dickson, Rose and Salter, Proc. Phys. Soc. (London) 68A, 361 (1955).

[3] I. Levintov, Dokl. Akad. Nauk SSSR 107, 240 (1956).

[4] Sach, Biedenharn and Breit, Phys. Rev. 93, 321 (1954).

[5] R. J. Blin-Stoyle, Phil. Mag. 96, 977 (1955).

[6] Melkanoff, Moszowski, Nodvik and Saxon, Phys. Rev. 101, 507 (1956).

[7] A.E.S. Green and K. Lee, Phys. Rev. 99, 772 (1955).

[8] J. A. Harvey, Canad. J. Phys. 31, 278 (1953).

[9] R. K. Adair, Phys. Rev. 92, 1491 (1953).

[10] W. Heisenberg, *Theorei des Atomkernes*, Goettingen, 1952.

Translated by H. Kasha
209

Modification of Double Proton Scattering Experiments

L.N. ROZENTZVEIG
Institute of Technical Physics, Academy of Sciences, Ukrainian SSR

(Submitted to JETP editor December 8, 1955)
J. Exptl. Theoret. Phys. (U.S.S.R.) 30, 597-598 (March, 1956)

SCATTERING of nonrelativistic protons by nuclei of zero spin is described by a two-row scattering matrix.

$$f(\theta, \varphi) = A(\theta) + B(\theta)(\vec{n\sigma}), \qquad (1)$$

where $\mathbf{n}$ denotes the normal to the plane of scattering, and functions A and B are expressed by phases according to known formulas. The function

$$P(\theta) = (AB^* + A^*B)/(|A|^2 + |B|^2) \qquad (2)$$

determines the polarization as a result of scattering of the originally nonpolarized beam as well as the azimuthal asymmetry observed when polarized protons are scattered.

For the experimental determination of P it is necessary to subject the protons to double scattering. By measuring the ratio of intensities for $\mathbf{n}_1 = \mathbf{n}_2$ and $\mathbf{n}_1 = -\mathbf{n}_2$ equal to

$$R = (1 + P_1P_2)/(1 - P_1P_2), \qquad (3)$$

we find the product P_1P_2, and if the factor P_1 is known we obtain P_2 (or vice versa). The success of measurement of this kind therefore depends on the existence of a "standard" scattering process for which the dependence of P on the angle of scattering and energy E is previously known. Note that even if both scatterings are by the same kind of nuclei and $\theta_1 = \theta_2$, $P_1 \neq P_2$ since the energy E_2 before the second scattering is smaller than the initial energy E_1 by the amount of energy imparted to the nucleus, which is considerable in the case of scattering by light nuclei.

The purpose of this note is to describe an experiment which in principle permits the direct determination of P_2. Let the beam of hydrogen molecular ions H_2^+ incident on the scattering target be such that its ratio q of the number of parahydrogen ions to the number of orthohydrogen ions is considerably different from the equilibrium value $q_0 = 1/3$. Upon entering the target the molecular ions "break up" and the two protons are scattered independently of each other. If two counters register coincidences due to protons from the same molecular ion scattered in directions θ, φ_1 and θ, φ_2, the number of coincidences D is proportional as follows:

$$D \sim \frac{q}{1+q}(F\chi_0, F\chi_0) + \frac{1}{3(1+q)} \sum_{m=-1}^{1} (F\chi_1^m, F\chi_1^m), \qquad (4)$$

where χ_0 and χ^m are wave functions of the proton spins for the para- and orthomolecules and F is the "direct product" of matrices f_1 and f_2

$$F = f_1(\theta, \varphi_1) \times f_2(\theta, \varphi_2); \qquad (5)$$

f_1 and f_2 act upon the spin variables of the first and second proton, respectively.

Indicating

$$\chi_{1x} = -2^{-1/2}(\chi_1^1 - \chi_1^{-1}); \quad (6)$$

$$\chi_{1y} = i2^{-1/2}(\chi_1^1 + \chi_1^{-1}); \quad \chi_{1z} = \chi_1^0$$

and making use of (1) we can write $F\chi_0$ in the form

$$F\chi_0 = A^2\chi_0 - B^2(\mathbf{n}_1\mathbf{n}_2)\chi_0 \quad (7)$$

$$+AB(\mathbf{n}_1 - \mathbf{n}_2, \vec{\chi}_1) - iB^2([\mathbf{n}_1\mathbf{n}_2], \vec{\chi}_1),$$

from which

$$(F\chi_0, F\chi_0) = \sigma_0^2(\theta)[1 - P^2(\theta)(\mathbf{n}_1\mathbf{n}_2)], \quad (8)$$

where $\sigma_0(\theta) = |A|^2 + |B|^2$ is the scattering cross section for the nonpolarized beam. The m summation in the right side of (4) is obtained from the condition that when $q = q_0$, $D \sim \sigma_0^2(\theta)$

$$\sum_m (F\chi_1^m, F\chi_1^m) = 4\sigma_0^2(\theta) - (F\chi_0, F\chi_0). \quad (9)$$

Accordingly, Eq. (4) takes the form:

$$D \sim \sigma_0^2(\theta)\left[1 - \frac{3q-1}{3(q+1)}P^2(\theta)(\mathbf{n}_1\mathbf{n}_2)\right], \quad (10)$$

and for the determination of P^2 it is sufficient to measure D for $(\mathbf{n}_1, \mathbf{n}_2) \sim 1$ and for $(\mathbf{n}_1\mathbf{n}_2) = -1$.

Unfortunately, the experiment under discussion will require considerably longer exposures than for usual double scattering. Indeed, the maximum permissible current in the incident beam is determined by the ratio of the effect under investigation to the background of chance coincidences. Let ν denote the number of scattered protons entering each of the counters, n the number of H_2^+ ions incident on the target, τ the resolving time of the coincidence circuit. The numbers of true and accidental coincidences are $\nu^2/2n$ and $2\tau\nu^2$, respectively, i.e., the condition $n \ll 1/4\,\tau$ must be fulfilled. Therefore, even when $\tau \sim 10^{-10}$ sec, the instantaneous value of the current into the target must not exceed 10^8 to 10^9 ion/sec, which is considerably less than current generally used in double scattering experiments. It should be noted that the formation of a molecular ion source of H_2^+ c $q \gg 1$ producing a current of the order of 10^9 ion/sec is apparently quite feasible.

Translated by J.L. Herson
116

Isomeric Transition of the Sn^{117*} Nucleus

S. M. KALEBIN

(Submitted to JETP editor December 22, 1955)
J. Exptl. Theoret. Phys. (U.S.S.R.) 30, 957-959
(May, 1956)

A RADIOACTIVE source containing the tin isotope Sn^{117*} was obtained by bombarding chemically pure cadmium with α-particles in the cyclotron. Radioactive tin was obtained by the reactions $Cd^{110}(\alpha, n)Sn^{113}$; $Cd^{114}(\alpha, n)Sn^{117*}$ [1,2]. In addition, reactions with the formation of radioactive indium isotopes took place. The separation of the radioactive tin into pure form was carried out chemically. The irradiated cadmium was first kept for five days. In this time all short lived radioactive isotopes decayed. The central feature of the chemical separation of radioactive tin into pure form was its distillation in the form of bromide, $SnBr_4$, into a collector filled with concentrated hydrochloric acid[3-7]. This sufficed to separate tin and indium. The distillation mentioned above was carried out twice; the first product was radioactive, the second, not. The contents of the distillation apparatus in both the first and second case were radioactive. The experiments carried out gave reason to believe that the source obtained in this way contained radioactive tin. Later on, the γ-spectrum, electron absorption curve, decay curve and electron spectrum of this source were obtained. The results of these experiments agree well with the data in the literature if we consider that Sn^{117*} and Sn^{113} are in the source obtained. The radioactive transformations of these isotopes, in agreement with the published data of Ref. 8, follow the scheme shown on Fig. 1.

Starting from this decay scheme, identification of the peaks of the γ-spectrum from this source was carried out. This spectrum is shown in Fig. 2. It was obtained on a 20-channel luminescence spectrometer developed by G. R. Kartashev. A crystal of NaI was used. Four peaks are indicated on the spectrum. The peak at 154 kev relates to the cascade γ-transition of Sn^{117*}; the peaks at 260 and 398 kev, to the cascade γ-transition of In^{113}. A peak at an energy of 325 kev is also present in the γ-spectrum. Of all possible combinations of

γ-transitions of radioactive In^{114} or Sn^{117*} isotopes, such an energy can be obtained only from the sum of two γ-transitions of Sn^{117*}; therefore, it is natural to assume that this peak comes from the direct transition of Sn^{117*} from the metastable to ground state. This transition has not previously been observed experimentally. Including this, the decay can be considered to follow the scheme shown on Fig. 3.

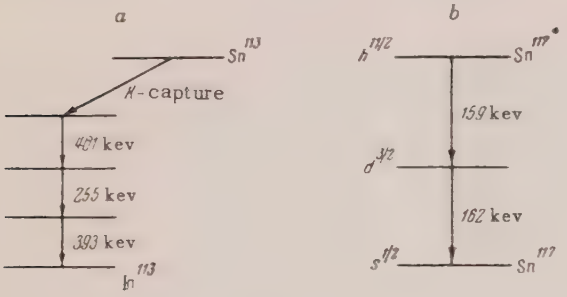

FIG. 1. a--Decay scheme of Sn^{113}. b--Transition scheme for isomeric Sn^{117*}.

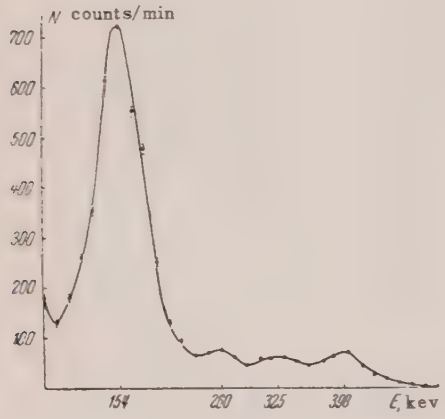

FIG. 2. γ-spectrum of the radioactive tin isotopes Sn^{113} and Sn^{117*}.

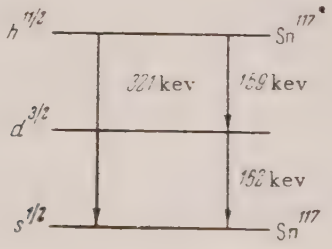

FIG. 3. Transition scheme for isomeric Sn^{117*}.

From selection rules the multipolarity of the new transition should be $E5$ or $M6$. Under the assumption that the 160 kev transition $h^{11/2} \rightarrow d^{3/2}$ of Sn^{117*} corresponds to an $M4$ multipolarity, and the new 320 kev transition to an $E5$, the relative probability of these transitions was calculated and found to be $W_{M4}/W_{E5} \sim 100$.

This theoretical calculation is in satisfactory agreement with the area of the 154 and 325 kev peaks. The large multipolarity of the radiation in the new transition indicates that this transition might be found by conversion electrons. In fact, such a transition was found when the electron spectrum of the source was obtained. This electron spectrum is shown in Fig. 4. This spectrum was obtained on a wide-aperture magnetic toroidal spectrometer developed by Vladimirskii, Trebukhovskii and Tarasov[9]. Spectrum a (Fig. 4) shows two electron peaks; the energy of the large peak was determined as 368 kev*. If we take into account the binding energy of the K-electron in indium of approximately 27 kev, then the electron energy of 368 kev obtained is in good agreement with the energy of the conversion electrons of the γ-ray from the isomeric transition of In^{113}. The energy of the small peak in this graph was determined as 291 kev. Taking into account the binding energy of about 29 kev of a K-electron in tin, this energy agrees very well with the energy of conversion electrons from the direct γ-transition of Sn^{117*} from the metastable state to the ground state. A month-and-a-half later this electron spectrum was taken again (Fig. 4b). The peak at 291 kev did not occur in the spectrum obtained. This is understandable if the 291 kev peak is considered to come from the isomeric transition of Sn^{117*}, which has a half-life of 14 days. Therefore, this confirms the assumed decay scheme (Fig. 3) of Sn^{117*}.

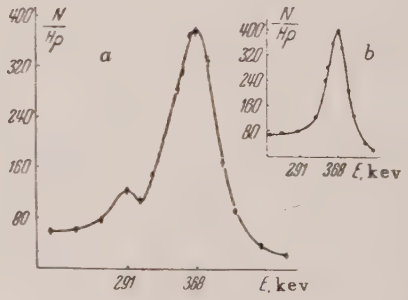

FIG. 4. a--Electron spectrum of the radioactive isotopes of tin, Sn^{113} and Sn^{117*}. b--The same spectrum 1½ months later.

The magnitude of the conversion coefficient of the observed 3 25 kev transition is of great interest. However, it is impossible to calculate a more or less reliable value from the data which were obtained in this experiment with spectrometers of poor resolution. A qualitative estimate of the magnitude of this conversion coefficient was carried out. To do this, the values of the conversion coefficients and the ratio N_K/N_L for In^{113} were assumed known. For the transition considered a ratio of $N_K/N_L \sim 0.3$ was obtained. The theoretical value of the conversion coefficient for a 320 kev, $E5$ transition in a nucleus with atomic number 50 is about unity. Therefore, the experimental and theoretical values of the conversion coefficients are near to each other.

In conclusion, I should like to use this opportunity to express my gratitude to Iu. V. Trebukhovskii, G. R. Kartashov and V. S. Kuryshev, who gave me the opportunity of using their apparatus for carrying out this experiment. The author is particularly thankful to V. V. Vladimirskii and N. P. Rudenko for valuable suggestions and advice.

* This transition is convenient to use for calibrating the β-spectrometer.

[1] J. J. Livingood et al., Phys. Rev. 55, 667 (1939).
[2] E. C. Mallary et al., Phys. Rev. 77, 743 (1950).
[3] W. Plato, Z. anorg. Chem 68, 26 (1910).
[4] H. Weber, Z. anal. Chem 50, 640 (1911).
[5] W. Hartman, Z. anal. Chem. 58, 148 (1919).
[6] J. Schwaibold et al., Biochem. Z. 306, 113 (1940).
[7] R. D. Maxwell et al., J. Chem Phys. 17, 1006 (1949).
[8] J. M. Cork et al., Phys. Rev. 84, 596 (1951).
[9] V. V. Vladimirskii, Iu. V. Trebukhovskii and E. K. Tarasov, *Experimental Apparatus and Technique* (in the press).

Translated by G. E. Brown
194

Theory of Interaction of Excitons with the Phonon Field

V. A. MOSKALENKO
Kishinevskii State University

(Submitted to JETP editor January 4, 1956)
J. Exptl. Theoret. Phys. (U.S.S.R.) 30, 959-961
(May, 1956)

THE presence of excitons in an ionic crystal lattice is responsible for its polarization [1-3] which, in turn, reacts on the exciton. This interaction with the lattice is small in crystals with a weak inertial polarization, and also when the effective mass of the electron and hole are approximately equal. In this case the exciton is called "nonpolarizing". The object of this note is to clarify the influence of the inertial polarization of the lattice on several properties of nonpolarizing excitons. The polarization of the medium is calculated by macroscopic methods. The Hamiltonian is written in the effective mass approximation.

The Hamiltonian of the system consists of two terms $H = H_0 + H_i$, where H_0 is the Hamiltonian of the exciton and free phonon field

$$H_0 = \frac{P_R^2}{2m} + H_r + \Sigma_f E(f)\, a_f^+ a_f, \qquad (1)$$

and H_i is the interaction

$$H_i = \sum_f A_f [e^{ifR} e_f(r)\, a_f + a_f^+ e_{-f}(r)\, e^{-ifR}]. \qquad (2)$$

Here we employ

$$H_r = \frac{P_r^2}{2\mu} - \frac{e^2}{xr}, \quad e_f(r) = e^{iy_1(f,r)} - e^{-iy_2(f,r)}; \qquad (3)$$

$$A_f = -(e/f)\sqrt{2\pi\hbar\omega c/V}, \quad y_1 = \mu_2/m, \quad y_2 = \mu_1/m,$$

where μ_1 and μ_2 are the effective masses of the electron and hole, respectively; m and R are the mass and coordinate of the center of mass of the electron and hole; μ and r, the reduced mass and relative coordinate of the electron and hole; f, $E(f) = \hbar\omega$, the wave vector and energy of the phonon; ω the limiting frequency of the longitudinal optical oscillations; $c = 1/x - 1/\epsilon$ with x the square of the index of refraction of the crystal and ϵ, the dielectric constant; a_f is the Bose operator. In zero-order approximation the coordinate R describes the free motion of a quasi-particle of mass m and momentum P_R. The energy spectrum of the system in this approximation consists of a continuum labelled by the quantum states of relative motion.

In calculating the interaction H_i it is convenient to introduce the total momentum of the system,

which is a constant of motion, according to the following canonical transformation[4-6]

$$\eta_f = a_f e^{i(\mathbf{f},\mathbf{R})}; \quad \eta_f^+ = a_f^+ e^{-i(\mathbf{f},\mathbf{R})}; \tag{4}$$

$$P_R = P - \hbar \sum_{\mathbf{f}} \mathbf{f}\eta_f^+ \eta_f; \quad \mathbf{P} = -i\hbar\, \partial/\partial \mathbf{R}.$$

In the new variables the Hamiltonian of the system is

$$H = \frac{P^2}{2m} + H_r + \sum_{\mathbf{f}} \mathcal{E}(f)\, \eta_f^+ \eta_f \tag{5}$$

$$+ \frac{\hbar^2}{2m} \sum_{\mathbf{f},\mathbf{g}} (\mathbf{f},\mathbf{g})\, \eta_f^+ \eta_g^+ \eta_f \eta_g +$$

$$+ \sum_{\mathbf{f}} A_f (e_f \eta_f + \eta_f^+ e_{-f}),$$

$$\mathcal{E}(f) = E(f) + \hbar f^2 f^2/2m - \hbar \mathbf{f}\mathbf{P}/m. \tag{6}$$

To obtain corrections to the total energy of the system we use the method of successive diagonalization of the Hamiltonian by a unitary transformation[4,6,7].

$$H' = U^{-1} H U. \tag{7}$$

We find the operator U to be

$$U = e^S; \quad S = \sum_g (\alpha_g \eta_g - \eta_g^+ \alpha_g^+). \tag{8}$$

The quantities α_g, which are of the same order as H_i, are assumed to depend on the operators H_r, r. For convenience, we expand the unitary operator U in powers of the small parameter of the theory

$$U = 1 + S + {}^1/_2 S^2 + \ldots \tag{9}$$

The transformed Hamiltonian will be diagonal to second order only if S, and consequently α_g, are defined from the condition $H_i = [S, H_0]$. Then H' is

$$H' = H_0 + {}^1/_2 [H_i, S].$$

It is easy to show that α_f is defined by the condition

$$[\alpha_f, H_r] + \alpha_f \mathcal{E}(f) + (\hbar/m)\, \alpha_f \mathbf{P}_F \mathbf{f} = A_f e_f, \tag{10}$$

where $\mathbf{p}_F = \hbar \sum_{\mathbf{f}} \mathbf{f} \eta_f^+ \eta_f$ is part of the total momentum belonging to the field.

If $\mathbf{P}_F$ is to be viewed as the mean value of the field momentum, then the operators α_f can be defined as matrices in the space of the eigenfunctions of the operator H_r:

$$(\alpha_f)_{n,m} = \frac{A_f (e_f)_{n,m}}{E_m - E_n + \mathcal{E}'(f)}, \tag{11}$$

$$(\alpha_f)^+_{n,m} = \frac{A_f (e_{-f})_{n,m}}{E_n - E_m + \mathcal{E}'(f)},$$

$$\mathcal{E}'(f) = E(f) + (\hbar^2 f^2/2m) - (\hbar/m)\, \mathbf{f}(\mathbf{P} - \mathbf{P}_F).$$

The diagonal matrix element of the Hamiltonian H' gives the energy of the system with inclusion of second-order corrections

$$(1, \ldots \bar{n}_f \ldots | H' | 1, \ldots \bar{n}_f \ldots) \tag{12}$$

$$= P^2/2m + E_1 + \sum \mathcal{E}(f)\, \bar{n}_f$$

$$- \sum_{\mathbf{f},m} (1 + \bar{n}_f) \frac{A_f^2 |(e_f)_{1,m}|^2}{E_m - E_1 + \mathcal{E}'(f)}$$

$$+ \sum_{\mathbf{f},m} \bar{n}_f \frac{A_f^2 |(e_{-f})_{1,m}|^2}{E_1 - E_m + \mathcal{E}'(f)} +$$

$$+ \frac{\hbar^2}{2m} \sum_{\mathbf{f},\mathbf{g}} (\mathbf{f},\mathbf{g})\, \bar{n}_g (\bar{n}_f - \delta_{f,g}),$$

where $\bar{n}_f$ is the mean Planck value, $(e_f)_{1,m}$ is the matrix element between hydrogen-like functions, m is the totality of the three hydrogen quantum numbers, E_m is the corresponding energy level. For zero phonon field and for small momenta P we obtain

$$E = \frac{P^2}{2m} + E_1 - \sum_{\mathbf{f},m} \frac{A_f^2 |(e_f)_{1,m}|^2}{E_m - E_1 + E_1(f)} \tag{13}$$

$$- \frac{\hbar^2 g^2}{3m^2} \sum_{\mathbf{f},m} \frac{A_f^2 f^2 |(e)_{1,m}|^2}{[E_m - E_1 + E_1(f)]^3},$$

where $E_1(f) = \hbar\omega + \hbar^2 f^2/2m$.

The discrete level of the exciton as a result of the interaction is lowered by an amount

$$E_1' = E_1 - \sum_{f,m} \frac{A_f^2 |(e_f)_{1,m}|^2}{E_m - E_1 + E_1(f)} . \qquad (14)$$

For the same reason the altered exciton mass μ_{eff} is equal to

$$\frac{1}{\mu_{eff}} = \frac{1}{m}\left[1 - \frac{2}{3}\frac{\hbar^3}{m}\sum_{f,m}\frac{A_f^2 f^2 |(e_f)_{1,m}|^2}{[E_m - E_1 + E_1(f)]^3}\right]. \qquad (15)$$

An approximate evaluation of the sum for the case $\mu_1 = \mu_2$ gives

$$E_1' = E_1\left(1 + \frac{5}{2} cx \frac{\hbar\omega}{|E_1|}\right); \qquad (16)$$

$$\mu_{eff} = m\left(1 + \frac{2}{3} cx \frac{\hbar\omega}{|E_1|}\right),$$

where $E_1 = -\mu e^4/2\hbar^2 x^2$.

[1] S. I. Pekar, *Investigation of the Electronic Theory of Crystals*, GITTL, 1951.

[2] I. M. Dykman and S. I. Pekar, Trudy Fiz. Inst., Akad. Nauk, Ukrainian SSR 3, 92 (1952).

[3] V. A. Moskalenko, Reports of the Kishinevskii State University 17, 103 (1955).

[4] S. V. Tiablikov, J. Exptl. Theoret. Phys. (U.S.S.R.) 21, 16 (1951); 22, 513 (1952).

[5] N. N. Bogoliubov, Ukrainian Journal of Mathematics 2, 3 (1950).

[6] N. N. Bogoliubov and S. V. Tiablikov, Dokl. Akad. Nauk SSR 5, 10 (1949).

[7] G. Wentzel, *Introduction to the Quantum Theory of Fields*, OGIZ, pp. 61, 81, 1947 (Russian Translation).

Translated by G.E. Brown
195

Correlation between the Planes of Production and Decay of Λ^0-Particles

V. I. KARPMAN
Minsk Pedagogical Institute

(Submitted to JETP editor January 7, 1956)
J. Exptl. Theoret. Phys. (U.S.S.R.) 30, 963-964
(May, 1956)

1. RECENTLY, correlations between planes of production and decay of hyperons have been found in a series of experiments[1-3]. These correlations consist in the fact that the angle between these planes is usually small. A theoretical analysis of the effect of correlation was carried out[4] and conclusions were drawn about the large spin of the Λ^0-particle and about the spin of the θ^0-meson being different from zero. It is not without interest, we believe, to consider another approach to this problem in addition to the method of Ref. 4.

2. We consider the z-axis to be perpendicular to the plane of production of the Λ^0-particle, and the direction of motion of the Λ^0-particle is taken as the y-axis. Then the angle between the planes of production and decay will be equal to the azimuthal angle φ. For calculation we now go to the system where the Λ^0 is at rest. it is not difficult to see that the angle φ does not change in this transition.

Let $\Phi_J^M(x, q)$ be the wave function of the system $\Lambda^0 + \theta^0$ describing the state with total angular momentum J and component $\hbar M$ along the z-axis; x and q denote dynamical variables of the Λ^0 - and θ^0-particles, respectively.

The Λ^0-particle as a sub-system of the system $\Lambda^0 + \theta^0$ is characterized by the density matrix $\rho(x', x)$[5]:

$$\rho(x', x) = \int \Phi_J^{M*}(x', q)\,\Phi_J^M(x, q)\,dq. \qquad (1)$$

The $\rho(x', x)$ can be expanded in the wave functions of the Λ^0-particle, which we denote by $\Lambda_m(x)$ (in which m can be considered the quantum number of the spin projection on the z-axis)

$$\rho(x', x) = \sum_{m_1, m_2} \rho_{m_1 m_2} \Lambda_{m_1}^*(x')\,\Lambda_{m_2}(x). \qquad (2)$$

3. We now turn to the calculation of the distribution of angles φ between the planes of production and decay of the Λ^0-particle.

The total moment of the proton and π^--mesons which are formed in the decay at rest of the Λ^0-particle, coincides with its spin j. If we designate by $\Psi_j^m(\theta, \varphi)$ the angular (and spin) part of the wave function of the stationary state of the system $p + \pi^-$, then

$$\Psi_j^m(\theta, \varphi) = c_1^m \chi^{+1/2} P_l^{m-1/2}(\theta)\, e^{i(m-1/2)\varphi} \qquad (3)$$

$$+ c_2^m \chi^{-1/2} P_l^{m+1/2}(\theta)\, e^{i(m+1/2)\varphi},$$

where c_1^m and c_2^m are Clebsch-Gordan coefficients, $\chi^{+1/2}$ are the spin wave functions of the proton, P_l^n is the spherical harmonic and $l = j + 1/2$ (depending on the relative parity of the Λ^0). In order to obtain the angular distribution, $f(\theta, \varphi)$, of the products of the Λ^0-decay it is obviously necessary to substitute in Eq. (2) the functions $\Psi_j^{m*1}(\theta, \varphi)$, $\Psi_j^{m2}(\theta,\varphi)$ from Eq. (3) instead of Λ^*_{m1} and Λ_{m2}, and carry out the summation over spin variables

$$f(\theta, \varphi) = \sum_{m_1,\, m_2 = \pm j,\, \pm(j-1),\ldots} \rho_{m_1 m_2} \Psi_j^{m_1 *}(\theta, \varphi)\, \Psi_j^{m_2}(\theta, \varphi). \tag{4}$$

The probability density for angle φ is $W(\varphi) = \int_0^\pi f(\theta,\varphi) \sin\theta\, d\theta$. If we substitute here from Eqs. (4) and (3), then one can see that $W(\varphi)$ takes the form

$$W(\varphi) = \sum_{k=0}^{(2j-1)/2} (a_k e^{2ik\varphi} + a_k^* e^{-2ik\varphi}), \tag{5}$$

where the coefficients a_k for $k \neq 0$ are linear combinations of off-diagonal elements only of the desnity matrix ($\rho_{m_1 m_2}$). Further, it must be noted that angle φ in the experiment is always measured in such a way that $\varphi < 90^\circ$ (that is, the angles φ, $\pi \pm \varphi$ and $2\pi - \varphi$ are considered as equivalent in the measurements). If we designate the probability density of the angle φ, defined in this way, through $\omega(\varphi)$, then we have $\omega(\varphi) = W(\varphi) + W(\pi+\varphi) + W(\pi - \varphi) + W(2\pi - \varphi)$ or

$$\omega(\varphi) = \sum_{k=0}^{(2j-1)/2} b_k \cos 2k\varphi, \tag{6}$$

$$b_k = 8\,|\,a_k\,|\cos(\arg a_k).$$

From Eq. (6) it follows that if the off-diagonal elements are zero, then the distribution of angles φ is isotropic and, consequently, there is no correlation between the planes of production and decay, even if $j \geq 3/2$.

Since $\omega(\varphi)$ satisfies the normalization condition

$$\int_0^{\pi/2} \omega(\varphi)\, d\varphi = 1,$$

then, substituting here from Eq. (6), we obtain the value of the coefficient b_0:

$$b_0 = 2/\pi \approx 0{,}637.$$

4. We consider in more detail the possible correlation effects, assuming that the spin of the Λ^0-particle is $j = 3/2$. In this case

$$\omega(\varphi) = 2/\pi + b_1 \cos 2\varphi. \tag{7}$$

We designate by $P(\varphi < \alpha)$ the probability that φ takes on a value less than α. From Eq. (7) we have

$$P(\varphi < \pi/4) = (1 + b_1)/2; \tag{8}$$

$$P(\pi/8 < \varphi < 3\pi/8) = 0{,}5.$$

On the other hand, we must have $\omega(\varphi) \geq 0$ for any $0 \leq \varphi \leq \pi/2$. This is possible only in case $b_1 \leq b_0 \approx 0.64$, i.e., $P(\varphi < \pi/4) \leq 0.82$. Thus, if the spin of the Λ^0-particle is equal to 3/2, then the probability that $\varphi > 45^0$ must be less than 18%, and the probability that $22.5^\circ \leq \varphi \leq 67.5^0$ should equal 50%. If this condition is not fulfilled (when correlation is present), then the spin of the Λ^0-particle j is greater than 3/2.

If we collect all experimental data relating to the angle φ given in Refs. 1-3 (including also the data of Table 8 in Ref. 3), we can conclude that the number of cases in which $\varphi > 45^0$ constitute 26%, and the number of cases in which $22.5^\circ \leq 67.5^\circ$ is 42%, which is comparatively near to 50%. Taking into account the fact that the statistics are still insufficient (there are data for only 19 decays) and that the accuracy of measurement is not high (this relates to the data of Table 8 in Ref. 3), one can say that the experimental data to date do not exclude the possibility that the spin of the Λ^0-particle is equal to 3/2. It must be noted that these data also do not exclude the possibility $j > 3/2$.

5. From the above development it follows simply that the spin of the θ^0-meson is different from zero. In fact, we shall assume the opposite. Then the wave function Φ_J^M of the $\Lambda^0 + \theta^0$ system defined in Sec. 2 can be expressed as

$$\Phi_J^M = \sum_m c_m \Lambda_m \varphi^{M-m}, \tag{9}$$

where φ^n is the wave function of the θ^0-meson and $n = M - m$ is the quantum number of the projection of its orbital moment. Substituting from Eq. (9) in Eq. (1), and taking account of the fact that functions φ^n with different n are orthogonal, we obtain an expression of the type Eq. (2), but with the off-diagonal elements of $\rho_{m_1 m_2}$ equal to zero. According to the preceding, correlation cannot be observed in this case, which contradicts experiment. Consequently, the spin of the θ^0-meson is different from zero. This result was obtained earlier[4] in a different way.

[1] J. Ballam, A. L. Hodson et al., Phys. Rev. 97, 245 (1955).

[2] W. B. Fowler, R. P. Shutt et al., Phys. Rev. 93, 861 (1954).

[3] W. B. Fowler, R. P. Shutt et al., Phys. Rev. 98, 121 (1955).

[4] L. D. Puzikov and Ia. A. Smorodinskii, Dokl. Akad. Nauk SSSR 104, 843 (1955).

[5] L. Landau and E. Lifshitz, *Quantum Mehanics*, Moscow, 1948.

Translated by G. E. Brown
197

Renormalization in the Equations of the New Tamm-Dancoff Method

V. I. Ritus
P. N. Lebedev Physical Institute, Academy of Sciences, USSR

(Submitted to JETP editor January 28, 1956)
J. Exptl. Theoret. Phys. (U.S.S.R.) 30, 965-967 (May, 1956)

IT is well known (see, for example, Ref. 1) that the equations of the new Tamm-Dancoff method for scattering of a meson by a nucleon, including only three virtual particles, contain divergent self-energy kernels of the meson and the nucleon and finite kernels corresponding to scattering with the meson being first absorbed ("graph with absorption") and scattering with the meson first emitted ("graph with emission"). We shall not consider renormalization of the self-energy kernels of the meson and nucleon and the difficulties arising with this[1], but shall assume that these kernels are corrections to the propagator of the system, which can be neglected in first approximation. We omit also all two-particle amplitudes containing antiparticles, assuming that in first approximation their influence on the amplitude " +meson, +nucleon" is small.

As a result, in first approximation an equation for one amplitude, " +meson, +nucleon" without self-energy kernel remains. In the solution of this equation, infinities of a vertex and self-energy type occur because of the kernel corresponding to the "graph with absorption." The renormalization of these divergences was studied recently by Dalitz and Dyson[2]; they came to the conclusion that the removal of these divergences was connected with the introduction of two renormalized charges into the theory (respectively, for the $s_{1/2}$ and $p_{1/2}$ states with isotopic spin $T = 1/2$) in addition to the fundamental charge g^2. Renormalization of these divergences was studied independently by us by a method used in Ref. 3* and it was shown that, contrary to the results of Dalitz and Dyson, the removal of divergences is connected with a finite charge renormalization and does not lead to any new constants.

In this note we give briefly our results and clarify the contradiction between them and the results of Ref. 2. For brevity of exposition and convenience in making a comparison, the notation of Ref. 2 will be used where possible.

2. The general solution of the integral equation for the amplitude "+meson, +nucleon" in state α (state α is characterized by angular momentum j and the parity of the system) has the form**

$$c_\alpha(p, l) = g_\alpha(p, l) + \frac{Qg^2}{8\pi^2}\int \sqrt{\frac{(E_p - \eta m)(E_l - \eta m)}{E_p \omega_p E_l \omega_l}}\,\frac{V_\alpha(p, \varepsilon)\, V_\alpha(l, \varepsilon)}{\varepsilon - \eta m - QS_\alpha(\varepsilon)} \qquad (1)$$

and is connected with the phase δ_α by the formula

$$\operatorname{tg}\delta_\alpha = -(\pi E_l \omega_l l \quad \varepsilon)\, c_\alpha(l, l).$$

In Eq. (1) $E_p = \sqrt{p^2 + m^2}$, $\omega_p = \sqrt{p^2 + \mu^2}$, $\epsilon = E_l + \omega_l$, $\eta = 1$ or -1, respectively, for even and odd states, $Q = 3$ or 0, respectively, for $T = 1/2$ and $3/2$; $g_\alpha(p, l)$ is the solution corresponding to the "graph" with emission." The integral equation for $g_\alpha(p, l)$ is obtained from the integral equation for $c_\alpha(p, l)$ if the term corresponding to the "graph with absorption" is omitted in the latter. Thus $g_\alpha(p, l)$ does not contain divergences. All divergences due to the "graph with absorption" are contained in the vertex function $V_\alpha(p, \epsilon)$ and the self-energy of the nucleon $S_\alpha(\epsilon)$. The divergence contained in the vertex function can be separated in

the form of a factor Z_α, such that $V_\alpha(p,\epsilon) = Z_\alpha(V_\alpha^R(p,\epsilon)$, where $V_\epsilon^R(p,\epsilon)$ is a finite function, defined by some integral equation and falls off with large p as p^λ, where $\lambda < 0$. The self-energy of the nucleon $S_\alpha(\epsilon)$ can be written in the form

$$S_\alpha(\varepsilon) = \frac{Z_\alpha^2 g^2}{8\pi^2}\left[\int_0^\infty \frac{P_\varepsilon(k)\,|\,v_\alpha(k)\,|^2 k^2 dk}{E_k\omega_k(E_k+m)}\right. \tag{2}$$

$$-\frac{1}{2}\frac{Q' g^2}{8\pi^2}$$

$$\left.\times\int_0^\infty\int_0^\infty \frac{q^2dqp^2dp}{E_q\omega_q E_p\omega_p} v_\alpha(p)\,P_\varepsilon(p)\,U_\alpha(\varepsilon,p,q)\,P_\varepsilon(q)\,v_\alpha(q)\right],$$

where

$$v_s(p) = (E_p+m)V_s^R(p,\varepsilon), \qquad v_p(p) = pV_p^R(p,\varepsilon)$$

(for the other notation, see Ref. 2). It is not difficult to show that both integrals in the brackets fall off more slowly than linearly; thus the factor Z_α^2 does not yet separate all divergences in $S_\alpha(\epsilon)$. Therefore, we consider the derivative $dS_\alpha(\epsilon)/d\epsilon = Z_\alpha^2\,\Lambda_\alpha(\epsilon)$. The function $\Lambda_\alpha(\epsilon)$ is given in Ref. 2 by Eq. (93). The authors of Ref. 2 assert that the integrals defining this function diverge. In fact, Eq. (93) is in error and

$$\Lambda_\alpha(\varepsilon) = \frac{g^2}{8\pi^2}\left[\left(\frac{d}{d\varepsilon}\int_0^\infty P_\varepsilon(k)\right)\frac{|\,v_\alpha(k)\,|^2 k^2 dk}{E_k\omega_k(E_k+m)}\right. \tag{3}$$

$$\left.+\frac{1}{2}\frac{Q'g^2}{8\pi^2}\int_0^\infty\int_0^\infty \frac{p^2dpq^2dq}{E_p\omega_p E_q\omega_q} v_\alpha(p)\,P_\varepsilon(p)\,\frac{dU_\alpha}{d\varepsilon}\,P_\varepsilon(q)\,v_\alpha(q)\right]$$

This formula differs from Eq. (93) in that in the denominator of the first term the factor m is changed to E_k and before the second term ½ occurs. It is easy to see that the first term in $\Lambda_\alpha(\epsilon)$ converges; thus $V_\alpha^R(k) \sim k^\lambda$, $\lambda < 0$ for $k \to \infty$. Investigation shows that the second integral also converges, rather than diverging as asserted in Ref. 2. In fact, we consider the integrals

$$J_1 = \int_{c'}^\infty dp\int_0^c dq\,\frac{p^2q^2}{E_p\omega_p E_q\omega_q} v_\alpha(p)\,P_\varepsilon(p)\,\frac{dU_\alpha}{d\varepsilon}\,P_\varepsilon(q)\,v_\alpha(q),$$

$$J_2 = \int_c^\infty\int_c^\infty \frac{p^2dpq^2dq}{E_p\omega_p E_q\omega_q} v_\alpha(p)\,P_\varepsilon(p)\,\frac{dU_\alpha}{d\varepsilon}\,P_\varepsilon(q)\,v_\alpha(q),$$

where $c' \gg c \gg m$. It is possible to show that for $p \gg q,\ m$; $dU_\alpha/d\epsilon \sim (2p^2)^{-1}$; for $p,\ q \gg m$: $dU_\alpha/d\epsilon \sim (pq)^{-1}\left[1 + 2x - \frac{(q+x)^2}{x}\ln(1+x)\right]$, where x is the smaller of the ratios q/p, p/q. Substituting these expressions in J_1 and J_2, respectively, and using also the fact that for large p, $V_\alpha^R(p,\epsilon) \sim p^\lambda$, $\lambda < 0$, we find that J_1 and J_2 converge. Insofar as the integrand in the second integral in Eq. (3) is symmetrical with respect to p and q, the convergence of the second integral in Eq. (3) follows from the convergence of J_1 and J_2.

Thus $\Lambda_\alpha(\epsilon)$ is finite, and not infinite as in Ref. 2. This means that the entire divergence in $S_\alpha(\epsilon)$ can be put into the first term of the expansion

$$S_\alpha(\varepsilon) = S_\alpha(\eta m) + Z_\alpha^2\int_{\eta m}^{\varepsilon}\Lambda_\alpha(x)\,dx \tag{4}$$

$$= S_\alpha(\eta m) + (\varepsilon-\eta m)\,Z_\alpha^2\Lambda_\alpha(\eta m) + Z_\alpha^2\frac{g^2}{8\pi^2}S_\alpha^R(\varepsilon)$$

and the factor Z_α^2. We substitute Eq. (4) and $V_\alpha^R \times (p,\epsilon) = Z_\alpha^2\,V_\alpha^R(p,\epsilon)$ into Eq. (1) and drop $S_\alpha(\eta m)$ in connection with the mass renormalization. Then, insofar as $Z_\alpha^2 = \infty$, we find that the second term in Eq. (1) has the form

$$\frac{g^2}{8\pi^2}\sqrt{\frac{(E_p-\eta m)(E_l-\eta m)}{E_p\omega_p E_l\omega_l}}\,\frac{V_\alpha^R(p,\varepsilon)\,V_\alpha^R(l,\varepsilon)}{-\int_{\eta m}^{\varepsilon}\Lambda_\alpha(x)\,dx} \tag{5}$$

$$= Q\frac{g_\alpha^2}{8\pi^2}\sqrt{\frac{(E_p-\eta m)(E_l-\eta m)}{E_p\omega_p E_l\omega_l}}$$

$$\times\frac{V_\alpha^R(p)\,V_\alpha^R(l)}{\varepsilon-\eta m-(Qg_\alpha^2/8\pi^2)\,S_\alpha^R(\varepsilon)},$$

where

$$g_\alpha^2 = Z_\alpha^2\,g^2/(1-Z_\alpha^2 Q\Lambda_\alpha(\eta m)) = -g^2/Q\Lambda_\alpha(\eta m),$$

because $Z_\alpha^2 = \infty$, and the remaining quantities are finite (it is possible to whos that $\Lambda_\alpha(\eta m) < 0$, so that $g_\alpha^2 > 0$). Thus, by virtue of a finite renormalization of the charge g_α^2, a completely determined function g^2 results and no new constants arise in the removal of divergences. In particular, for small g^2: $g_\alpha^2 = 2/3\ g^2$.

We mention by the way that the finite expressions Eqs. (96a) and (96b) in Ref. 2 are erroneous because of an incorrect sign in front of Q in Eqs. (55), (64), (67), (70) and (95), and in front of the second

term in Eqs. (76) and (92), and also because of incorrect factors in front of $V_\alpha^R(p)$ and $V_\alpha^{R+}(l)$.

3. The integral equations for $g_\alpha(p, l)$ and $V_\alpha^R(p, \epsilon)$ have an infinite upper limit of integration. The solution of these equations should be taken as limits of the solutions of these equations with a finite upper limit of integration, p_{max}, as $p_{max} \to \infty$. Then further investigation shows that the equations for $g_\alpha(p, l)$ and $V_\alpha^R(p, \epsilon)$ have finite solutions, behaving for large p as p^ν and p^λ, respectively, where ν and λ are those roots of the equations

$$-Q'g^2/16\pi^2 = F_j(\nu + 1/2), \quad -Q'g^2/16\pi^2 = F_j(\lambda),$$

$$F_{1/2}^{-1}(\lambda) = \pi[\lambda(\lambda+1)\sin\pi\lambda]^{-1} - \lambda^{-2} - (\lambda+1)^{-2} + (\lambda^2-1)^{-1} + (\lambda^2+2\lambda)^{-1},$$

which for $g^2 \to 0$ go over into the exponent of the first argument in the asymptotic kernel. For $T = j = 1/2$ with $g^2/4\pi > 3\pi(3\pi-8)^{-1} \approx 6.61$, ν and λ are complex, and it is possible to show that in this case the equations for $g_\alpha(p, l)$ and $V_\alpha^R(o, \epsilon)$ do not have solutions in the sense that the solutions of the equations with a finite upper limit do not have a well-defined limit for $p_{max} \to \infty$. Thus $g^2/4\pi$ should be less than 6.61. This limit on $g^2/4\pi$ is not connected with the condition of normalization of the full solution, as taken in Ref. 2. In fact, from the integrability of the wave function in **x**-space for $\mathbf{x} = 0$, it follows that the wave function in **p**-space for $p \to \infty$ should fall off faster than $p^{-3/2}$. However, the wave functions in p-space are the functions $\langle b_{-pu}\, a_{p\alpha}\rangle$, and not

$$\psi(p) = \sqrt{\omega_p} \sum_{u^+} u \langle b_{-pu} a_{p\alpha}\rangle,$$

as taken in Ref. 2. Therefore, the functions $f(p)$ and $g(p)$ in Ref. 2 should fall off faster than const and not faster than $p^{-1/2}$. But this condition does not limit g^2.

I am very thankful to Academician I.E. Tamm and his colleagues for discussions and advice.

Note added in proof: It is necessary to note that the removal of divergences from the "graph with absorption" are connected with a finite charge renormalization not only in the equations of the new Tamm-Dancoff method, but also in covariant equations in the approximation considered here. For the finite renormalization it is necessary that the renormalized vertex function falls off with a negative power of p for large momenta.

* This method is essentially the same as that of Ref. 2.

** This equation is obtained from the initial equation for the amplitude "+meson, +nucleon" by decomposition of angle variables using spherical harmonics (see Ref. 1).

[1] Silin, Tamm and Fainberg, J. Exptl. Theoret. Phys. (U.S.S.R.) 29, 6 (1955); Soviet Phys. JETP 2, 3 (1956).

[2] R. H. Dalitz and F. J. Dyson, Phys. Rev. 99, 301 (1955).

[3] M. Levy, Phys. Rev. 94, 460 (1954); S. Chiba, Progr. Theor. Phys. 11, 494 (1954).

Translated by G. E. Brown
193

Two τ-Mesons Detected in Photographic Emulsions

I. M. Gramenitskii, E. A. Zamchalova, M. I. Podgoretskii, M. I. Tret'iakova and M. N. Shcherbakova
P. N. Lebedev Physical Institute, Academy of Sciences, USSR

(Submitted to JETP editor February 6, 1956)
J. Exptl. Theoret. Phys. (U.S.S.R.) 30, 967-969 (May, 1956)

A STACK, consisting of 126 layers of unbacked electron-sensitive emulsions of type *R*, thickness 450μ and diameter 10 cm, were exposed for 7 hours at a height of 27 km. Two τ-mesons were found in the scanning; the characteristics of these are given in the table.

One of the τ-mesons was observed by following the track of a π^+-meson which had come to rest. All of the prongs of the star in which the τ-meson was produced were followed either to their end or to the point where they left the stack. No further heavy particle decay was found among the prongs coming to their end.

Two π-mesons (π^+ and π^-) coming from the decay of the τ-meson stopped; the third left the stack. The tracks of these π-mesons lay in a plane; coplanarity was established to an accuracy of 3°. The decay energy was $Q = (74.2 \pm 2)$ mev, and the mass, determined from the decay scheme, $m_\tau = (965 \pm 4) m_e$. The second τ-meson was found by area-scanning. A microprojection of it is shown on the picture. All black and grey tracks from the primary star end in the stack; additional heavy unstable particles did not appear among them.

All of the π-mesons produced in the decay also stopped in the stack; two of them were positively

TABLE

No. of the case	Primary star	Track length of τ-meson in mm	Energy of τ-meson in mev	Secondary Particles: Type	Secondary Particles: Track length in mm	Secondary Particles: Energy in mev	Decay energy Q in mev	Mass of τ-meson in units m_e	Angles between π-mesons in degrees	Θ	φ	Ψ
1	$12+0n$	$15\pm0,5$	50 ± 1	π	—	18 ± 1	$74,2\pm2$	965 ± 4	$\alpha_{12}=89\pm2$	56,5	176	59
				π^-	$8,5\pm0,4$	$21,0\pm0,15$			$\alpha_{23}=144\pm3$			
				π^+	$21,2\pm0,8$	$35,2\pm1,0$			$\alpha_{31}=126\pm3$			
2	$14+2n$ или $14+1p$	$10,5\pm0,3$	$40,8\pm0,8$	π^-	$7,7\pm0,3$	$19,8\pm0,4$	$74,9\pm1,4$	965 ± 3	$\alpha_{12}=33,5\pm1,5$	50	42	33
				π^+	$2,14\pm0,1$	$9,5\pm0,2$			$\alpha_{23}=159\pm2$			
				π^+	$33,2\pm1,5$	$45,6\pm1,2$			$\alpha_{31}=167\pm2$			

Key: Θ is the angle between the direction of flight of the τ-meson and the normal to its decay plane; φ is the angle between the direction of flight of the τ-meson and that of the π^--meson; ψ is the angle between the decay plane of the τ-meson and the plane of the emulsion. Both τ-mesons came off at a large angle with the vertical.

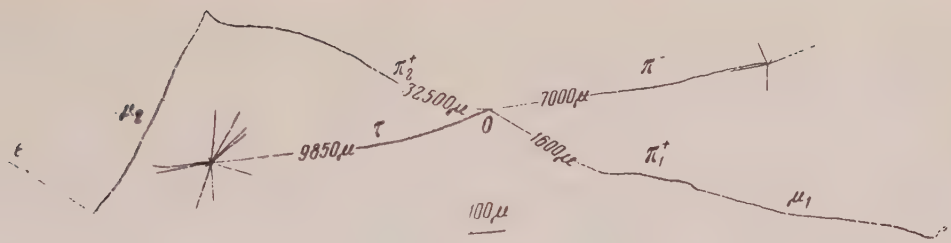

charged, the third, negatively. The tracks of the π-mesons lay in a plane to an accuracy of 2°. The decay energy was* $Q = (74.1 \pm 1.4)$ mev and the mass, determined from the decay scheme, $m_\tau = (964 \pm 3) m_e$. The first τ-meson came out at a very large angle to the plane of the emulsions, which made a direct measurement of its mass impossible. The track of the second τ-meson was gently sloping. A direct determination of its mass by multiple scattering and range led to the value $m_\tau = (1097 \pm 105) m_e$.

The comparatively small energy of one of the π^+-mesons produced in the decay of the second τ-meson stands out. Such a case supports, as is well known (see Ref. 1), the hypothesis that the τ-mesons and χ-mesons are different particles, and not different modes of decay of a single particle. Such a conclusion possible follows from the analysis of nuclear disintegrations in which heavy unstable particles are produced[2].

* In determination of the decay energies of both τ-mesons, several differences in the stopping power of emulsions of type R and type G-5 were taken into account. In order to carry out the corresponding corrections, we measured the track lengths of 110μ-mesons, produced in the decay of π-mesons which stopped. The mean length of track of these μ-mesons was (584 ± 2.4)μ, which differs by 2% from the value in G-5 emulsions.

[1] R. H. Dalitz, Phys. Rev. 94, 1046 (1954).

[2] Gramenitskii, Zamchalova, Podgoretskii, Tret'iakova and Shcherbakova, J. Exptl. Theoret. Phys. (U.S.S.R.) 28, 616 (1955); Soviet Phys. JETP 1, 562 (1955).

Translated by G. E. Brown
199

On Mass Renormalization in the Tamm-Dancoff Method

D. A. KIRZHNITS
P. N. Lebedev Physical Institute, Academy of Sciences, USSR

(Submitted to JETP editor February 6, 1956)
J. Exptl. Theoret. Phys. (U.S.S.R.) 30, 971-973 (May, 1956)

THE present article is concerned with the consistent application of the counterterm technique for mass renormalization in the Tamm-Dancoff method (abbreviated as the TD method). Because of the mathematical difficulties that arise, we also consider a renormalization method which does not require separation of the counterterms.

Mass renormalization in the TD method is usually accomplished by separation of the counterterms in the Hamiltonian[1]

$$H = H_0(M_1, \mu_1) + H' = H_0(M, \mu) + H' + \delta H',$$

$$H' = ig_1 \bar{\psi}(x) \gamma_5 \tau \varphi(x) \psi(x),$$

$$\delta H' = \delta M \bar{\psi}(x) \psi(x) + \delta \mu^2 \varphi(x) \varphi(x),$$

where M_1 and μ_1 are bare masses, and M and μ are renormalized masses. The equations of motion for the amplitude A are then given by the relationship

$$i\delta A / \delta\sigma = [A, H'] + [A, \delta H'].$$

The state vector of the system is resolved into states with different numbers of free particles (but possessing renormalized mass), and all amplitudes with a number of particles smaller than the given number are taken into consideration in each approximation of the method.

I.E. Tamm has noted that there is usually some inconsistency in the manner of application of these amplitude selection rules. These rules are strictly adhered to in relation to terms arising from H' in

the equation for A, whereas some of the terms associated with $\delta H'$ are simply dropped despite the fact that they contain terms which should be considered in a given approximation. This procedure corresponds to the Levy-Klein procedure (the retention in the integral equation kernels of only the lowest order terms in g_1^2) but is, strictly speaking, in contradiction with the TD method. Mass renormalization is considered below for the one-nucleon problem in the lowest TD approximation with the inclusion of all essential amplitudes.

Without dwelling on the details of the calculation (see Ref. 1) we shall present the final results (the meson counterterm can be neglected in this approximation):

$$\langle\psi(x)\rangle_t = \int S_R(x-x')\,[ig_1\gamma_5\tau\langle\psi(x')\varphi(x')\rangle_{t'} + \delta M\langle\psi(x')\rangle_{t'}]\,d^4x', \tag{1}$$

$$\langle\psi(x)\varphi(x)\rangle_t = g_1\int\Gamma(x-x')\langle\psi(x')\rangle_{t'}\,d^4x' + \delta M\int S_R(x-x')\langle\psi(x')\varphi(x)\rangle_{t'}\,d^4x'. \tag{2}$$

Here

$$S_R(x) = -\frac{1+\varepsilon(x)}{2}S(x),$$

$$\Gamma(x) = \frac{1}{2}\varepsilon(x)\,[S^+(x)\Delta(-x) - S(x)\Delta^+(-x)]\,\gamma_5\tau.$$

In the solution of this type of equation the terms with δM in the equations of intermediate amplitudes [in this case the last term in Eq. (2)] were usually dropped. The term with δM was retained only in the equation of the principal amplitude, where it compensated the divergence.

Retaining both terms with δM in (1) and (2) we first solve (2) with respect to $\langle\varphi(x)\psi(x)\rangle_t$; this is easily accomplished because of the different kernel contained in (2). Substituting this solution in (1) we obtain

$$\langle\psi(x)\rangle_t = \int S_R(x-x')\left[\int\mathfrak{M}(x'-x'')\langle\psi(x'')\rangle_{t''}\,d^4x'' + \delta M\langle\psi(x')\rangle_{t'}\right]d^4x', \tag{3}$$

where the Fourier representation of the mass operator $\mathfrak{M}$ is

$$\mathfrak{M}(p) = 3g_1^2 i\int d^4k\gamma_5\left(1+\frac{\delta M}{i\gamma k + M - \delta M}\right)[(S^+\varepsilon)_k\Delta_{k-p} - (S\varepsilon)_k\Delta^+_{k-p}]\,\gamma_5. \tag{4}$$

A transition is easily made from (3) to the equation [where $\psi(p)$ is the Fourier transform of $\langle\psi(x)\rangle_t$]:

$$[i\gamma p + M + \delta M + (2\pi)^4\mathfrak{M}(p)]\cdot\psi(p) = 0. \tag{5}$$

We now transform to the system in which the nucleon is at rest ($p = 0$). For the mass renormalization δM must now be chosen to satisfy the relationship

$$\delta M + (2\pi)^4\mathfrak{M}(p_0) = 0 \text{ where } p_0 = -i\gamma_0 M. \tag{6}$$

When the term with δM in (2) and (4) is dropped, this gives the usual result (L is the cutoff momentum):

$$\delta M \sim g_1^2 M\ln(L/M). \tag{7}$$

When all terms with δM are taken into consideration (4) becomes

$$\int_0^L\frac{1+a(\delta M)^3}{k^2+b(\delta M)^4}\,k\,dk,$$

where a and b are constants and δM is given by the expression

$$\delta M \sim \sqrt{g_1^2}L. \tag{8}$$

Thus in the simplest case considered above, the inclusion of all essential amplitudes in mass renormalization does not give rise to any additional difficulties. But it does lead to a change in the character of the divergences of the theory; for this reason considerable care must be used in perturbation theory renormalization in the TD method.

When all amplitudes with δM are retained in a more complicated problem such as the scattering of mesons by nucleons the equations of the intermediate amplitudes are very complicated and cannot be solved explicitly.

We shall therefore consider another method of renormalization which is not associated with separation of the counterterms but which is based, instead, on the direct use of the relationships between the bare and renormalized constants (see

Ref. 2). The Hamiltonian remains expressed in terms of the bare masses; the state vector will therefore be resolved into states with different numbers of particles possessing bare masses. For this reason the solution of any problem concerning particle interactions will be expressed in terms of bare constants, and, in addition, relationships will be required between these constants and the renormalization constants in order to express the solution in terms of observed quantities. For this purpose it is essential to solve another problem along with the fundamental problem, that is, the problem of the "envelopment" of an isolated meson and nucleon, i.e., their interaction with their own field.

The latter problem may be reduced to the following equations (in the lowest approximation of the TD method):

$$(\gamma\nabla + M_1)\langle\psi(x)\rangle_t = -ig\gamma_5\tau\langle\varphi(x)\psi(x)\rangle_t \qquad (9a)$$

$$= -\int \mathfrak{M}(x-x')\langle\psi(x')\rangle_t d^4x',$$

$$(\Box - \mu_1^2)\langle\varphi(x)\rangle_t = ig\tau(\gamma_5)_{\mu\nu}\langle\bar{\psi}_\mu(x)\psi_\nu(x)\rangle_t$$

$$= \int P(x-x')\langle\varphi(x')\rangle_t d^4x'.$$

Transforming to momentum space and using the definitions

$$\gamma\nabla\langle\psi(x)\rangle_t = -M\langle\psi(x)\rangle_t, \quad \Box\langle\varphi(x)\rangle_t = \mu^2\langle\varphi(x)\rangle_t,$$

we obtain equations which enable us to express M_1 and μ_1 in terms of M and μ:

$$-M + M_1 + (2\pi)^4\mathfrak{M}(M_1, \mu_1^2, M) = 0, \qquad (10)$$

$$\mu^2 - \mu_1^2 - (2\pi)^4 P(M_1, \mu^2) = 0.$$

We note in explanation that the mass operators $\mathfrak{M}$ and the polarization operator P in (9) depend on bare masses, whereas their Fourier representations $\mathfrak{M}(p)$ and $P(k)$ enter into (10), in which we have put $ip = -M$, $k^2 = -\mu^2$. The divergent integrals in $\mathfrak{M}$ and P are cut off by the substitution

$$(p^2 + M_1^2)^{-2} \to 2\int_{M_1^2}^{L^2} (p^2 + x)^{-3}\, dx.$$

As a result of the simultaneous solution of Eqs. (10) the following relationships are obtained ($\lambda = g_1^2/4\pi^2$):

$$\mu_1^2 = \mu^2 + \lambda L^2 + O(\ln L^2); \qquad (11)$$

$$M_1 = M\frac{(1-\lambda)(4-\lambda) + 3\lambda(4\lambda-3)\ln\lambda}{4(1-\lambda)^2 + 6\cdot\lambda(1-\lambda)\ln\lambda} + O\left(\frac{1}{L^2}\right).$$

It is important to note that the bare nucleon mass and δM are finite and different from (7). This results from the fact that the meson distribution function appearing in the mass operator contains in its denominator the square of the bare meson mass, which increases with L:

$$\lim_{L\to\infty}\int_0^{L^2}\frac{dk^2}{k^2 + \lambda L^2 + \mu^2} = \int_0^1 \frac{dx^2}{x^2 + \lambda}, \quad x = \frac{k}{L}.$$

Passing now to the scattering of mesons by nucleons, we confine ourselves to a state with isotopic spin $I = 3/2$, since in the state with $I = 1/2$ the mass operator is more complicated than in (9). The meson-nucleon equation is[1]:

$$\langle\varphi(x_1)\psi(x_2)\rangle_t = \langle\varphi(x_1)\psi(x_2)\rangle_{-\infty} \qquad (12)$$

$$+ \int (K_1 + K_2)\langle\varphi(x')\psi(x'')\rangle_{t'''} dx'\, dx''\, dx''',$$

where K_1 represents the self-energy kernels corresponding to (9), and K_2 represents the scattering kernels; both of these are expressed in terms of the bare masses.

The renormalization of (12) reduces simply to the substitution in (12) of M_1 and μ_1 expressed in terms of M and μ, using the relationships in (11). In some of the propagation functions which correspond to scattering, M_1 and μ_1 are simply replaced by M and μ due to "envelopment" of the corresponding lines. There will also appear, however, the propagation functions of the "undeveloped" particles to which the bare mass corresponds. To the last category belong, for example, the propagation function of a nucleon which has already emitted, but not yet absorbed, a meson; the inclusion of four-particle amplitudes would correspond to its "envelopment", i.e., a higher approximation of the TD method.

As a result of the use of the above-described renormalization method a solution is obtained which does not contain infinities but which is in general different from the usual solution[1], in which renormalized masses correspond to all propagation functions.

After the mass renormalization in the TD method it is still necessary to renormalize the charge; the

associated difficulties are also inherent in the method here described. This hampers the comparison of the solution of (12) and of the expression derived therefrom for the scattering phases, etc., with the results obtained by the usual renormalization method[1].

I wish to express my profound gratitude to Academician I. E. Tamm and to his collaborators for their discussion of this note and for valuable suggestions.

---

[1] Silin, Tamm and Fainberg, J. Exptl. Theoret. Phys. (U.S.S.R.) 29, 6 (1955); Soviet Phys. JETP 2, 3 (1956).

[2] M. Neumann, Phys. Rev. 85, 129 (1952).

Translated by I. Emin
201

Neutrino Induced Deuteron Disintegration

A. B. GOVORKOV

(Submitted to JETP editor February 12, 1956)
J. Exptl. Theoret. Phys. (U.S.S.R.) 30, 974-975
(May, 1956)

IT has recently been clearly established that the β-interaction is a mixture of the scalar and tensor types. The scalar interaction constant has been determined by measuring f^t for the β-decay of 0^{14} to N^{14} [2]. The nuclear matrix element of β^+-decay of 0^{14} can be obtained by an exact theoretical calculation since this is an $0 \to 0+$ transition with identical nucleonic wave functions in the initial and final nuclei.

The tensor interaction constant cannot be determined directly from β-decay since the matrix element for the tensor type cannot be calculated exactly. In this case the spin direction of the decaying nucleus is changed, and since spin-orbit coupling and the relative orientation of nucleonic spins play an important part in nuclear interactions the nucleonic wave functions of the initial and final nuclei will differ. But since we must know the form of the initial and final nucleonic wave functions in order to calculate the matrix element of the nucleus, whereas the exact form of a nucleonic wave function in the nucleus is unknown, the matrix element for the tensor type of β-interaction cannot be calculated exactly.

The only nucleus for which the nucleonic wave functions are known well is the deuteron, which is not β-active. However, it is possible to determine the tensor interaction constant directly and independently of the scalar interaction constant by measuring the cross section for the absorption of an antineutrons by a deuteron:

$$D + \tilde{\nu} \to n + n + e^+ \qquad \text{(I)}$$

(ν denotes a neutrino and $\tilde{\nu}$ an antineutrino). This process, as is indicated by an estimate given below, has a cross section which is smaller by an order of magnitude than the $p + \tilde{\nu} \to n + e^+$ cross section; this process has apparently been observed by the annihilation radiation of the positrons. The cross section is of the order of magnitude 10^{-44} cm^2.

The present note deals with the determination of the antineutrino absorption cross section for deuterons.

The following simple considerations show that the scalar interaction makes a small contribution to the cross section as compared with the tensor interaction. The neutrons emitted in process (I) will possess very small velocities since the larger part of the energy evolved in the interaction is borne off by the electron. We can therefore assume that both neutrons are formed in an S-state. By the Pauli principle the spin part of the wave function for the final state of the neutrons must be antisymmetric, i.e., the neutrons spins must be antiparallel. The spin part of the deuteron wave function is symmetric--the nucleonic spins in the deuteron are parallel,. Consequently, the relative direction of the spins must be changed. This is possibly only by a tensor interaction type and is impossible by a scalar type.

For the purpose of obtaining the differential cross section of process (I) the deuteron wave function was taken in the usual form; the wave function of the final state was made antisymmetrical in all variables of the neutrons.

For the differential cross sections, summed over all polarizations of the final states and averaged over all polarizations of the initial states of the particles, the following expressions are obtained:

$$d\sigma_S = \frac{2\pi\varkappa}{(2\pi)^5} G_S^2 \left(\frac{1}{\varkappa^2 + p_1^2} - \frac{1}{\varkappa_2 + p_2^2}\right) \qquad (1)$$
$$^2\,\frac{E_e E_\nu - \mathbf{p}_e \mathbf{p}_\nu}{E_e E_\nu}\,\frac{p_1 E_1\, do_1 p_e E_e\, do_e\, dE_e}{1 - (E_1 p_2 / p_1 E_2)\cos\theta_{1,2}},$$

$$d\sigma_T = \frac{2\pi\varkappa}{(2\pi)^5} G_T^2 \left\{\frac{2}{(\varkappa^2 + p_1^2)^2}\right. \qquad (2)$$
$$\left. + \frac{2}{(\varkappa^2 + p_2^2)^2} + \left(\frac{1}{\varkappa^2 + p_1^2} - \frac{1}{\varkappa^2 + p_2^2}\right)^2\right\}$$
$$\times\ \frac{E_e E_\nu + {}^1/_3\, \mathbf{p}_e \mathbf{p}_\nu}{E_e E_\nu}\,\frac{p_1 E_1\, do_1 p_e E_e\, do_e\, dE_e}{1 - (E_1 p_2 / p_1 E_2)\cos\theta_{1,2}}.$$

Here $\mathbf{p}_e$, $\mathbf{p}_\nu$, E_e, E_ν are the momentum and the total energy of the positron and antineutrino, respectively; $\mathbf{p}_1$, $\mathbf{p}_2$, E_1, E_2 are the momenta and total energies of the emitted neutrons; $\theta_{1,2}$ is the angle between $\mathbf{p}_1$ and $\mathbf{p}_2$; do_1 and do_2 are the element of solid angle of one of the emitted neutrons and of the positron, respectively; G_T and G_s are the dimensionless tensor and scalar interaction constants, $\varkappa$ is the reciprocal of the deuteron radius (units have been chosed to give $\hbar = c = m_0 = 1$). The following momentum and energy conservation laws are satisfied:

$$\mathbf{p}_\nu - \mathbf{p}_1 - \mathbf{p}_2 - \mathbf{p}_e = 0, \qquad E_D + E_\nu - E_1 - E_2 - E_e = 0. \tag{3}$$

Here $E_D = W + M_p + M_n$, where M_p and M_n are the mass of the proton and neutron, respectively, and W is the deuteron binding energy.

In the cross section for process (I) we neglected the term resulting from the interference of the scalar and tensor interactions. As can be shown by a direct calculation, this term is directly proportional to the velocity difference of the initial and final states of the nucleon which absorbs the neutrino and can therefore be neglected (an error $\sim 0.1\%$ is thus introduced).

From (1) and (2) it can be seen that

$$\frac{d\sigma_s}{d\sigma_T} \approx \left(\frac{G_s}{G_T}\right)^2 \frac{(E_1 - E_2)^2}{2(\varkappa^2/2M_n + E_1 - M_n)^2 + 2(\varkappa^2/2M_n + E_2 - M_n)^2 + (E_1 - E_2)^2}. \tag{4}$$

An estimate of the ratio of the integral cross sections gives $\sigma_s/\sigma_T \approx 10^{-2}$. Since (as has been indicated above) the energy evolved in the reaction is borne off by the electron, it is possible to estimate the total cross section of the process without an exact integration of (1) and (2). For this estimate we can use certain average values of the energies and momenta. Then $\overline{E}_1 \approx \overline{E}_2 \approx \overline{\overline{E}}$, where $\overline{\overline{E}}$ is the average energy of a nucleon in the deuteron and

$$\sigma_s \approx 0, \quad \sigma \approx \sigma_T \approx \frac{2\varkappa}{3\pi^2} \frac{G_T^2}{(\overline{p}^2 + \varkappa^2)^2} \overline{p}\,\overline{\overline{E}}\,\overline{p}_e^3. \tag{5}$$

By substituting in (5) the calculated values $G_T \approx 4 \times 10^{-12}$ (see, for example, Ref. 2), $\overline{\overline{E}} \approx 2 \times 10^3$, $\overline{p} \approx \varkappa \approx 87$, $\overline{p}_e \approx 1$ to 2 (the energy of the antineutrino must then be $E_\nu \approx 4.2 - 4.6$ mev; the reaction threshold $E_\nu = 4.03$ mev; the average energy of the antineutrinos emitted by a reactor* is 2.5 mev) we obtain as an estimate of the total cross section $0.1 \times 10^{-45} - 1 \times 10^{-45}$ cm^2.

In conclusion, the author wishes to thank I. S. Shapiro for suggesting the problem and for valuable comments.

* For an estimate of the average energy of antineutrinos emitted by a nuclear reactor, see Refs. 3 and 4.

[1] Maxson, Allen and Jentschke, Phys. Rev. **97**, 109 (1955).

[2] I. B. Gerhart, Phys. Rev. **95**, 288 (1954).

[3] F. Reines and C. L. Cowan, Phys. Rev. **92**, 830 (1953).

[4] K. Way and E. P. Wigner, Phys. Rev. **73**, 1318 (1948).

Translated by I. Emin
202

Diffraction Scattering of High Energy π-Mesons by Nuclei

S. Z. Belen'kii
P. N. Lebedev Physical Institute, Academy of Sciences, USSR

(Submitted to JETP editor February 16, 1956)
J. Exptl. Theoret. Phys. (U.S.S.R.) **30**, 983-985 (May, 1956)

EXPERIMENTAL data indicate that the elastic collisions between high energy π-mesons (1.4 bev and more) and nucleons are of a markedly diffractive character, i.e, small angle scattering is prevalent[1-4]. In Ref. 3 an attempt was made to analyze the diffraction scattering theoretically. However, the authors assumed for the nucleonic model a sphere with sharp boundaries and certain transparency, an assumption which is usually made with respect to the nucleus. In the case of a nucleon, nevertheless, there is no cause to choose such a model. In the present note the diffraction

scattering is treated on the basis of general theory, without any special assumption as to the nucleonic model.

We shall take the following relations[5] as the basis:

$$\sigma_c = \pi\lambda^2 \sum_{l=0}^{\infty} (2l+1)(1-|\beta_l|^2), \qquad (1)$$

$$\sigma_s = \pi\lambda^2 \sum_{l=0}^{\infty} (2l+1)|\beta_l - 1|^2.$$

We are neglecting here the spin dependence of nuclear forces and the change of the charge of π-mesons in collision with protons[6]. Here σ_c is particle absorption cross section, σ_s is the elastic scattering cross section, $\lambda\!\!\!^{-}$ is the wavelength of the incident particle, $\lambda\!\!\!^{-} l$ is the orbital momentum and $\beta_l = \exp\{2i\eta_l\}$ where η_l is the phase of scattering.

The differential cross section for elastic scattering is given by the following expression:

$$\frac{d\sigma_s}{d\omega} = |f(\vartheta)|^2, \qquad (2)$$

$$f(\vartheta) = -\frac{i\lambda\!\!\!^{-}}{2} \sum_{l=0}^{\infty} (2l+1)(\beta_l - 1) P_l(\cos\vartheta).$$

where ϑ is the scattering angle, $d\omega$ is the solid angle element and $P_l(\cos\vartheta)$ are the Legendre polynomials.

On the basis of the results of Ref. 6 we assume that in high energy region the imaginary part of the scattering amplitude is much larger than the real part and β_l is therefore real. This fact greatly simplifies the phase analysis. If the function $d\sigma_s/d\omega$ were known sufficiently well from the experimental data, it would be possible to find a unique function β_l. In reality the present degree of precision of the experiments does not allow for unique phase determination. The experimental results obtained with high energy accelerators permit, nevertheless, an approximate phase analysis.

We shall turn now to the most complete experimental data available on the scattering of 1.4 bev π-mesons by nucleons[3]. The other experimental results[1,2,4] are in satisfactory agreement with the results of Ref. 3. Estimating the cross sections, its authors referred a part of the observed elastic scattering to processes directly connected with the absorption of pions. Indeed, as the result of the π-meson capture and the following decay of the compound system a noncoherent, almost isotropic elastic scattering should take place, which should be regarded as inelastic collision, contrary to the diffraction scattering. This division is not completely unambiguous. We shall note, however, that the number of elastic nondiffractive collisions found by the authors of Ref. 3 is in good agreement with the value obtained from the statistical theory[7]. According to the predictions of the statistical theory, the inelastic scattering practically disappears at high energies (4.5 bev). The cross section found for the inelastic and elastic collisions in Ref. 3 are: $\sigma_c = 26.7 \pm 1.3$ mbn and $\sigma_s = 7.3 \pm 1.0$ mbn. The ratio σ_s/σ_c changes from 0.33 to 0.23. The angular distribution for the diffractive scattering was obtained as well (Fig. 1). In order to analyze the obtained data, we shall proceed as follows: for sufficiently large energies it is possible to pass over to integration in Eqs. (1) and (2):

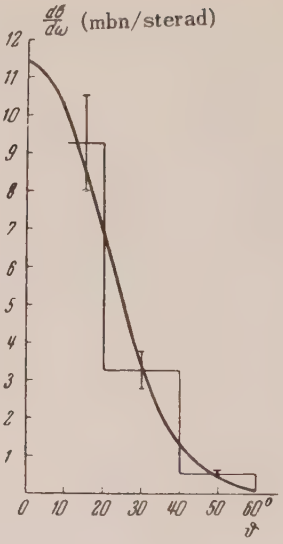

Angular distribution of the diffraction scattering of π-mesons by a nucleon in the center-of-mass system according to Ref. 3. The solid theoretical curve calculated according to Eq. (2) and (6).

$$\sigma_c = \pi\lambda^2 \int_0^{\infty} 2la_l(2-a_l)\,dl; \quad \sigma_s = \pi\lambda^2 \int_0^{\infty} 2la_l^2\,dl; \qquad (3)$$

$$f(\vartheta) = -i\lambda \int_0^{\infty} la_l J_0(l\vartheta)\,dl, \qquad (4)$$

where $a_l = 1 - \beta_l$ and $J_0(l\vartheta)$ is the Bessel function of order zero.

We shall make the simplest assumption, namely, we shall put $\alpha_l = \alpha \exp(-\lambda\!\!\!^{-2} l^2/R^2)$ where the

values α and R have to be determined from experiment. Substituting the function a_l into Eq. (3) we obtain:

$$\sigma_c = \frac{\pi\alpha^2}{2} R^2 \left(\frac{4}{\alpha} - 1\right); \qquad \sigma_s = \frac{\pi\alpha^2}{2} R^2. \tag{5}$$

The values of α and R corresponding to the experimental results lie within the following limits: from $R = 0.86 \times 10^{-13}$ cm and $\alpha = 0.74$ to $R = 0.74 \times 10^{-13}$ and $\alpha = 0.99$. The values, corresponding to the mean values of σ_s and σ_c, are $R = 0.8 \times 10^{-13}$ and $\alpha = 0.85$. Furthermore, substituting the function a_l into Eq. (4), we can calculate the function $f(\vartheta)$:

$$|f(\vartheta)| = \lambda\!\!\!^{-} \int_0^\infty \alpha J_0(l\vartheta)\, e^{-\lambda\!\!\!^{-}_2 l^2/R^2}\, l\,dl \tag{6}$$

$$= \alpha \frac{R^2}{\lambda\!\!\!^{-}} \int_0^\infty e^{-y^2} J_0\left(\vartheta \frac{R}{\lambda\!\!\!^{-}} y\right) y\,dy =$$

$$= (\alpha R^2/2\lambda\!\!\!^{-}) \exp\{-\vartheta^2 R^2 4\lambda\!\!\!^{-2}\}.$$

The angular distribution $d\sigma/d\omega$ is determined by the function $|f(\vartheta)|^2$. The angular distribution calculated according to the formula (6) using the values $\lambda\!\!\!^{-} = 2.7 \times 10^{-14}$ cm, $R = 0.8 \times 10^{-13}$ cm and $\alpha = 0.9$, which correspond to $\sigma_c = 28$ mbn and $\sigma_s = 81$ mbn, is given in Fig. 1. The experimental data fit satisfactorily the theoretical curve.

The value $Z_l = 1 - |\beta_l|^2$, the physical meaning of which is the ' sticking probability " of particle, is of interest:

$$Z_l = \alpha e^{-\rho^2/R^2} (2 - \alpha e^{-\rho^2/R^2}), \tag{7}$$

where $\rho = \lambda\!\!\!^{-} l$. We shall note that for $\rho = 0$ the value of Z is close to unity for a wide interval of values of d. Thus, even for $\alpha = 0.73$ $Z_{\rho=0} = 0.93$.

The mean square value of the impact parameter [averaged over the function (7)] is:

$$\rho_{cp} = \overline{(\rho^2)}^{1/2} = \sqrt{\frac{1 - \alpha/8}{1 - \alpha/4}}\, R. \tag{8}$$

The values $\bar{\rho}$, satisfying the experimental data are contained in the interval $(0.8 - 0.9) \times 10^{-13}$ cm. We shall note that, contrary to what is maintained in Ref. 3, the fact that the nucleon cannot be regarded as a black body does not imply that the statistical theory of multiple production is not applicable.

The function (7) gives the probability of inelastic scattering taking place for the impact parameter ρ. The inelastic scattering can be treated on the basis of the statistical theory, too[8]. It is of interest to perform a similar analysis for nucleon-nucleon collisions.

[1] Crussard, Walker and Koshiba, Phys. Rev. **94**, 736 (1954).

[2] Walker, Crussard and Koshiba, Phys. Rev. **95**, 852 (1954).

[2] Eisberg, Fowler, Lea, Shephard, Shutt, Thorndike and Whittemore, Phys. Rev. **97**, 797 (1955).

[3] Maenchen, Powell, Saphir and Wright, Phys. Rev. **99**, 1619 (1955).

[5] A. Akhiezer and I. Pomeranchuk, *Problems of Nuclear Theory*, GTTI, 1950.

[6] L. Okun' and I. Pomeranchuk, J. Exptl. Theoret. Phys. (U.S.S.R.) **30**, 424 (1956).

[7] A. Nikishov, J. Exptl. Theoret. Phys. (U.S.S.R.) **30**, 601 (1956); Soviet Phys. JETP **3**, 634 (1956).

[8] L. D. Landau, Izv. Akad. Nauk SSSR, Ser. Fiz. **17**, 51 (1953).

Translated by H. Kasha
207

Radiative Disintegration of Λ^0-Particle

P. V. VAVILOV

(Submitted to JETP editor February 17, 1956)
J. Exptl. Theoret. Phys. (U.S.S.R.) **30**, 985-987
(May, 1956)

BESIDES the normal decay scheme of the Λ^0-particle

$$\Lambda^0 \to p + \pi^-, \tag{1}$$

the following decay scheme is possible:

$$\Lambda^0 \to p + \pi^- + \gamma. \tag{2}$$

It is known from the experimental data that the spin of the π^--meson is zero and therefore the spin of the Λ^0-particle must be half-integral. In the present work the influence of the spin of Λ^0-particle upon the shape of the γ-quanta spectrum is investigated.

SPIN OF Λ^0 EQUAL TO ½

We shall use the notation of Ref. 1 and a system of units in which $h = c = 1$. The density of the interaction energy is given by the following expression:

$$U = ieN(\bar{\psi}_p \gamma_\mu \psi_p) A_\mu - ie\left(\varphi \frac{\partial \varphi^*}{\partial x_\mu} - \varphi^* \frac{\partial \varphi}{\partial x_\mu}\right) A_\mu + V, \tag{3}$$

where ψ_p and φ are the wave functions of the proton and of the meson, respectively, A_μ is the electromagnetic potential, V is the interaction energy of Λ^0, p and the π^--meson, of the following form:

$$V = gN(\bar{\psi}_p \gamma_5 \psi_{\Lambda^0})\varphi \quad (P\text{-coupling}) \tag{4, P}$$

$$V = \frac{f}{M+\Lambda} N(\bar{\psi}_p \gamma_5 \gamma_\mu \psi_{\Lambda^0}) \frac{\partial \varphi}{\partial x_\mu} \quad (A\text{-coupling}) \tag{4, A}$$

M, Λ and m are the masses of the proton, Λ^0-particle and the meson. (4, P) and (4, A) represent the pseudoscalar P-coupling and the pseudovector A-coupling. The normalization of the constant of (4, A) is chosen so that (4, P) and (4, A) give the same result for the probability of decay (1) in the first approximation of the perturbation theory.

The matrix element of the decay (2) is of the following form in the first non-vanishing approximation of the perturbation theory:

$$M = \frac{ieg(2\pi)^4}{2\sqrt{E_\pi k}} \bar{u}_p \left(\frac{2p_e + \hat{e}\hat{k}}{M^2 \varkappa} + \frac{2q_e}{m^2 \varkappa_1}\right) \times \gamma_5 u_\Lambda \delta(p_\Lambda - p - q - k), \tag{5, P}$$

$$M = \frac{ief(2\pi)^4}{2\sqrt{E_\pi k}} \bar{u}_p \left(\frac{2p_e + \hat{e}\hat{k}}{M^2 \varkappa} + \frac{2q_e}{m^2 \varkappa_1} - i\frac{\hat{e}}{\Delta}\right) \times \gamma_5 u_\Lambda \delta(p_\Lambda - p - q - k). \tag{5, A}$$

Here $\bar{u}_p$, u_Λ are the Dirac spinors of the proton and of the Λ^0-particle; $\hat{e} = e_\nu \gamma_\nu$, $p_e = e_\nu p_\nu$, $\Delta = M + \Lambda$, $M^2 \varkappa = 2(pk)$, $m^2 \varkappa_1 = 2(qk)$ and p, q, k are the 4-momenta of the proton, of the meson and of the γ-quantum, respectively. According to general rules, we obtain from (5) the probability of the decay (2), given by

$$dw = \frac{e^2 f^2}{8 E_\pi E_p k} \left\{\frac{1}{(pk)^2}\left[\left(q^2 - \frac{1}{k^2}(qk)^2\right) \times \left(E_p + k - M + 2\frac{(pk)}{\Delta}\right) - k(pk) + 2(E_p + M)\frac{(pk)^2}{\Delta^2} + 2(kM - (pk)\frac{(pk)}{\Delta}\right] + \frac{1}{(qk)^2}\left(q^2 - \frac{1}{k^2}(qk)^2\right)(E_p - M) - \frac{1}{(pk)(qk)}\left(q^2 - \frac{1}{k^2}(qk)^2\right)\left(k + 2E_p - 2M + 2\frac{(pk)}{\Delta}\right)\right\} \times \frac{d^3k d^3q}{(2\pi)^5} \delta(E_\lambda - E_p - E_\pi - k). \tag{6, A}$$

The probability for pseudoscalar interaction will be obtained from (6, A) dropping the terms in $1/\Delta$ and putting g instead of f.

2. SPIN OF Λ^0 EQUAL TO 3/2

The equations for the case of particle with spin $^3/_2$ were studied in Ref. 2. The wave function of a particle with spin $^3/_2$ has mixed transformation properties of a usual spinor and of a 4-vector, each component of which satisfies the equation

$$(i\hat{p} + M)\psi_\mu = 0, \tag{7}$$

with the auxiliary conditions:

$$\partial \psi_\mu / \partial x_\mu = 0, \quad \gamma_\mu \psi_\mu = 0.$$

For a particle at rest the wave function is[3]:

$$\vec{\psi}^{(1)} = \mathbf{e}_1 u^{(1)}, \quad \vec{\psi}^{(2)} = \mathbf{e}_2 u^{(2)}, \tag{8}$$

$$\vec{\psi}^{(3)} = \frac{\mathbf{e}_2}{\sqrt{3}} u^{(1)} + \sqrt{\frac{2}{3}}\, \mathbf{e}_3 u^{(2)},$$

$$\vec{\psi}^{(4)} = \frac{\mathbf{e}_1}{\sqrt{3}} u^{(2)} - \sqrt{\frac{2}{3}}\, \mathbf{e}_3 u^{(1)},$$

$$\psi_0^{(i)} = 0; \quad \mathbf{e}_1 = 2^{-1/2}(1, i, 0),$$

$$\mathbf{e}_2 = 2^{-1/2}(1, -i, 0), \quad \mathbf{e}_3 = (0, 0, 1);$$

$u^{(1)}$ and $u^{(2)}$ are spinors with polarization $\pm ½$.

The condition $\gamma_\mu \psi_\mu = 0$ implies that it is possi-

ble to form an invariant combination of the wave functions ψ, $\vec{\psi}$ only with the help of vector q_ν:

$$V = \frac{f}{m} N (\bar{\psi}_p \gamma \psi_\mu) \frac{\partial \varphi}{\partial x_\mu}, \tag{9}$$

where $\gamma = \gamma_5$ when $\bar{\psi}_p \psi_\mu q_\mu$ is a scalar and $\gamma = 1$ when it is pseudoscalar. The matrix element for the decay (2) can be written on the basis of Eq. (5) by putting $\hat{q} \to q_\nu$, $u_\lambda \to u_\nu$ therein. The expression for the decay proabability for the case of spin $^3/_2$ is:

$$dw = \frac{e^2 f^2}{24 m^2 E_p E_\pi k} \left\{ \left(\mathbf{q}^2 - \frac{1}{k^2} (\mathbf{qk})^2 \right) \right. \tag{10}$$

$$\times \left[\frac{\mathbf{q}^2}{(pk)^2} (E_p + k \pm M) + \frac{\mathbf{p}^2}{(qk)^2} (E_p \pm M) \right] -$$

$$\times - \frac{1}{(pk)(qk)} \left[2 \left(\mathbf{q}^2 + (\mathbf{qk}) + \frac{1}{4} | \mathbf{q} | k \right) \cdot \right.$$

$$(E_p \pm M) + k (\mathbf{q}^2 + (\mathbf{qk})) \Big] - \frac{k \mathbf{q}^2}{(pk)^2} \Big\}$$

$$\times \frac{d^3k \, d^3q}{(2\pi)^5} \delta (E_\lambda - E_p - E_\pi - k).$$

The signs (+) and (–) correspond to the cases $\gamma = 1$ and $\gamma = \gamma_5$, respectively. For small photon frequency ($k \ll 1$) we obtain from (6) and (10)

$$\frac{dw}{dw_e} = \frac{\alpha}{2\pi} \left(\mathbf{q}^2 - \frac{1}{k^2} (\mathbf{qk})^2 \right) \tag{11}$$

$$\left(\frac{1}{(pk)} - \frac{1}{(qk)} \right)^2 k \, dk \sin\theta \, d\theta,$$

where dw_e is the probability of decay mode (1) and $\alpha = 1/137$.

When the particles can be regarded as nonrelativistic, Eq. (11) simplifies to the well-known relation[4]

$$dw/dw_e = (2\alpha/3\pi) (q^2/E_\pi^2) \, dk/k. \tag{12}$$

For small photon frequencies the spin of the Λ^0-particle has, therefore, no influence upon the decay probability. In the Table below, values are given for the ratio of the total probability w_2 of decay with emission of a photon with energy $\geq E$ to the probability w_1 of decay without emission of radiation. This ratio is calculated for spin $^3/_2$ ($\gamma = 1$) and for spin $^1/_2$ (P-interaction). The following values are taken for the masses of the particles: $M = 1837\, m_e$, $m = 270\, m_e$, $\Lambda = 2180\, m_e$.

E (mev)	1	5	10	Spin
$10^4\, w_2/w_1$	13	4,6	2,8	1/2
	10	3,0	0,97	3/2

It is evident from the above that the spin of Λ^0-particle has an influence upon the shape of the spectrum. This difference in forms of spectra is very substantial at high energies. Comparing theory with experiment we can try to determine the spin of the Λ^0-particle and the type of coupling as well.

I wish to express my gratitude to I.I. Pomeranchuk for his constant help and advice.

[1] A.I. Akhiezer and V.B. Berestetskii, *Quantum Electrodynamics*, GITTL, Moscow, 1953.

[2] W. Rarita and J. Schwinger, Phys. Rev. 60, 61 (1942).

[3] S. Kusaka, Phys. Rev. 60, 61 (1942).

[4] I.I. Pomeranchuk and I.M. Shmushkevich, Dokl. Akad. Nauk SSSR 64, 499 (1949).

Translated by H. Kasha
208

CONTENTS

(*Contents continued on inside back cover*)